EVALUATION OF LOW WING-LOADING
FUEL CONSERVATIVE, SHORT-HAUL TRANSPORTS

By

L.H. Pasley and T.A. Waldeck

By

THE *BOEING* COMPANY
WICHITA DIVISION - WICHITA KANSAS 67210

For

NASA
National Aeronautics and
Space Administration

EVALUATION OF LOW WING-LOADING
FUEL CONSERVATIVE, SHORT-HAUL TRANSPORTS

By

L.H. Pasley and T.A. Waldeck

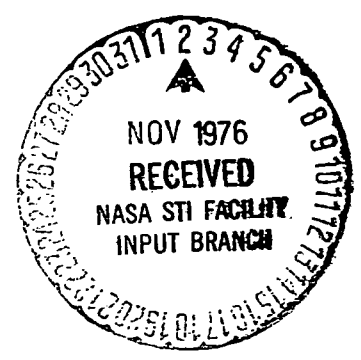Prepared under Contract No. NAS 1-13714

By

THE **BOEING** COMPANY
WICHITA DIVISION · WICHITA KANSAS 67210

For

NASA
National Aeronautics and
Space Administration

ABSTRACT

The objective of this study was to determine the fuel
conservation that could be attained with two technology
advancements, Q-fan propulsion system and Active Control
Technology (ACT). Aircraft incorporating each technology
were sized for a Federal Aviation Regulation (FAR) field
length of 914 meters (3,000 feet), 148 passengers, and a
926 kilometer (500 nautical mile) mission. The cruise
Mach number was .70 at 10100 meter (33,000 foot) altitude.
The improvement resulting from application of the Q-fan
propulsion system was computed relative to an optimized
fuel conservative transport design. The performance
improvements resulting from application of ACT technology
were relative to the optimized Q-fan propulsion system
configuration.

FOREWORD

An evaluation of recent advancements in Q-fan propulsion
technology and active control technology, on a short-haul
transport, was conducted under NASA-Langley Research
Center Contract NAS1-13714. Work was initiated in January
1975 and completed January 1976. This work represents a
part of NASA continuing effort to provide the technology
needed to meet the challenge of designing fuel conservative,
quiet, economical transports.

This study was under the direction of W. J. Rohling, Program
Manager. The Principal Investigator was L. H. Pasley. Val-
uable contributions were made by the following members of the
Technical Staff; C. R. Hanke, N. E. Conley, G. E. Hodges,
O. E. Visor, H. F. Veldman, C. T. Havey and M. P. Schaefer.

The work was administered under the direction of W. C.
Sleeman, Jr., and D. W. Conner, Transport Aircraft
Projects Office, NASA-Langley Research Center.

SUMMARY

The objective of this study was to determine the fuel conservation that could be attained with two technology advancements, Q-fan propulsion system and Active Control Technology (ACT). Aircraft incorporating each technology were sized for a Federal Aviation Regulation (FAR) field length of 914 meters (3,000 feet), 148 passengers, and a 926 kilometer (500 nautical mile) mission. The cruise Mach number was .70 at 10100 meter (33,000 foot) altitude. The improvement resulting from application of the Q-fan propulsion system was computed relative to an optimized fuel conservative transport design. The performance improvements resulting from application of ACT technology were computed relative to the optimized Q-fan propulsion system configuration.

The baseline airplane specified had a mechanical flap, low wing loading, 2.8 kPa (58 psf), and was powered by a turbofan engine (1.35 fan pressure ratio). The design utilized the advantage of supercritical wing technology and acoustical noise treatment.

The optimum Q-fan propulsion system configuration yielded a 14 percent reduction in total mission fuel (including reserves) and a four percent reduction in maximum gross weight. The optimized airplane was essentially identical to the baseline airplane in all other design parameters. In both cases, the optimum Fan Pressure Ratio (FPR) was 1.35. There was no significant noise improvement found with the Q-fan.

Application of ACT technology yielded a seven percent reduction in total mission fuel relative to the optimized Q-fan propulsion system airplane and a ten percent reduction in maximum gross weight. Three ACT technology concepts were included, Gust Load Alleviation (GLA), Relaxed Static Stability (RSS) and Ride Quality Improvement (RQI). The GLA reduced the Q-fan baseline airplane critical design gust load factor from 4.2 g's to 2.65 g's or approximately the maneuver limit of 2.5 g's. Horizontal and vertical tail size reductions of 43 percent and 36 percent, respectively, were attained with the RSS concept. The necessity for ride quality improvement was based on the finding that the low wing loading produced approximately twice as rough a ride in turbulence as that on a modern jet transport. The RQI provided the ride quality of a modern jet transport in cruise.

The performance improvements resulting from application of the ACT concepts to configurations optimized for field lengths greater than 914 meters (3,000 feet) showed that the relative percentage improvement decreased.

TABLE OF CONTENTS

TABLE OF CONTENTS (Cont'd)

INTRODUCTION

The design of future transport aircraft will need to give increased attention to energy consumption and environmental impact. This study is part of an overall study by NASA to help provide the technology needed to meet the challenge of designing a fuel conservative, quiet, economical transport. Two recent advancements in technology are evaluated in this report. The first is the Q-fan propulsion system that employs a very high bypass, variable pitch fan. The second is Active Control Technology (ACT) to provide gust load alleviation, relaxed static stability and ride quality improvement.

The study addresses the short-haul market, 926 kilometer (500 nautical mile) design range. A previous NASA-Langley sponsored study (Reference 1) showed that for the shorter field lengths and stage lengths that are associated with the structure of this market, a low wing loading aircraft is competitive with the high wing loading blown flap design. A low wing loading mechanical flap design was selected as the baseline for evaluating the further improvement that could be realized with Q-fan propulsion and active controls technology. The ACT serves two purposes: a direct payoff resulting from a reduction of both the design gust load factor and the empennage surface areas, and from ride quality improvement to provide the low wing loading airplane with a ride quality as desirable as a current jet airplane.

The specific low wing-loading baseline airplane design was selected from NASA-Ames studies (References 2 and 3) that addressed various design ranges, field lengths and number of passengers. The baseline airplane selected was a 148-passenger configuration designed for a 926 kilometer (500 nautical mile) range and 914 meter (3,000 foot) FAR field length. The baseline design included mid-1980 technology turbofan engine performance, supercritical airfoil technology and a conventional flight control system.

The technology advantages of the Q-fan propulsion system are the improved fuel consumption and reduced noise level potentially available with the very high-bypass ratio variable pitch fan blades. Q-fan technology demonstration engines are currently being tested with a full-scale engine test scheduled for the near future.

The three concepts of ACT that were evaluated were Gust Load Alleviation (GLA), Relaxed Static Stability (RSS) and Ride Quality Improvement (RQI). These concepts have been demonstrated in flight and are being incorporated into some of the new airplane designs. The present study evaluated the potential use of each separately, and then combined use of all three in a multipurpose active control system configuration.

The design objective was to minimize the total energy expended per passenger for gate-to-gate operations. To achieve fuel economy, the cruise speed was allowed to be reduced at a reasonable sacrifice in trip time from that normally achieved in present day jet airline schedule operations. A sacrifice of four minutes per each 185 kilometers (100 nautical miles) of stage length was considered reasonable. The design goal for community noise level was to reduce the 90 EPNdb footprint during terminal-area operations to an area not to exceed 2.59 square kilometers (one square mile).

SYMBOLS AND ABBREVIATIONS

$\bar{A}$ — Acceleration per unit gust velocity, g's/m/s (g's/ft/sec)

ACT — Active Control Technology

APU — Auxiliary Power Unit

AR — Aspect Ratio

ASAMP — Airplane Sizing and Mission Performance

ATA — Air Transportation Association

a_H — Horizontal tail lift curve slope, per degree

a_V — Vertical tail lift curve slope, per degree

a_{WB} — Wing body lift curve slope, per degree

b — Wing span, m(ft)

C — Comfort rating

c — Chord, m(in)

$\bar{c}$ — Wing mean aerodynamic chord, m(in)

CCD — Customer Computer Deck

C_D — Airplane drag coefficient

C_{D_α} — Drag due to angle of attack, per degree

C_{D_δ} — Drag due to control surface deflection, per degree

C_{D_0} — Zero lift or parasite drag coefficient with no compressibility

CG — Airplane center of gravity, percent MAC

C_L — Airplane lift coefficient

C_{L_0} Initial airplane lift coefficient

$C_{L_{APP}}$ Airplane approach lift coefficient

C_{L_H} Horizontal tail lift coefficient

$C_{L_{MAX}}$ Maximum lift coefficient

C_{L_q} Lift due to pitch rate, per rad.

C_{L_S} Airplane lift coefficient corresponding to stall speed

$C_{L_{WB}}$ Wing body lift coefficient

$C_{L_{V_{\delta_R}}}$ Vertical tail lift coefficient due to rudder, per degree

C_{L_α} Airplane lift curve slope, per degree

$C_{L_{\dot\alpha}}$ Lift due to angle of attack rate, per rad.

C_{L_δ} Lift due to control surface deflection, per degree

C_M Pitching moment coefficient

C_{M_q} Pitching moment due to pitch rate, per rad.

C_{M_0} Initial pitching moment (assumed zero when trimmed)

$C_{M_{0_{WB}}}$ Wing body pitching moment coefficient at zero lift

$C_{M_{.25\bar{c}}}$ Pitching moment about quarter wing MAC

C_{M_α} Pitching moment due to angle of attack, per rad.

$C_{M_{\dot\alpha}}$ Pitching moment due to angle of attack rate, per rad.

C_{M_δ} Pitching moment due to control surface deflection, per degree

C_{n_β} Yawing moment coefficient due to sideslip, per degree

$C_{n_{\beta_V}}$ Vertical tail yawing moment coefficient due to sideslip, per degree

$C_{n_{\beta_{WB}}}$ Wing body yawing moment coefficient due to sideslip, per degree

D   Drag or diameter, newtons (lb), M(ft)

dB   Decibel

DOC   Direct Operating Cost

EPNdb   Equivalent perceived noise level, db

EPR   Engine Pressure Ratio

f   Frequency, Hz

FAR   Federal Airworthiness Regulation

FBW   Fly-by-Wire

FCT   Fuel Conservative Transport

F_N Scaled engine sea level static thrust, newtons (lb)

$F_{N_{REF}}$ Reference engine sea level static thrust, newtons (lb)

FPR   Fan Pressure Ratio

g   Acceleration of gravity, m/sec^2 (ft/sec^2)

GLA   Gust Load Alleviation

i_t Horizontal tail incidence, degree

I_{xx} Airplane yaw moment of inertia about roll axis, $kg-m^2$ $(slug-ft^2)$

I_{yy} Airplane yaw moment of inertia about pitch axis, $kg-m^2$ $(slug-ft^2)$

KEAS   Knots Equivalent Airspeed,(knots)

I_B Fuselage length, m (ft)

ℓ_H Horizontal tail arm measured from the wing aerodynamic center to the horizontal tail aerodynamic center, m (ft)

L_p	Rolling moment variation with roll rate, /sec
ℓ_V	Vertical tail arm measured from the wing aerodynamic center to the vertical tail aerodynamic center, m (ft)
L_δ	Rolling moment variation with lateral control, /sec^2
M	Free stream Mach number
MAC	Mean Aerodynamic Chord, m (in)
MF	Mechanical Flap
MTBF	Mean-Time-Between-Failure, hours
N	Number of engines
n	Load factor, g's
OWE	Operating Weight Empty, newtons (lb)
PNL	Perceived Noise Level, db
PNdb	Perceived noise level in decibels, db
PSF	Pounds Per Square Foot
q	Dynamic pressure, kg/m^2 (lb/ft^2)
RQI	Ride Quality Improvement
RSS	Relaxed Static Stability
S	Wing area, m^2 (ft^2)
S	Laplace operator or percent passengers satisfied
S_B	Body cross-sectional area, m^2 (ft^2)
SFC	Engine specific fuel consumption, Mkg/N·S (Lbm/Lbf-Hr)
S_H	Horizontal tail area, m^2 (ft^2)
S_{REF}	Reference area, m^2 (ft^2)

S_V	Vertical tail area, m^2 (ft^2)
T	Thrust, newtons (lb) or time, seconds
t/c	Wing thickness ratio, fractional part of local chord
U_{de}	Gust velocity equivalent airspeed, m/s (ft/sec)
V_{APP}	Aircraft approach speed, m/s (knots)
V	Velocity, m/s (knots)
V_C	Velocity cruise, m/s (knots)
V_{CW}	Cross-wind component perpendicular to aircraft flight path, m/s (knots)
V_D	Velocity Dive, m/s (knots)
V_e	Equivalent airspeed, m/s (knots)
$\bar{V}_H$	Horizontal tail volume coefficient
V_{LO}	Lift-off speed, m/s (knots)
V_{MC}	Airplane engine-out minimum control speed, m/s (knots)
V_{MCG}	Airplane engine-out ground minimum control speed, m/s (knots)
V_{MU}	Airplane minimum unstick speed, m/s (knots)
V_R	Airplane takeoff rotation speed, m/s (knots)
V_S	Airplane stall speed, m/s (knots)
$\bar{V}_V$	Vertical tail volume coefficient
V_1	Critical engine failure speed, m/s (knots)
V_2	Takeoff climb speed, m/s (knots)
W	Gross weight, newton (lbf)
W	Vertical gust velocity, m/s (ft/sec)

WRBM/α	Wing-Root-Bending-Moment due to angle of attack, N·m/deg (ft-lbs/deg)
WRBM$_\delta$	Wing-Root-Bending-Moment due to control surface deflection, N·m/deg (ft-lbs/deg)
$X_{AC_{WB}}$	Wing body aerodynamic center measured relative to the leading edge of the mean aerodynamic chord, m (in)
X_{CG}	Center of gravity measured relative to the leading edge of the mean aerodynamic chord, m (in)
X/C	Fractional percent of local chord
X_{MG}	Main landing gear location measured relative to the leading edge of the mean aerodynamic chord, m (in)
y_e	Critical engine moment arm, m (in)
$\ddot{Z}$	Vertical acceleration, m/s^2 (ft/sec^2)
Z_T	Engine pitching moment arm, m (in)
α_S	Angle of attack, degree
α_S	Stall angle of attack, degree
β_W	Sideslip angle, degree
γ	Flight path angle, degree
Δ	Incremental change
δ	Control surface deflection, degree
δ	Atmospheric pressure ratio
η	Percent semispan
$\dot{\theta}$	Pitch rate, degree/second
$\dot{\theta}_{ss}$	Steady state pitch rate, degree/second
$\ddot{\theta}$	Pitch acceleration, degree/second^2

θ	Atmospheric temperature ratio
Λ	Sweep angle, degree
$\Lambda c/4$	Sweep of quarter chord, degree
λ	Wing or horizontal tail taper ratio
ρ	Atmospheric density, kg/m^3 (slugs/ft^3)
$\dfrac{d\epsilon}{d\alpha}$	Change in downwash with respect to angle of attack
$\dfrac{d\sigma}{d\beta}$	Change in sidewash with respect to sideslip

BASELINE DEFINITION AND ANALYTICAL CORRELATION

The initial phase of this study involved definition of the baseline configuration utilizing The Boeing Company preliminary design methodology and computer programs and correlation of these results to the specified Reference 2 baseline airplane. Such a correlation was necessary to establish a meaningful reference for comparing the performance benefits due to Q-fan propulsion technology and active control technology to previous fuel conservative studies.

The baseline airplane was selected from two NASA sponsored studies reported in References 2 and 3 which addressed a wide range of operating and design parameters and concepts. Among these were passenger size, operating range, field length, cruise altitude and speed, wing geometry, thrust-to-weight ratio and types of propulsion systems and high lift devices. The selected airplane design characteristics are as follows:

- Mission

Design range	=	926 km	(500 nm)
Design field length	=	914 m	(3,000 ft)
Cruise Mach number	=	0.7	
Cruise altitude	=	10100 m	(33,300 ft)

- Wing Geometry

Aspect ratio	=	10
Taper ratio	=	0.3
Quarter chord sweep angle	=	10 degrees
Supercritical airfoil technology		

- Propulsion

Two wing mounted engines

Fan pressure ratio	=	1.35	
Bypass ratio	=	12	
Engine rated thrust	=	118.4 kN	(26,610 lbf)

- Fuselage

Five abreast seating
148 passengers

A three-view of the baseline airplane is presented in Figure 1.
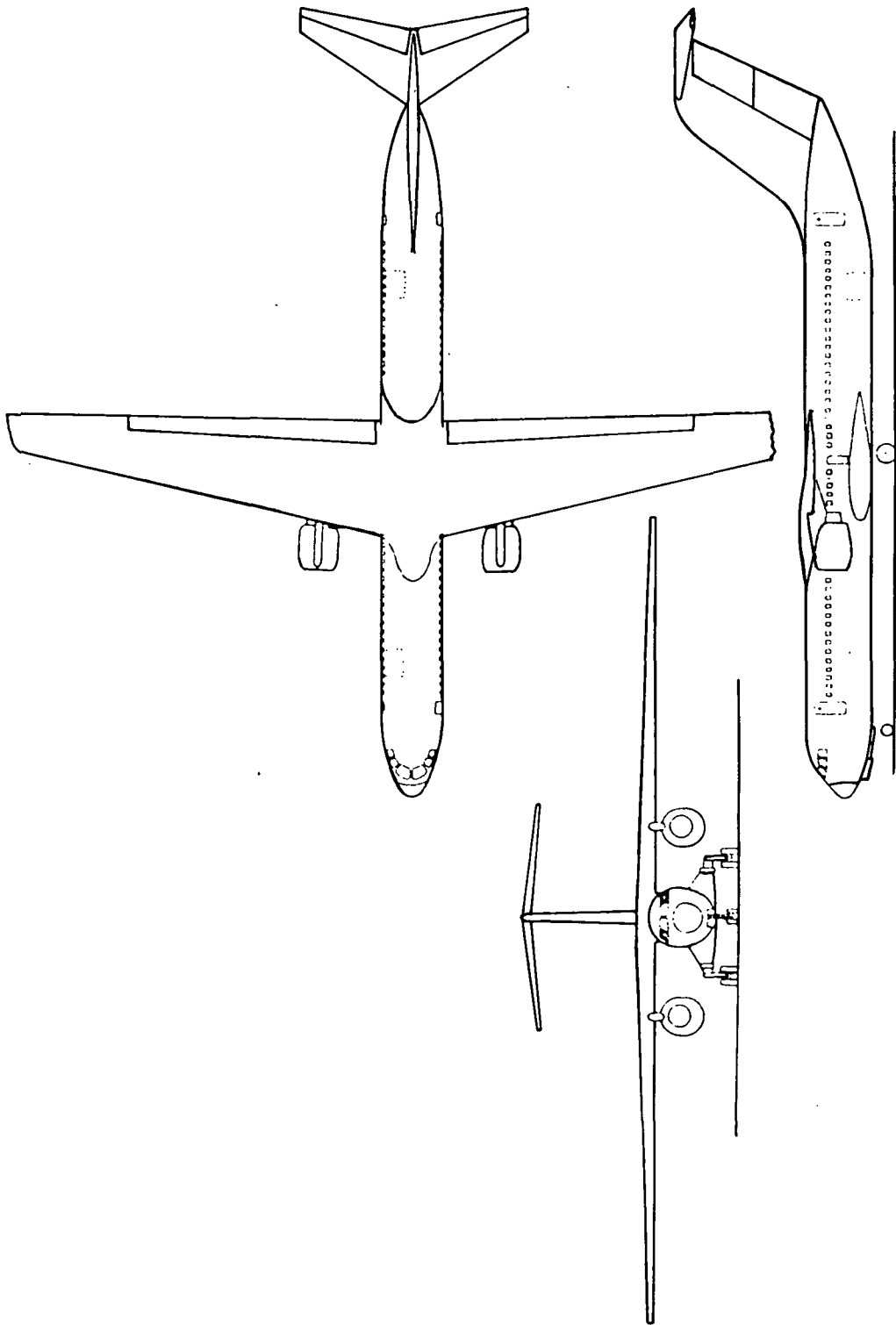
BASELINE MECHANICAL FLAP CONFIGURATION 914m (3000 FT) FIELD LENGTH
FIGURE 1

A design mission profile is shown in Figure 2. This mission is identical to that used in Reference 2, except the 1524 meter (5,000 foot) maneuvers were performed at 129 m/s (250 knots) equivalent airspeed instead of maximum endurance speed. The gate-to-gate time for the mission is 96 minutes at a cruise Mach number of .70. This time is 12 minutes longer than the 926 kilometer (500 nautical mile) mission time of a modern jet which cruises at .78 Mach. A comparison of the mission profiles of the study airplane and the Boeing 727 in terms of distance and time are presented in Figures 3 and 4, respectively.

Baseline Configuration

The baseline configuration selected from Reference 2 was defined parametrically. No detailed aerodynamic, weight-and-balance and propulsion data were provided. The aerodynamic three-view for the baseline configuration was drawn using the tabulated data contained in Reference 2. The fuselage length of 41.5 meters (136.3 feet) was held constant in this study. The airplane geometric characteristics are presented in Table 1.
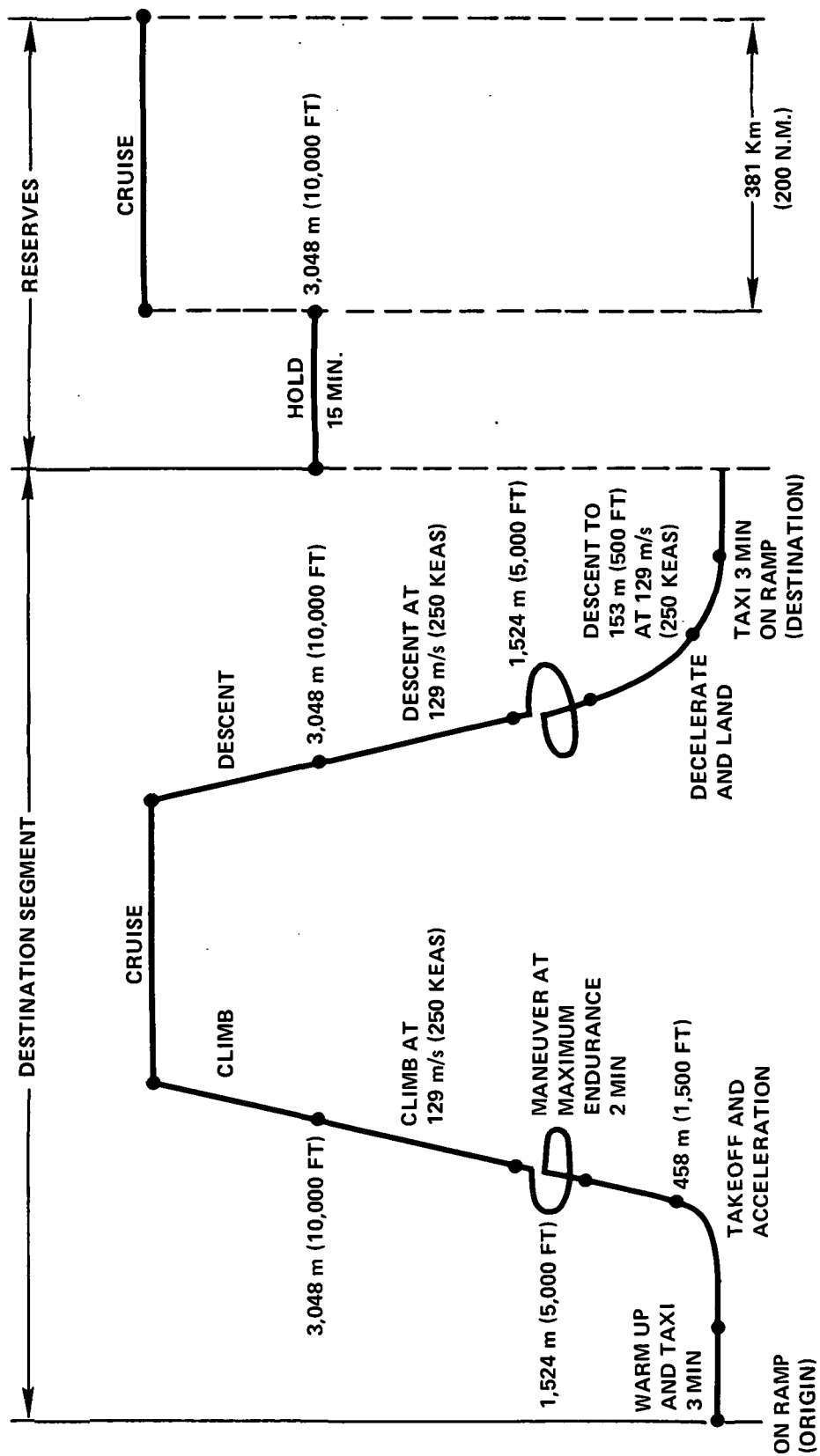

Aerodynamics

The aerodynamic data necessary to define the baseline configuration aerodynamic characteristics were estimated since the information was not available in Reference 2. The low-speed lift, drag and pitching moment data were computed based on the baseline flap geometry shown in Figure 5. The wing trailing edge flap extends from the wing-body junction to 70 percent semispan. The wing leading edge flap is a 17 percent wing-chord full-span Kreuger flap deflected 70 degrees. The computed low-speed aerodynamic lift and drag data are shown in Figures 6 and 7.

Tail Sizing

The horizontal and vertical tail size were determined for the baseline airplane using the following stability, control and handling quality criteria. This aspect of the design was particularly important for the relaxed static stability trade studies.

Horizontal Tail Sizing. - The horizontal tail size was based on the following requirements:

- Static longitudinal stability margin of three percent.
- Adequate nose wheel steering at the aft center of gravity limit.

FLIGHT PROFILE INCLUDING RESERVES
FIGURE 2
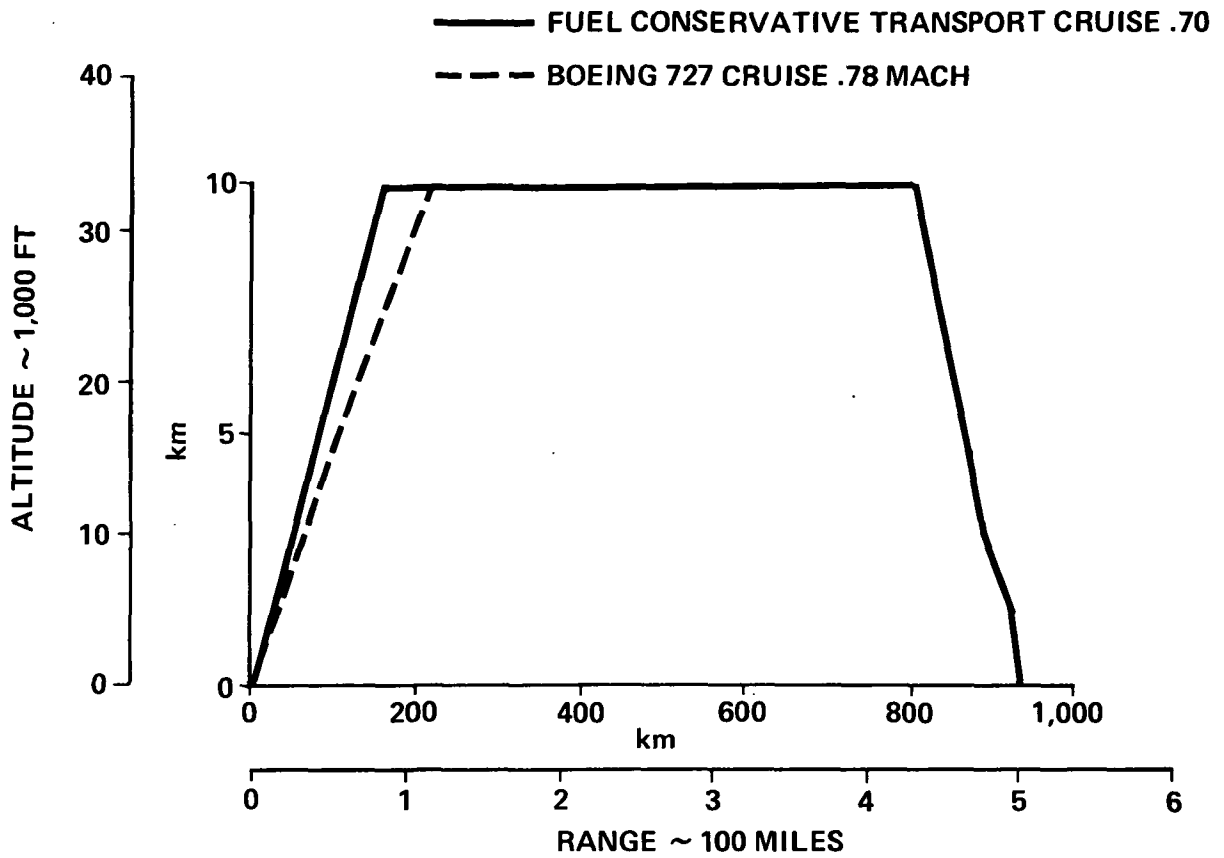
DESIGN MISSION RANGE PROFILE COMPARISON
FIGURE 3

DESIGN MISSION TIME PROFILE COMPARISON
FIGURE 4

TABLE 1
BASELINE FUEL CONSERVATIVE TRANSPORT AERODYNAMIC GEOMETRY

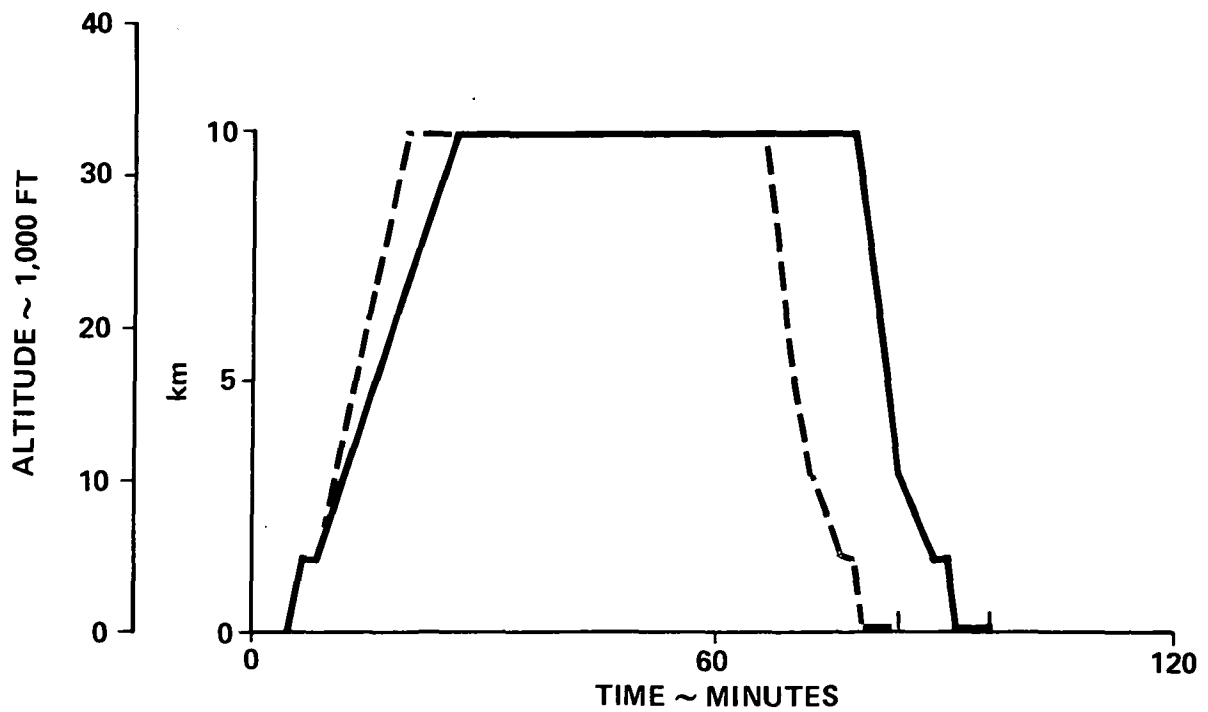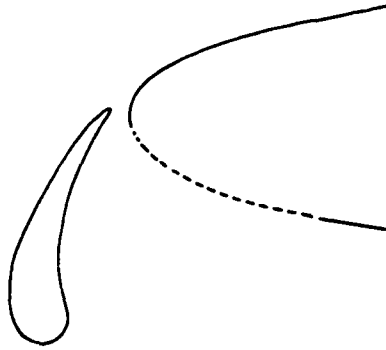|				
Fuselage				
LF	Length	41.5 m	(136.3	Ft)
WF	Width	3.66 m	(12.0	Ft)
SF	Wetted Area	433.0 m^2	(4,661.	Sq Ft)
Wing				
AR	Aspect Ratio		10.00	
SW	Area	487.0 m^2	(2,289.5	Sq Ft)
B	Span	46.1 m	(151.3	Ft)
CBARW	Geom. Mean Chord	5.06 m	(16.6	Ft)
LAMBDA C/4	Quarter Chord Sweep		10.0	Deg
LAMBDA	Taper Ratio		0.300	
(T/C)R	Root Thickness		0.183	
(T/C)T	Tip Thickness		0.140	
WG/SW	Wing Loading	2.78 kPa	(58.0	lb/Sq Ft)
Horizontal Tail				
ARHT	Aspect Ratio		4.50	
SHT	Area	38.03 m^2	(409.4	Sq Ft)
BHT	Span	13.1 m	(42.9	Ft)
CBARHT	Mean Chord	2.90 m	(9.5	Ft)
(T/C)HT	Thickness/Chord		0.120	
Vertical Tail				
ARVT	Aspect Ratio		1.40	
SVT	Area	50.23 m^2	(540.7	Sq Ft)
BVT	Span	8.38 m	(27.5	Ft)
CBARVT	Mean Chord	6.00 m	(19.7	Ft)
(T/C)VT	Thickness/Chord		0.130	
Primary Engine Nacelle				
LN	Length	4.05 m	(13.3	Ft)
DBARN	Mean Diameter	2.35 m	(7.7	Ft)
SN	Wetted Area	59.93 m^2	(645.1	Sq Ft)

LEADING EDGE FLAP
$\delta = 70^{\circ}$

WING REFERENCE
PLANE (WRP)

FWD
FLAP
SEGMENT

AFT
FLAP
SEGMENT

65%   76%   85%   100%

TRAILING EDGE FLAP ~ % CHORD
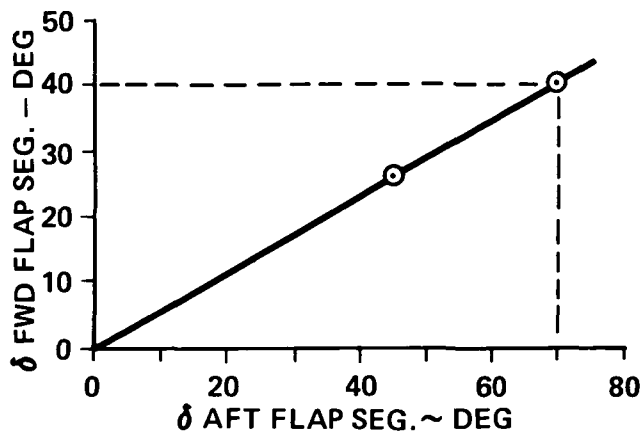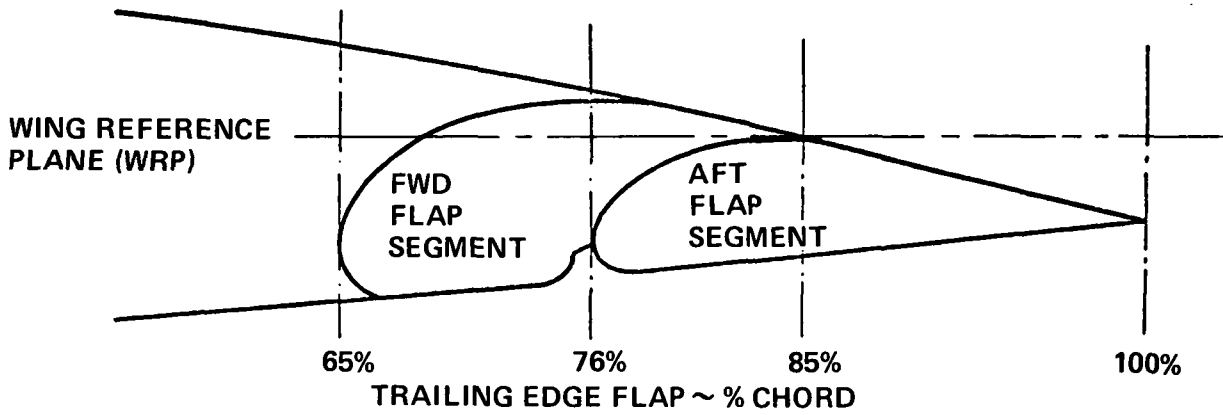
FLAP GEOMETRY
FIGURE 5
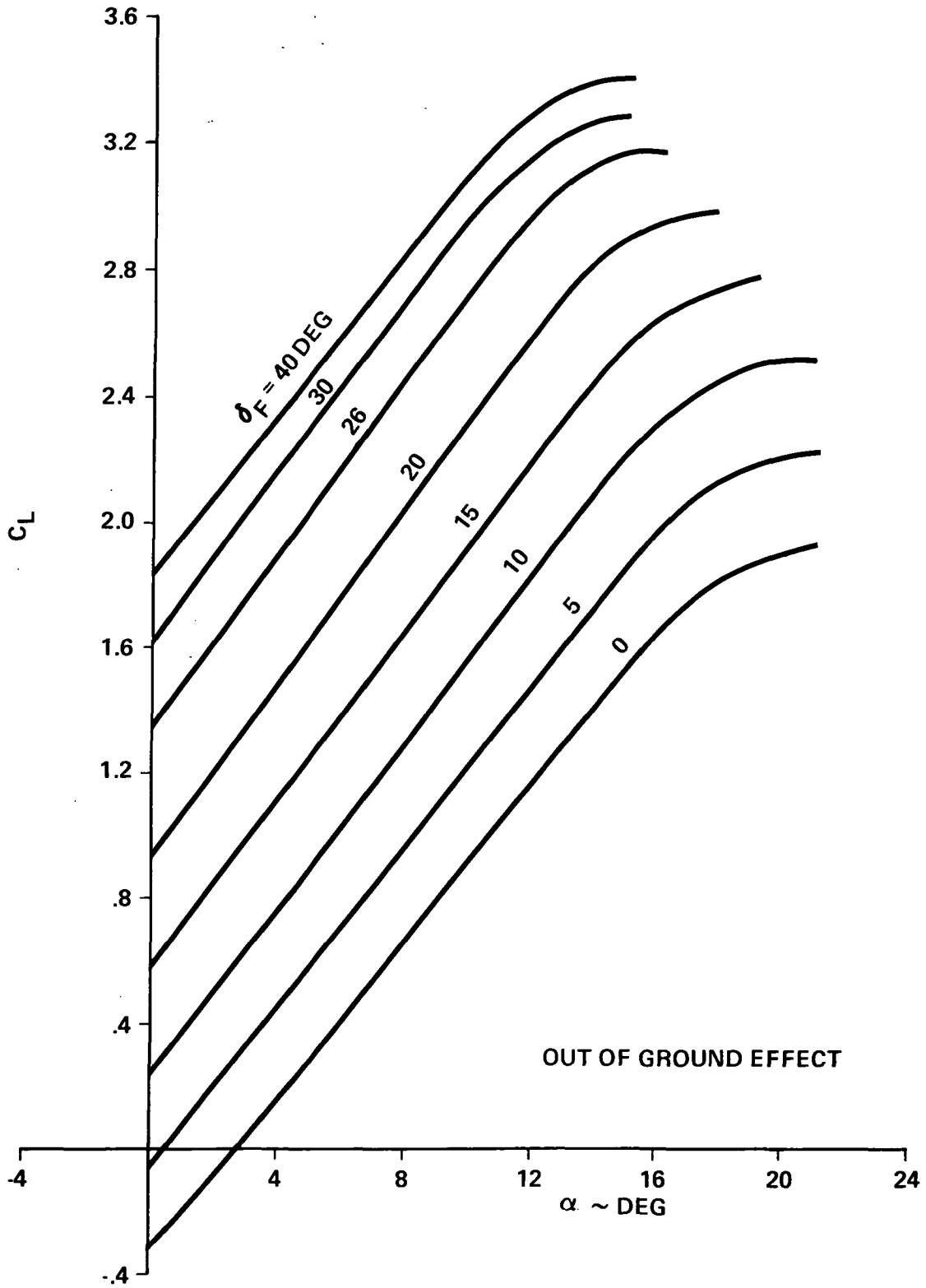
LOW-SPEED LIFT CHARACTERISTICS FOR BASELINE AIRPLANE CONFIGURATION
FIGURE 6

LOW-SPEED MAXIMUM C_L AND LIFT TO DRAG RATIO FOR BASELINE CONFIGURATION
FIGURE 7

- The ability to rotate the aircraft to takeoff attitude at the rotation speed.
- The ability to trim the aircraft at the approach speed.
- The center of gravity travel range of 20 percent MAC.

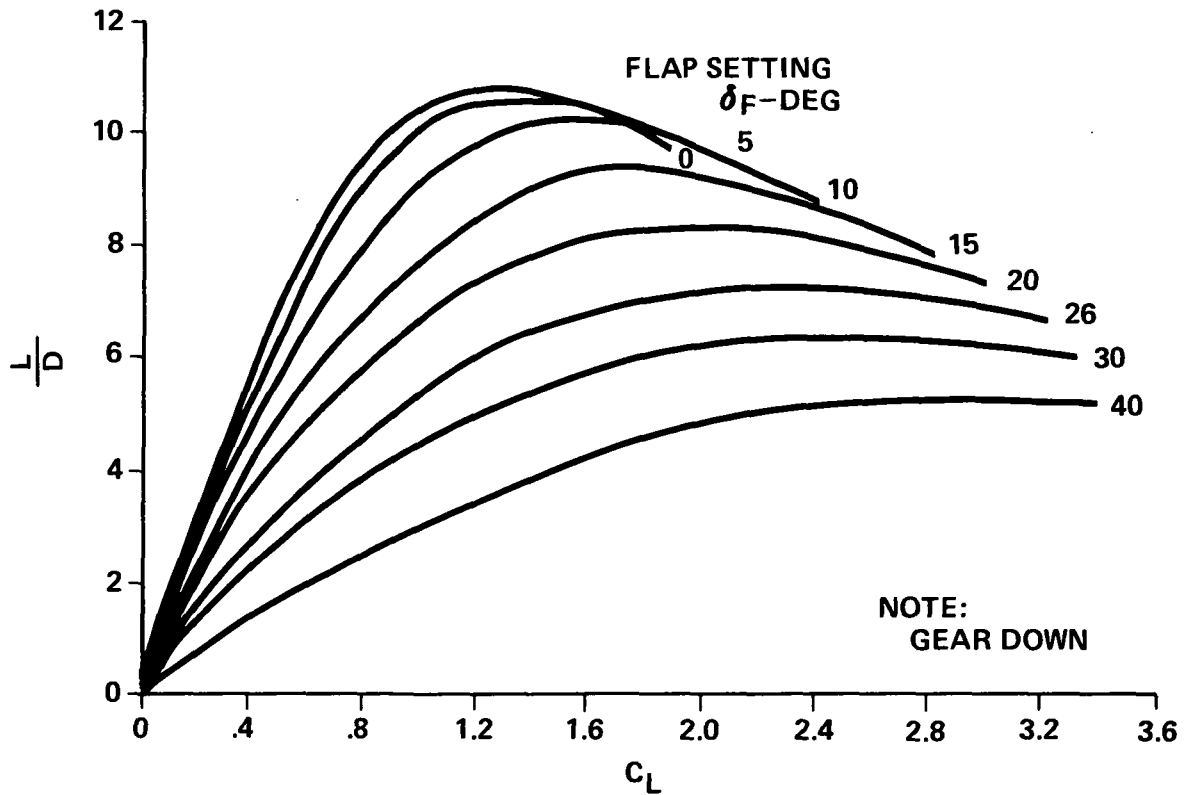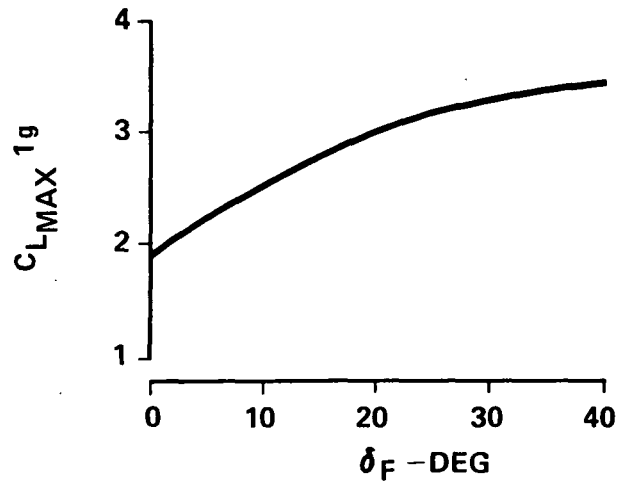The first two items determine the aft center of gravity limit while the third and fourth items determine the forward center of gravity limit for a given tail size. Figure 8 schematically illustrates the horizontal tail area requirements as a function of center of gravity position. The optimum tail area was achieved by varying the wing position until a location was found in which the forward and aft aerodynamic center of gravity limits encompass the forward and aft weight-and-balance loading limits as well as the required center of gravity travel range.

Static Longitudinal Stability. - The static longitudinal stability criteria chosen for this study was to provide the aircraft with a three percent static stability margin when flying with the center of gravity on the aft limit. The horizontal tail area-to-wing area ratio (S_H/S) required to provide the aircraft with neutral static stability $(dC_m/dC_L = 0)$ was computed by:

$$\frac{S_H}{S} = \frac{\left(\dfrac{X_{CG}}{\bar{c}} - \dfrac{X_{AC_{WB}}}{\bar{c}}\right)}{\dfrac{a_H}{a_{WB}}\left(1 - \dfrac{d\epsilon}{d\alpha}\right)\left(\dfrac{l_H}{\bar{c}} + .25 - \dfrac{X_{CG}}{\bar{c}}\right)}$$

The wing-body neutral point $(X_{AC_{WB}})$ is presented in Figure 9 as a function of Mach number. The wing-body lift curve slope, (a_{WB}) and horizontal tail lift curve slope, (a_H) are presented as a function of Mach number in Figures 10 and 11, respectively. The change in downwash angle at the tail per unit change in wing angle of attack,$(1-d\epsilon/d\alpha)$ is presented in Figure 12.

The horizontal tail area to wing area ratio required for a three percent static margin is then obtained by limiting the center of gravity position to three percent ahead of the values determined from the above equation.

Nose Wheel Steering. - When the aft center of gravity limit as a function of the horizontal tail area to wing area ratio has been determined which will satisfy the static longitudinal requirements, the nose wheel steering requirement can be satisfied by proper placement of the main landing gear. With the center of gravity at the aft limit for the static stability requirement, the main landing gear can be located so that adequate nose wheel steering is available for the aircraft considering power on and off effects.

STATIC LONGITUDINAL
STABILITY AND NOSE
WHEEL STEERING

REQUIRED
CG RANGE

TRIM AT APPROACH
SPEED

NOSE WHEEL LIFT-OFF
AT ROTATION SPEED
(MAIN LANDING GEAR
PLACED FOR STEERING
REQUIREMENT AT AFT
CG LIMIT)

REQUIRED
HORIZONTAL
TAIL SIZE

CG

S_H/S
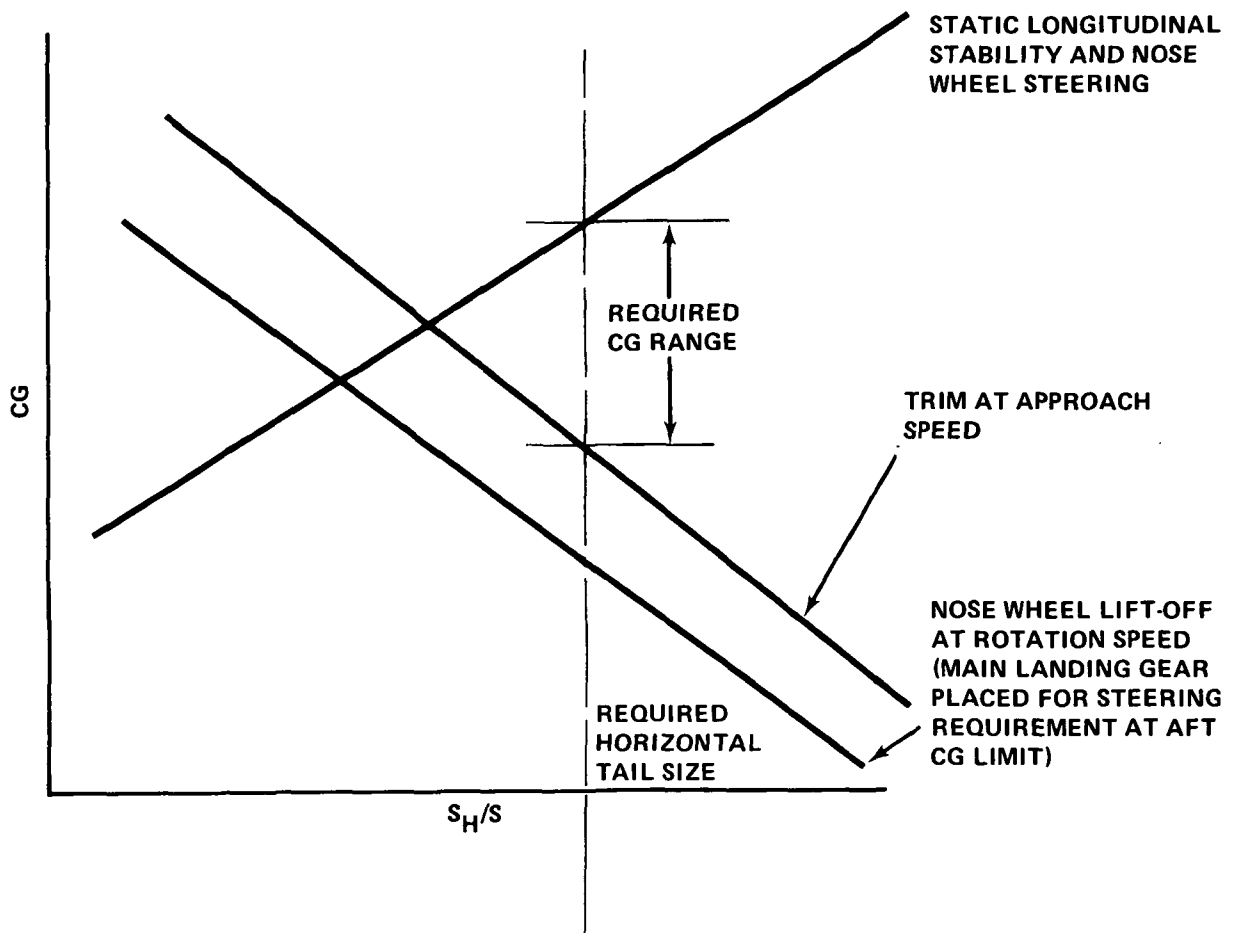
HORIZONTAL TAIL SIZING SCHEMATIC
FIGURE 8

WING-BODY AERODYNAMIC CENTER $(X_{AC_{WB}})$

MACH NUMBER
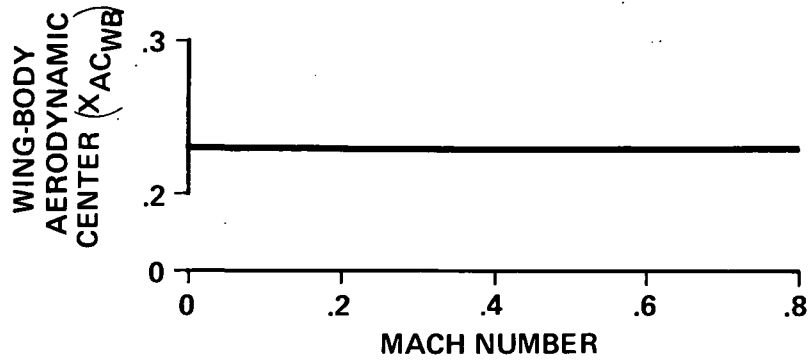
WING-BODY AERODYNAMIC CENTER
FIGURE 9

WING-BODY LIFT CURVE SLOPE $(a_{W.B.}) \sim 1/DEG.$

MACH NUMBER
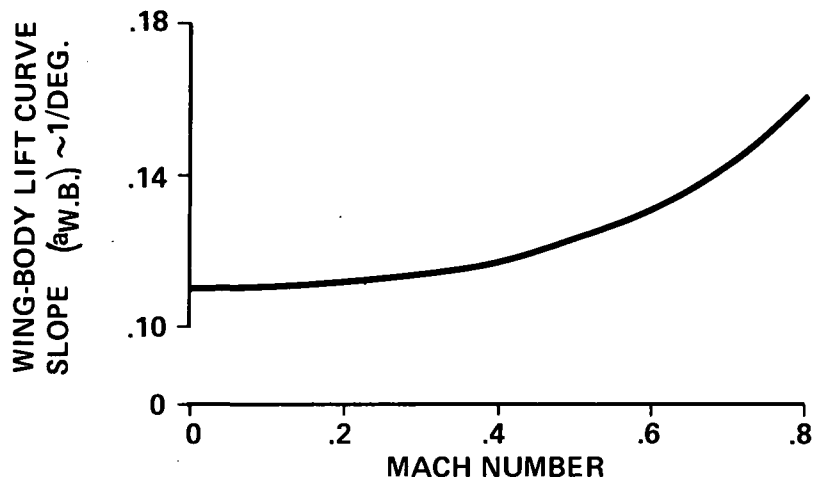
WING-BODY LIFT CURVE SLOPE
FIGURE 10

HORIZONTAL TAIL LIFT CURVE SLOPE $(a_H) \sim 1/DEG$

MACH NUMBER
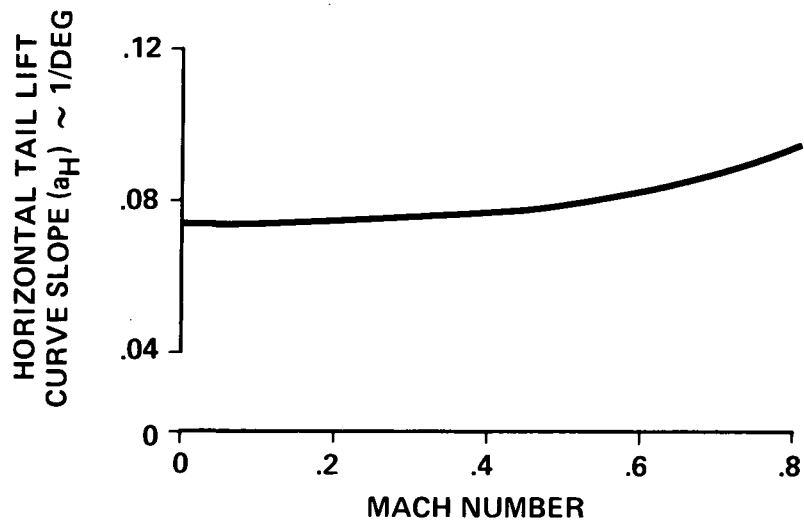
HORIZONTAL TAIL LIFT CURVE SLOPE
FIGURE 11

22
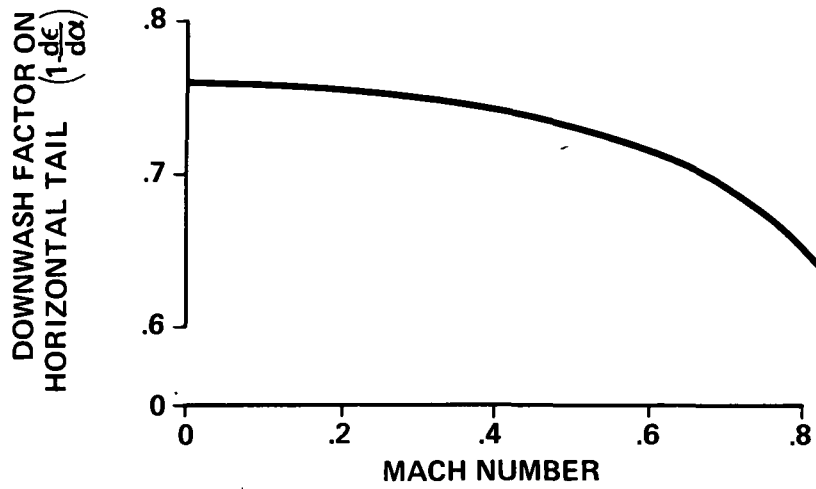
DOWNWASH ON HORIZONTAL TAIL
FIGURE 12
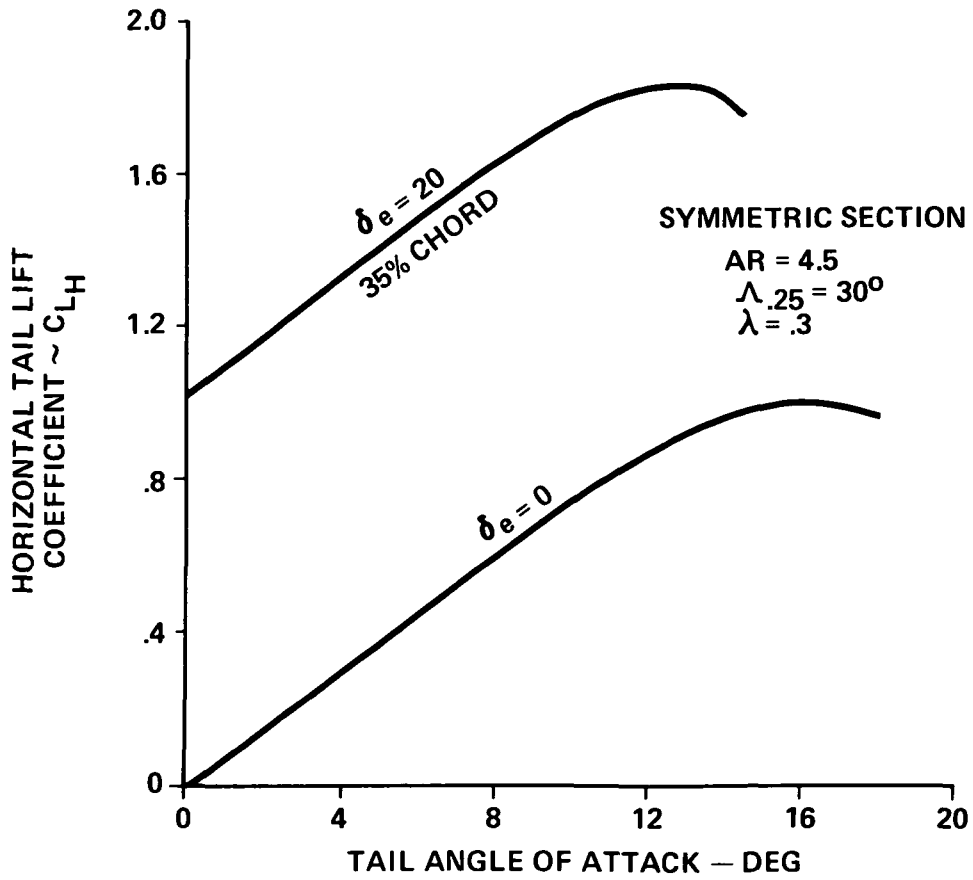
HORIZONTAL TAIL LIFT COEFFICIENT
FIGURE 13

Use of this technique forces the aft center of gravity limit to satisfy simultaneoulsy the static longitudinal stability requirement and the nose wheel steering requirement. The main landing gear was placed so that the loading on the nose wheel was always equal to or greater than five percent of the total gear load at zero velocity. This loading is comparable to the gear load distribution on Boeing commercial aircraft. The horizontal tail area which will satisfy the forward center of gravity limit criteria can now be determined.

Nose Wheel Lift Off Requirement. - When the rotation speed is reached during the takeoff ground roll, the aircraft must be capable of rotating to the takeoff attitude at the most forward center of gravity location and with the takeoff power setting. The horizontal tail area to wing area ratio (S_H/S) required to rotate the aircraft about the main gear was determined as follows:

$$\frac{S_H}{S} = \frac{\left(\frac{W/S}{q} - C_{L_{WB}}\right)\left(\frac{X_{MG}}{\bar{c}} - \frac{X_{CG}}{\bar{c}}\right) + C_{L_{WB}}\left(\frac{X_{AC_{WB}}}{\bar{c}} - \frac{X_{CG}}{\bar{c}}\right) - C_{m_{o_{WB}}} - \frac{1}{q}\left(\frac{T}{W}\right)\left(\frac{W}{S}\right)\frac{Z_T}{\bar{c}}}{C_{L_H}\left(\frac{X_{MG}}{\bar{c}} - \frac{\ell_H}{\bar{c}} - .25\right)}$$

A horizontal tail lift coefficient (C_{L_H}) of -1.4 was used to rotate the aircraft. The tail lift coefficient for rotation was determined by setting the horizontal tail for tim on climb-out at the forward center of gravity limit $(C_{L_H} = -.4)$ and applying full airplane nose-up elevator deflection.

A 35 percent chord elevator with 20 degree deflection was utilized. The horizontal tail/elevator lift authority is presented in Figure 13.

Trim at the Approach Speed. - At the landing approach speed in the landing configuration, it must be possible to trim the aircraft with the stabilizer only (no elevator control). The horizontal tail area to wing area ratio required to trim the landing approach was determined by the following equation:

$$\frac{S_H}{S} = \frac{C_{m_{o_{WB}}} + \frac{W}{q\bar{Sc}}\left(X_{CG} - X_{AC_{WB}}\right)}{C_{L_H}\left(\frac{\frac{\ell_H}{\bar{c}} + .25 - X_{AC_{WB}}}{\bar{c}}\right)}$$

The low-speed tail-off pitching moment $(C_{m_{.25}})$ variation with lift coefficient (C_L) is presented in Figure 14 as a function of flap setting. A usable
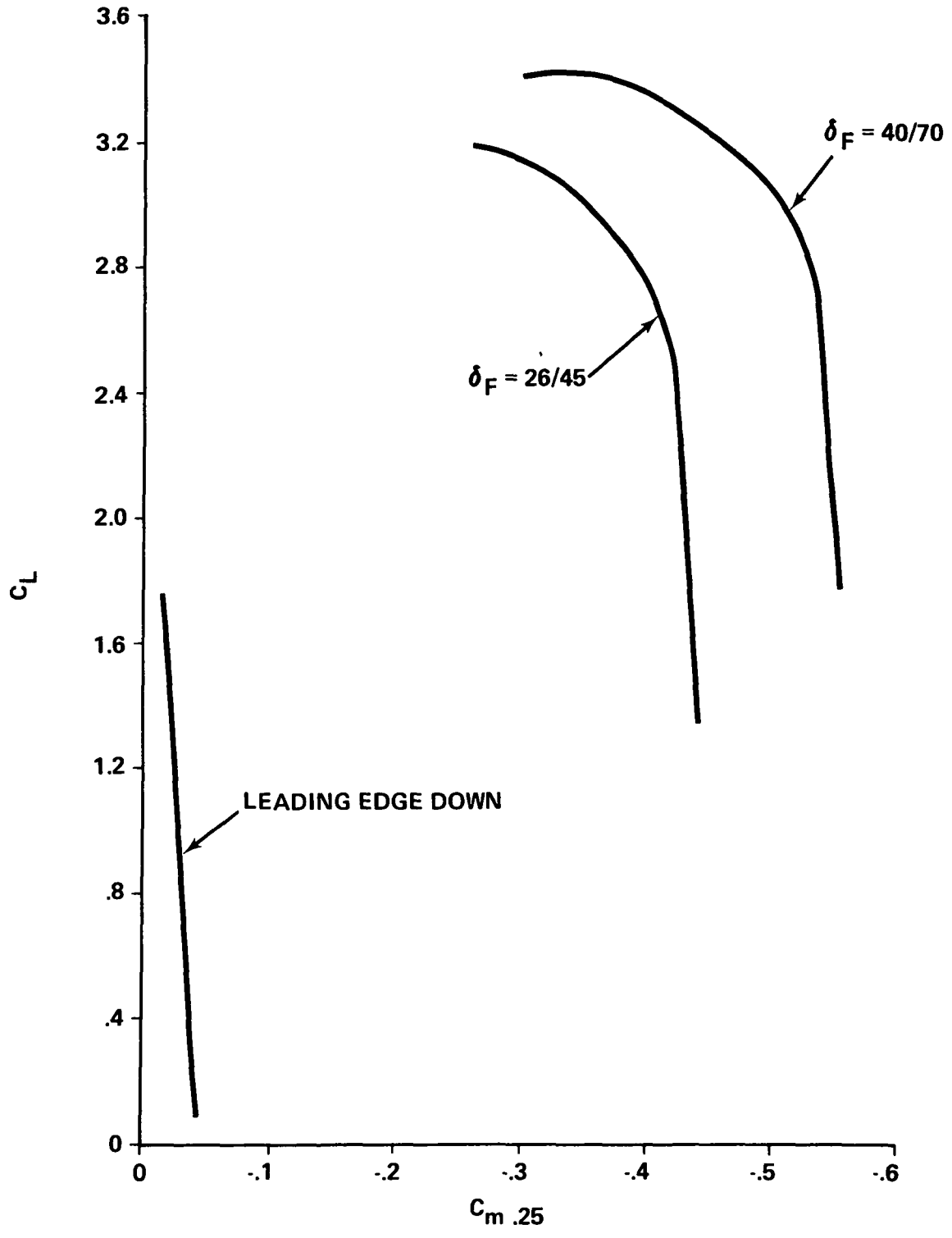
LOW SPEED TAIL OFF PITCHING MOMENT COEFFICIENT
FIGURE 14

tail lift coefficient of -.8 will provide adequate tail stall margin. The total elevator authority is then available for maneuvering the aircraft.

Baseline Configuration. - The Reference 2 baseline configuration horizontal tail sizing chart is presented in Figure 15. These data are based on a reference tail arm to wing mean chord ratio $(\ell_H/\bar{c})$ of 4.7. Based on these data, a horizontal tail area to wing area ratio of .38 ($\bar{V}_H$ = .648) would satisfy the aerodynamic requirements. However, a weight and balance analysis showed that the center of gravity range for the maximum gross weight and OWE was not within the required limits (.26 $\bar{c}$ to .46 $\bar{c}$). The configuration was rebalanced so that the center of gravity travel required coincided with the aerodynamic limits by moving the wing .762 meters (30 inches) forward.

Vertical Tail Sizing. - Vertical tail size was determined by considering:

- Ground minimum control speed, V_{MCG}
- Boeing tameness criteria
- Static directional stability
- Crosswind landing

Figure 16 illustrates the vertical tail area requirements as a function of the critical engine moment arm. For multiengine aircraft with wing-mounted engines, the minimum critical engine moment arm is usually spanwise limited by the need for adequate clearance between engines or between engine and fuselage to minimize interference effects which would penalize cruise performance. The maximum allowable vertical tail area is dictated by the crosswind requirement. The minimum vertical tail size is determined from the ground minimum control speed requirement and/or static and dynamic stability requirements. The tameness depends primarily on static directional stability (C_{n_β}) whereas the ground minimum control speed depends on the rudder authority. Crosswind landing capability is also directly dependent on the rudder authority and inversely related to the static directional stability.

Ground Minimum Control Speed Requirement. - During the takeoff run, it must be possible to maintain control of the aircraft following a sudden loss of thrust on the most critical engine. If the critical engine fails prior to reaching the ground minimum control speed (V_{MCG}), the takeoff must be aborted. If the critical engine fails at or above V_{MCG}, the aircraft must have adequate aerodynamic control power to continue the ground roll with takeoff thrust on the remaining engines. A maximum deviation of 7.62 meters (25 feet) from the intended ground roll path is allowed following an engine failure. No credit is allowed for nose wheel steeering.
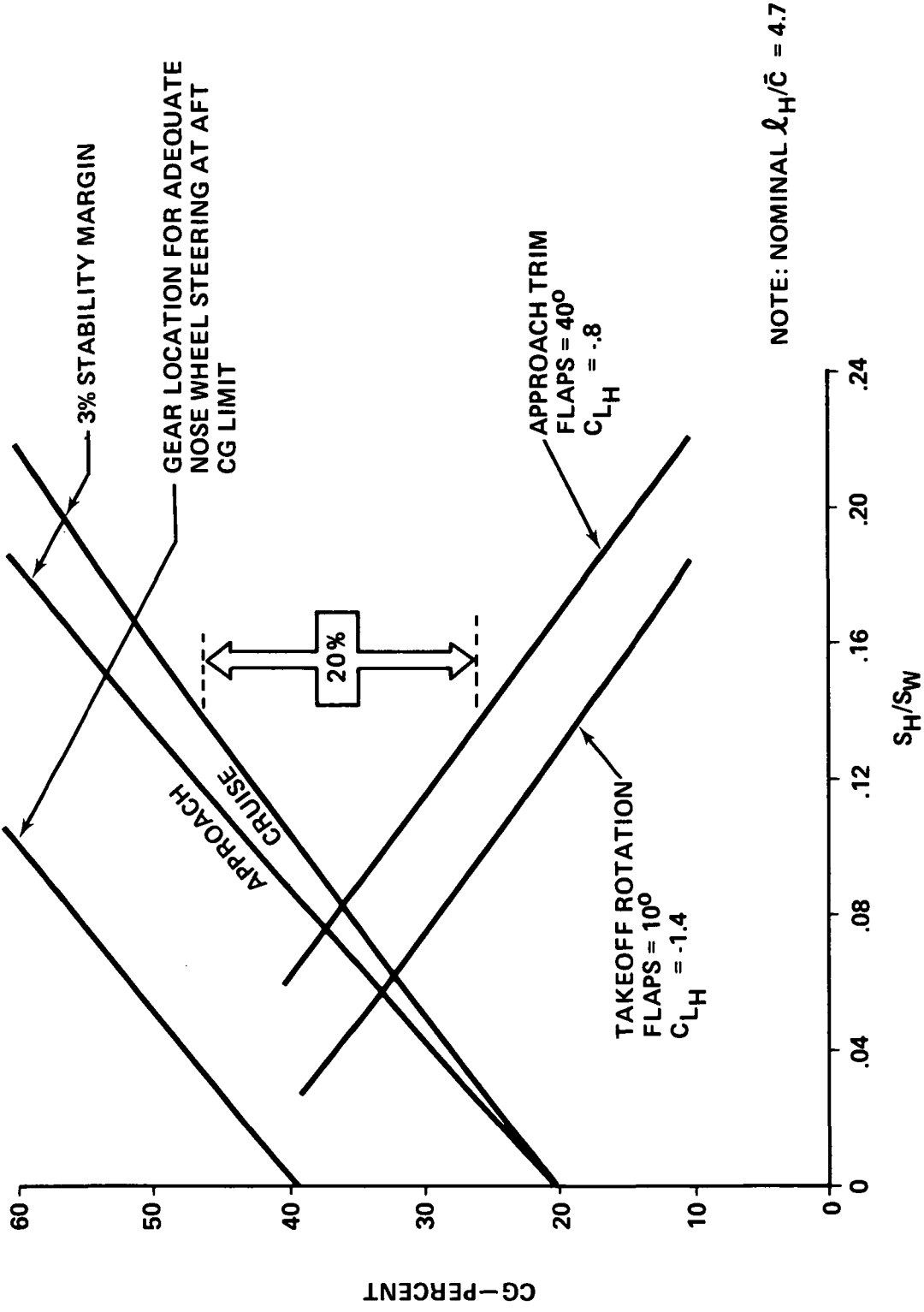
HORIZONTAL TAIL SIZING BASELINE CONFIGURATION

FIGURE 15

Sizing the vertical tail to allow a 7.62 meter (25 foot) deviation from the runway centerline allows the most critical engine to fail prior to a speed at which the rudder controls can statically balance the engine-out yawing moment. If the takeoff run is continued following an engine failure, the speed continues to increase as the aircraft departs from its originally intended flight path. Prior to reaching the maximum allowed 7.62 meter (25 foot) deviation from the intended ground path, the speed has increased and at this speed the rudder control must be able to overcome the engine-out yawing moment. The aircraft is then able to return to its originally intended flight path without exceeding the 7.62 meter (25 foot) allowed deviation. This vertical tail sizing method (besides being cumbersome to solve because the airplane dynamics are involved) gives a V_{MCG} which is less than a static analysis in which the rudder yawing moment exactly balances the engine-out yawing moment.

For this study, the vertical tail area required to satisfy the ground minimum control speed requirement was determined from a static balance of engine-out yawing moment and rudder yawing moment at the takeoff decision speed, V_1. The takeoff decision speed was chosen equal to the takeoff rotation speed.

The ratio of vertical tail area to wing area required to provide static balance of the engine-out yawing moment using only rudder control is given by:

$$\frac{S_V}{S} = \frac{295 \left(\frac{T}{NW}\right)\left(\frac{Y_e}{\ell_v}\right) \frac{W}{S}}{C_{L_V} V_1^2}$$

Because of the low speeds at which low-wing-loading aircraft operate, the critical engine moment arm must be kept small if reasonably sized vertical tails with conventional aerodynamic controls are used. Also of importance is the amount of usable vertical tail lift coefficient which can be generated by the rudder to produce a yawing moment. This vertical tail lift coefficient is determined primarily by the size of the rudder and the complexity of the rudder. A 40 percent chord rudder with 25 degrees deflection was utilized providing a maximum vertical tail lift coefficient of .9.

Tameness. - Tameness is a Boeing criteria for engine-out control. At a gross weight 25 percent above OWE and at a speed 40 percent above stall, constant heading after takeoff must be maintained following the loss of the critical engine with no rudder pedal application. Airplane steady state sideslip cannot exceed 15 degrees and the lateral control requirement cannot exceed 100 percent of the lateral control available.

The ratio of vertical tail area to wing area required to provide static balance of the engine-out yawing moment for tameness is given by:

$$\frac{S_V}{S} = \left(\frac{1}{a_V}\right)\left(\frac{b}{\ell_V}\right)\left[\left(\frac{T}{NW}\right)\left(\frac{Y_e}{b}\right)\left(\frac{C_L}{\beta}\right) - C_{n_{\beta_{WB}}}\right]$$

This expression neglects the yaw due to lateral control input. The lateral control input is small for the small wing sweep angles considered for this study. Also, the favorable yaw associated with the spoilers normally offsets the adverse yaw of the ailerons.

Static Dynamic Directional Stability Requirements. - The static directional derivative C_{n_β} (weathercock stability) does not have an explicit required value; however, when the aircraft is in a sideslip, the yawing moment produced must tend to restore the aircraft to symmetric flight. In terms of rudder required to sideslip the aircraft, right rudder pedal must produce left sideslip and left rudder pedal must produce right sideslip.

The total airplane weathercock stability is composed of the wing body contribution (usually unstable) and the vertical tail contribution (stable) and may be expressed as:

$$C_{n_\beta} = C_{n_{\beta_{WB}}} + C_{n_{\beta_V}}$$

The wing body contribution $(C_{n_{\beta_{WB}}})$ is primarily a function of the body volume coefficient $\frac{S_B \ell_B}{Sb}$ and was estimated using data from the Boeing family of airplanes. The vertical tail contribution $(C_{n_{\beta_V}})$ is estimated by:

$$C_{n_{\beta_V}} = a_V \left(\frac{S_V}{S}\right)\left(\frac{\ell_V}{b}\right)\left(1 - \frac{d\sigma}{d\beta}\right)$$

The sidewash factor is difficult to estimate and wind tunnel tests are required to determine the value. In general, sidewash factors are favorable and tend to increase the level of directional stability above the value predicted if the effect is neglected. For this study, the sidewash factor was neglected, therefore, the static directional stability level should be conservative.

Crosswind Landing Requirement. - At a landing weight 15 percent above OWE, the airplane must have sufficient directional control power to hold a constant ground track in an 18 m/s (35 knot) crosswind. Boeing design criteria permits a maximum crab angle of four degrees at touchdown. If the yawing moment due to lateral control (required to balance the rolling moment) is assumed to be small, the crosswind capability can be approximated by:

$$V_{cw} = V \sin \left[\frac{C_{Lv_{\delta R}} \; \delta_{R_{max}} \left(\frac{Sv}{S}\right)\left(\frac{\ell v}{b}\right)}{\left(C_{n_{\beta WB}} + a_v \; \frac{Sv}{S} \; \frac{\ell v}{b}\right)} + \delta_{crab} \right]$$

Since the wing body directional stability is a relatively small term in this equation, it shows that the crosswind capability is independent of the tail area but varies directly proportional to the rudder maximum authority. For this study, the value of wing body directional stability ($C_{n_{\beta WB}}$) was -.0008, unstable, and the lift curve slope of the vertical tail was .054 per degree.

Baseline Vertical Tail Size. - Figure 17 shows the vertical tail area ratio as a function of the vertical tail moment arm ratio with the aforementioned vertical fin design criteria. As can be seen, the tameness criteria is critical for sizing the vertical tail. To assure good crosswind capability which happens to be coincident with C_{n_β} = .002, the vertical tail area should not exceed the values shown. Sizing the vertical tail on the tameness criteria, results in a level of static weathercock stability (C_{n_β}) of .00186 per degree.

The vertical tail sized by Boeing is considerably smaller than the vertical tail sized in Reference 2. The Reference 2 study used only one-half the available rudder deflection to control an engine-out condition.

Propulsion

The baseline airplane was powered by two Allison engines with a fan pressure ratio of 1.35. These engines, as described in Reference 2, are based on mid-1980 technology levels and result in a baseline airplane which has low fuel consumption.

Engine data were computed for takeoff, climb and cruise using the Boeing-Wichita Master Customer Computer Deck (MCCD) program. This program facilitates a standard input/output format for all such engine company furnished computer programs. The engine computer deck was furnished by the Detroit Diesel Allison Division of General Motors Corporation. The installation losses presented in Reference 2 were used. Where the MCCD program required definition of installation losses not presented in Reference 2, nominal values were used to assure realistic representation of installed engine performance.
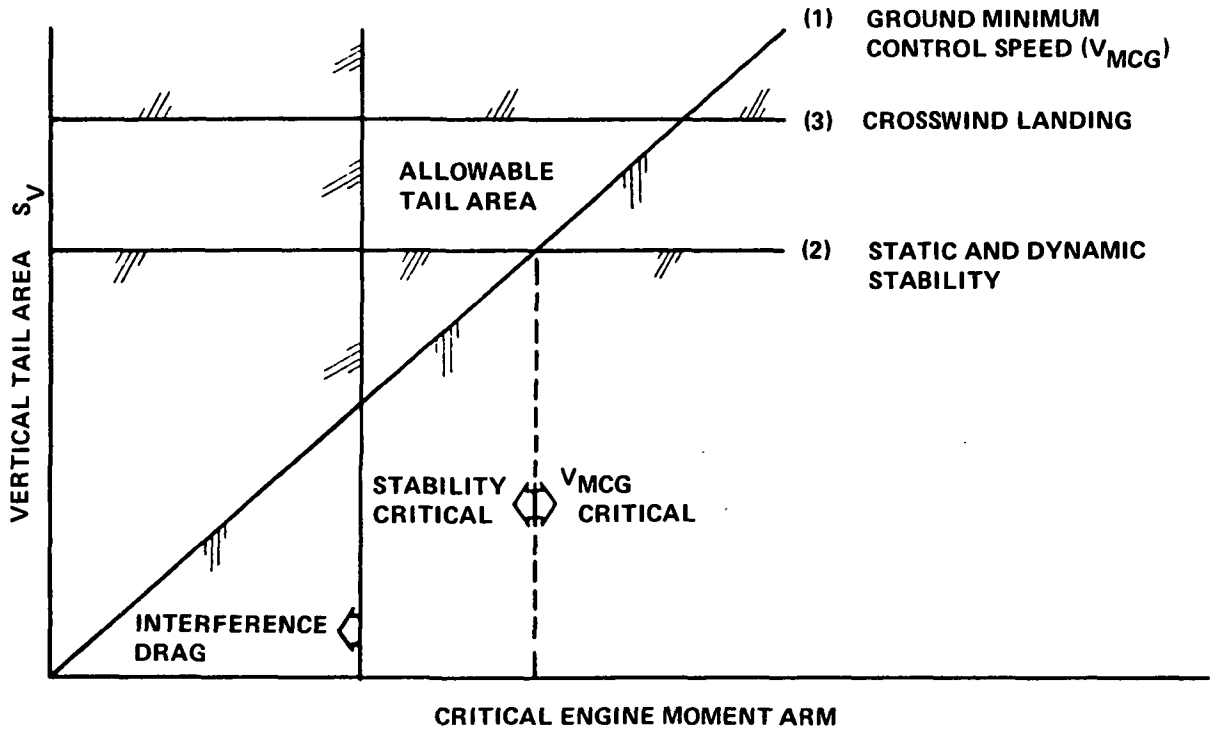
VERTICAL TAIL SIZING SCHEMATIC
FIGURE 16
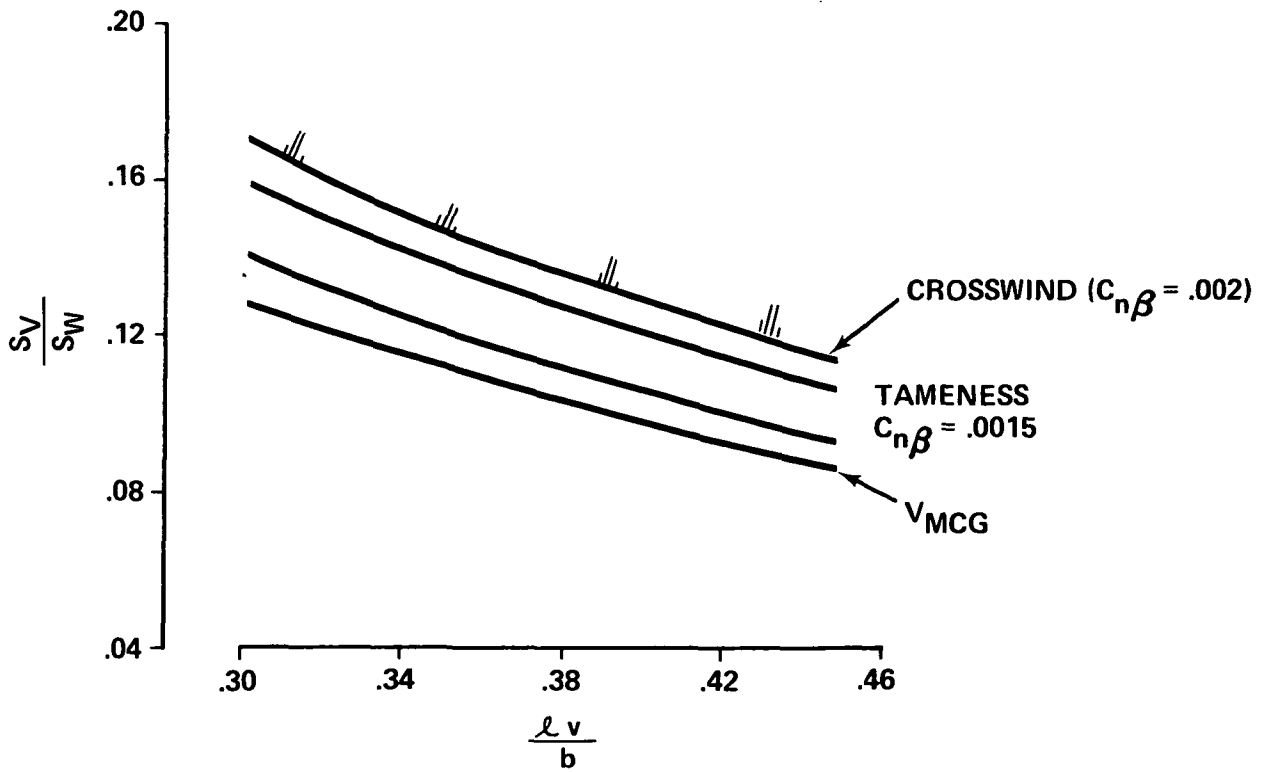
VERTICAL TAIL SIZING BASELINE CONFIGURATION
FIGURE 17

Recognizing that this (MCCD) program is not readily adept to handle engine modification and that a part of this study would investigate the application of a Q-fan in combination with the basic engine core, another more general engine performance program was utilized. This program, Generalized Simulator Analyzer (GSA) uses basic scaled component engine data to compute installed performance.

The engine performance computed by the GSA program was found to be in good agreement with that computed by the MCCD program. Figures 18 through 20 present the comparison of installed Allison MCCD data and the installed engine data from the GSA program. The deviation in SFC for the data at 9144 meter (30,000 foot) altitude (Figure 18) is less that 3-1/2 percent, and at sea level (Figure 19) this deviation is less than 2-1/2 percent. Figure 20 shows a comparison of the takeoff thrust lapse rate with Mach number.

The engine thrust and specific fuel consumption (computed by the GSA program) used to compute the baseline airplane performance is presented in Appendix A. These data are presented as a function of Mach number and altitude for standard atmosphere. The takeoff thrust for $35^{\circ}C$ ($95^{\circ}F$) sea level conditions is also presented.

Baseline Noise

The takeoff and landing noise footprint areas were computed for the baseline airplane based on component noise analysis. Data required to compute noise characteristics were obtained from Reference 2. For those items not defined in Reference 2, the data were developed by Boeing.

Four noise components were considered: inlet fan, aft fan, turbine and jet. The amount of acoustic treatment used is consistent with the state-of-the-art sound suppression technology. PNdB were computed for the various components and are tabulated in Table 2.

The noise footprints were determined for the takeoff and landing profiles shown in Figures 21 and 22, respectively. The 80 and 90 EPNdB footprints are presented in Figure 23. The 90 EPNdB area is 1.04 square kilometers (.4 square mile), well within the 2.59 square kilometers (1 square mile) design guidelines for this study and meets FAR Part 36, Reference 7.

Weights

The Airplane Sizing and Mission Performance (ASAMP) computer program (Reference 4) contains a Class I weight prediction subroutine. Class I weight
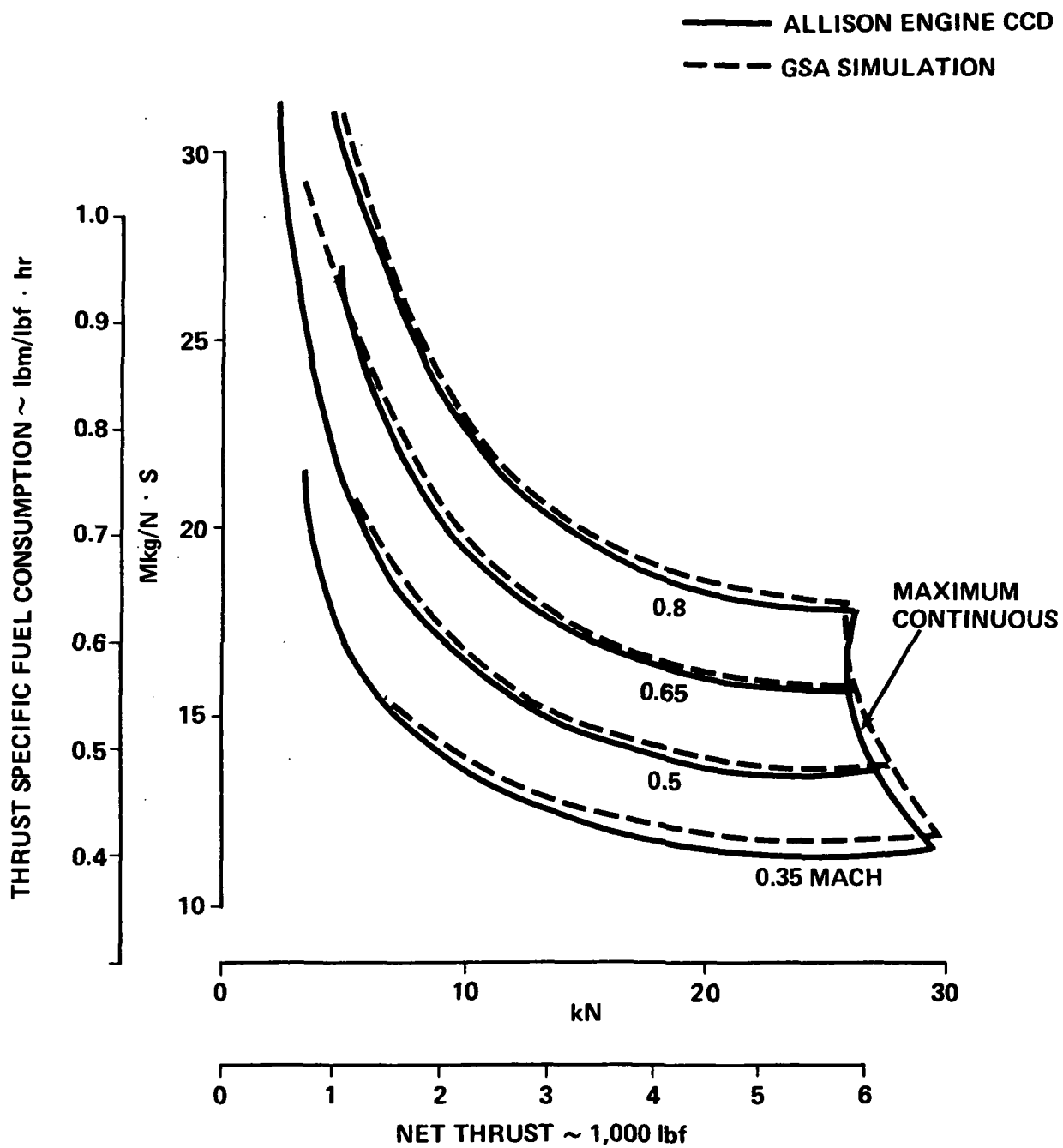
THRUST SPECIFIC FUEL CONSUMPTION BASELINE
CONFIGURATION — 9,144 m (30,000 FT), STANDARD DAY
FIGURE 18
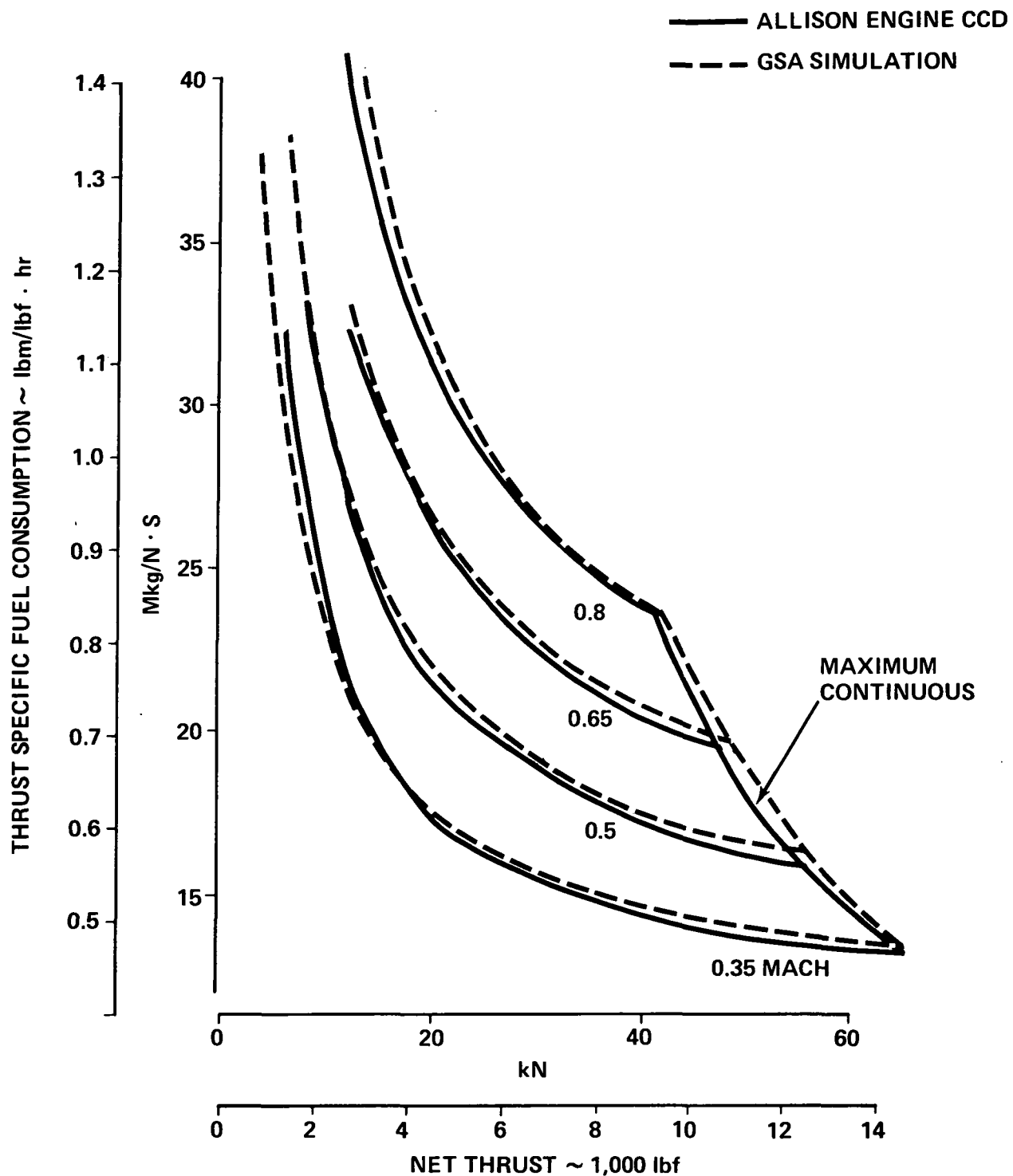
THRUST SPECIFIC FUEL CONSUMPTION BASELINE
CONFIGURATION — SEA LEVEL, STANDARD DAY
FIGURE 19
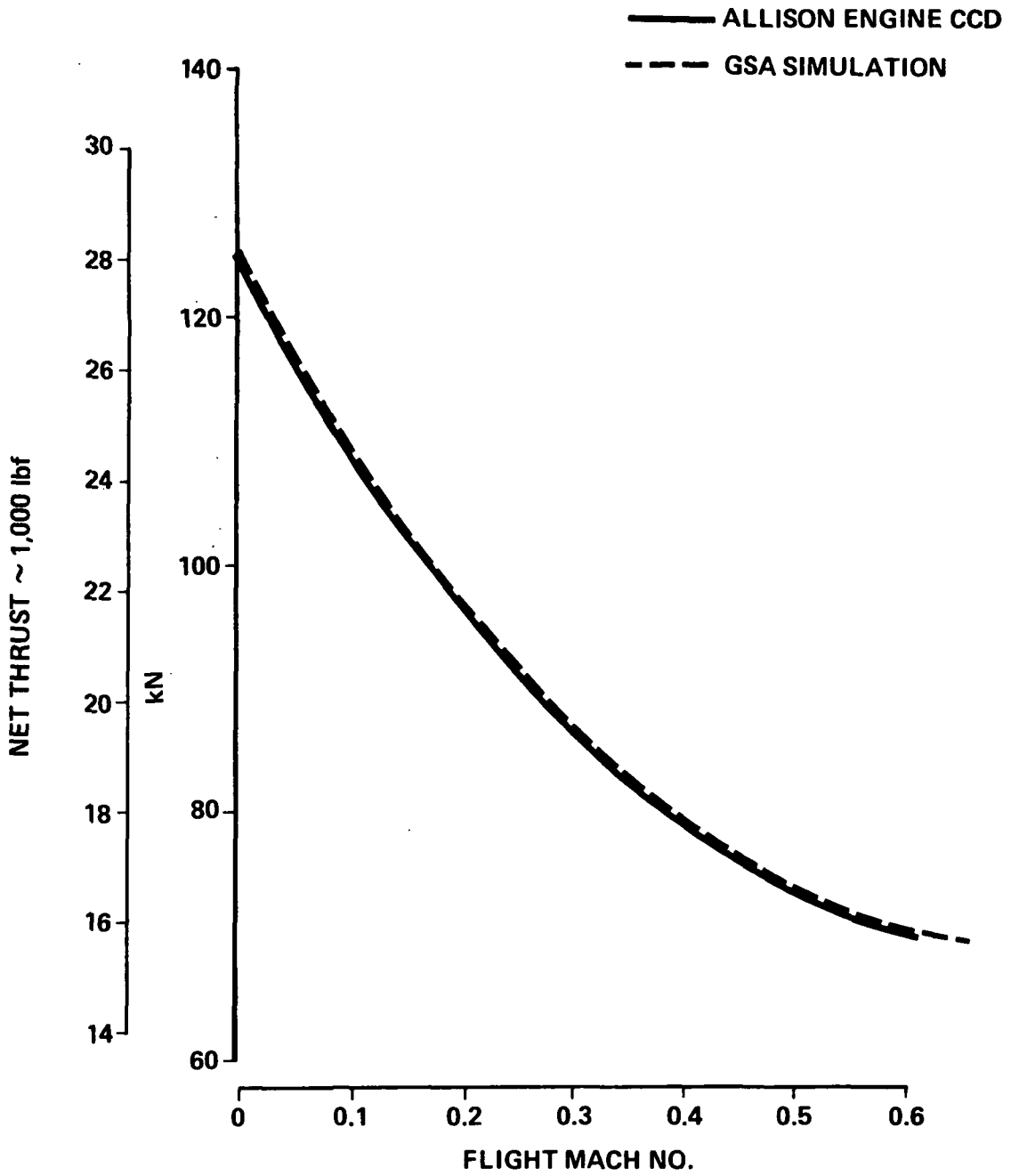
NET THRUST BASELINE CONFIGURATION TAKEOFF SEA LEVEL
FIGURE 20

TABLE 2
COMPONENT NOISE LEVEL COMPARISON

Component	Boeing		Reference 2
	Baseline	Q-Fan	
Fan Unsuppressed (PNdB)	107.4	106.1	105.9
Fan Suppressed (PNdB)	93.0	91.1	94.5
Jet (PNdB)	88.9	61.4	88.5
Aero (PNdB)	83.6	85.0	84.4
Core (PNdB)	91.1	89.0	—
Total (PNdB)	97.5	94.1	98.1
Total (EPNdB)	94.2	92.0	93.9

Conditions

    Takeoff

    Altitude: 89.9 m (290 Ft)

    Sideline: 152.4 m (500 Ft)

    Velocity: 51.5 m/s (169 Ft/Sec), Boeing
                  66.4 m/s (218 Ft/Sec), Reference 2
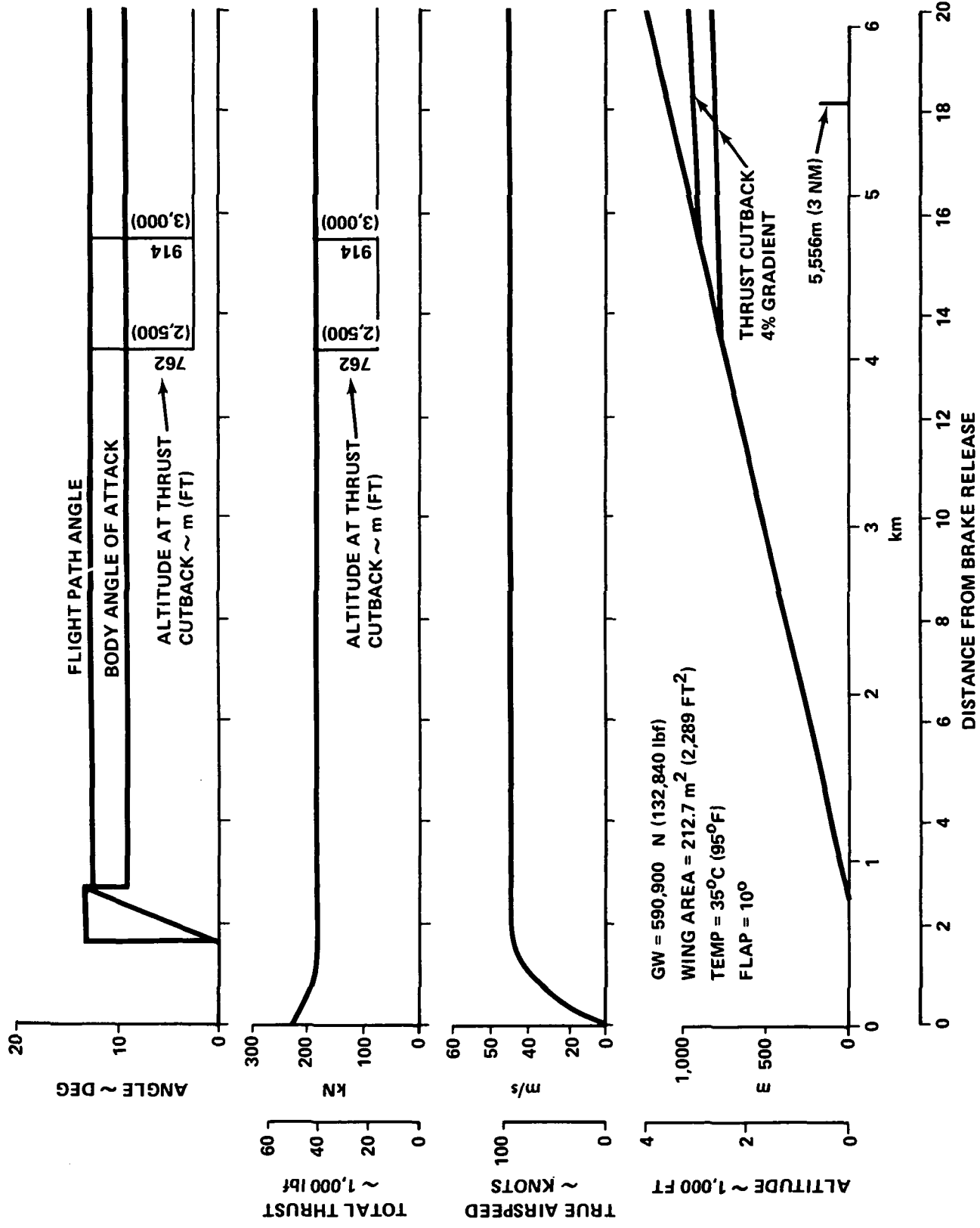
BASELINE CONFIGURATION TAKEOFF PROFILE
FIGURE 21
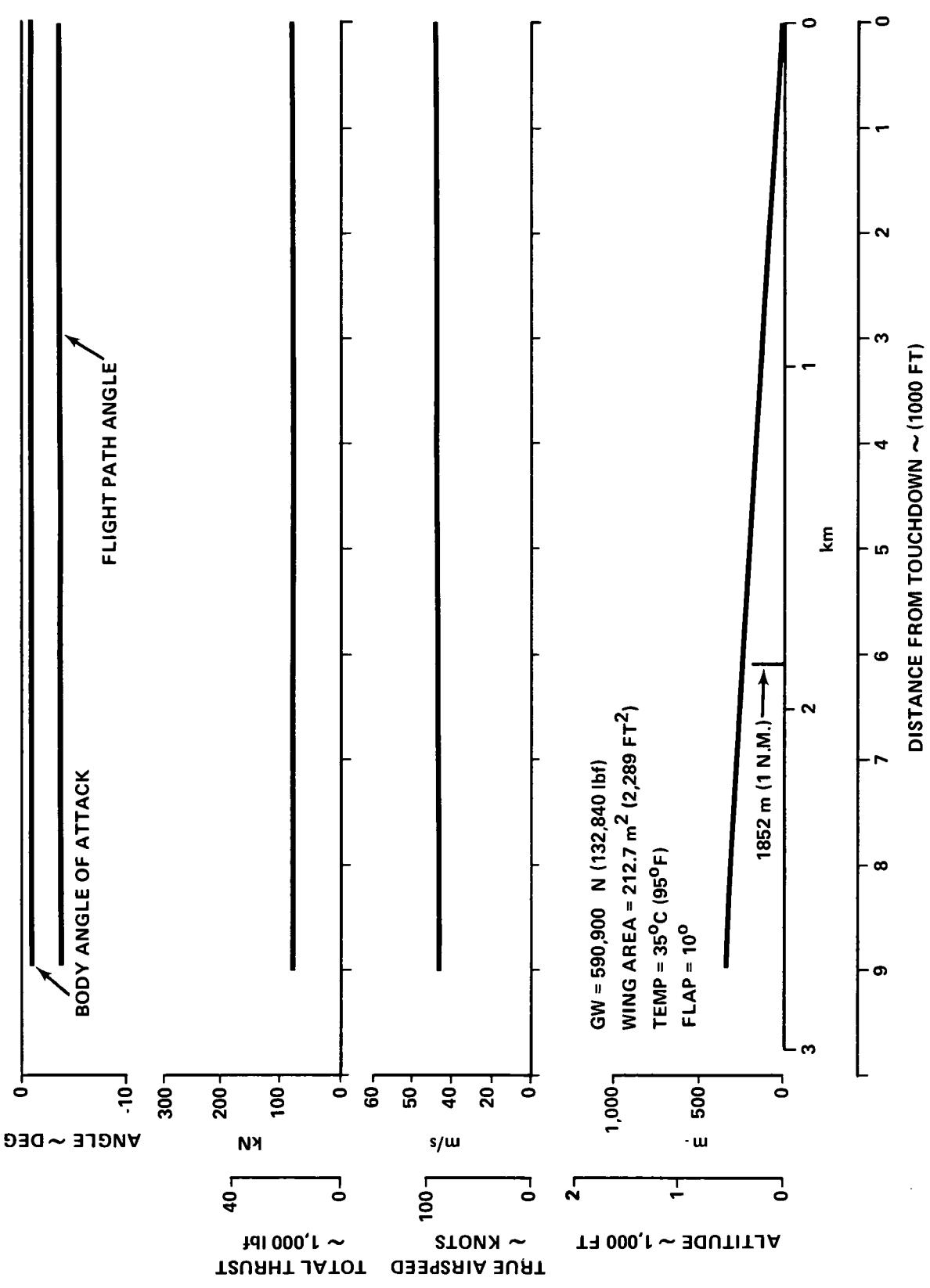
37

BASELINE CONFIGURATION LANDING PROFILE
FIGURE 22

GW = 590,900 N (132,840 lbf)
WING AREA = 212.7 m^2 (2,289 FT^2)
TEMP = 35°C (95°F)
FLAP = 10°

1852 m (1 N.M.)

DISTANCE FROM TOUCHDOWN ~ (1000 FT)

FLIGHT PATH ANGLE
BODY ANGLE OF ATTACK

ANGLE ~ DEG
kN
m/s
ALTITUDE ~ 1,000 FT

TOTAL THRUST ~ 1,000 lbf
TRUE AIRSPEED ~ KNOTS

38
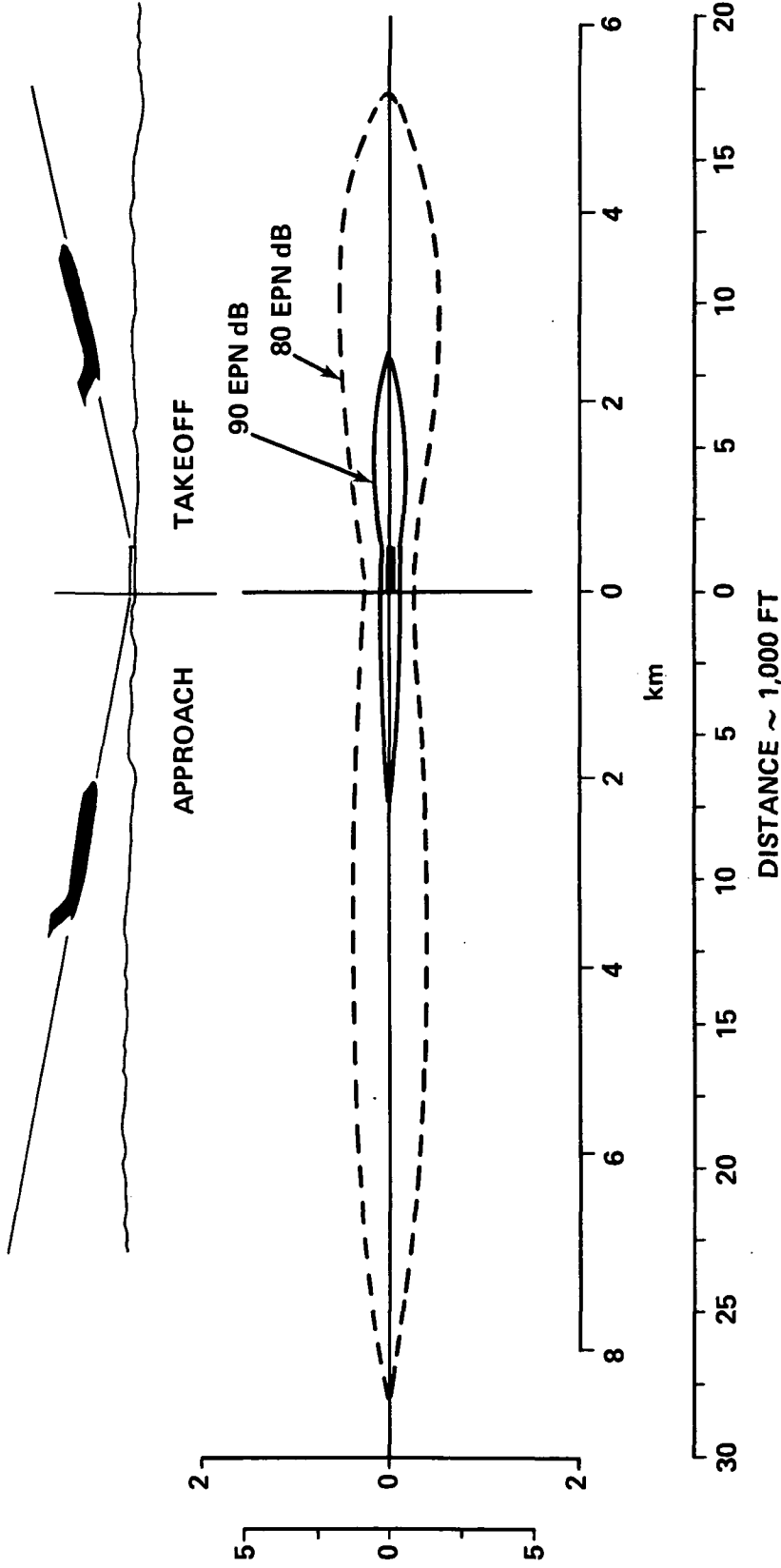
BASELINE CONFIGURATION NOISE FOOTPRINT
FIGURE 23

predictions are developed parametrically based on preliminary configuration data. Class I weight prediction methods are expected to yield relative weight accuracies between 5 and 10 percent when comparing several aircraft design to do similar transport tasks.

Weights Methodology. - The weight prediction method is based on breaking the airplane down into the basic items that can be described in terms of the parameters that dictate its weight. The items are defined to a level of detail commensurate with preliminary design. For example, the basic wing structure is defined as a function of design gross weight, wing thickness ratio, aspect ratio, taper ratio, sweepback, deadweight relief, material, landing gear support, fatigue life, load factor, high lift devices and control surfaces.

The Structures group contains the following items:

- Wing
- Horizontal tail
- Vertical tail
- Fuselage
- Landing gear
- Engine struts
- Engine nacelles
- Engine duct
- Engine mount

Figure 24 is a correlation of actual versus ASAMP predicted wing weight for a wide range of airplanes using the method of Reference 5. A correlation of the total actual Structures group weights compared to the ASAMP predicted summation is shown on Figure 25. The ±10 percent accuracy lines are included.

The Propulsion group contains the following items:

- Primary engines
- Engine accessories
- Engine controls
- Engine starting system
- Thrust reversers
- Fuel system

The total Propulsion group weight correlation by ASAMP is shown on Figure 26.
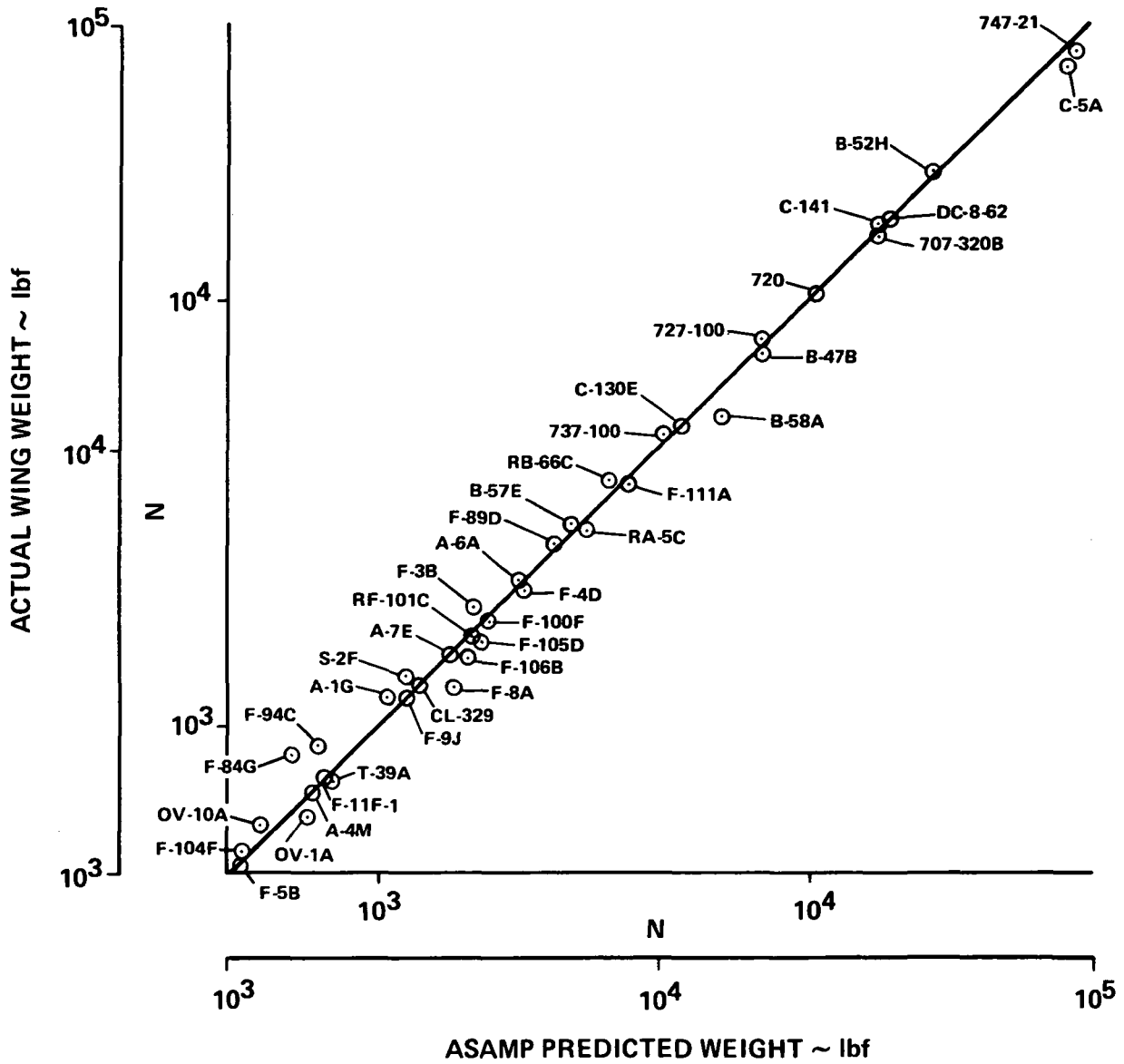
WING WEIGHT CORRELATION
FIGURE 24
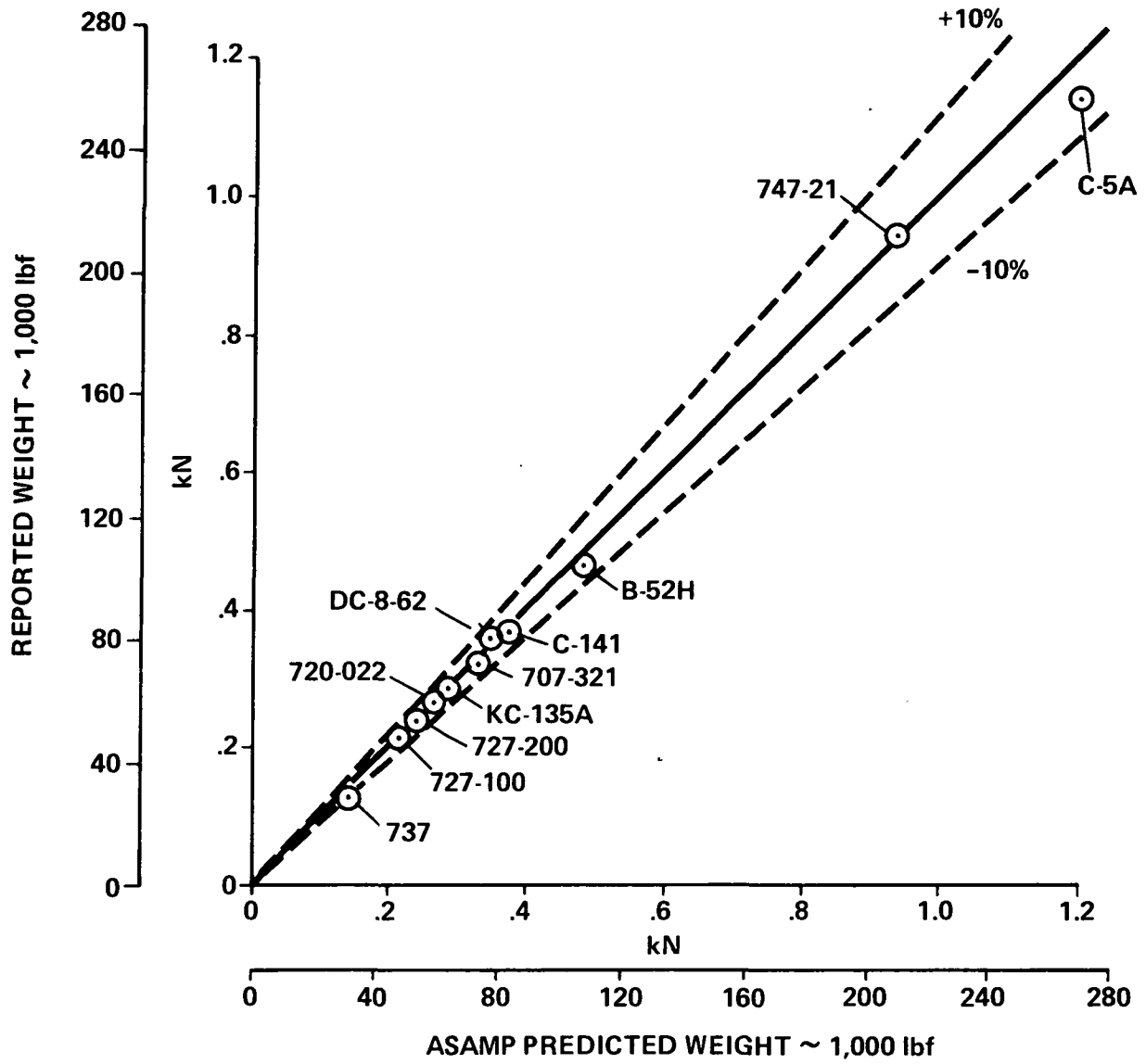
STRUCTURES GROUP PREDICTION ACCURACY
FIGURE 25
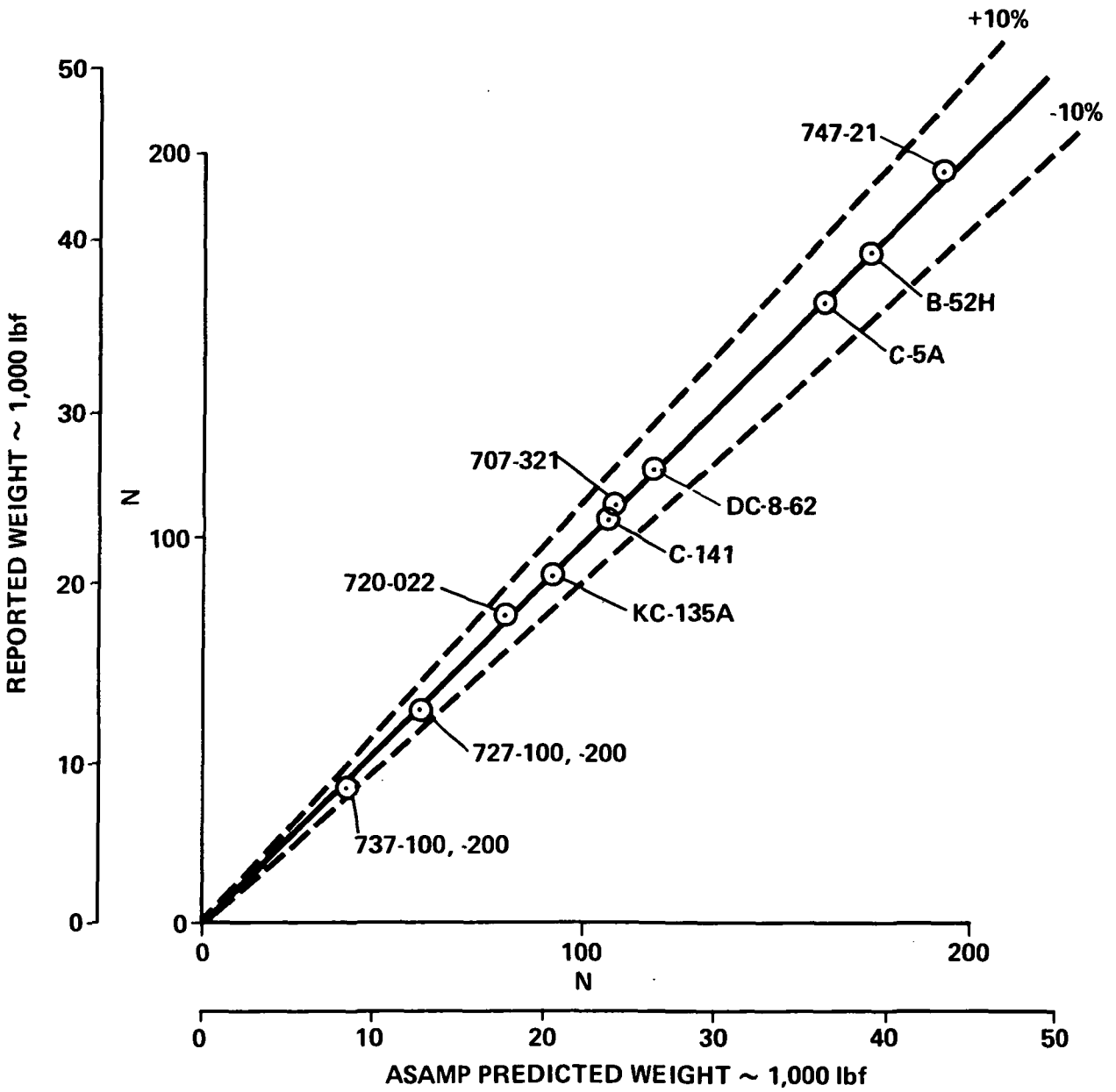
PROPULSION GROUP PREDICTION ACCURACY
FIGURE 26

The Fixed Equipment group contains the following items:

- Instruments
- Surface controls
- Hydraulics
- Pneumatics
- Electrical
- Electronics
- Flight deck accommodations
- Passenger accommodations
- Cargo accommodations
- Emergency equipment
- Air conditioning
- Anti-icing
- APU

The ASAMP predicted correlation with actual total fixed equipment is shown on Figure 27.

Standard and operational items
Standard items

Standard items are equipment and fluids not an integral part of a particular aircraft and not a variation for the same type of aircraft. These items may include, but are not limited to the following:

- Unusable fuel and other unusable fluids
- Engine oil
- Toilet fluid and chemical
- Fire extinguishers, pyrotechnics, emergency oxygen equipment
- Structure in galley, buffet and bar
- Supplementary electronic equipment

Operational items are personnel, equipment and supplies necessary for a particular operation but not included in basic empty weight. These items may vary for a particular aircraft and may include, but are not limited to the following:

- Crew and baggage
- Manuals and navigational equipment
- Removable service equipment for cabin, galley and bar
- Food and beverages
- Usable fluids other than those in useful load
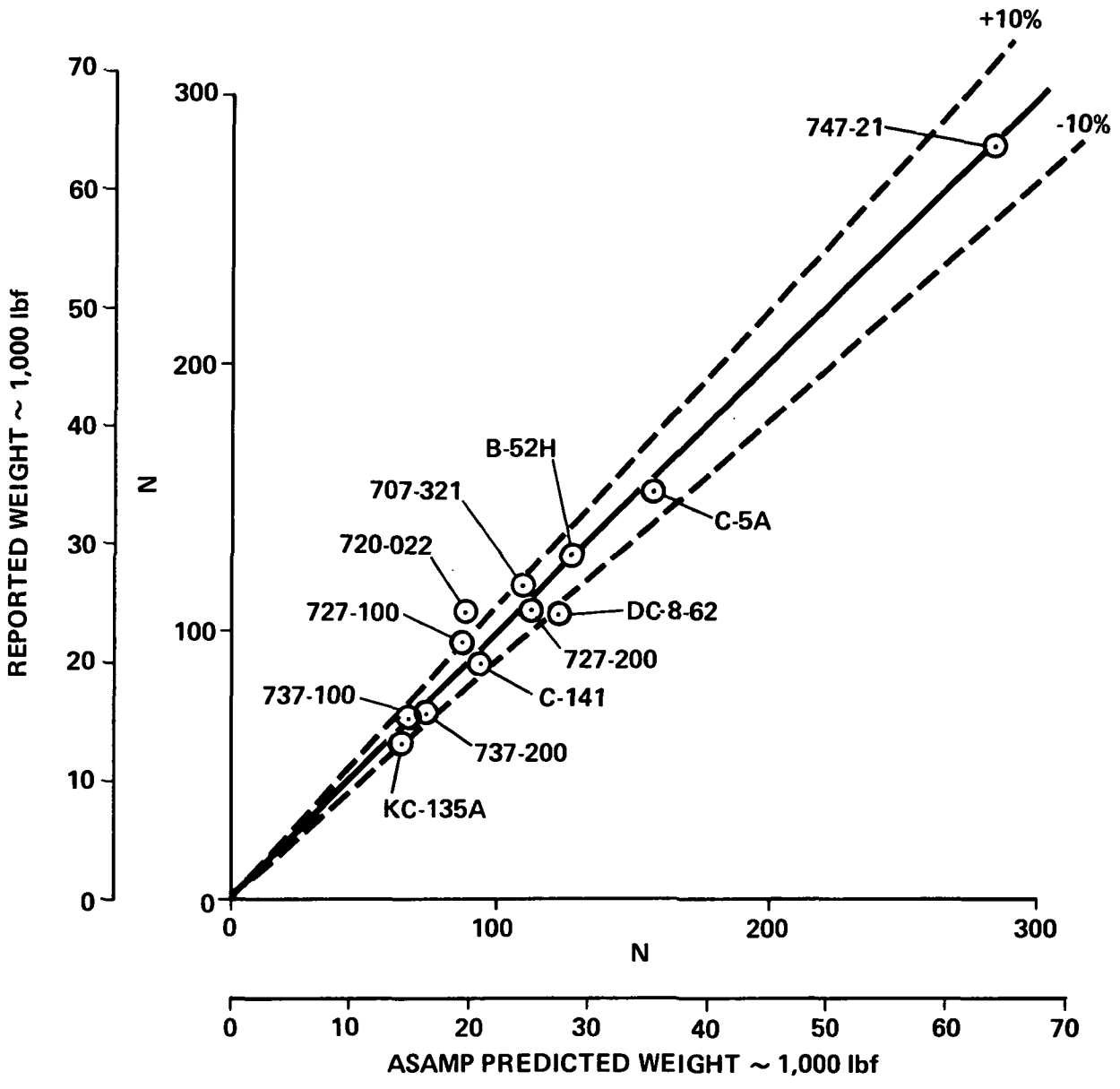
FIXED EQUIPMENT GROUP PREDICTION ACCURACY
FIGURE 27

- Life rafts, life vests and emergency transmitters
- Aircraft cargo handling system and cargo container

The correlation is shown on Figure 28.

Baseline Airplane. - The weights computed for the baseline airplane are presented in Table 3. The longitudinal center of gravity was determined for the baseline configuration based on the Class I group weight statement. A longitudinal arm was estimated for each individual item of the group weight statement building up to the operational empty weight and gross weight of the aircraft. The longitudinal arms were predicted from current Class I center of gravity prediction procedures along with ASAMP generated geometric data and the three-view of the baseline mechanical flap configuration shown in Figure 1. The following assumptions were also used to compute the center of gravity.

- 148 all-economy class passengers
- 3 lavatories (1 forward and 2 aft)
- 2 galleys (1 forward and 1 aft)
- Forward and aft below floor baggage areas of equal volume
- 3 flight and 4 cabin crew members
- Passenger weights = 734 N (165 lbf)
- Baggage allowance = 178 N (40 lbf)/passenger, 133 N (30 lbf) luggage, 44.5 N (10 lbf) carry on
- Auxiliary power unit is located aft of the aft pressure bulkhead
- Air conditioning pack bay is located just forward of the wing front spar
- Main electrical distribution center is located in aft flight crew compartment
- Main electronics bay is located under flight compartment
- No fuel in center wing area
- Tip of nose is designated as Body Station "0"

The computed balance data are also presented in Table 3. The data presented were used as a baseline weight and balance model for wing placement. It was necessary to move the wing .762 meter (30 inches) forward relative to the body to balance the airplane at a center of gravity of 35 percent MAC. This location is midway between the aerodynamic forward and aft center of gravity limit.
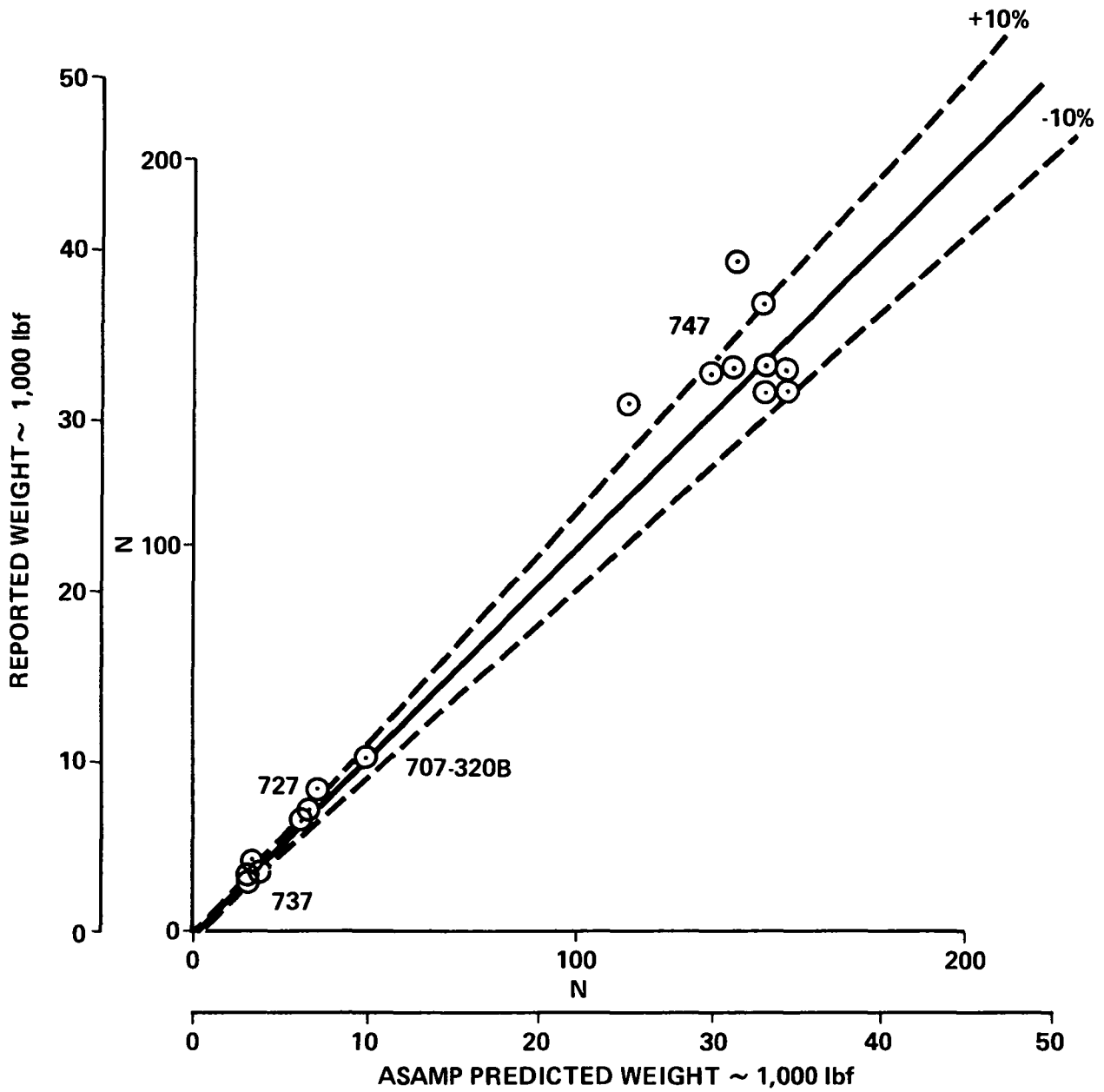
STANDARD AND OPERATIONAL ITEMS PREDICTION ACCURACY
FIGURE 28

TABLE 3
BASELINE CONFIGURATION WEIGHT AND BALANCE SUMMARY

Weight Group	N	Weight (lbf)	Horizontal Arm (Body Station)
Wing	98,525	(22,150)	742
Horizontal Tail	9,105	(2,047)	1,687
Vertical Tail	12,028	(2,704)	1,512
Fuselage	65,509	(14,727)	744
Landing Gear	23,633	(5,313)	688
Engine Struts	8,278	(1,861)	636
Engine Nacelles	10,858	(2,441)	590
Total Structure Group Weight	Σ 227,939	Σ (51,243)	804
Primary Engines	33,748	(7,589)	580
Engine Accessories	1,503	(338)	451
Engine Controls	667	(150)	451
Engine Starting System	347	(78)	580
Thrust Reversers	10,106	(2,272)	599
Fuel System	1,753	(394)	657
Total Propulsion Group Weight	Σ 48,124	Σ (10,819)	581
Instruments	2,834	(637)	330
Surface Controls	9,119	(2,050)	972
Hydraulics	3,158	(710)	747
Pneumatics	2,197	(494)	706
Electrical	6,939	(1,560)	414
Electronics	4,635	(1,042)	284
Flight Deck Accommodations	3,465	(779)	108
Passenger Accommodations	48,597	(10,925)	758
Cargo Accommodations	5,480	(1,232)	740
Emergency Equipment	1,886	(424)	582
Air Conditioning	8,069	(1,814)	622
Anti-Icing	1,566	(352)	462
APU	4,395	(988)	1,359
Total Fixed Equipment Group Weight	Σ 102,340	Σ (23,007)	703
Manufacturers Empty Weight	Σ 378,404	Σ (85,069)	749
Standard and Operational Items	22,321	(5,018)	669
Operational Empty Weight	Σ 400,725	Σ (90,087)	744 26% MAC
Payload	134,958	(30,340)	750
Fuel	55,202	(12,410)	737
Gross Weight	Σ 590,885	Σ(132,837)	745 26.5% MAC

Correlation

Reference Baseline Correlation. - The initial baseline airplane sized
by the ASAMP computer program to do the design mission showed a large differ-
ence in mission fuel required relative to the Reference 2 study. This analysis
was based on the airplane geometry as shown in Table 4. The weight comparison
between the two studies was in good agreement as shown in Table 5. For the
same thrust-to-weight (T/W) and wing loading (W/S) ratios, the Reference 2
and the Boeing baseline airplane OWE's are in close agreement (a difference of
1.16 kN (260 lbf). The fuel requirements (mission and reserves) did not agree.
The fuel quantity required to fly the mission computed by Boeing is 19 percent
less than the mission fuel shown in the Reference 2 study. The reserve fuel
requirement computed in this study is 17 percent greater than the Reference 2
results. The total fuel (mission plus reserves) is approximately 10 percent
less than shown in the Reference 2 study. These fuel quantity differences led
to the initiation of a study into the differences between this study and the
Reference 2 mathematical models.

A comparison was made of the Boeing and Reference 2 drag data at the
start of the cruise. The comparison is shown in Table 6. The total airplane
cruise drag prediction for this study agrees within six drag counts of the
Reference 2 drag prediction. The low nacelle and pylon drag predicted in the
Reference 2 study was first thought to be unrealistic. A more thorough inves-
tigation showed the drag value to be only the drag of the pylons and nacelle
interference drag. The complete nacelle installation (excluding pylons) was
treated as a thrust loss, while Boeing has chosen to include only the nacelle
area scrubbed by the engine bypass as a thurst loss. Thus, the drag difference
is principally due to the drag "bookkeeping" methods. The Reference 2 trim
drag is considered to be excessively conservative. An airplane that is prop-
erly balanced and optimized for cruise usually has no more than one or two
drag counts due to trim requirements.

Since a good correlation was obtained between the weight and drag data
for the two studies, the propulsion model became suspect. The Reference 2
study treated nacelle drag as an engine penalty. Since the nacelle drag was
not reported in this reference, the Boeing nacelle drag was subtracted from
the Reference 2 propulsion model for cruise at 9144 meters (30,000 feet). Fig-
ure 29 shows maximum cruise thrust as a function of Mach number for the 9144
meter (30,000 foot) condition. The data points represent discrete points from
the Reference 2 and this study propulsion models. Removal of the predicted
nacelle drag from the Reference 2 propulsion model gave good thrust correlation
at and above the cruise Mach number of .7. At Mach numbers less than .7, a
slightly different characteristic is obtained between the two models. The afore-
mentioned cruise thrust data are shown for the primary fan efficiencies as

TABLE 4
BASELINE AIRPLANE GEOMETRY COMPARISON

	Reference 2 Configuration	Boeing Configuration*
Wing		
Aspect Ratio	10	10
Taper Ratio	.3	.3
Quarter Chord Sweep ~ Deg.	10	10
Area ~ m^2 (Ft^2)	215.4 (2,318.6)	212.7 (2,289.5)
Fuselage		
Overall Length ~ m (Ft)	41.53 (136.25)	41.53 (136.25)
Maximum Width ~ m (Ft)	3.66 (12)	3.66 (12)
Maximum Depth ~ m (Ft)	3.96 (13)	3.96 (13)
Number of Passengers	148	148
Vertical Tail		
Aspect Ratio	—	1.2
Taper Ratio	—	.7
Quarter Chord Sweep ~ Deg.	—	35
Area ~ m^2 (Ft^2)	50.23 (540.7)	50.23 (540.7)
Horizontal Tail		
Aspect Ratio	—	4.5
Taper Ratio	—	.3
Quarter Chord Sweep ~ Deg.	—	30
Area ~ m^2 (Ft^2)	38.03 (409.4)	38.03 (409.4)

*Based on the vertical and horizontal tail areas used by Reference Study

TABLE 5
BASELINE AIRPLANE WEIGHT COMPARISON

	Reference 2 Configuration	Boeing Configuration
T/W	.39	.39
W/S ~ kPa (PSF)	2.8 (58)	2.8 (58)
OWE ~ N (lbf)	401,895 (90,350)	400,725 (90,090)
Payload ~ N (lbf)	134,958 (30,340)	134,958 (30,340)
Mission Fuel ~ N (lbf)	47,151 (10,600)	38,299 (8,610)
Reserve Fuel ~ N (lbf)	14,368 (3,230)	16,859 (3,790)
Total Fuel ~ N (lbf)	61,519 (13,830)	55,202 (12,400)
Gross Weight ~ N (lbf)	598,372 (134,520)	590,885 (132,830)

TABLE 6
DRAG CORRELATION ΔC_D (COUNTS) AT START CRUISE

Item	Reference 2 10,100 m (33,000 Ft) MF	Boeing 10,100 m (33,000 Ft) MF
Fuselage and Landing Gear Pod	48	44
Wing — Parasite	62	66
Wing — Induced	31	29
Horizontal Tail	11	12
Vertical Tail	13	14
Pylons and Nacelle Interference	3	2
Nacelle	*	8
Miscellaneous, Roughness and Interference	14	15
Trim	5	2
Compressibility	2	0
Total Drag**	189	184
Start Cruise L/D	15.2	15.5

*Included in Propulsion Data

**Does Not Include Nacelle Drag

1 count = .0001 ΔC_D
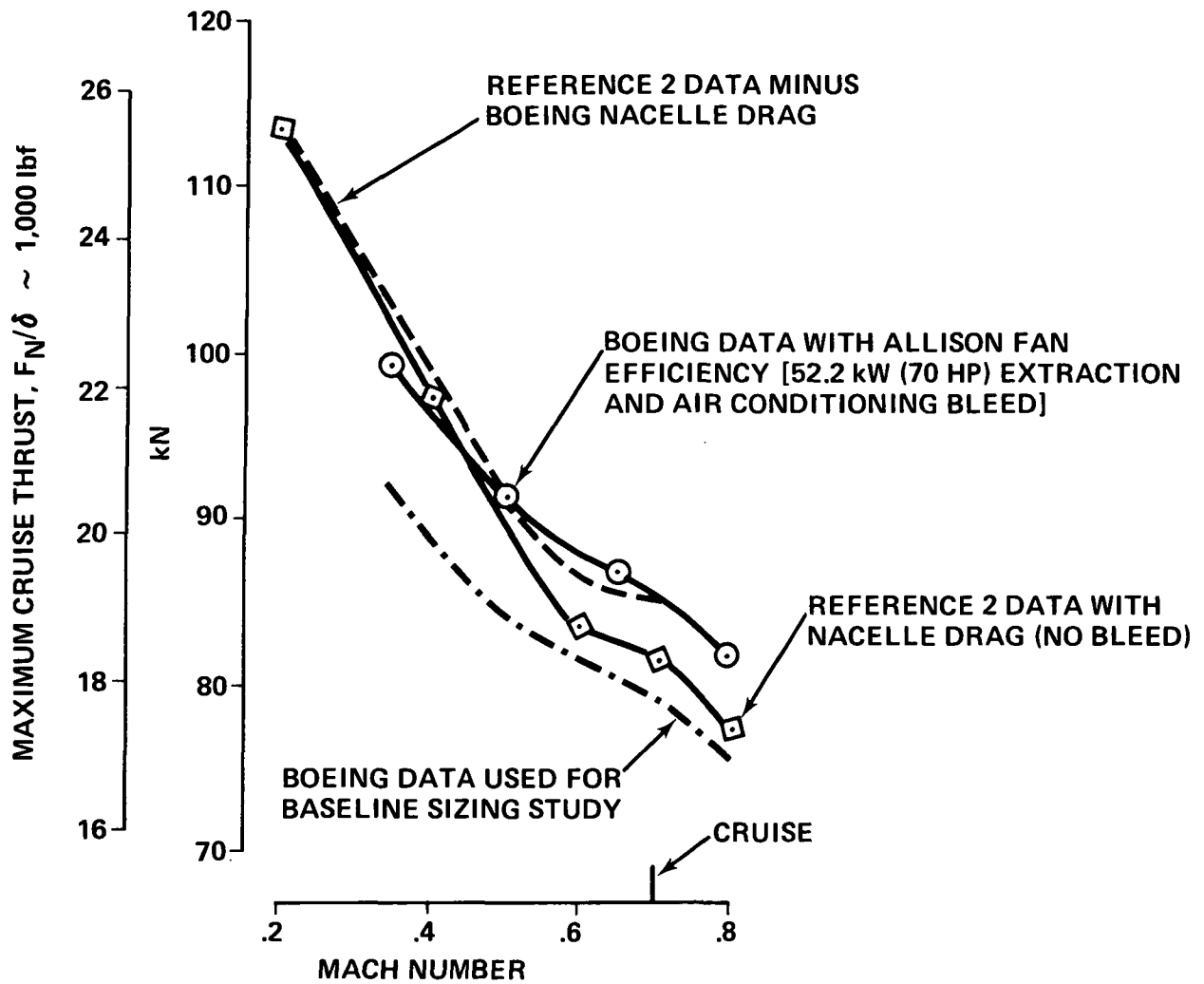
MAXIMUM CRUISE THRUST COMPARISON — 9,144 m (30,000 FT)
FIGURE 29

defined by the Detroit Diesel Allison Division. In evaluating the engine components in anticipation of simulating the engine with the generalized Boeing program, it was determined that the fan efficiency was excessively high for that type of engine. Fan efficiency characteristics which seem more realistic were incorporated to modify the Allison Division data. The maximum cruise thrust was approximately 7 percent less than the Reference 2 propulsion model.

Figure 30 shows specific fuel consumption as a function of Mach number for maximum cruise thrust at 9144 meters (30,000 feet). Removal of the predicted nacelle drag from the Reference 2 propulsion model gave a good specific fuel consumption correlation for the Mach number range shown. Incorporating the revised fan efficiency characteristics gave a specific fuel consumption approximately 8 percent higher than the Reference 2 propulsion model.

Figure 31 compares this study and Reference 2 partial thrust propulsion data for the .7 cruise Mach number at 9144 meters (30,000 feet). With the fan efficiencies as specified by Allison, a good specific fuel consumption comparison is obtained between this study and the Reference 2 propulsion models for maximum cruise thrust. Partial thrust operation shows the Reference 2 specific fuel consumption to be higher than this study specific fuel consumption (with Allison fan efficiencies). Since the weight and drag data correlate quite well, a typical cruise thrust level (F_n/δ) of 74,730 N (16,800 lbs.) could be expected for both the Reference 2 and this study configurations. At a typical cruise thrust level, the specific fuel consumption for this study propulsion model (with the reduced fan efficiency) is higher than the Reference 2 data.

It is not understood why the Reference 2 mission fuel as shown in Table 5 is greater than the results of this study. The Boeing mathematical models have been reviewed and the fuel consumption was independently checked for the cruise condition. Based on the results of the propulsion model comparison at the 9144 meter (30,000 foot) altitude, the Reference 2 study might be expected to use slightly less fuel than this study. No further investigation was conducted on the difference of mission fuel required for the baseline configuration.

The Reference 2 geometry, weight, airframe and engine costs for the baseline configuration shown in Figure 1 were input to the Boeing Direct Operating Cost (DOC) computer program. The program uses the 1967 standard Air Transport Association mathematical model. The program was modified to incorporate the changes used in the Reference 2 study, shown in Table 7. A comparison of the DOC data shown in Table 8 agrees for the baseline configuration with the Reference 2 weight and fuel consumption. The differences in the block fuel requirements as derived by Boeing will result in a decrease in DOC for this configuration.
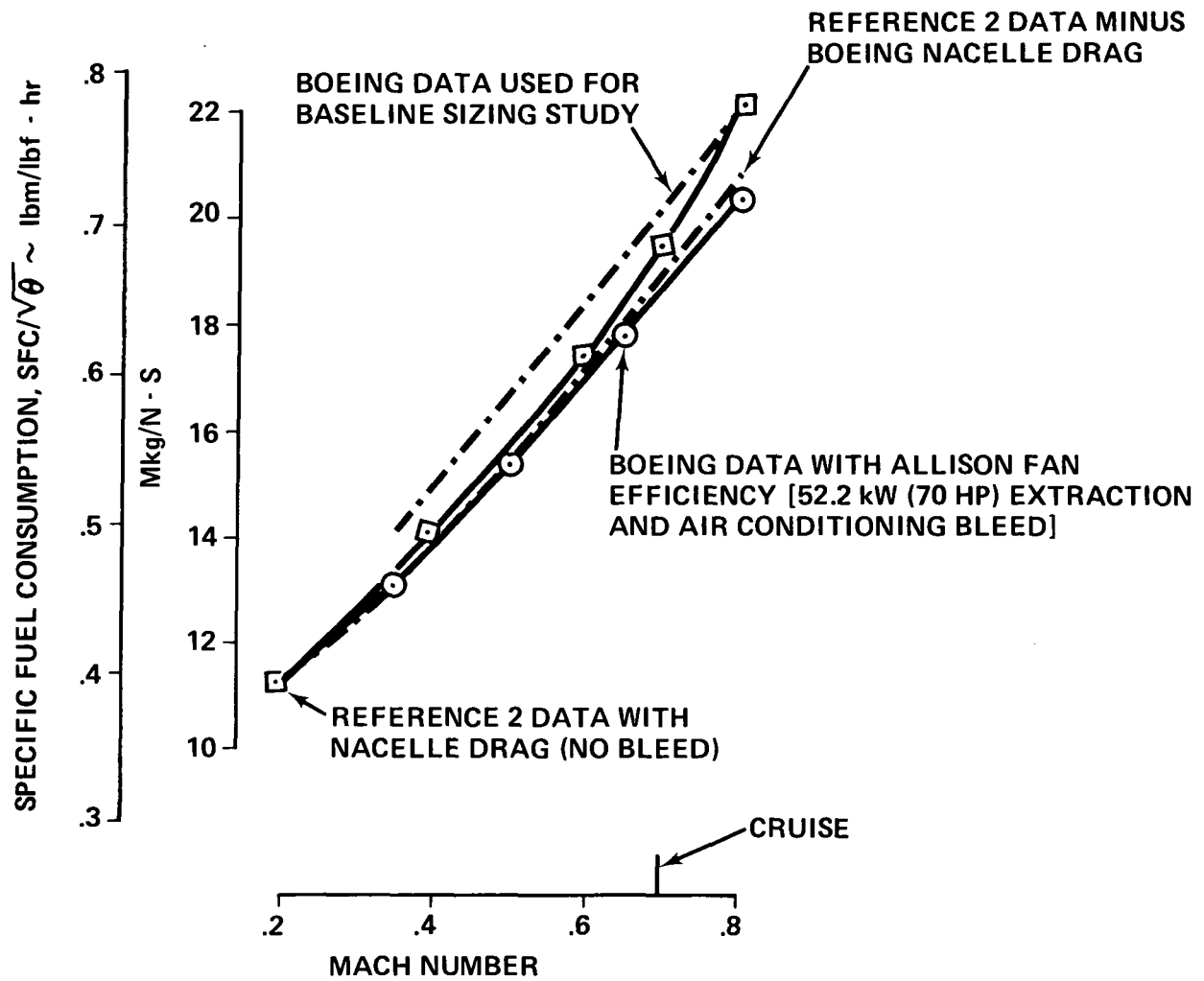
SPECIFIC FUEL CONSUMPTION COMPARISON AT
MAXIMUM CRUISE THRUST — 9,144 m (30,000 FT)
FIGURE 30
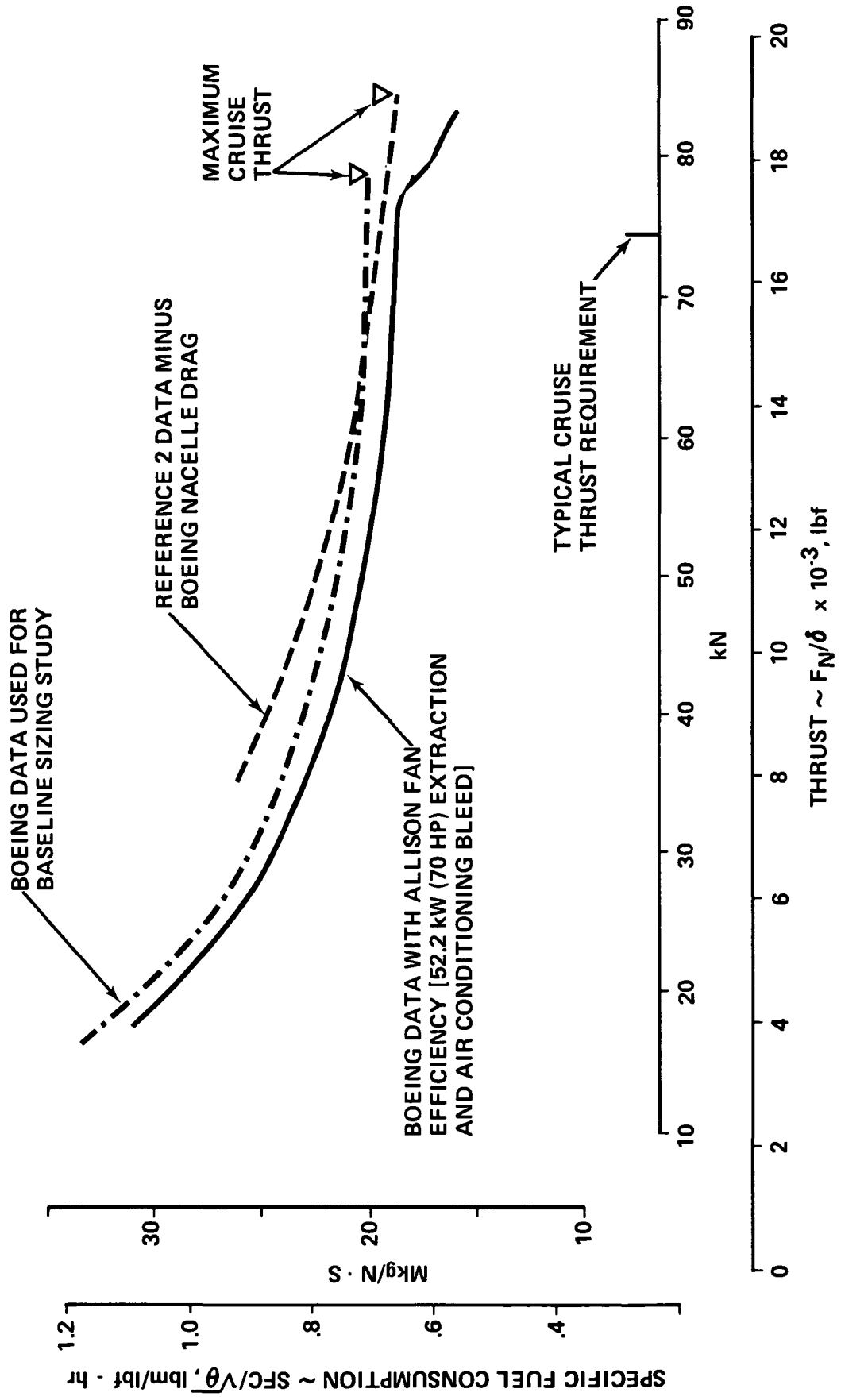
BASELINE CONFIGURATION PARTIAL THRUST CHARACTERISTICS —
9,144 m (30,000 FT) MACH NO. .70
FIGURE 31

TABLE 7
CHANGES TO ATA DOC MATHEMATICAL MODEL

Block Time — Flight Time:	10 Min (ATA is 20 Min)
Reserve Fuel:	370 km (200 NM) at Cruise Altitude to Alternate field; 15 Min hold at 3,048 m (10,000 Ft) at Maximum Endurance
Block Fuel:	Per Mission Profile but using 6 Min Ground Time + 4 Min. Air Maneuver Time
Crew Costs:	Increase ATA to Current Crew Cost (40% Higher than ATA); 3-Man Crew
Fuel Cost:	$30.40/m^3 ($.115/Gal) [ATA is $25.10/m^3 ($.095/Gal)]
Hull Insurance:	Retain ATA 2% Rate
Utilization:	Will be an Output of Systems Studies but for Parametric Purposes will use 2,500 Hr/Yr
Labor Rate:	$6/Hr (ATA is $4/Hr)
Maintenance Flight Hour Costs:	Engine Labor — 75% of ATA Value Airplane Labor — 67.5% of ATA Value
Maintenance Flight Cycle Costs:	75% of ATA Value
Maintenance Burden:	Retain ATA Factor of 1.8
Depreciation:	Use ATA 12 Years, 0 Residual but 25% Engine Spares in Lieu of 40%

TABLE 8
CORRELATION OF DOC ANALYSIS

Trip Conditions	
Trip Distance = 927 km (576 Stat. Miles)	Block Time = 1.580 Hrs.
Block Fuel = 47,138 N (10,597 lbf)	Altitude = 10,100 m (33,000 Ft)
Winds = 0	Temperature = SA + 0°C
Load Factors Passengers = 100.0%	
Cargo = 100.0%	

Cost Item	Boeing Analysis Block Hour Cost	Air km (Mile) Cost		Ref 2 Data Air km (Mile) Cost	
Flight Operations					
Crew	$ 202.220	$0.3450	($0.5552)	$0.3450	($ .5552)
Fuel	117.421	0.2003	(0.3224)	0.1998	(.3215)
Oil	0.255	0.0004	(0.0007) }	0.0988	(.159)
Insurance	56.823	0.0969	(0.1560) }		
Total	$ 376.718	$0.6427	($1.0343)	$0.6436	($1.0357)
Maintenance (ATA Factored)					
Airplane					
Labor	$ 35.503	$0.0606	($0.0975)	$0.0603	($ .097)
Materials	27.024	0.0461	(0.0742)	0.0459	(.0738)
Engines					
Labor	17.240	0.0294	(0.0473)	0.0291	(.0469)
Materials	49.535	0.0845	(0.1360)	0.0831	(.1338)
Maintenance Burden	94.937	0.1619	(0.2606)	0.1609	(.2589)
Total	$ 224.239	$0.3825	($0.6156)	$0.3793	($ .6104)
Depreciation	$ 269.591	$0.4599	($0.7401)	$0.4695	($ .7555)
Total D.O.C.	$ 870.548	$1.8485	($2.3900)	$1.4922	($2.4014)
Seat Mile Cost		0.0100	(0.0161)	0.0101	(.01623)
Pass. Mile Cost		0.0100	(0.0161)	0.0101	(.01623)
Ton Mile Cost		0.0000	(0.0000)		
Trip Cost	$1,375.4650				

Verification of Field Length. - Using the low-speed aerodynamic data
determined for this study, FAR takeoff field length and second-segment climb
gradient capability were computed as a function of flap setting for the take-
off gross weight, Figure 32. A flap setting of 6.5 degrees will meet the
914 meter (3,000 foot) field length requirement for a sea level takeoff on
a 35°C (95°F) day. The engine-out second segment climb gradient exceeds the
FAR minimum requirement. The field length was computed using a preliminary
design prediction technique specifically developed for 2-engine aircraft.
The aircraft was assumed to lift off at 1.2 times the stall speed.

Figure 33 shows FAR landing distance as a function of landing speed and
flap setting for a landing at the takeoff gross weight. The Reference 2 study
used a 4.572 meters per second (900 feet per minute) descent rate and touched
down at 3.05 meters per second (10 feet per second). With a 40 degree flap
setting, the FAR landing distance is 732 meters (2,400 feet). If a more con-
ventional glideslope is used (3.5 degrees) with a 3.05 meters per second
(20 feet per second) touchdown (excessively high), the FAR landing distance
is 844 meters (2,770 feet). A 3.5 degree glideslope with a conventional
touchdown rate of sink .914 meter per second (3 feet per second) will allow an
FAR landing distance of 853 meters per second (2,800 feet) at takeoff design
gross weight.

In general, the takeoff and landing performance computed by Boeing shows
the airplane can operate in and out of airfields with runways less than 914
meters (3,000 feet) long. The discrepancy between the Boeing and the Reference
2 takeoff and landing analysis is believed to be primarily in the maximum lift
coefficient. The Reference 2 study used maximum lift data based on a 30 degree
wing sweep. No credit was given to the maximum lift coefficient when the wing
sweep was changed to 10 degrees. In order to avoid reoptimizing the baseline
airplane, the design field length for the baseline study will be 853 meters
(2,800 feet) instead of 914 meters (3,000 feet). At the design gross weight,
a takeoff flap setting of 10 degrees and a landing flap setting of 40 degrees
will provide the airplane with 853 meters (2,800 feet) field length capability.

Noise Correlation. - The PNdB values calculated for the various noise
components as compared to those in Reference 2 are tabulated in Table 2. The
suppression necessary on the inlet fan duct to achieve the predicted level is
shown on Figure 34. The total noise spectra calculated by the Reference 2
study was made up of component noise due to the fan, jet and aerodynamic shape.
The Boeing program also considers turbine and core-related noise. Due to the
high rotational speed of the turbine, no significant contribution was found in
the audible range. The core noise, however, required a small amount of sup-
pression to attain the desired EPNL value (Figure 35).

GW = 590,885 N (132,830 lbf)
SEA LEVEL
TEMP = 35°C (95°F)
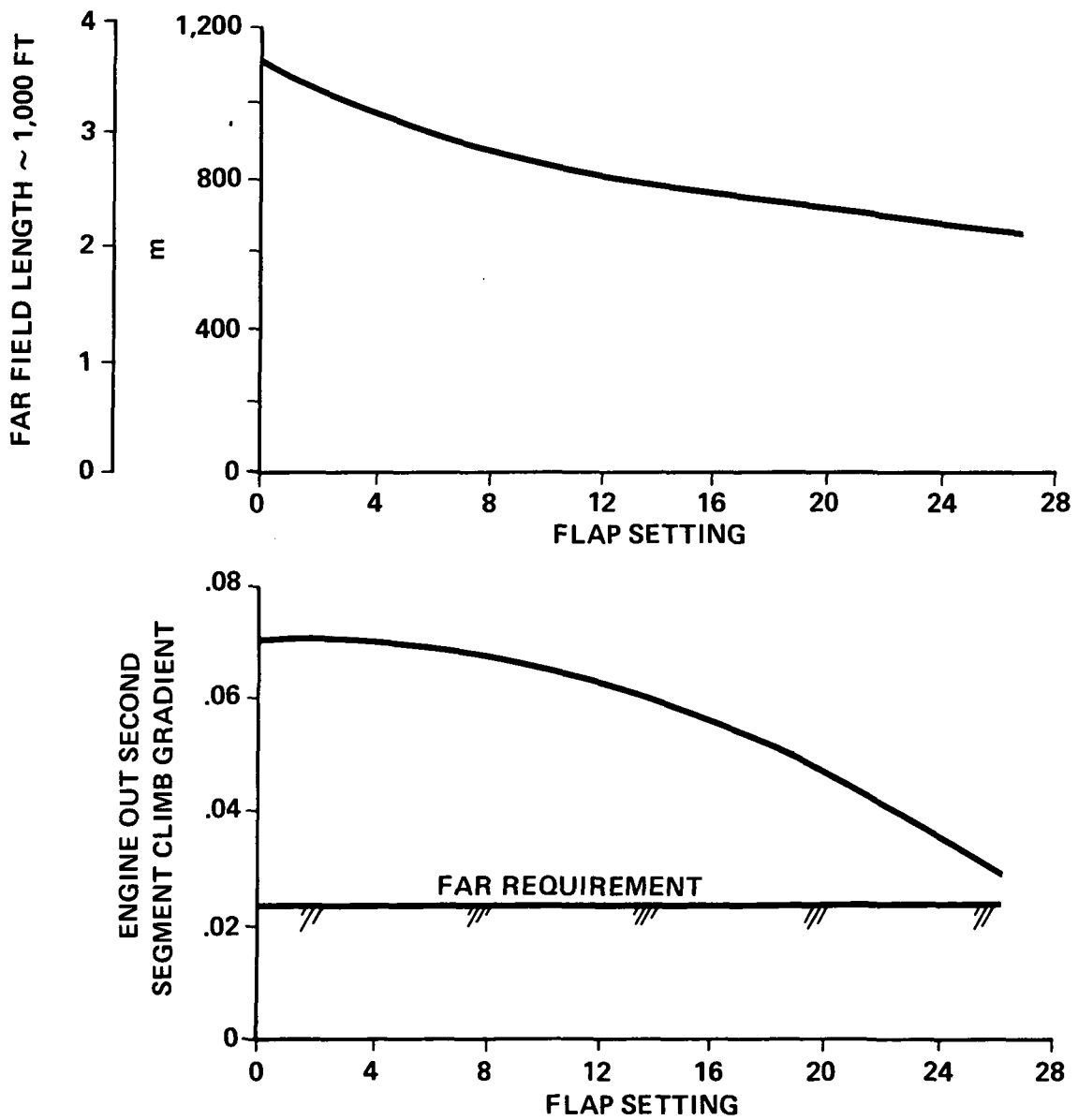
BASELINE CONFIGURATION TAKEOFF FLAP SETTING
FIGURE 32

59
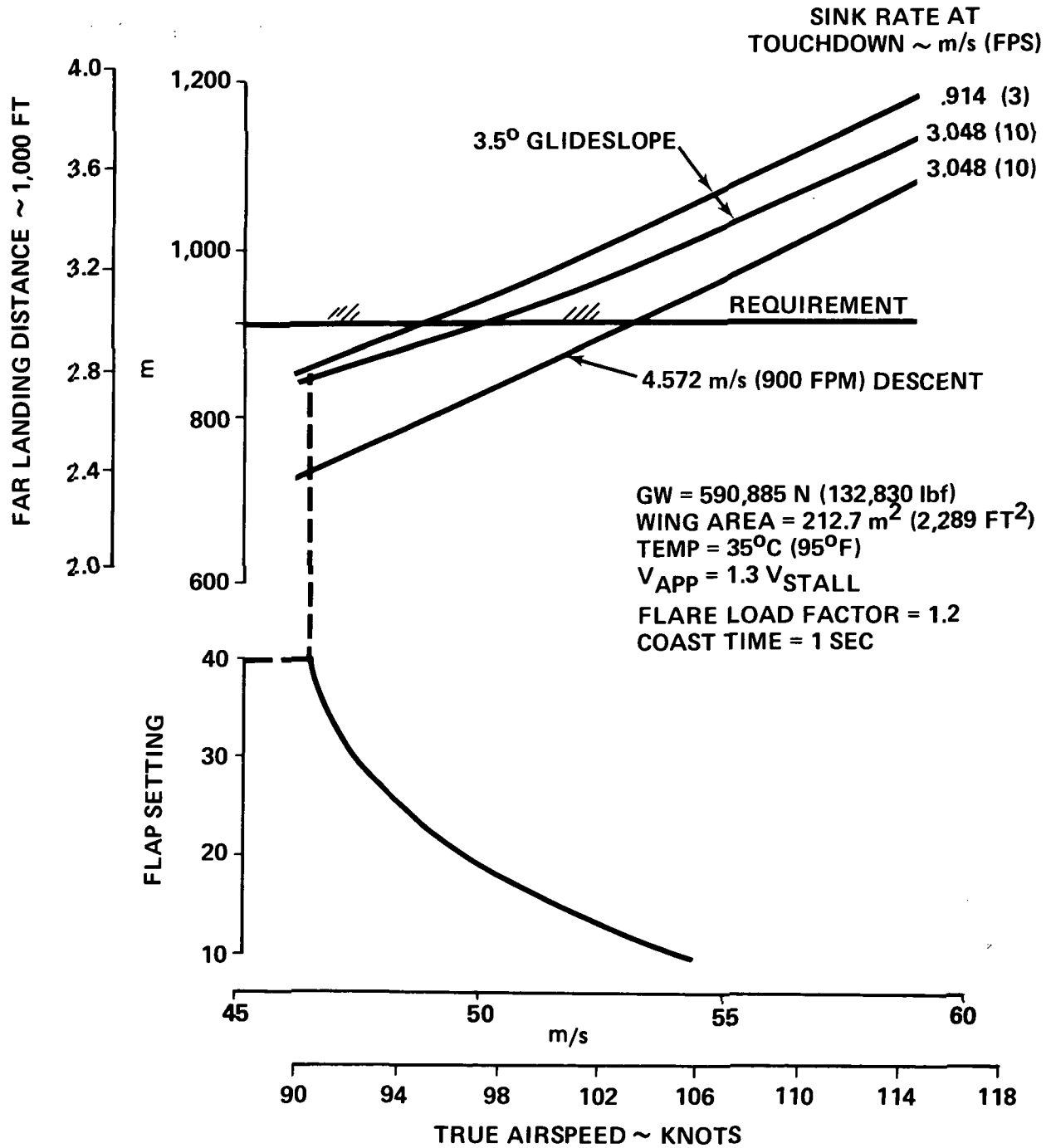
BASELINE MECHNICAL FLAP LANDING DISTANCE
FIGURE 33
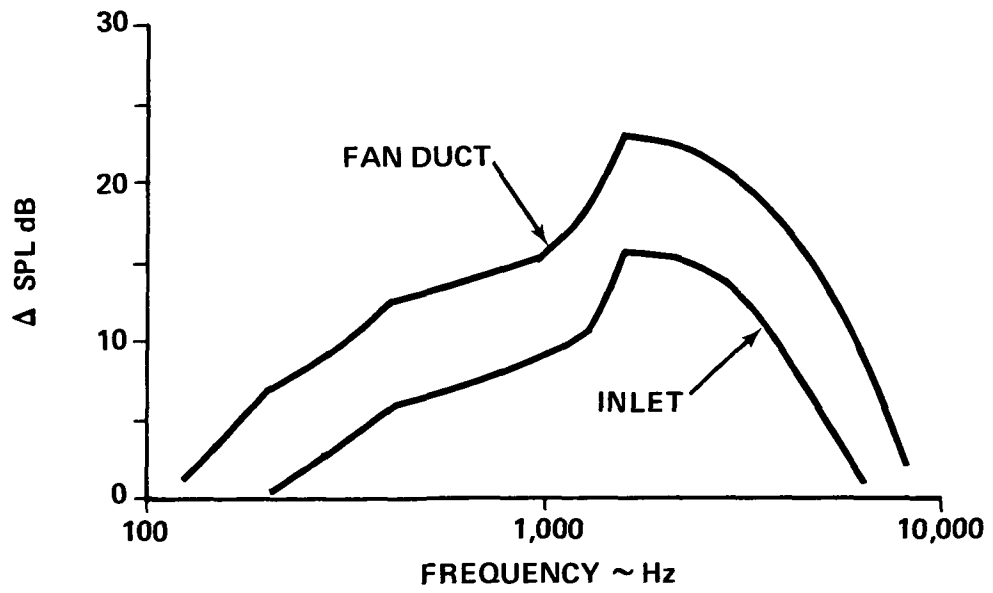
FAN ATTENUATION SPECTRA FOR THE BASELINE ENGINE
FIGURE 34
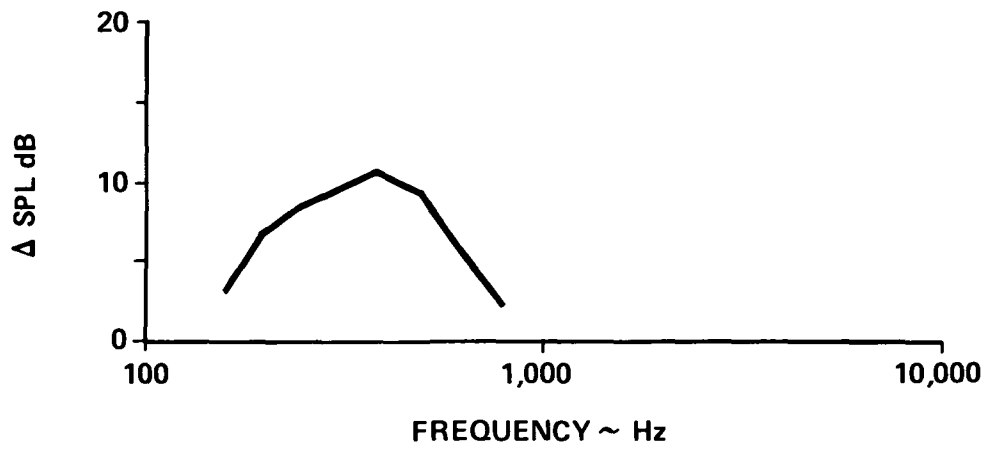
CORE ATTENUATION SPECTRA FOR THE BASELINE ENGINE
FIGURE 35

Footprint areas computed for the baseline airplane as compared to that for the reference study are shown on Figure 36. Contours are drawn for 80 and 90 EPNdB values. The upper portion of the footprint, calculation for this study, is larger than the lower half, Reference 2 calculations. The sound pressure level (SPL) values for the various subcomponents of the fan were calculated and evaluated to determine which component caused the approach contour to be larger than in the Reference 2 study. The buzz saw noise of the fan inlet, as calculated by the Boeing program, is large at the lower frequencies. These low frequencies exhibit very small atmospheric attenuation rates. The approach contour was recalculated without the buzz saw noise and is in good agreement with the Reference 2 noise contour data.

Gust Load Critical Baseline Design. - The Reference 2 aircraft, which was compared to the Boeing baseline configuration, was assumed to be maneuver load critical (2.5 g limit, 3.75 g ultimate). An evaluation of the aircraft in accordance with the gust load criteria of FAR 25 shows that both of the aircraft are gust load critical, not maneuver load critical.

Because the Boeing baseline study had shown so many differences with the Reference 2 study, a design constraint chart was developed to evaluate the airplane sizing parameters and is given in Figure 37. Shown on the chart are takeoff, landing, second segment climb and start cruise thrust limits for an aircraft with 853 meter (2,800 foot) FAR field length capability. The airplane is landing critical for wing loadings higher that 2.8 kPa (58 lbf/ft^2). The thrust-to-weight ratio used in Reference 2 for the aspect ratio 10 wing is high. With a thrust-to-weight ratio of .33 and a wing loading of 2.8 kPa (58 lbf/ft^2) the airplane will be thrust limited at the start of cruise and landing critical. If the aspect ratio is increased to 14, a thrust-to-weight ratio of .307 and a wing loading of 2.8 kPa (58 lbf/ft^2) the airplane will be start cruise thrust limited, landing critical and second segment climb critical.

Shown in Figure 38 are the airplane OWE, block fuel and DOC as a function of aspect ratio for the start cruise thrust critical airplane wing loading of 2.8 kPa (58 lbf/ft^2). The OWE increases rapidly with aspect ratio whereas the DOC shows a slight increase with aspect ratio. Minimum block fuel occurs at an aspect ratio of 12. The small decrease in block fuel obtained by increasing the aspect ratio is not considered to be significant. Therefore, the baseline configuration has retained the aspect ratio 10 wing and has been sized to be landing critical and start of cruise thrust critical.

Incorporating the aforementioned tail sizing criteria, rebalancing the aircraft and including FAR 25 gust load criteria, the final baseline configuration was defined and is shown in Figure 39. The basic airplane geometry comparison for the maneuver load critical and the gust load critical designs is

AREA ~ Mm² (SQ MI)		
EPN dB	BOEING CONFIGURATION	REFERENCE 2 CONFIGURATION
90	1.04 (0.40)	.548 (.46)
80	10.5 (4.06)	8.03 (3.10)

TAKEOFF

APPROACH

90 EPN dB

80 EPN dB

BOEING CONFIGURATION

REFERENCE 2 CONFIGURATION

DISTANCE ~ 1,000 FT

km
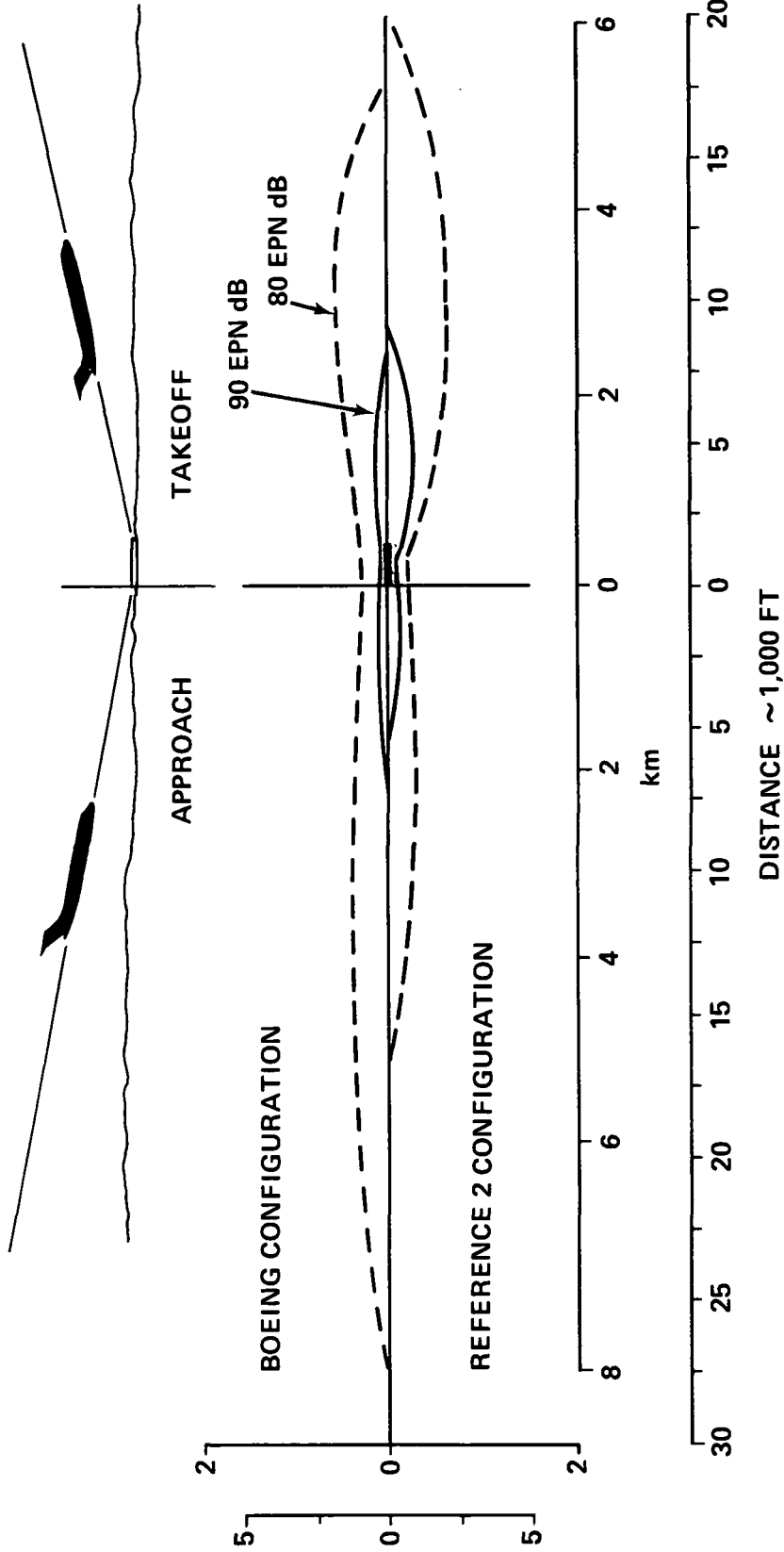
BASELINE AIRPLANE NOISE FOOTPRINT CORRELATION
FIGURE 36

63

853 m (2,800 FT) FIELD
35°C (95°F) TEMPERATURE
SEA LEVEL
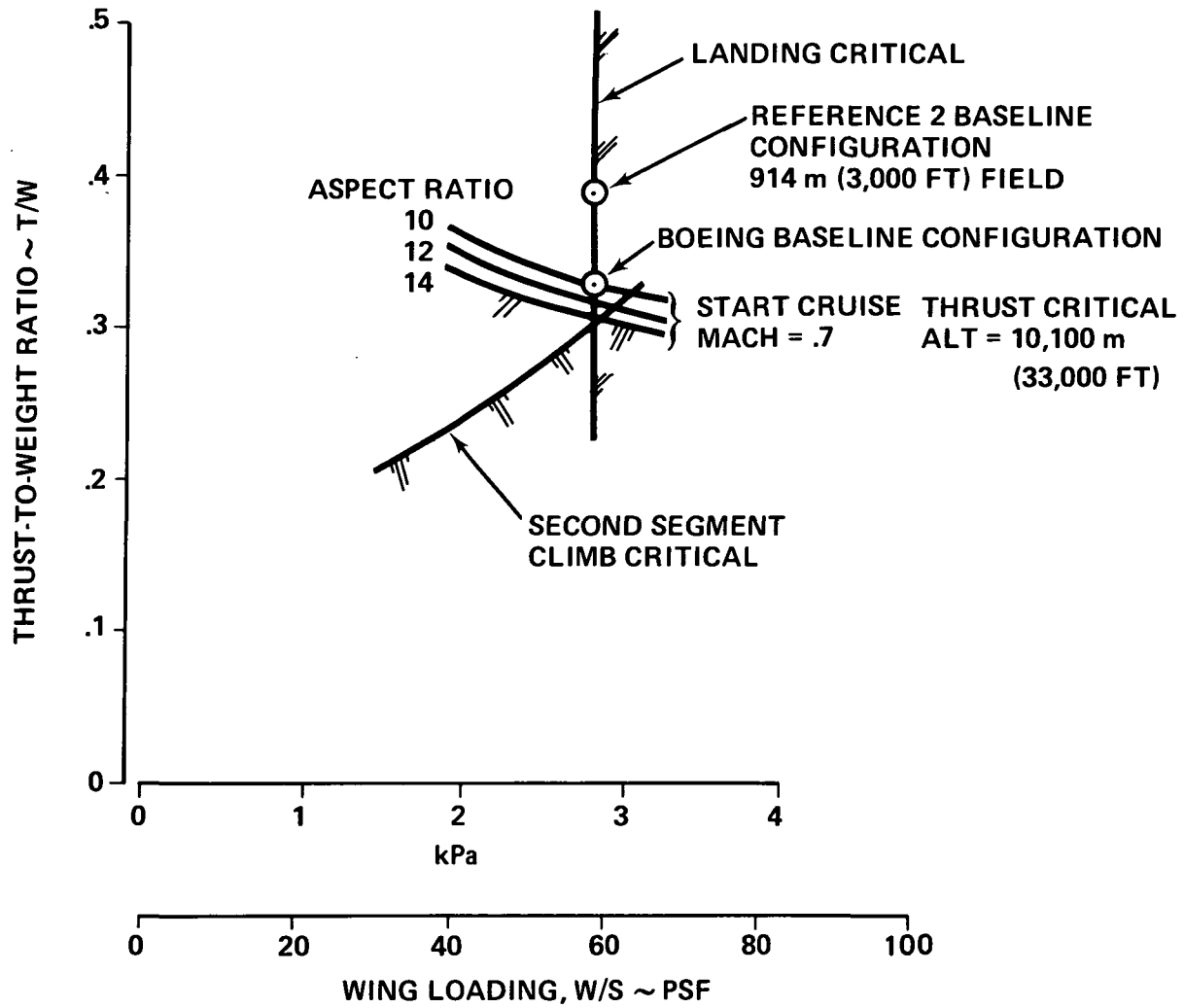
BASELINE CONFIGURATION DESIGN CONSTRAINTS
FIGURE 37

START CRUISE THRUST CRITICAL AT MACH = .7
10,100 m (33,000 FT)   W/S = 2.8 kPa (58 PSF)
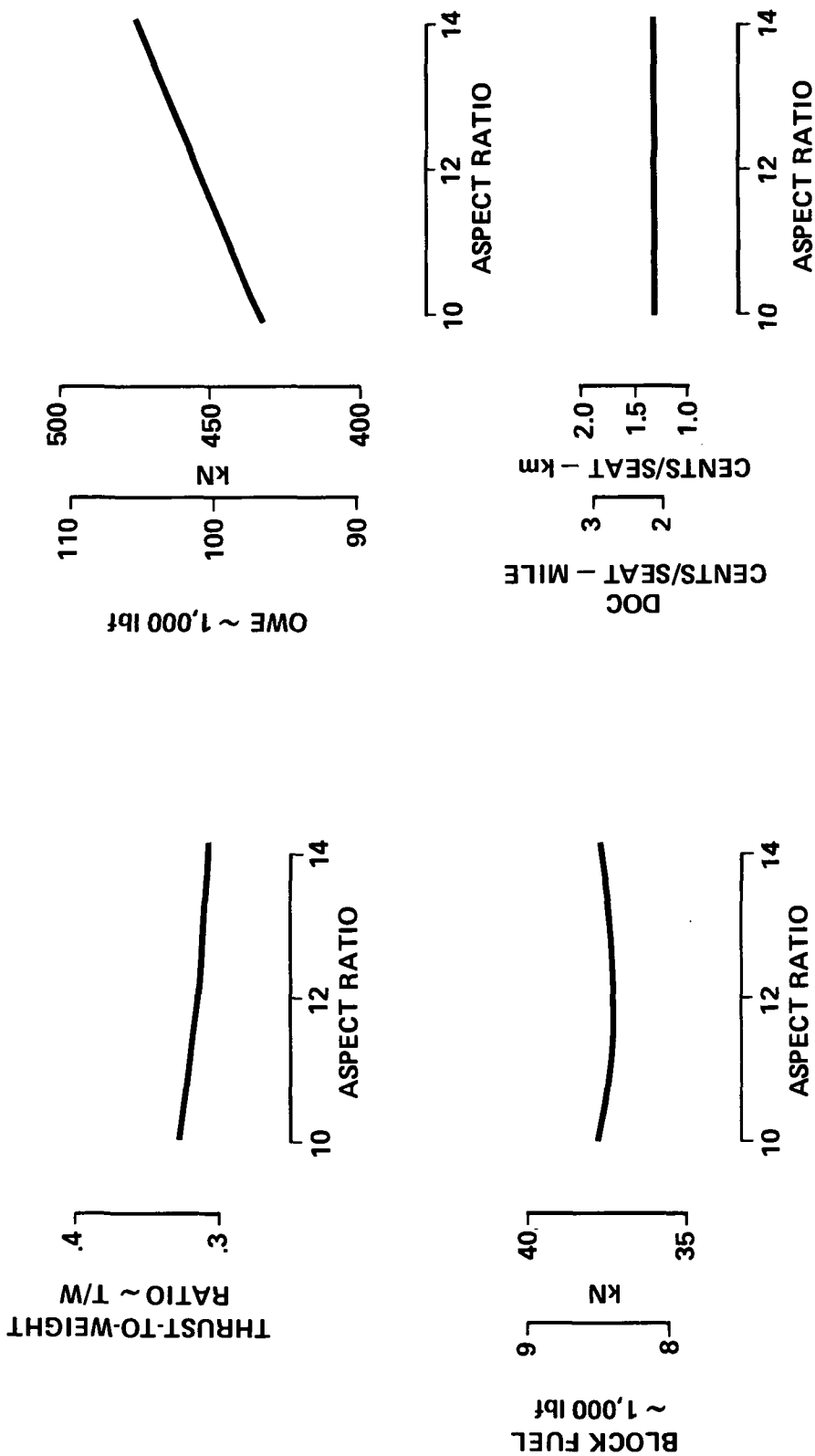
BASELINE CONFIGURATION CRUISE SIZING
FIGURE 38
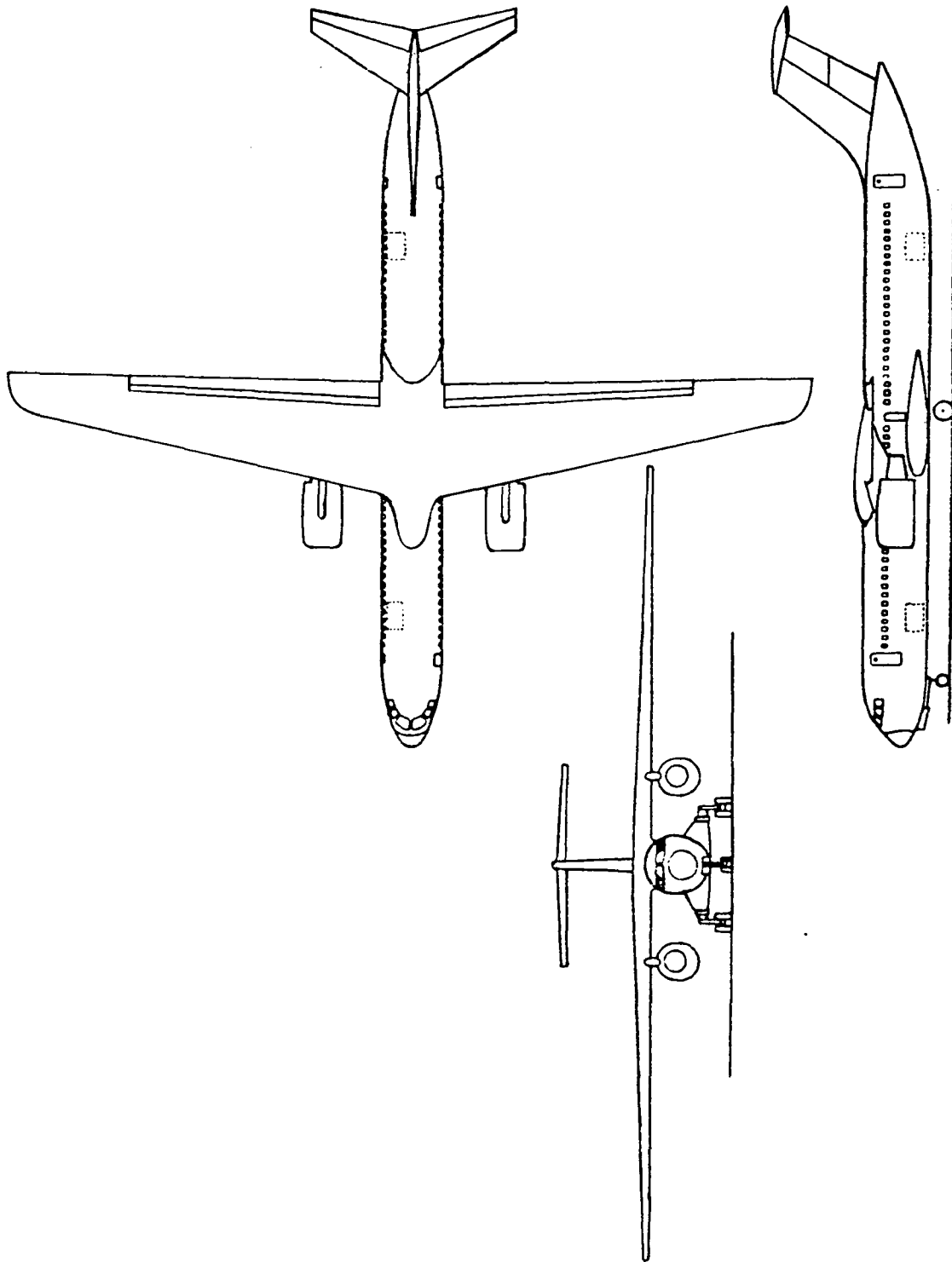
**BOEING BASELINE MECHANICAL FLAP CONFIGURATION
914 m (3,000 FT) FIELD LENGTH
FIGURE 39**

shown in Table 9 and the weight comparison is shown in Table 10. The increase in airplane size relative to the initial correlation is due to the aircraft being gust load critical instead of maneuver load critical. The Boeing baseline mechanical flap configuration to be used for the remainder of the subject contract study will be the gust load critical design as described by the three-view of Figure 39 and the geometry and weights as presented in Tables 11 and 12, respectively. The DOC for the gust load critical Boeing baseline configuration is shown as a function of fuel cost in Figure 40.

TABLE 9
BASELINE AIRPLANE GEOMETRY COMPARISON

| | Maneuver Load Critical | | Gust Load Crit. |
	Reference 2 Configuration	Boeing Configuration*	Boeing Configuration
Wing			
Aspect Ratio	10	10	10
Taper Ratio	.3	.3	.3
Quarter Chord Sweep ~ Deg.	10	10	10
Area ~ m^2 (Ft^2)	215.4 (2,318.6)	212.7 (2,289.5)	223.9 (2410)
Fuselage			
Overall Length ~ m (Ft)	41.54 (136.25)	41.54 (136.25)	41.54 (136.25)
Maximum Width ~ m (Ft)	3.66 (12)	3.66 (12)	3.66 (12)
Maximum Depth ~ m (Ft)	3.96 (13)	3.96 (13)	3.96 (13)
Number of Passengers	148	148	148
Vertical Tail			
Aspect Ratio	–	1.2	1.2
Taper Ratio	–	.7	.7
Quarter Chord Sweep ~ Deg.	–	35	35
Area ~ m^2 (Ft^2)	50.23 (540.72)	50.23 (540.72*)	25.56 (275)
Horizontal Tail			
Aspect Ratio	–	4.5	4.5
Taper Ratio	–	.3	.3
Quarter Chord Sweep ~ Deg.	–	30	30
Area ~ m^2 (Ft^2)	38.03 (409.38)	38.03 (409.38*)	31.49 (339)

*Based on the vertical and horizontal tail areas used in Reference Study

TABLE 10
BASELINE AIRPLANE WEIGHT COMPARISON

| | Maneuver Load Critical | | Gust Load Critical |
	Reference Configuration	Boeing Configuration	Boeing Configuration
T/W	.39	.39	.33
W/S ~ kPa (PSF)	2.8 (58)	2.8 (58)	2.8 (58)
OWE ~ N (lb)	401,895 (90,350)	400,725 (90,090)	432,240 (97,170)
Payload ~ N (lb)	134,958 (30,340)	134,958 (30,340)	134,958 (30,340)
Mission Fuel ~ N (lb)	47,151 (10,600)	38,299 (8,610)	37,854 (8,510)
Reserve Fuel ~ N (lb)	14,368 (3,230)	16,859 (3,790)	16,948 (3,810)
Total Fuel ~ N (lb)	61,519 (13,830)	55,202 (12,400)	54,800 (12,320)
Gross Weight ~ N (lb)	598,372 (134,520)	590,885 (132,830)	622,010 (139,830)

TABLE 11
BOEING BASELINE CONFIGURATION AERODYNAMIC GEOMETRY

Fuselage				
LF	Length	41.54 m	(136.3	Ft)
WF	Width	3.66 m	(12.0	Ft)
SF	Wetted Area	433.0 m²	(4,661.	Sq Ft)

Wing				
AR	Aspect Ratio		10.00	
SW	Area	223.9 m²	(2,410.1	Sq Ft)
B	Span	47.30 m	(155.2	Ft)
CBARW	Geom. Mean Chord	5.18 m	(17.0	Ft)
LAMBDA C/4	Quarter Chord Sweep		(10.0	Deg)
LAMBDA	Taper Ratio		0.300	
(T/C)R	Root Thickness		0.183	
(T/C)T	Tip Thickness		0.140	
WG/SW	Wing Loading	2.8 kPa	(58.0	lb/Sq Ft)

Horizontal Tail				
ARHT	Aspect Ratio		4.50	
SHT	Area	31.49 m²	(339.3	Sq Ft)
BHT	Span	11.92 m	(39.1	Ft)
CBARHT	Mean Chord	2.65 m	(8.7	Ft)
(T/C)HT	Thickness/Chord		0.120	
LTH	Moment Arm	23.71 m	(77.8	Ft)

Vertical Tail				
ARVT	Aspect Ratio		1.40	
SVT	Area	25.56 m²	(275.1	Sq Ft)
BVT	Span	5.97 m	(19.6	Ft)
CBARVT	Mean Chord	4.27 m	(14.0	Ft)
(T/C)VT	Thickness/Chord		0.130	
LTV.	Moment Arm	20.06 m	(65.8	Ft)

Primary Engine Nacelle				
LN	Length	4.05 m	(13.2	Ft)
DBARN	Mean Diameter	2.23 m	(7.3	Ft)
SN	Wetted Area	56.45 m²	(607.6	Sq Ft)

TABLE 12
BOEING BASELINE CONFIGURATION WEIGHT AND BALANCE SUMMARY

Weight Group	N	Weight (lbf)	Horizontal Arm (Body Station)
Wing	126,267	(28,386)	742
Horizontal Tail	7,549	(1,697)	1,687
Vertical Tail	6,121	(1,376)	1,512
Fuselage	81,669	(18,360)	744
Landing Gear	24,879	(5,593)	688
Engine Struts	7,500	(1,686)	636
Engine Nacelles	9,884	(2,222)	590
Total Structure Group Weight	Σ 263,867	Σ (59,320)	(774)
Primary Engines	29,936	(6,730)	580
Engine Accessories	1,397	(314)	451
Engine Controls	667	(150)	451
Engine Starting System	347	(78)	580
Thrust Reversers	8,985	(2,020)	599
Fuel System	1,739	(391)	657
Total Propulsion Group Weight	Σ 43,072	Σ (9,683)	(581)
Instruments	2,856	(642)	330
Surface Controls	9,395	(2,112)	972
Hydraulics	3,220	(724)	747
Pneumatics	2,277	(512)	706
Electrical	6,939	(1,560)	414
Electronics	4,751	(1,068)	284
Flight Deck Accommodations	3,465	(779)	108
Passenger Accommodations	48,592	(10,924)	758
Cargo Accommodations	5,480	(1,232)	740
Emergency Equipment	1,975	(444)	582
Air Conditioning	8,069	(1,814)	622
Anti-icing	1,557	(350)	462
APU	4,395	(988)	1,359
Total Fixed Equipment Group Weight	Σ 102,971	Σ (23,149)	(703)
Manufacturers Empty Weight	Σ 409,919	Σ (92,154)	(736)
Standard and Operational Items	22,317	(5,017)	669
Operational Empty Weight	Σ 432,236	Σ (97,171)	(732) 20.2% MAC
Payload	134,958	(30,340)	750
Fuel	54,815	(12,323)	737
Gross Weight	Σ 622,005	Σ(139,833)	(737) 21.6% MAC
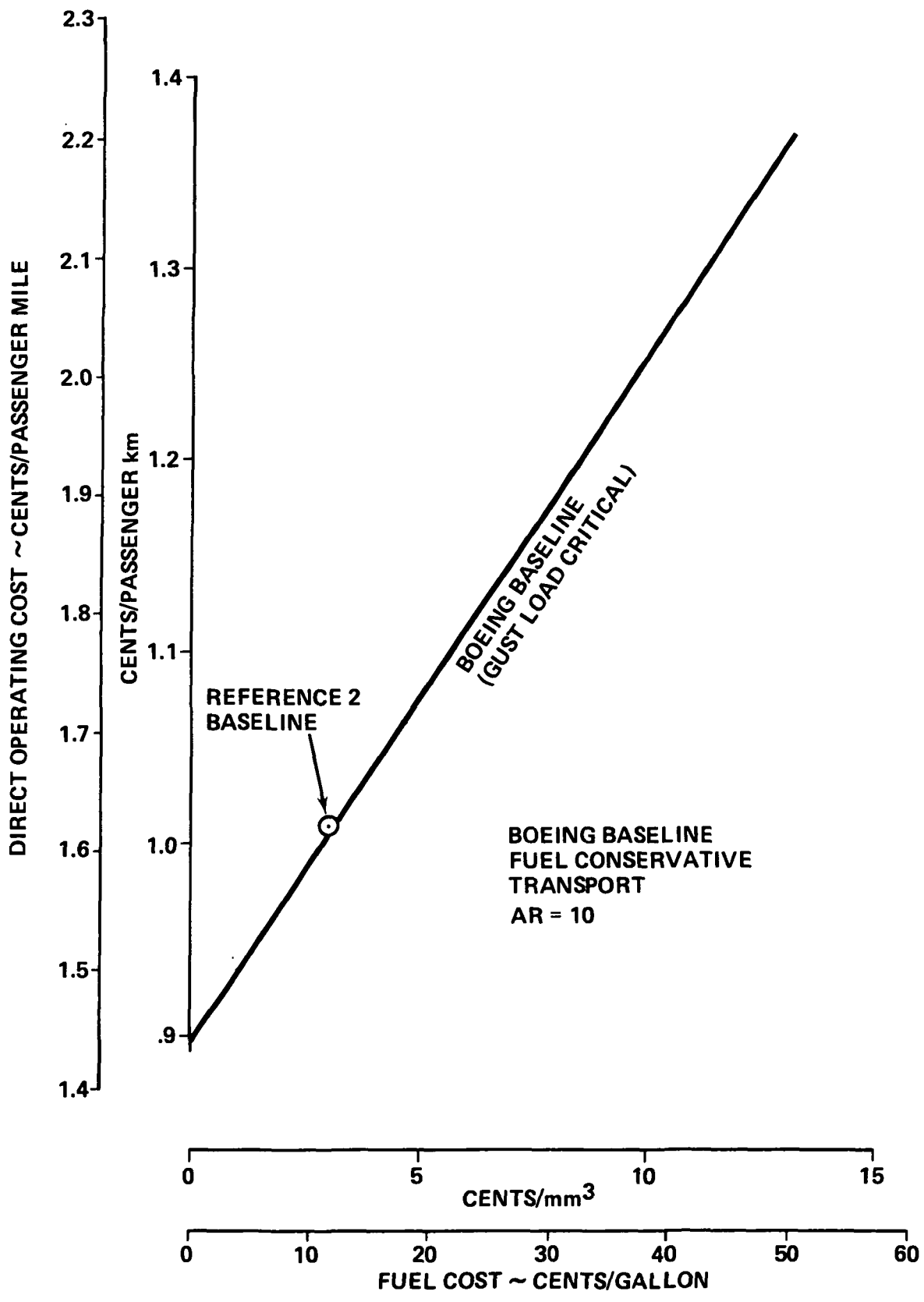
THE EFFECT OF FUEL COST ON DIRECT OPERATING COST
FIGURE 40

Page Intentionally Left Blank

Q-FAN PROPULSION

The Q-fan propulsion is a recent innovation that combines the salient features of the turbofan engines and the shrouded propeller. The Q-fan employs a variable pitch fan blade to optimize performance over a wide operating range. The fan speed is reduced such that the tip speed is below sonic speed by having the turbine drive the fan through a gear reduction. The complexity and weight of the variable pitch fan blades and gear reduction mechanism is more than offset by the improved efficiency and other attractive features, i.e., the improved specific fuel consumption, the reduced noise levels and a more effective simplified reverse thrust system.

Q-Fan Propulsion Development

A family of Q-fan engines were developed from Hamilton Standard Q-fan component map data using the baseline engine gas generator as shown in Figure 41. The generalized Boeing engine performance computer program (GSA) was used to compute the Q-fan data for FPR's of 1.25, 1.35 and 1.40. Installed engine data were calculated including the effect of scrub drag, typical inlet recovery, bleed and power extractions for the two-engine baseline airplane. The Q-fan propulsion data generated for the ASAMP computer program is presented in Appendix B.

Propulsion thrust-to-weight ratio for the Q-fan and the high bypass fan baseline configuration are shown in Figure 42. Weight savings of the simplified thrust reversing mechanism can be seen to offset the added weight of the variable fan blades pitch and gear reduction mechanism, based on static sea level thrust. The Q-fan fuel consumption characteristics compared to the baseline airplane are presented in Figure 43. The FPR 1.35 Q-fan engine shows approximately a 10 percent improvement over the baseline engine which represents a significant performance improvement inasmuch as the baseline engine is a fuel conservative propulsion system based on the mid-1980 technology.

Nacelle Drag

The nacelle drag was computed by the same method used to compute the baseline engine nacelle drag. The nacelle sizes for the Q-fan engines are shown in Figure 44 for the FPR's of 1.25, 1.35 and 1.40. The Q-fan engine does not require a larger nacelle diameter than the baseline for a given FPR.

BASELINE GAS GENERATOR

BASELINE ENGINE FPR = 1.35

F_N = 125,440 N (28,200 lbf)*

Q-FAN FPR = 1.4

F_N = 127,220 N (28,600 lbf)*

Q-FAN FPR = 1.35

F_N = 135,670 N (30,500 lbf)*

Q-FAN FPR = 1.25

F_N = 167,700 N (37,700 lbf)*
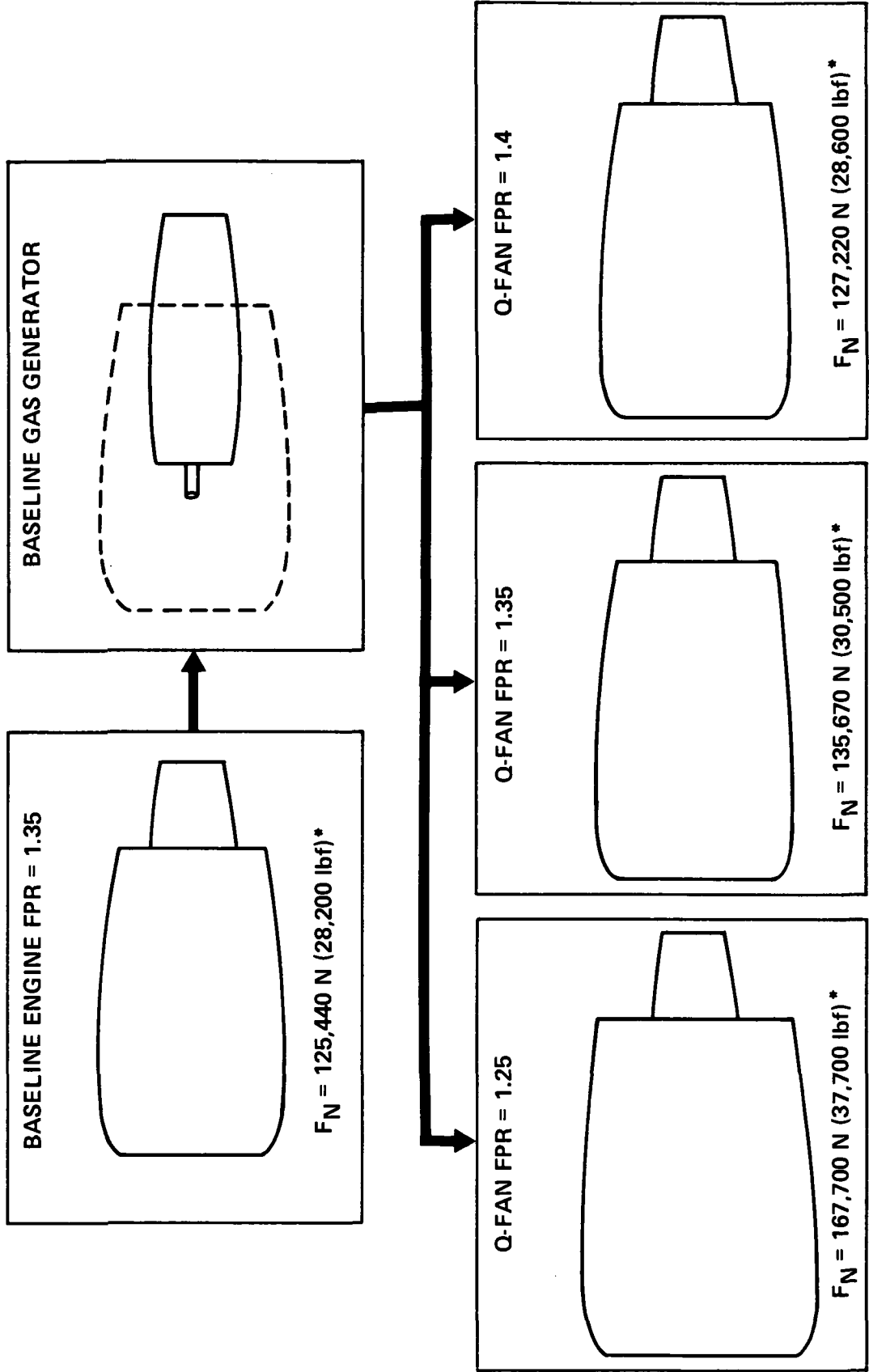
*SEA LEVEL STANDARD DAY STATIC INSTALLED THRUST

DEVELOPMENT OF Q-FAN PROPULSION MODEL
FIGURE 41

SEA LEVEL
TEMPERATURE = 35°C (95°F)
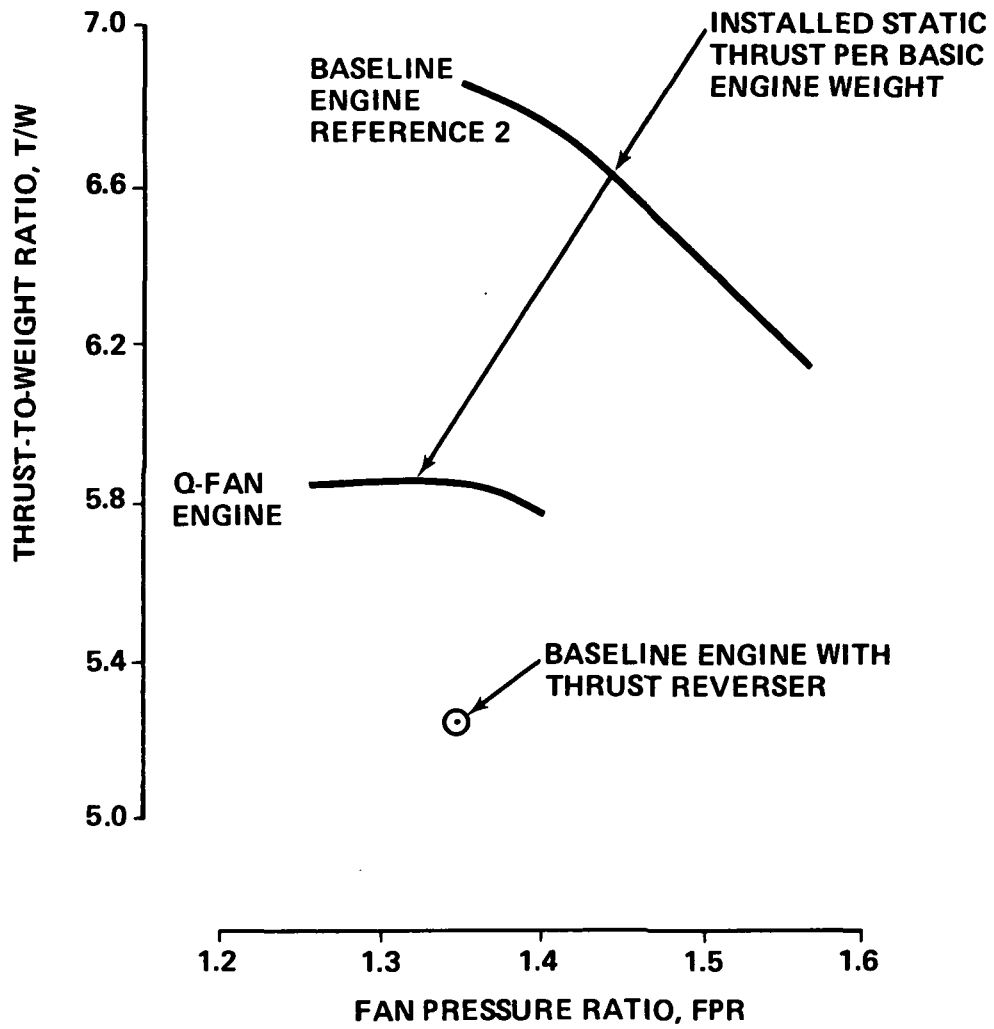
ENGINE STATIC THRUST-TO-WEIGHT RATIO
FIGURE 42
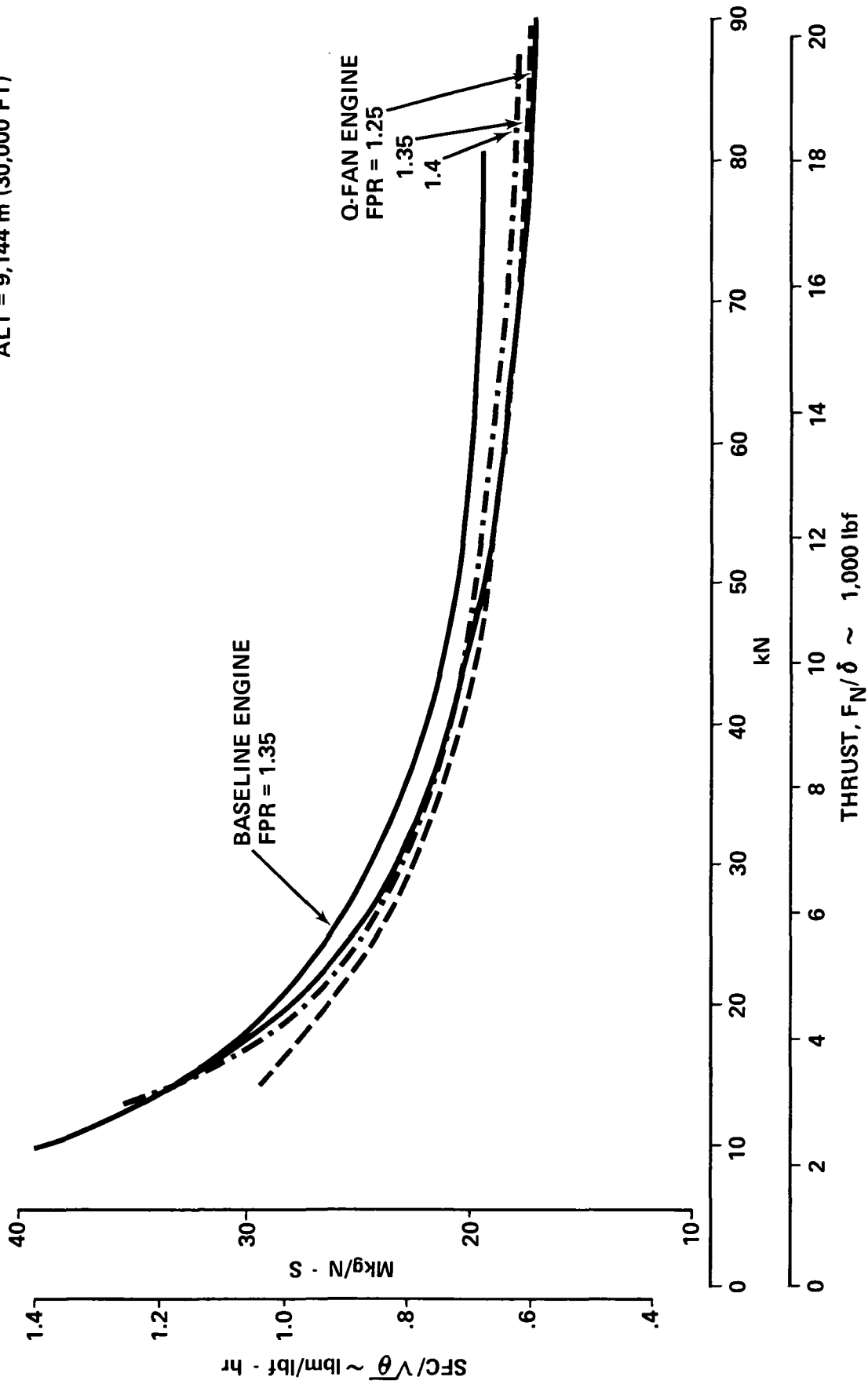
Q-FAN FUEL CONSUMPTION CHARACTERISTICS
FIGURE 43

TABLE 13
Q-FAN PROPULSION CONFIGURATION NOISE COMPONENT

152 m (500 Ft) Sideline

88.4 m (290 Ft) Altitude

35°C (95°F) Sea Level Day

Component		Component Noise	
		Boeing Baseline	Boeing Q-Fan
Fan Unsuppressed	(PNdB)	107.9	106.1
Fan Suppressed	(PNdB)	90.2	91.9
Jet	(PNdB)	83.1	61.3
Core Unsuppressed	(PNdB)	97.1	95.5
Core Suppressed	(PNdB)	88.3	89.0
Total	(PNdB)	94.2	94.9
Total	(EPNdB)	93.9	93.7
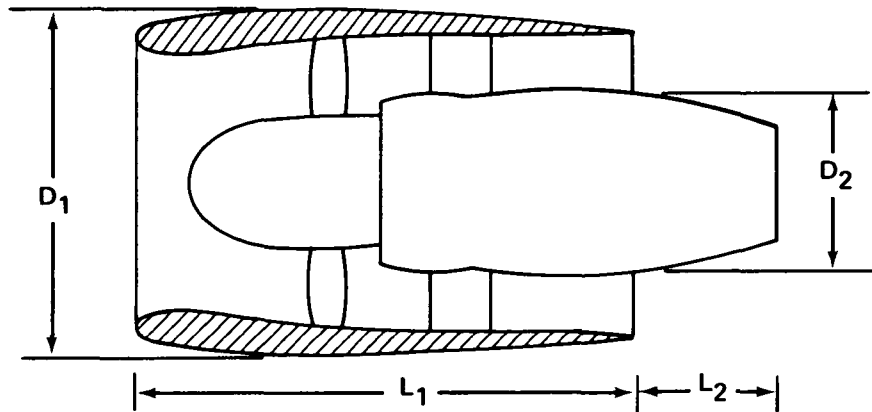
ENGINE	BASELINE		Q-FAN PROPULSION					
FPR	1.35		1.25		1.35		1.40	
REF THRUST N (lbs)	125,370 (28,185)		120,600 (27,113)		135,820 (30,534)		127,190 (28,593)	
D_1 m (FT)	2.46	((8.06)	3.16	(10.36)	2.62	(8.58)	2.49	(8.18)
D_2 m (FT)	1.12	(3.66)	1.12	(3.66)	1.12	(3.66)	1.12	(3.66)
L_1 m (FT)	4.04	(13.27)	4.47	(14.65)	4.18	(13.73)	4.12	(13.52)
L_2 m (FT)	1.18	(3.86)	1.18	(3.86)	1.18	(3.86)	1.18	(3.86)

ESTIMATED Q-FAN PROPULSION NACELLE DIMENSIONS
FIGURE 44

Noise

The Q-fan noise levels were computed in the same manner as for the base-line engine. A comparison of the component noise levels are presented in Table 13.

The Q-fan jet noise level is considerably lower than that of the base-line engine. The core noise, however, obscures the benefits of the lowered jet noise level since in both engines the core noise exceeds the jet noise. The contribution of the fan noise, however, remains at approximately the same level as the baseline because both engines are operating at similar fan pressure ratios.

The footprint area for the Q-fan engine was computed based on the take-off and landing approach profiles shown in Figures 45 and 46, respectively, and the Q-fan footprint noise contours are presented in Figure 47. The footprint noise area can be seen to be essentially equal to the baseline because the component noise levels are similar in magnitude.

Q-Fan Propulsion Optimization

Prior to the Q-fan optimization study, a design constraint chart, Figure 48, was prepared for the Q-fan configuration (FPR = 1.35). The purpose of this chart was to ensure that all configurations examined in the parametric study would meet the basic design requirements. The second segment climb constraints shown in Figure 48 have been presented for a wing aspect ratio of 10 only (increasing aspect ratio will lower the thrust-to-weight ratio required for a given wing loading). For a range of wing aspect ratio of 8 to 14, the minimum thrust-to-weight ratio is determined by the start cruise thrust requirement which is well above the second segment climb requirement as presented for aspect ratio 10.

Figure 49 shows block fuel, gross weight and direct operating cost as a function of wing aspect ratio for the three Q-fan configurations investigated. The airplane is sized for cruise at .7 Mach number at 10100 meter (33,000 foot) altitude. A FPR of 1.35 requires the least fuel, is the lightest airplane and has the lowest DOC for the design flight profile. The minimum block fuel required for the flight profile occurs at an aspect ratio of 12. However, in going from aspect ratio 10 to 12, the gross weight increases 30700 N (6,900 lbf) with a reduction of only 222 N (50 lbf) block fuel. The small savings in block fuel, by increasing aspect ratio from 10 to 12, is not considered to be of significant magnitude to warrant a wing aspect ratio any greater than 10.

78
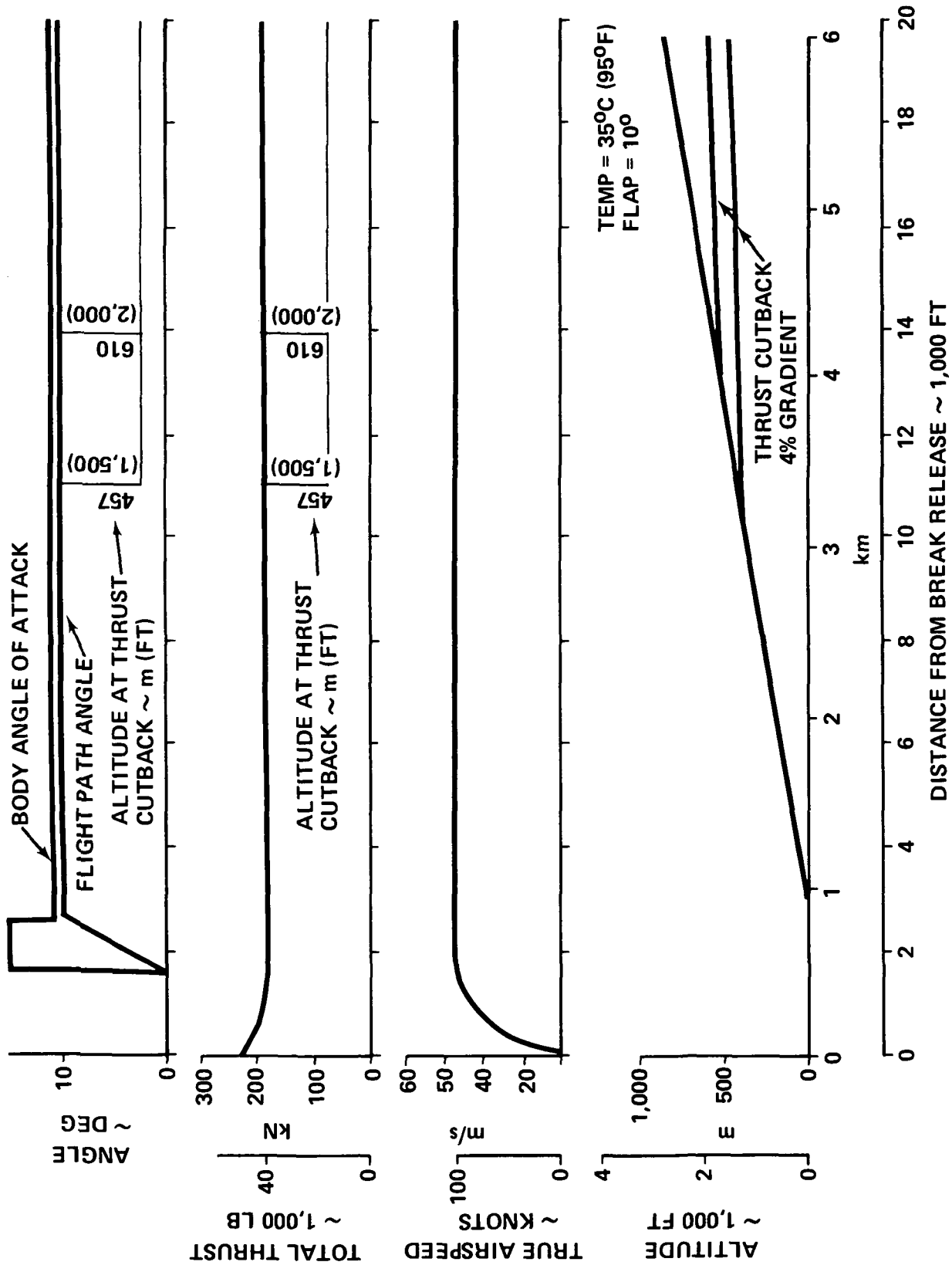
Q-FAN PROPULSION CONFIGURATION TAKEOFF PROFILE
FIGURE 45
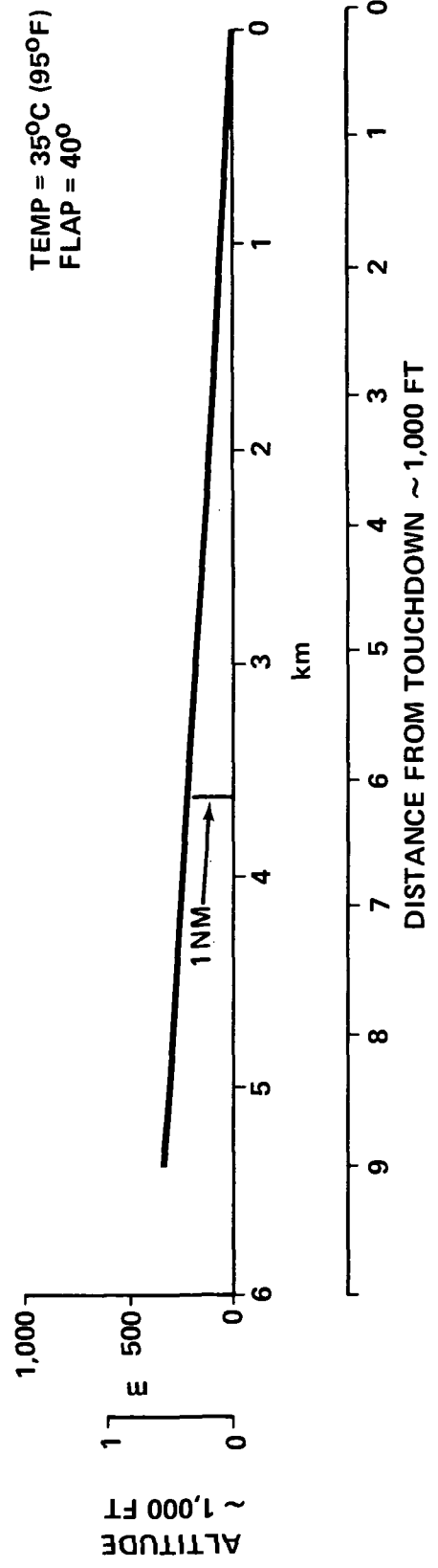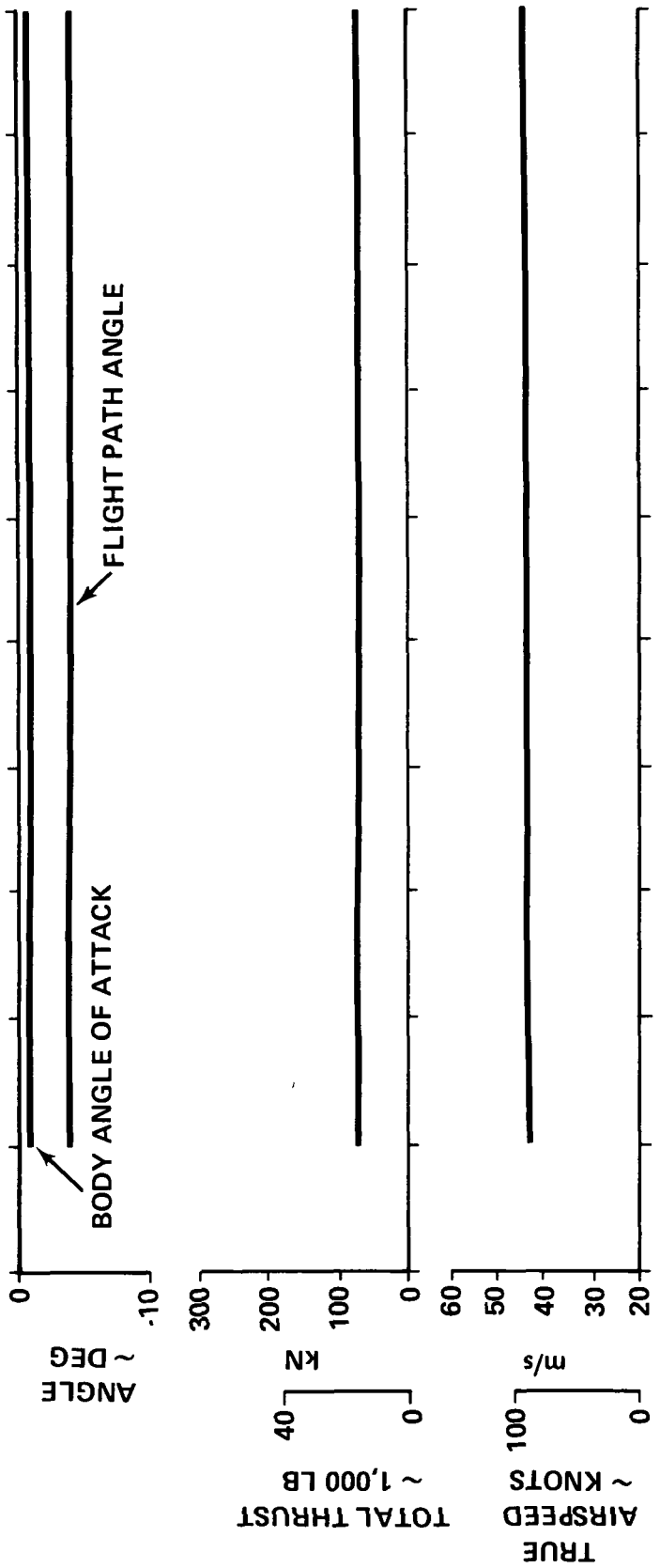
Q-FAN PROPULSION CONFIGURATION LANDING PROFILE
FIGURE 46

80
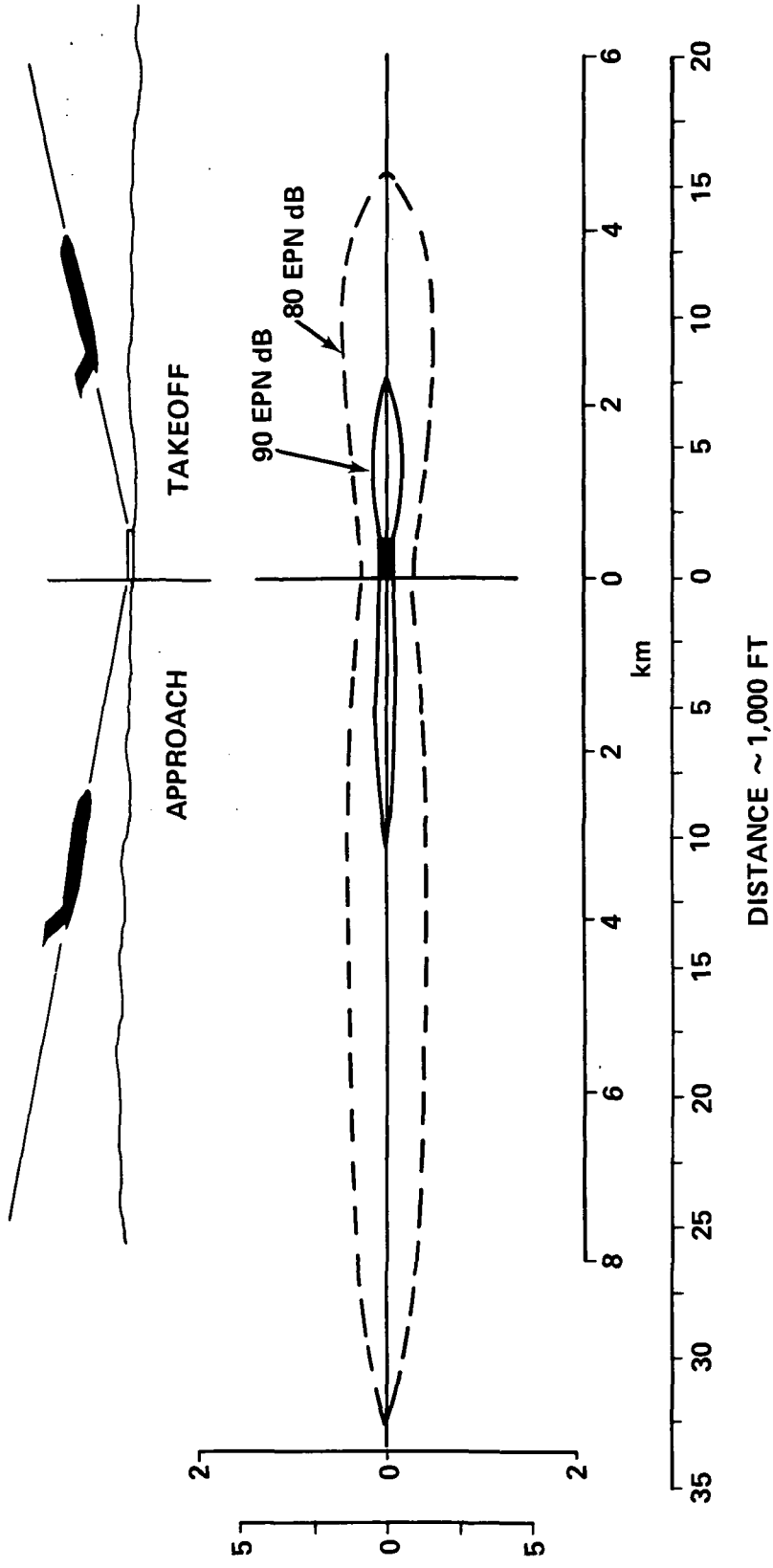
Q-FAN PROPULSION CONFIGURATION NOISE FOOTPRINT CONTOURS
FIGURE 47

853 m (2,800 FT) FIELD
35°C (95°F) TEMPERATURE
SEA LEVEL
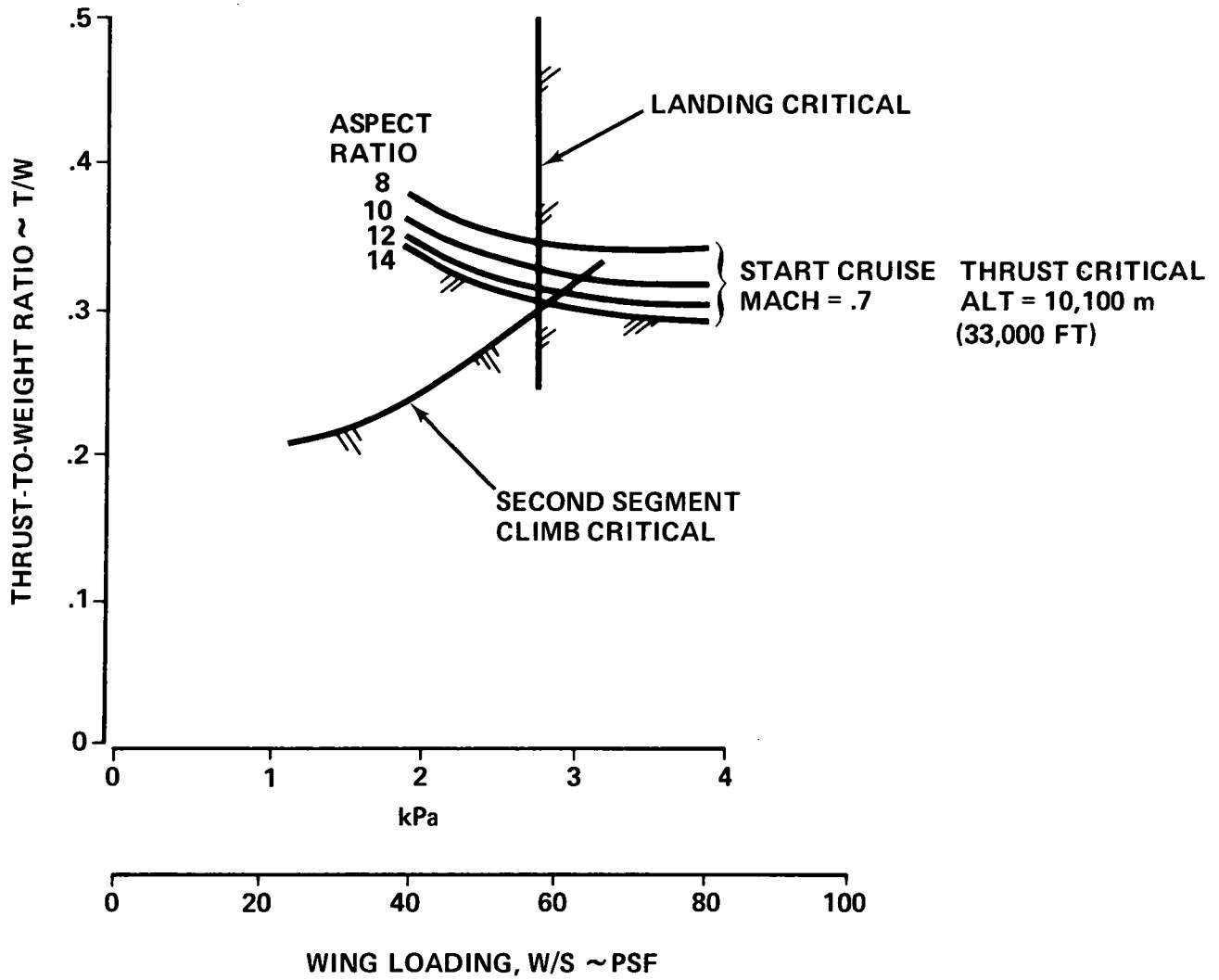
Q-FAN CONFIGURATION DESIGN CONSTRAINTS FPR = 1.35
FIGURE 48
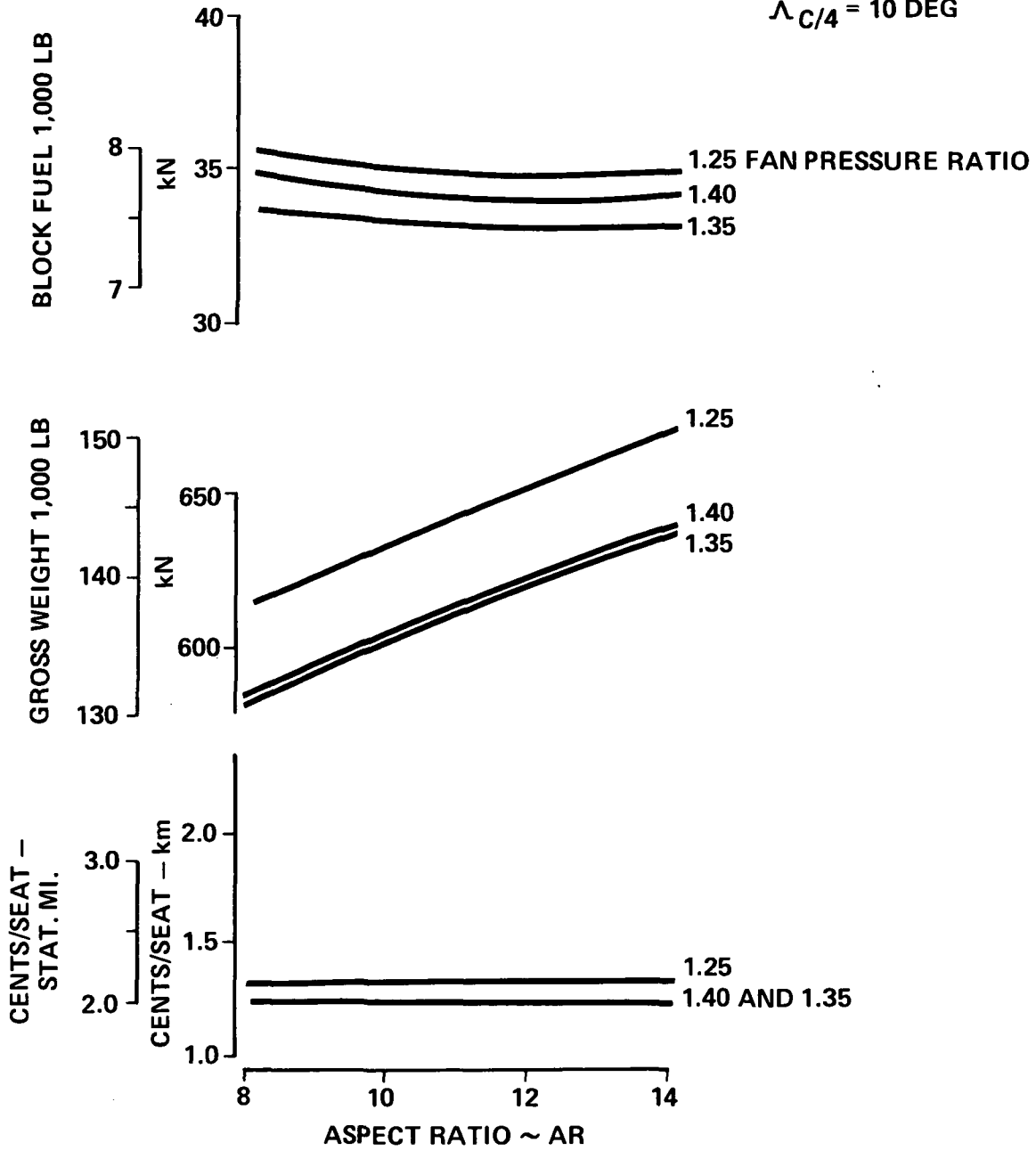
AIRPLANE SIZED FOR CRUISE AT M = .7,
10,100 m (33,000 FT) WITH Q-FAN PROPULSION
FIGURE 49

Figure 50 shows the effect of sizing the aircraft for cruising at .75 Mach number at 10100 meter (33,000 foot) altitude. Minimum block fuel, gross weight and DOC are still obtained with an engine FPR of 1.35.

Figure 51 compares block fuel requirements, gross weight and DOC as a function of wing aspect ratio and cruise Mach number for an engine FPR of 1.35. For a wing aspect ratio 10, cruise at .75 Mach number instead of .70 Mach number increases the block fuel requirement 3780 N (850 lbf), the aircraft gross weight 29800 N (6,700 lbf) and the DOC 0.03 cents/seat-kilometer (0.05 cents/ seat-mile).

The effects of wing sweep on airplane sizing is presented in Figure 52. For cruise at .7 Mach number at 10100 meter (33,000 foot) altitude, a reduction in block fuel, gross weight and DOC can be obtained by unsweeping the wing.

Figure 53 shows the effect of wing taper ratio. A taper ratio of less than .3 is not considered to provide a beneficial savings in fuel, gross weight or DOC. The minimum allowed wing taper ratio is usually determined by the physical thickness of the wing near the tips. If ailerons or other control surfaces are located on the outboard portion of the wing, sufficient thickness must exist for structural requirements.

A summary of the benefits of Q-fan propulsion as applied to and compared to the Boeing baseline configuration is shown in Table 14. The aircraft geometry (aspect ratio, taper ratio, sweep, etc.) with the Q-fan propulsion system is identical to the geometry of the baseline configuration. All aircraft are start cruise thrust critical at 10100 meters (33,000 feet), 0.7 Mach number (determines the minimum allowable thrust-to-weight ratio) and landing critical (determines the maximum allowable wing loading 2.8 kPa (58 psf). The most favorable Q-fan FPR is 1.35. This aircraft is the smallest, lightest, requires the least fuel and has the lowest DOC's.

Q-Fan Baseline Configuration

The optimum Q-fan configuration sized by the ASAMP computer program to do the design mission with 1.35 FPR Q-fan propulsion is shown in Figure 54. A detailed description of the geometry is shown by Table 15 and the weight statement is shown by Table 16.

Table 17 presents a comparison of the Boeing baseline configuration and the 1.35 FPR Q-fan propulsion system configuration. The Q-fan configuration

W/S = 2.8 kPa (58 PSF)
λ = .30
$\Lambda_{C/4}$ = 10 DEG
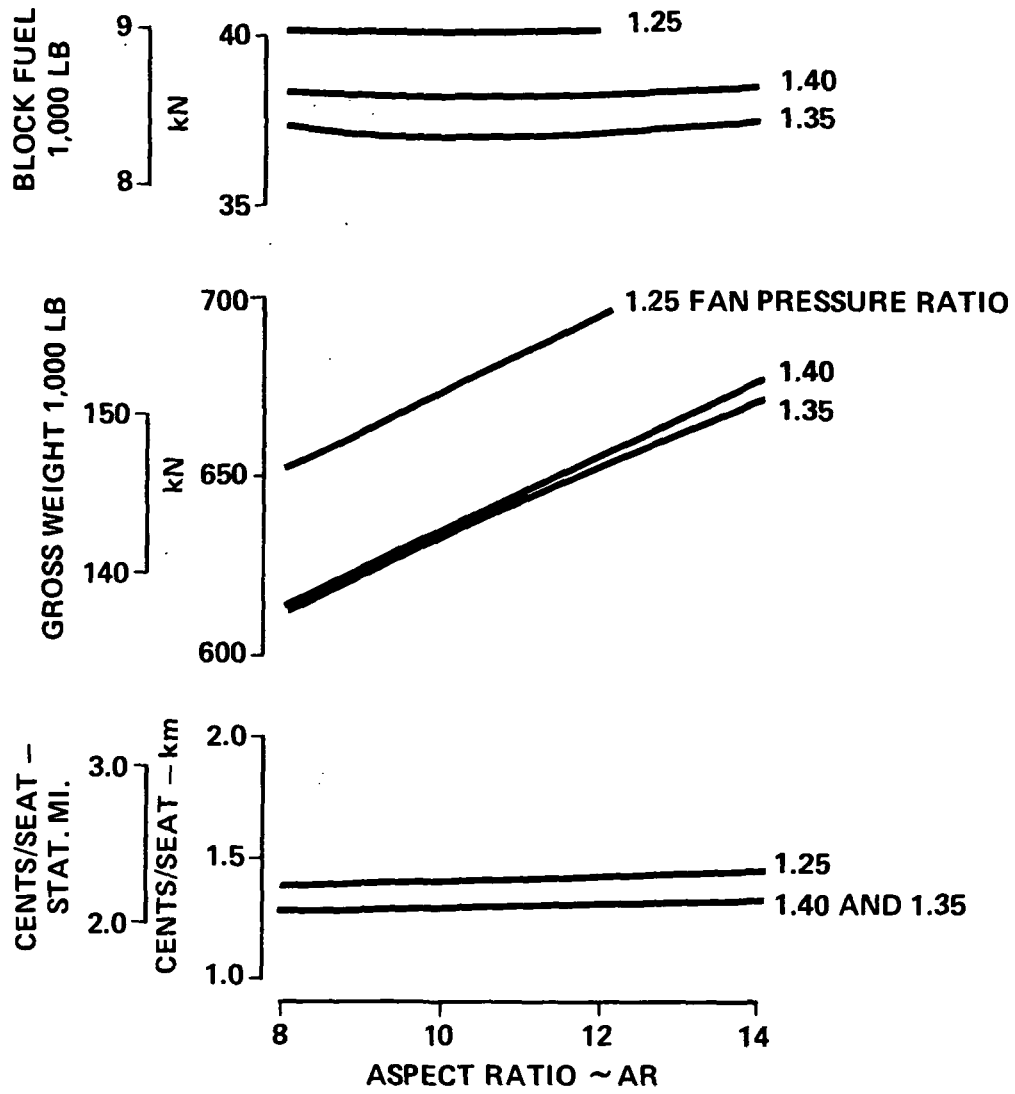
AIRPLANE SIZED FOR CRUISE AT M = .75,
10,100 m (33,000 FT) WITH Q-FAN PROPULSION
FIGURE 50

W/S = 2.8 kPa (58 PSF)
FPR = 1.35
λ = .3
$\Lambda_{C/4}$ = 10 DEG
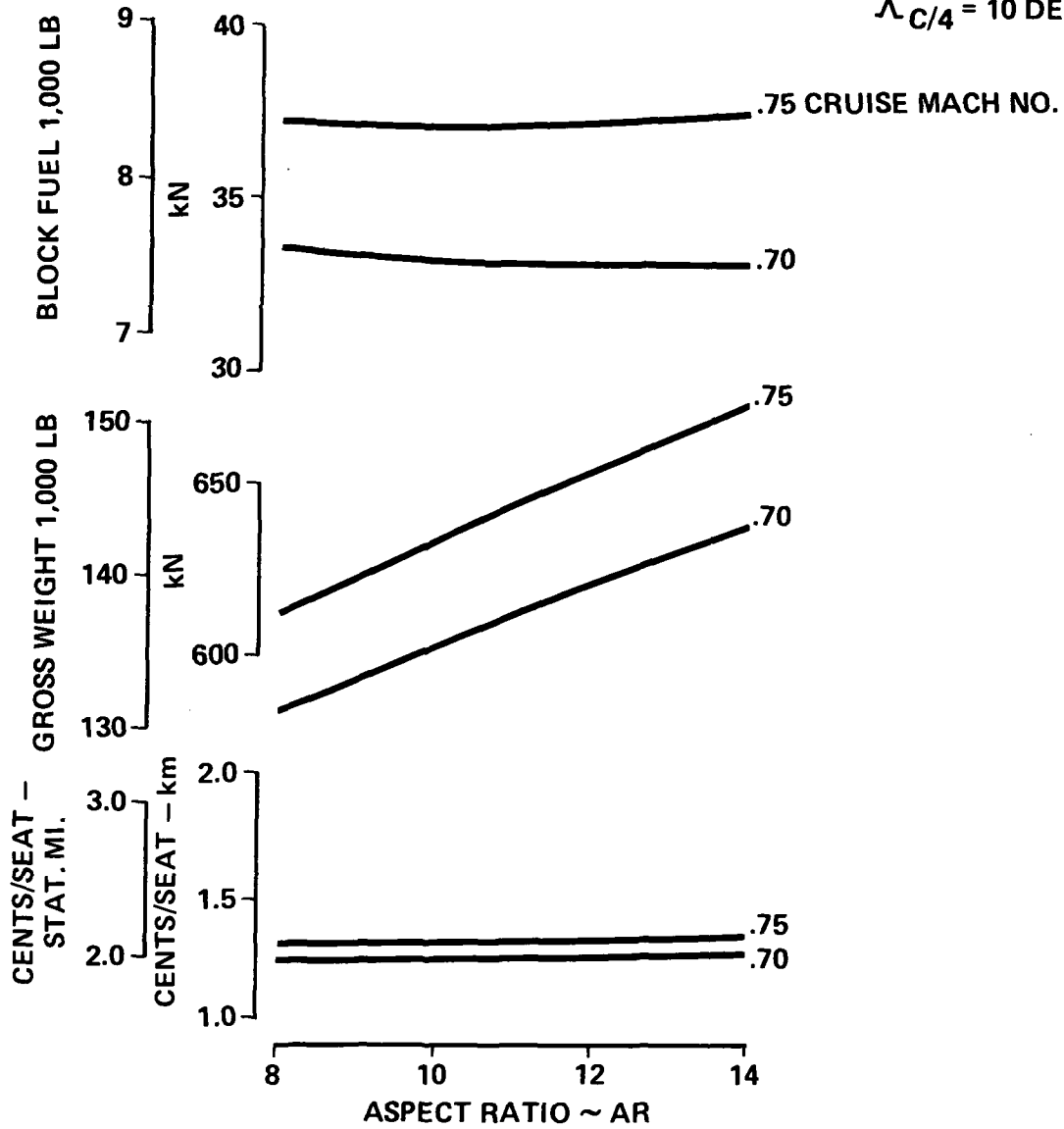
EFFECT OF CRUISE MACH NUMBER AT
10,100 m (33,000 FT) Q-FAN PROPULSION
FIGURE 51

W/S = 2.8 kPa (58 PSF)
FPR = 1.35
λ = .3
CRUISE AT M = .7
10,100 m (33,000 FT)
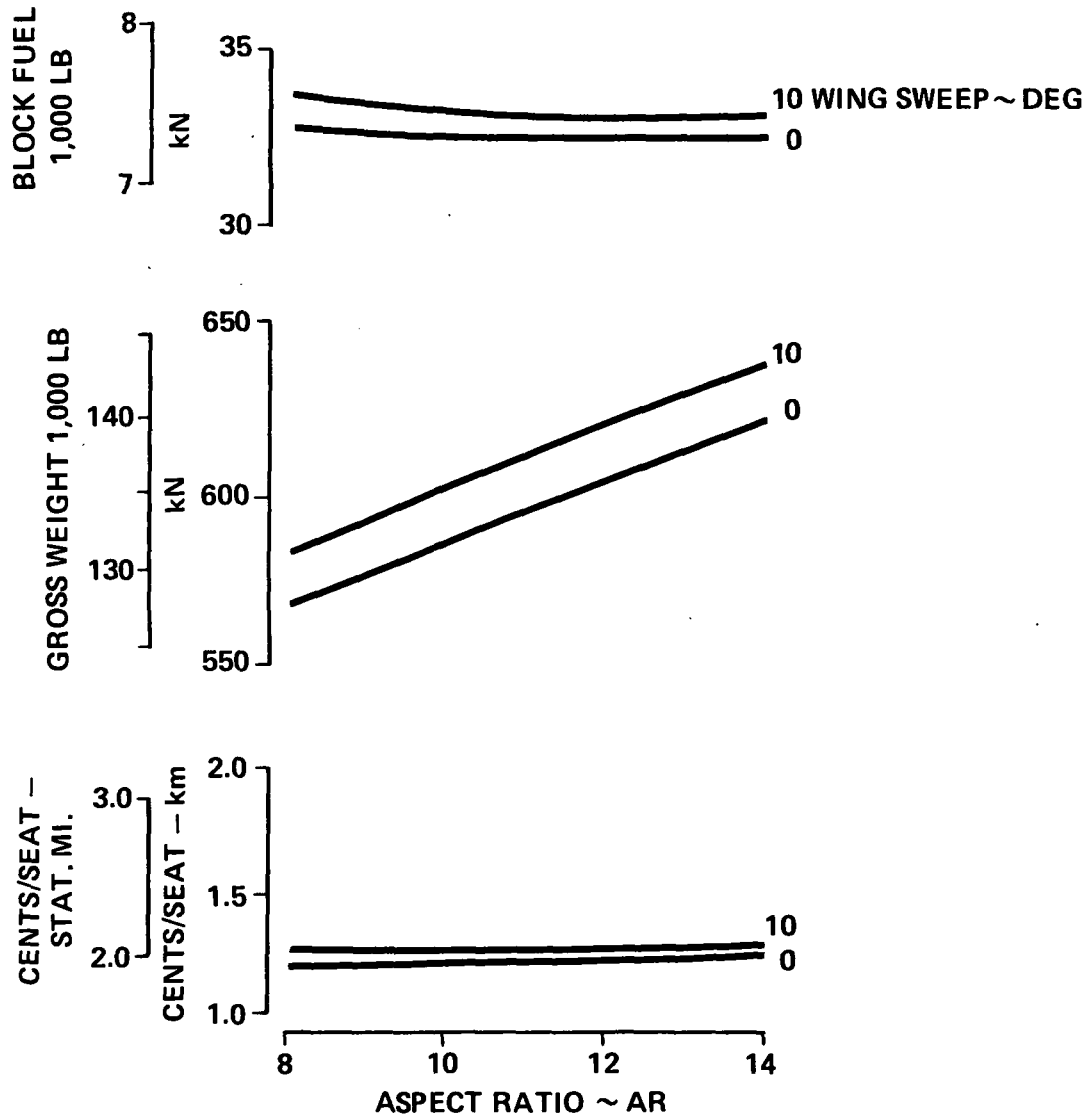
EFFECT OF WING SWEEP, Q-FAN PROPULSION
FIGURE 52

W/S = 2.8 kPa (58 PSF)
FPR = 1.35
$\lambda_{C/4}$ = 10 DEG
CRUISE AT M = .7,
10,100 m (33,000 FT)
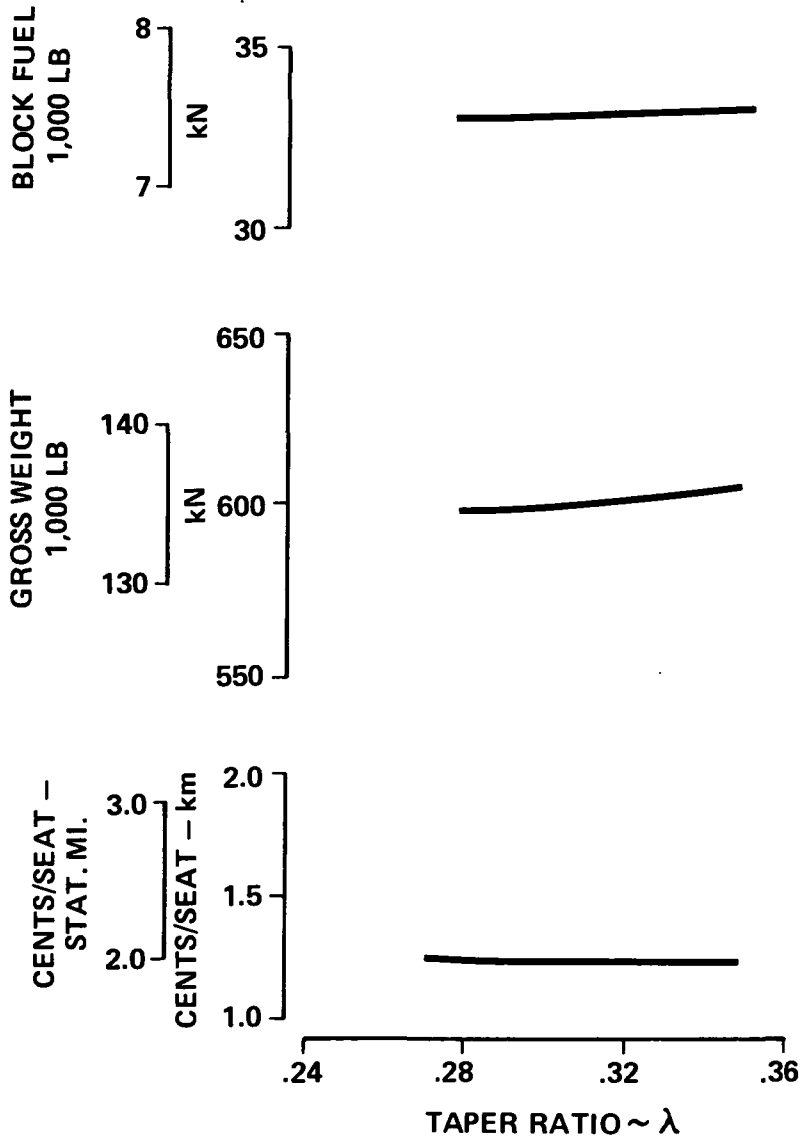
EFFECT OF TAPER RATIO, Q-FAN PROPULSION
FIGURE 53
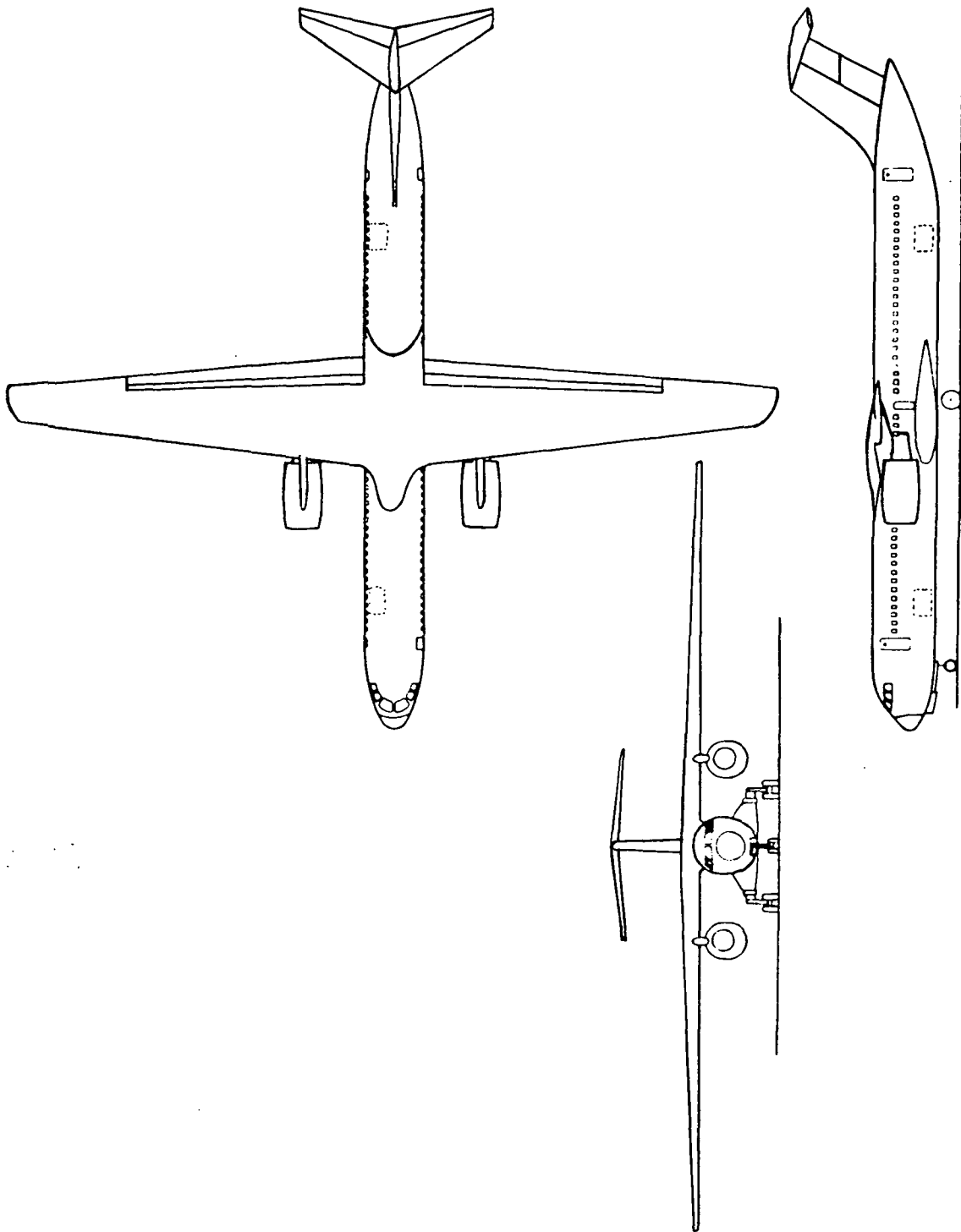
BOEING OPTIMIZED Q-FAN MECHANICAL FLAP CONFIGURATION,
FPR = 1.35, 914 m (3,000 FT) FIELD LENGTH
FIGURE 54

TABLE 14

Q-FAN PROPULSION CONFIGURATION COMPARISON TO BOEING BASELINE CONFIGURATION

	Boeing Baseline Configuration	Q-Fan Propulsion		
FPR	1.35	1.25	1.35	1.40
T/W	.33	.40	.33	.32
W/S ~ kPa (PSF)	2.8 (58)	2.8 (58)	2.8 (58)	2.8 (58)
OWE ~ N (lbf)	432,240 (97,170)	448,200 (100,760)	420,000 (94,420)	419,550 (94,320)
Payload ~ N (lbf)	134,958 (30,340)	134,958 (30,340)	134,958 (30,340)	134,958 (30,340)
Block Fuel ~ N (lbf)	37,854 (8,510)	35,010 (7,870)	33,270 (7,480)	34,210 (7,690)
Reserve Fuel ~ N (lbf)	16,948 (3,810)	15,260 (3,430)	14,410 (3,240)	14,770 (3,320)
Total Fuel ~ N (lbf)	54,800 (12,320)	50,260 (11,300)	47,680 (10,720)	48,970 (11,010)
Gross Weight ~ N (lbf)	622,010 (139,830)	633,420 (142,400)	602,640 (135,480)	603,490 (135,670)
DOC Cents/Seat – km (Cents/Seat – Statute Mi)	1.31 (2.11)	1.33 (2.14)	1.24 (1.99)	1.25 (2.01)
Wing Area ~ m^2 (Ft^2)	223.9 (2,410)	228.0 (2,454)	216.9 (2,335)	217.2 (2,338)
Vertical Tail Area ~ m^2 (Ft^2)	25.56 (275)	26.29 (283)	24.34 (262)	24.43 (263)
Horizontal Tail Area ~ m^2 (Ft^2)	31.49 (339)	32.42 (349)	30.10 (324)	30.10 (324)

TABLE 15
OPTIMIZED Q-FAN PROPULSION CONFIGURATION AERODYNAMIC GEOMETRY

Fuselage				
LF	Length	41.54 m	(136.3	Ft)
WF	Width	3.66 m	(12.0	Ft)
SF	Wetted Area	433.0 m^2	(4,661.	Sq Ft)

Wing				
AR	Aspect Ratio		(10.00)	
SW	Area	213.9 m^2	(2,302.5	Sq Ft)
B	Span	46.24 m	(151.7)	Ft)
CBARW	Geom. Mean Chord	5.06 m	(16.6	Ft)
LAMBDA C/4	Quarter Chord Sweep		(4.3	Deg)
LAMBDA	Taper Ratio		(0.300)	
(T/C)R	Root Thickness		(0.183)	
(T/C)T	Tip Thickness		(0.140)	
WG/SW	Wing Loading	2.8 kPa	(58.0	lb/Sq Ft)

Horizontal Tail				
ARHT	Aspect Ratio		(4.50)	
SHT	Area	29.44 m^2	(316.9)	Sq Ft)
BHT	Span	11.52 m	(37.8	Ft)
CBARHT	Mean Chord	2.56 m	(8.4	Ft)
(T/C)HT	Thickness/Chord		(0.120)	
LTH	Moment Arm	23.71 m	(77.8	Ft)

Vertical Tail				
ARVT	Aspect Ratio		(1.40)	
SVT	Area	23.87 m^2	(256.9	Sq Ft)
BVT	Span	5.79 m	(19.0	Ft)
CBARVT	Mean Chord	4.11 m	(13.5	Ft)
(T/C)VT	Thickness/Chord		(0.130)	
LTV	Moment Arm	20.06 m	(65.8	Ft)

Primary Engine Nacelle				
LN	Length	4.11 m	(13.5	Ft)
DBARN	Mean Diameter	2.23 m	(7.3	Ft)
SN	Wetted Area	56.44 m^2	(607.5	Sq Ft)

TABLE 16
OPTIMIZED Q-FAN PROPULSION CONFIGURATION WEIGHT AND BALANCE SUMMARY

Weight Group	N	Weight (lbf)	Horizontal Arm (Body Station)
Wing	118,980	(26,748)	742
Horizontal Tail	7,046	(1,584)	1,687
Vertical Tail	5,716	(1,285)	1,512
Fuselage	77,323	(17,383)	744
Landing Gear	23,771	(5,344)	688
Engine Struts	7,340	(1,650)	636
Engine Nacelles	9,884	(2,222)	590
Total Structure Group Weight	Σ 250,060	Σ (56,216)	773
Primary Engines	33,655	(7,566)	580
Engine Accessories	1,361	(306)	451
Engine Controls	667	(150)	451
Engine Starting System	347	(78)	580
Thrust Reversers	0	(0)	—
Fuel System	1,508	(339)	657
Total Propulsion Group Weight	Σ 37,538	Σ (8,439)	576
Instruments	2,834	(637)	330
Surface Controls	9,017	(2,027)	972
Hydraulics	3,167	(712)	747
Pneumatics	2,206	(496)	706
Electrical	6,939	(1,560)	414
Electronics	4,648	(1,045)	284
Flight Deck Accommodations	3,465	(779)	108
Passenger Accommodations	48,597	(10,925)	758
Cargo Accommodations	5,480	(1,232)	740
Emergency Equipment	1,895	(426)	582
Air Conditioning	8,069	(1,814)	622
Anti-icing	1,530	(344)	462
APU	4,395	(988)	1,359
Total Fixed Equipment Group Weight	Σ 102,242	Σ (22,985)	703
Manufacturers Empty Weight	Σ 389,840	Σ (87,640)	735
Standard and Operational Items	22,263	(5,005)	669
Operational Empty Weight	Σ 412,103	Σ (92,645)	732 20.0% MAC
Payload	134,958	(30,340)	750
Fuel	47,182	(10,607)	737
Gross Weight	Σ 594,244	Σ (133,592)	736 21.5% MAC

TABLE 17
SUMMARY OF Q-FAN PROPULSION BENEFITS

AR = 10

W/S = 2.8 kPa (58 PSF)

λ = .3

	Boeing Baseline Configuration	Q-Fan Propulsion	Percent Reduction
FPR.	1.35	1.35	—
T/W	.33	.33	—
Λc/4 ~ Deg	10	4.3	—
OWE ~ N (lbf)	432,240 (97,170)	412,080 (92,640)	5
Payload ~ N (lbf)	134,958 (30,340)	134,958 (30,340)	—
Block Fuel ~ N (lbf)	37,854 (8,510)	32,920 (7,400)	13
Reserve Fuel ~ N (lbf)	16,948 (3,810)	14,280 (3,210)	16
Total Fuel ~ N (lbf)	54,800 (12,320)	47,200 (10,610)	14
Gross Weight ~ N (lbf)	622,010 (139,830)	594,240 (133,590)	4
*DOC ~ Cents/Seat — km (Cents/Seat — Statute Mi)	1.31 (2.11)	1.23 (1.98)	6

*Based on 12 cents/km^3 (46 cents/gal) fuel cost

selected for further study with Active Controls Technology (ACT) has a wing quarter chord sweep of 4.3 degrees. This configuration, although slightly heavier than the upswept wing has 0 degree sweep of the aft wing spar. It is anticipated that implementation of aerodynamic surfaces for the application of ACT will be simplified with an unswept aft spar.

In summary, the 13 percent fuel savings possible with the Q-fan propulsion system makes it a serious candidate for low-wing-loading transport aircraft designed to operate in the short-haul market. These findings indicate this propulsion concept warrants further development that would lead to the demonstration of an engine.

ACTIVE CONTROL TECHNOLOGY

The application of active control technology to low-wing-loading, short-haul transport configurations has two main purposes. The first purpose is to obtain the fuel savings possible from the reduced structural weight by reduction of design gust load.factor and tail sizes. The second purpose is to improve the ride quality and make the low-wing-loading performance advantages possible without degrading the passenger ride comfort in turbulence. The objective of the ride quality concept is to restore the ride quality to the comfort level experienced on jet transports of today.

The ACT features evaluated were Gust Load Alleviation (GLA), Relaxed Static Stability (RSS) and Ride Quality Improvement (RQI). The analytical approach taken to evaluate these ACT features was to determine first how applicable each are to the low-wing-loading, short-haul transport configuration separately and then to combine them into a single multipurpose active control system configuration. This section covers the study results of each of the three ACT features separately. The combined analysis results are reported in the next Section.

The fuel conservative transport configuration, used as a baseline for the ACT analysis, was the optimized Q-fan propulsion configuration described in "Q-Fan Baseline Configuration." The important parameter relevant to the application of ACT to this configuration is that the design was gust load critical at V-cruise design condition. The FAR Part 25 gust load factor was 4.2 g's which means there is a potential reduction of 1.7 g's for the GLA system to reduce the design load factor to the maneuver limit, (2.5 g's).

The maximum speed flight envelope for the baseline configuration is presented in Figure 55.

The longitudinal response characteristics of the Q-fan propulsion system baseline configuration is presented in Table 18 for cruise, high-speed dive and landing approach flight conditions. The longitudinal stability derivatives for the respective flight conditions are presented in Table 19. All ACT analyses were conducted based on the assumption of a rigid system.

Gust Load Alleviation

The design philosophy for applying the gust load alleviation concept to the fuel conservative transport was to keep the control surfaces as simple and

TABLE 18
Q-FAN PROPULSION BASELINE STABILITY CHARACTERISTICS

Mid CG = 36 % MAC	Cruise	High-Speed Dive	Approach
Configuration	Clean	Clean	Flaps 40
Mach/$V_E \sim$ m/s (Kts)	.70/121 (236)	.75/180 (350)	.13/44 (86)
Altitude $\sim$ m (Ft)	10,100 (33,000)	5,500 (18,000)	S.L.
Gross Weight $\sim$ N (lbf)	578,300 (130,000)	549,400 (123,500)	562,300 (126,400)
Short Period			
Freq. $(\omega_\eta) \sim$ Hz	.26	.45	.12
Period (T) $\sim$ Sec	5.2	4.1	16.8
Damping (ζ)	.67	.83	.87
Time ½ Ampl. $(T_{1/2}) \sim$ Sec	.62	.30	1.05
Phugoid			
Freq. (ω_η) Hz	.0086	.0067	.031
Period (T) $\sim$ Sec	115.7	150.0	32.9
Damping (ζ)	.039	.111	.108
Time ½ Ampl. $(T_{1/2}) \sim$ Sec	323.	148.	33.1

TABLE 19

Q-FAN PROPULSION BASELINE STABILITY AND CONTROL DERIVATIVES

	Flight Conditions		
	Cruise	High Speed Dive	Landing
Configuration	Clean	Clean	Flaps 40/Gear Down
Mach No./V_e ~m/s (Knots)	.70/121 (236)	.75/180 (350)	.13/44 (86)
Altitude~m (Ft)	10,100 (33,000)	5,500 (18,000)	S.L.
Gross Weight~N (lbs)	578,300 (130,000)	549,400 (123,500)	562,300 (126,400)
I_{yy} ~kg-M^2 (Slugs-FT^2)	5,420,000 (4,000,000)	5,290,000 (3,900,000)	5,360,000 (3,950,000)
CG ~ % MAC	36.0	36.0	36.0
C_{L_o}	.300	.130	2.23
C_{L_α} ~1/Rad	8.65	9.14	7.73
$C_{L_{\hat\alpha}}$ ~1/Rad	2.01	2.20	1.38
$C_{L_{\hat q}}$ ~1/Rad	6.56	6.78	5.66
C_{D_o}	.0192	.0156	.4462
C_{D_α} ~1/Rad	.184	.0713	1.113
dC_D/dC_L	.0225	.0078	.144
C_{M_o}	0	0	0
C_{M_α} ~1/Rad	-1.02	-1.02	-.873
$C_{M_{\hat\alpha}}$ ~1/Rad	-9.42	-10.3	-6.44
$C_{M_{\hat q}}$ ~1/Rad	-30.6	-31.7	-26.5

conventional as possible. Therefore, aileron and spoiler control surfaces were selected as opposed to a movable trailing edge flap. The amount of elevator control available for gust load alleviation was limited by consideration of passenger ride quality at the rear of the passenger compartment. For the elevator to provide gust load alleviation, the airplane must be rotated and the elevator input required to produce this rotation causes accelerations that could be unacceptable to passengers.

Two design limitations were considered in defining the gust load alleviation design flight conditions. The first was the maximum flight load factors specified in FAR Part 25 Airworthiness Standards for Transport Category airplanes. The second was the maximum wing root bending moment while operating within the flight envelope. The peak load factor for FAR Part 25 occurs at maximum gross weight. Since the wing weight algorithm is based on the peak wing root bending moment, the design condition was based on the maximum gross weight.

Wing loads for analysis of wing structural weight assumed an elliptical lift distribution. The design objective was to reduce the outboard portion of the lift so as to attain the largest reduction in wing root bending moment. The method of computing the wing structural weight reduction, assuming an elliptical lift distribution, is therefore conservative. A detailed analysis should take into account the resultant GLA lift distribution.

Design Flight Condition. - The limiting design flight condition was determined by computing the FAR Part 25 gust load factor as a function of altitude. The variation of load factor with altitude for the V-dive and V-cruise flight speeds are presented in Figures 56 and 57, respectively. At V-cruise, the maximum load factor occurs at 5500 meters (18,000 feet) where the maximum operating Mach number and airspeed coincide (see Figure 55). Although the minimum gross weight has a larger gust load factor, the peak wing lift occurs at the maximum product of gust load factor and gross weight. This product is 2490000 N (560,000 lbf) for the maximum gross weight condition and 2140000 N (482,000 lbf) for the minimum gross weight condition. Therefore, the maximum gross weight condition is considered the most severe wing design condition.

The FAR Part 25 V-n diagram for two design gross weights are presented in Figure 58. The GLA system was evaluated at each of the cardinal points as defined in Table 20. Each GLA design point is lettered for convenient reference.

Flight Controls

Control System Description and Authority. - The analytical approach taken to determine the control surface area for the gust load alleviation was to size
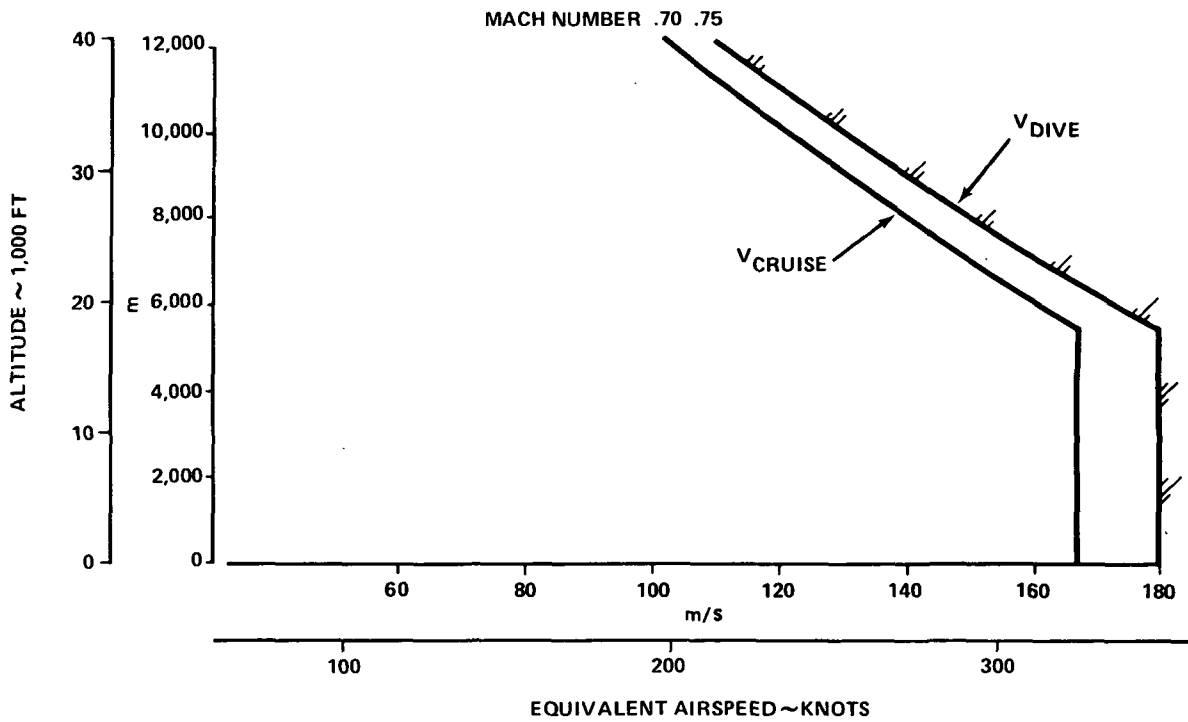
Q-FAN PROPULSION BASELINE FLIGHT ENVELOPE
FIGURE 55

TABLE 20. GUST LOAD ALLEVATION DESIGN FLIGHT CONDITIONS

	Flight Conditions					
	GLA – A	GLA – B	GLA – C	GLA – D	GLA – E	GLA – F
FAR Part 25 Design Condition	V_D		V_C		V_B	
Gust ~ m/s (FPS)	7.6 (25)		15.2 (50)		20.1 (66)	
Mach No.	.75		.70		.39	.34
V_E ~m/s (Kts)	180 (350)		167 (325)		94 (182)	78 (152)
Altitude ~ m (Ft)	5,500 (18,000)		5,500 (18,000)		5,500 (18,000)	
Gross Weight ~ N (lbf)	*588,900 (132,400)	**414,600 (93,200)	588,900 (132,400)	414,600 (93,200)	588,900 (132,400)	414,600 (93,200)

*Maximum Inflight Gross Weight

**Minimum No Reserve Gross Weight
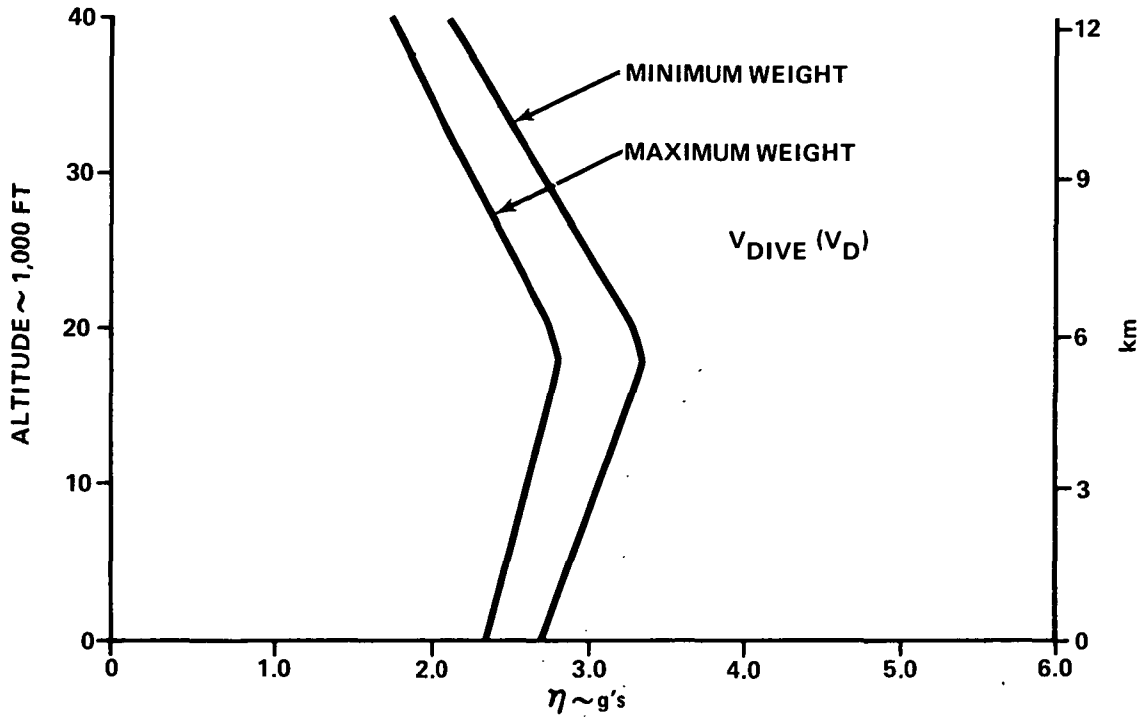
V_{DIVE} MAXIMUM GUST LOAD FACTOR VARIATION WITH ALTITUDE
FIGURE 56
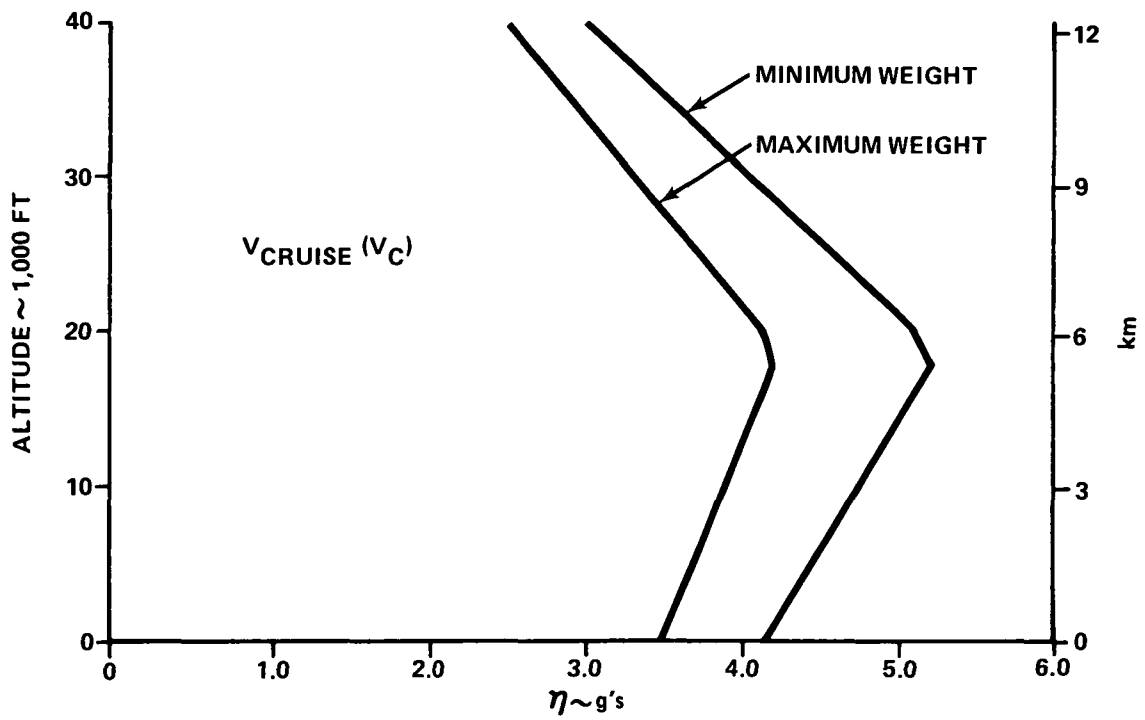
V_{CRUISE} MAXIMUM GUST LOAD FACTOR VARIATION WITH ALTITUDE
FIGURE 57

100

MINIMUM INFLIGHT WEIGHT

GW = 414,600 N (93,200 lbf)
ALT = 5,500 m (18,000 FT)
━━━ MANEUVERING ENVELOPE
━ ━ GUST ENVELOPE
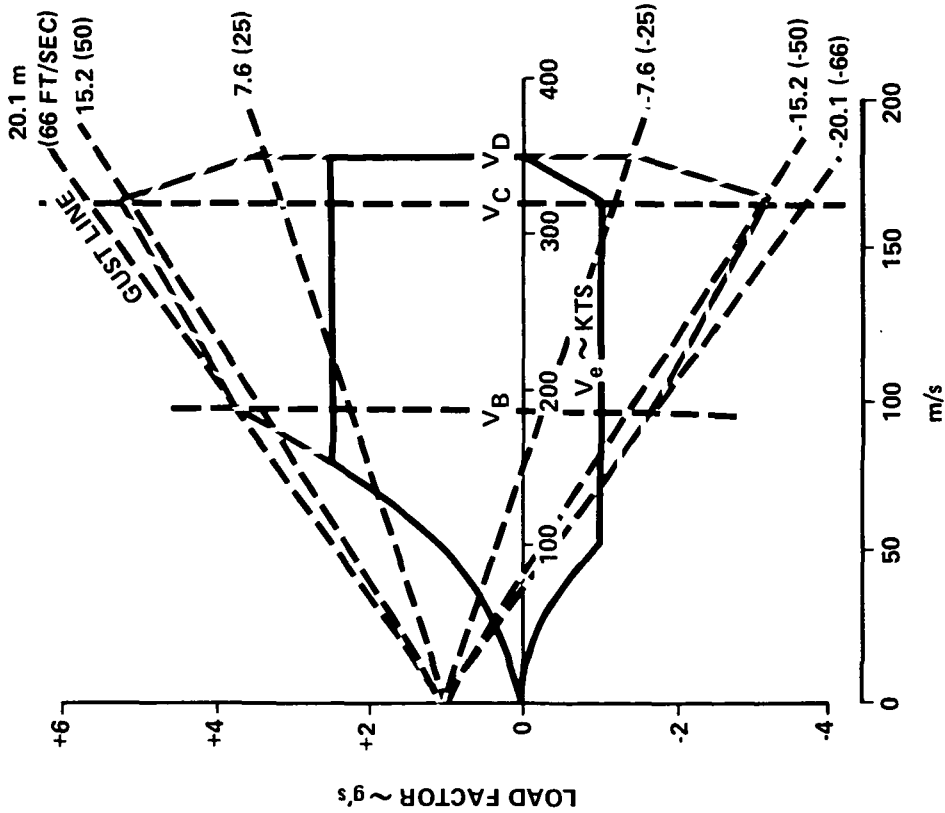
MAXIMUM INFLIGHT WEIGHT

GW = 588,900 N (132,400 lbf)
ALT = 5,500 m (18,000 FT)
━━━ MANEUVERING ENVELOPE
━ ━ GUST ENVELOPE
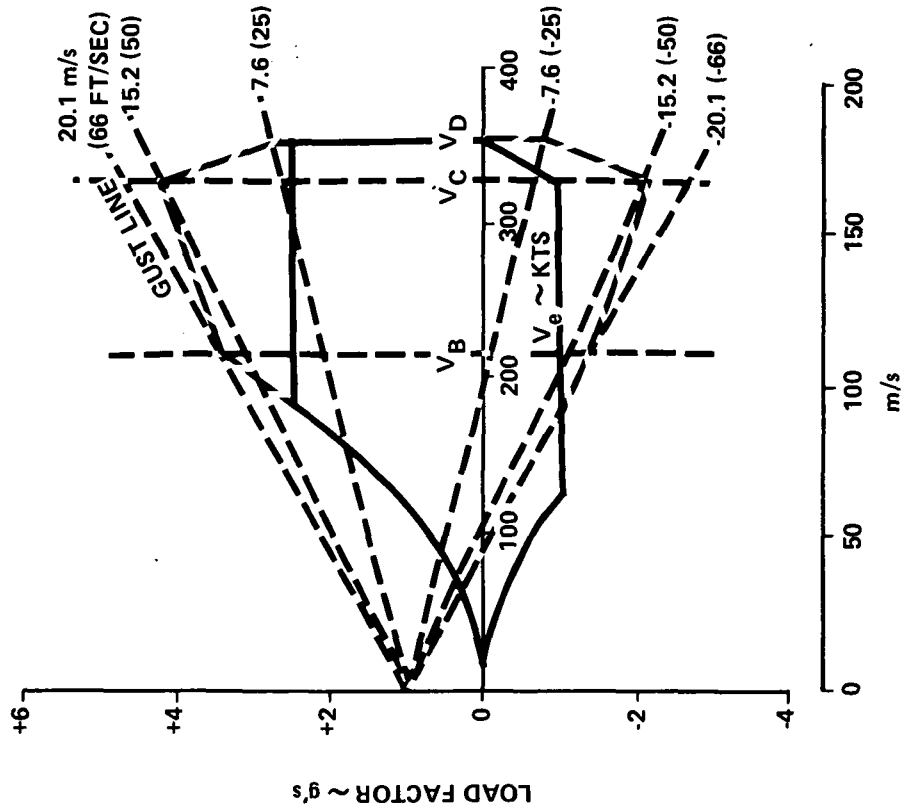
Q-FAN PROPULSION BASELINE V-N DIAGRAM
FIGURE 58

101

first the lateral control surface for roll control and then determine the gust load alleviation capability. The compatibility of these two functions is based on the maximum gust load alleviation, being an improbable event on the order of 10^{-7} and at airspeeds where the lateral control required for roll control is small. It is therefore assumed that the design objectives for these two functions can be met essentially concurrently, i.e., the pilot does not need full roll capability for the short duration of the peak gust.

The design objectives for the gust load alleviation system are to reduce the wing root bending moment and load factor due to gusts to the same level as that specified for maneuvering flight. The design objective for roll control is to achieve a 30 degree bank angle change in 2.5 seconds. The roll authority required to achieve this design objective can be approximated as follows based on a single degree-of-freedom roll response.

$$L_\delta = \frac{\phi(T)}{-\dfrac{T}{L_p} + \dfrac{e^{L_p T} - 1}{L_p^2}}$$

Outboard ailerons which can be deflected symmetrically as flaperons to reduce the wing root bending moment and asymmetrically as ailerons to provide roll control were considered in the first iteration. In this report these surfaces will be referred to as ailerons even though they do act as flaperons when performing the gust load alleviation function.

The space available for lateral controls was limited to the 27 percent of the wing span outboard of the flaps for aileron type control surfaces. The spoiler span was limited to be equivalent to the 66 percent span flaps. The requirement for full flap-span spoilers was considered to exist for reducing wing lift during landing. These spoilers were divided into three equal segments for lateral control consideration. The full 27 percent span aileron and the outboard spoiler segment referred to as Segment A control surfaces are required to meet the roll requirement on the baseline configuration. The geometry of these controls is shown in Figure 59.

The GLA capability of the outboard aileron and spoiler Segment A produce a substantial wing root bending moment reduction but failed to reduce the gust load factor as desired.

A second GLA control configuration was designed again trying to maintain the philosophy of a simple conventional control system not involving the trail edge flap segment.

OUTBOARD AILERON
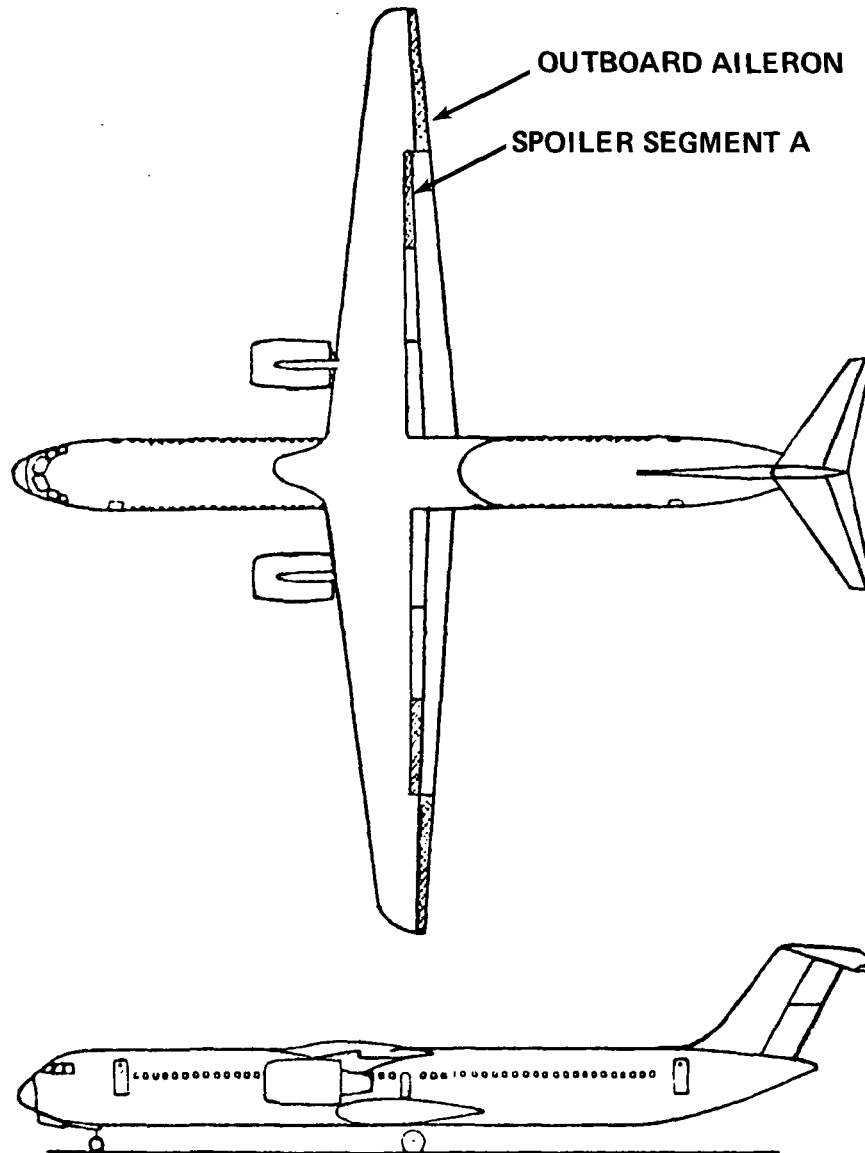
SPOILER SEGMENT A

	CONTROL SURFACE GEOMETRY PER SIDE	
	OUTBOARD AILERON	SPOILER SEGMENT A
SPAN ~ % b/2	27	22
CHORD ~ % c	25	14
AREA ~ m² (FT²)	4.57 (49.2)	2.82 (30.4)
HINGE LINE ~ % c	75	65

Q-FAN PROPULSION BASELINE CONFIGURATION CONTROL SURFACES
FIGURE 59

The wing flaps were moved outboard seven percent of the wing span to make room for an inboard aileron between the body and flaps. The primary function of this aileron was to obtain the maximum direct lift capability to reduce the load factor. This surface would then also provide the load factor control needed to perform the ride quality function on the multipurpose active control configuration. Moving the flaps outboard reduced the outboard aileron size to only 15 percent of the span. The outboard aileron plus spoiler Segments A and B were required to meet the roll control design objective on this control configuration. The geometry of these controls is shown in Figure 60.

Stability, Control and Wing Root Bending Moment Derivatives. - The airplane stability and control derivatives for the gust load alleviation analysis are summarized in Appendix C. The data are presented for the GLA control system with outboard ailerons and spoiler Segment A only and with outboard/inboard ailerons and spoiler Segments A and B.

The incremental change in wing root bending moments was determined for each of the design flight conditions as a function of wing angle of attack and deflection of each of the gust load alleviation control surfaces. The wing root bending moments were computed by integrating the change in spanwise life distribution. For this analysis, a basic elliptical lift distribution was assumed. Since this study is primarily concerned with determining the incremental improvement with a gust load alleviation system and not the absolute value of the wing root bending moment, the assumed basic lift distribution does not significantly affect the results. The incremental change in wing root bending moment due to deflecting each of the gust load alleviation control surfaces was determined by integrating the change in the spanwise lift distribution for the respective surface. The incremental change in wing root bending moments were computed to include the effect of the mass relief due to the wing structure, fuel and engines. The fuel provided less than 10 percent of the relief because of the relatively small fuel quantity. Based on a forward spar located at 15 percent chord and rear spar at 60 percent, only 17 percent of the span was required for fuel tanks. The wing root bending moment (WRBM) derivatives are presented in Appendix C.

Gust Load Alleviation System. - A preliminary gust load alleviation system was synthesized to determine the potential gains in terms of both vertical load factor and wing root bending moment reduction for the Q-fan baseline configuration. A block diagram of the system utilizing the four wing control surfaces, two ailerons and two spoilers per side is presented in Figure 61.

Gust Load Alleviation Capability. - Pursuant to the definition of gust load alleviation control concepts, airplane equations of motion were generated and programmed on an analog computer. Airplane rigid body equations of motion were generated for the gust load alleviation airplane configuration at the six flight conditions. The equations of motion generated reflect the airplane

OUTBOARD AILERON

SPOILER SEGMENT A

SPOILER SEGMENT B
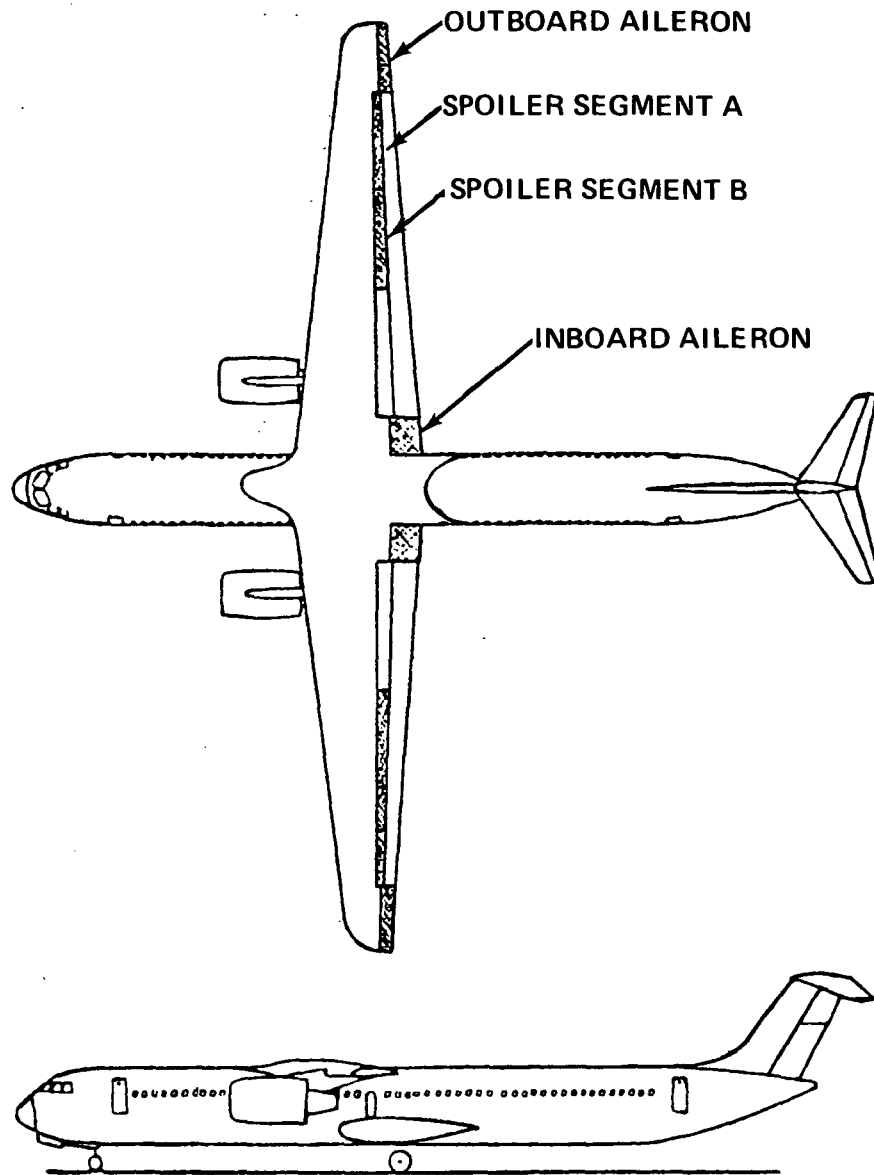
INBOARD AILERON

	CONTROL SURFACE GEOMETRY PER SIDE			
	INBOARD AILERON	OUTBOARD AILERON	SPOILER SEGMENT A	SPOILER SEGMENT B
SPAN ~ % b/2	7	15	22	22
CHORD ~ % c	25	25	14	14
AREA ~ m² (FT²)	2.81 (30.2)	2.25 (24.2)	2.60 (28.0)	3.34 (36.0)
HINGE LINE ~ % c	75	75	65	65

GUST LOAD ALLEVIATION CONFIGURATION CONTROL SURFACES
FIGURE 60
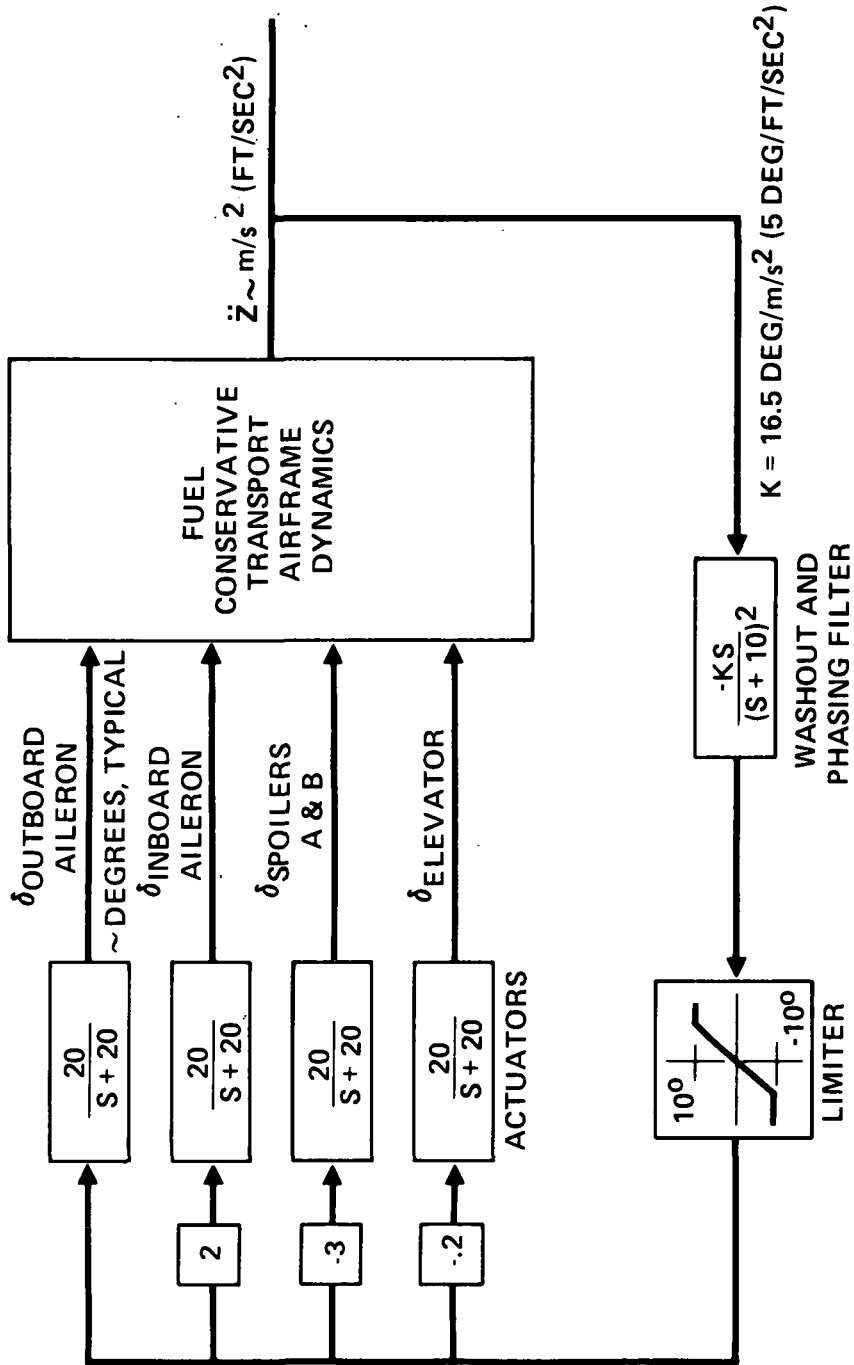
GUST LOAD ALLEVIATION CONTROL SYSTEM BLOCK DIAGRAM
FIGURE 61

106

stability and control derivatives summarized in Appendix C.

- Three airplane symmetric degrees-of-freedom
  - Vertical translation
  - Pitch
  - Longitudinal velocity perturbation

- Three control surfaces
  - Elevator
  - Outboard aileron
  - Spoiler

- Wing root bending moment equation

- (1-cos ωt) gust generating circuit

Analog computer programming was verified by comparing analog time responses to solutions obtained from a digital computer linear analysis program.

Initial definition of a GLA system considered individual control surface effectiveness for reduction of peak load factor and WRBM due to (1 - cos) gust. The first control surfaces evaluated were those defined for the baseline airplane shown in Figure 59. Elevator control had virtually no effect on the initial peak response of the load factor or WRBM.

Individual wing control surfaces provided limited reduction in peak load factor as shown in the analog time response of Figure 62. Individual outboard surfaces provided a substantial reduction in WRBM, Figure 63. To obtain a proportionate reduction in load factor, systems utilizing multiple control surfaces shown in Figure 60 were evaluated. Increased wing control surface authority utilizing multiple wing surfaces substantially reduced peak load factor, but reduced airplane short period stability. Adding a control loop with vertical acceleration feedback to the elevator compensated for the destabilizing effect of the wing control system as shown in the maneuver response of Figure 64.

The reduction in load factor attainable is determined by the available wing control surface authority, providing the elevator can be utilized to compensate for the destabilizing effect of the wing control authority. The following maximum attainable wing control surface authorities were defined for operation at the GLA design flight condition:

- Inboard ailerons ± 20 degrees

- Outboard ailerons ± 10 degrees

- Spoilers + 30 degrees

$$W_{GUST} = -\frac{U_{de}}{2} \ (1 - COS \ 11.07t)$$

CONTROL SYSTEM:

$$\delta_{\substack{OUTB'D \\ AIL.}} = K\left(\frac{S}{S+.01}\right)\left(\frac{20}{S+20}\right)\ddot{Z}_{CG}$$

FLIGHT CONDITION GLA-C
HIGH GROSS WEIGHT
CRUISE
$U_{de} = 15.2 \ m/SEC \ (50 \ FT/SEC)$
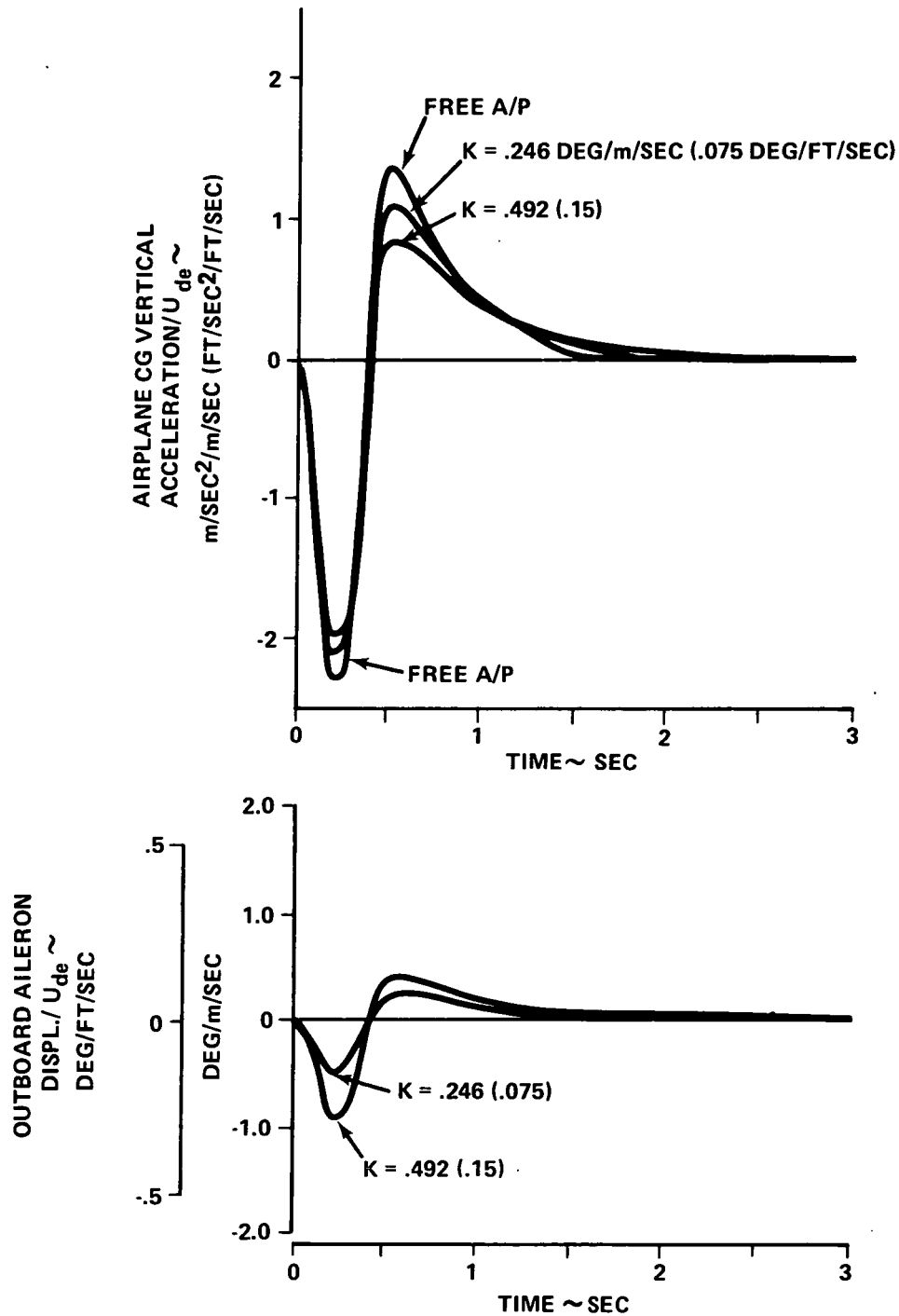
AIRPLANE VERTICAL ACCELERATION AND CONTROL SURFACE
DISPLACEMENT WITH OUTBOARD AILERON CONTROL SYSTEM
FIGURE 62

$$W_{GUST} = -\frac{U_{de}}{2} \ (1 - COS\ 11.07t)$$

CONTROL SYSTEM:

$$\delta_{\substack{OUTB'D \\ AIL.}} = K \left(\frac{S}{S+.01}\right)\left(\frac{20}{S+20}\right)\ddot{Z}_{CG}$$

FLIGHT CONDITION GLA-C
HIGH GROSS WEIGHT
CRUISE
U_{de} = 15.2 m/SEC (50 FT/SEC)

FREE A/P

$K = .246$ DEG/m/SEC (.075 DEG/FT/SEC^2)

$K = .492$ (.15)

INCREMENTAL AERODYNAMIC WING ROOT
BENDING MOMENT/U_{de}
100,000 FT-lbf/FT/SEC

MN · m/m/SEC

TIME ~ SEC
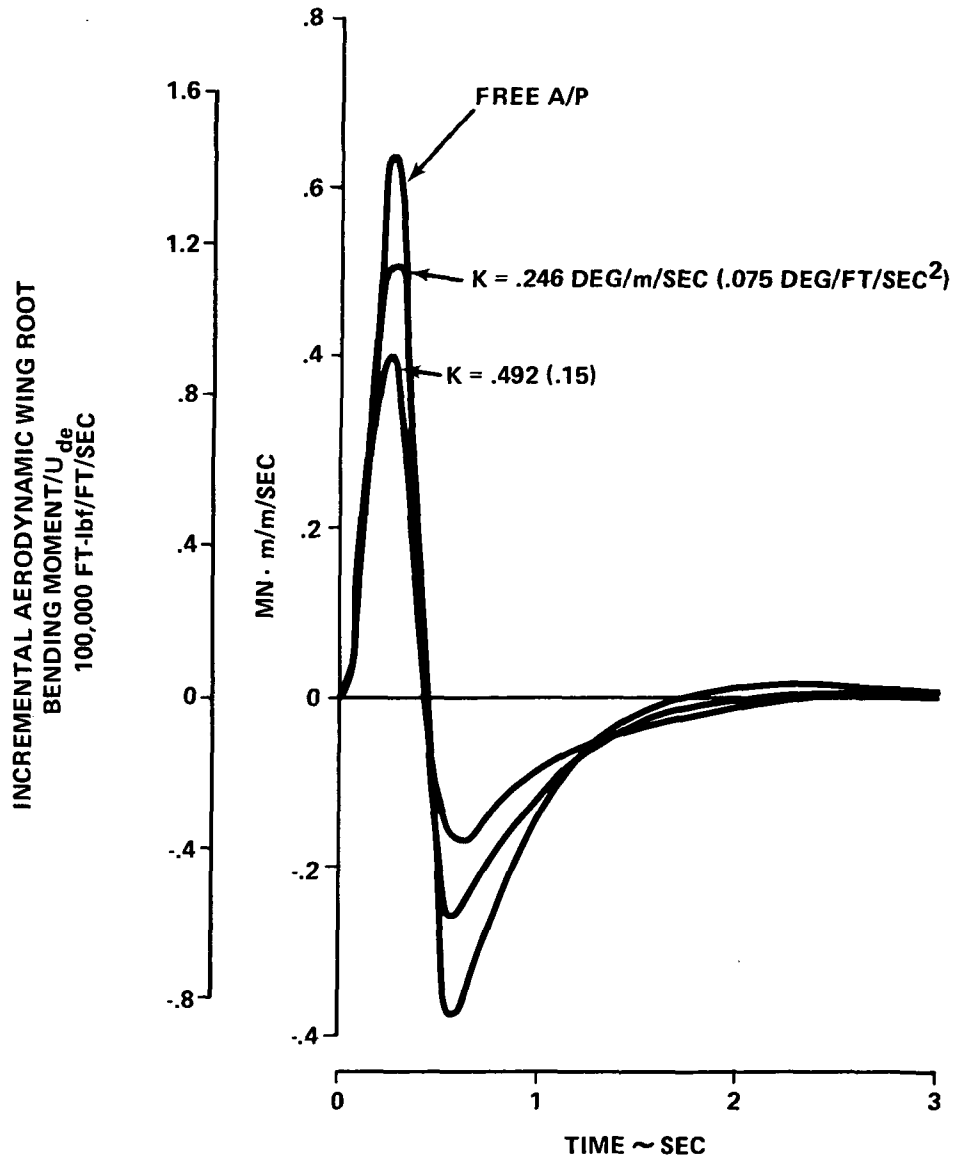
WING ROOT BENDING MOMENT REDUCTION WITH OUTBOARD
AILERON CONTROL SYSTEM
FIGURE 63

STEP ELEVATOR

CRUISE CONDITION:
WT = 414,600 N (93,200 lbf)
M = .7
ALT = 5,500 m (18,000 FT)
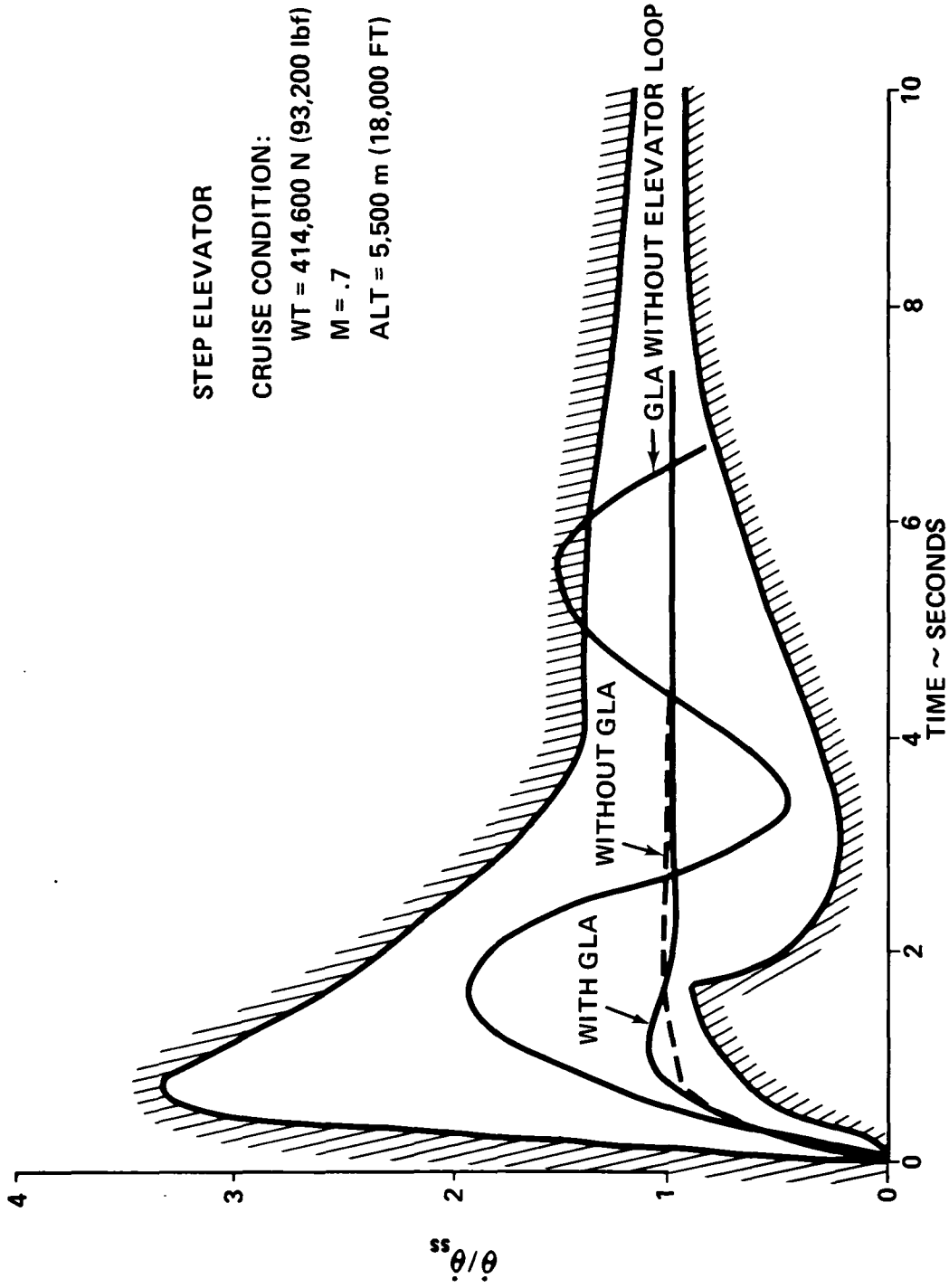
HANDLING QUALITY EVALUATION
FIGURE 64

GLA WITHOUT ELEVATOR LOOP

WITHOUT GLA

WITH GLA

TIME ~ SECONDS

$\dot{\theta}/\dot{\theta}_{ss}$

A GLA system designed to utilize the maximum wing control surface authority is shown in the block diagram of Figure 61.

The gust load factor reduction possible with the GLA was determined for each of the design conditions in Table 20. The reduction in gust load factors obtained with GLA are presented in Figure 65. The reduction can be seen to fall short of the 2.5 maneuver limit; however, it does substantially reduce the Q-fan baseline design gust load factor from 4.2 g's to 2.9 g's for the maximum gross weight condition, which is the critical condition in terms of bending moments. The peak incremental wing root bending moments are presented in Figure 66. The wing root bending moments can be seen reduced in all positive wing bending cases to values below the maneuver design loads.

The vertical load factor time response for gust load alleviation Flight Condition D is shown in Figure 67 and wing root bending moment time response for Flight Condition C is shown in Figure 68. The control surface time responses for Flight Condition D are shown in Figure 69. Maximum elevator authority required to provide acceptable stability and handling qualities with the GLA was ±2 degrees.

The time response of pitch rate due to an elevator step input shown in Figure 64 shows that the gust load alleviation system has a minimal effect on airplane handling qualities. The criteria shown were derived from References 16 and 17.

Performance Benefits. - The benefits of applying ACT concepts to a configuration are highly dependent on the particular airplane design requirements. Airplanes that have long range requirements and relatively low payload to gross weight ratios are in general more susceptible to improvements by the incorporation of ACT. It also follows that airplanes with relatively short range requirements and high payload to gross weight ratios will show a relatively small improvement due to the incorporation of ACT. For an ACT concept to show a significant improvement for an airplane with short range/high payload requirements, the concept must have a large impact on the airplane empty weight.

The relative performance improvement for the GLA and RSS systems were determined separately to help understand the net performance gain resulting from combining the three ACT systems (GLA, RSS and RQI) into the multipurpose active controls configuration. The analysis did not include a weight penalty for the respective system and therefore represents the maximum potential gain. The gross weight reduction possible with the GLA system is presented in Figure 70. For this particular design, the GLA system offers a significant improvement because it offers a very large reduction in the design load factor, and hence the structural weight of the airplane. From Figure 70, it appears that

MANEUVERING ENVELOPE
GUST ENVELOPE WITHOUT GLA SYSTEM
GUST ENVELOPE WITH GLA SYSTEM
REDUCTION IN GUST ENVELOPE

MINIMUM INFLIGHT WEIGHT
GW = 414,600 N (93,200 lbf)
ALT = 5,500 m (18,000 FT)

MAXIMUM INFLIGHT WEIGHT
GW = 588,900 N (132,400 lbf)
ALT = 5,500 m (18,000 FT)
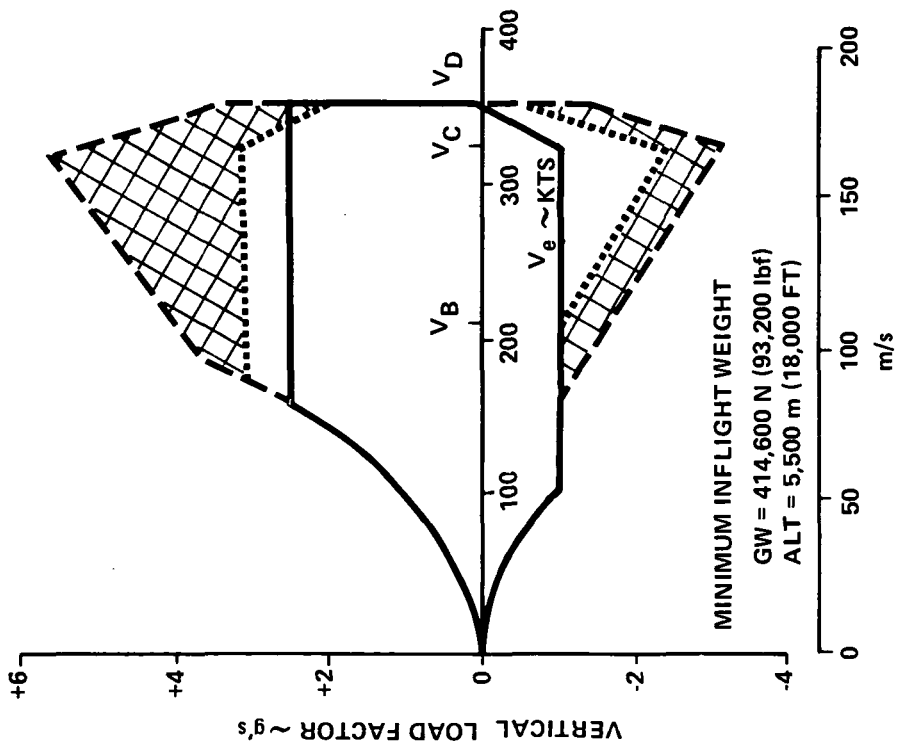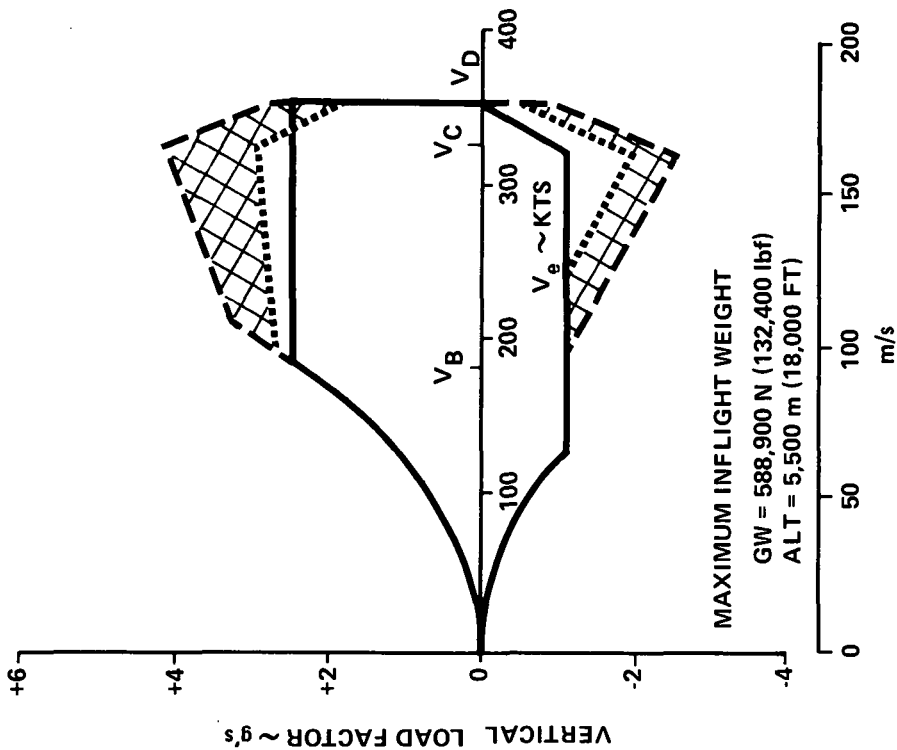
GUST LOAD ALLEVIATION IMPROVEMENT
FIGURE 65

112
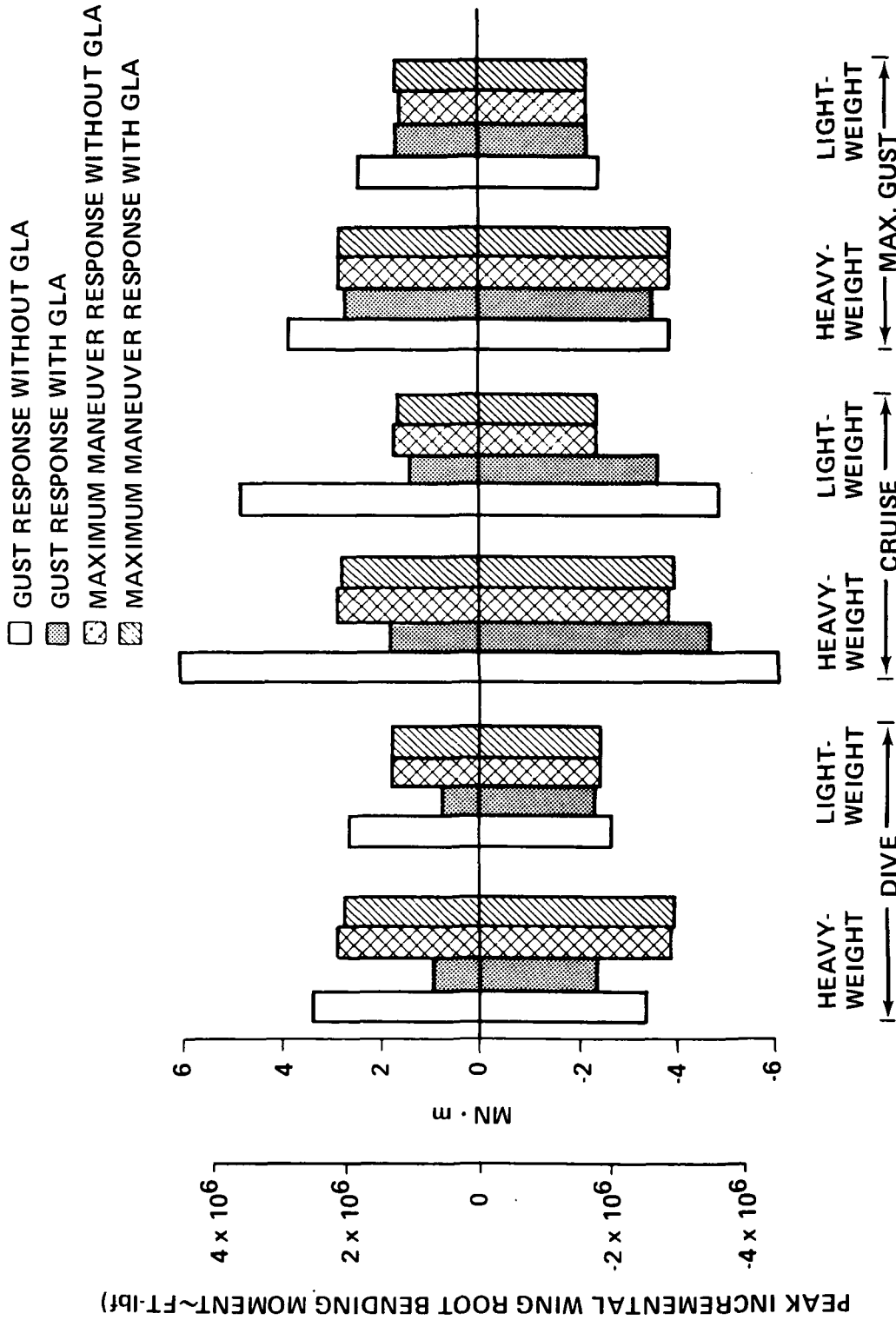
PEAK WING ROOT BENDING MOMENT FOR DESIGN 1-COS
GUST AND MAXIMUM MANEUVER
FIGURE 66

113

CRUISE CONDITION:

WT = 414,600 N (93,200 lbf)

M = .7

ALT = 5,500 m (18,000 FT)

U_{de} = 15.2 m/s (50 FT/SEC)

$$Wg = -\frac{U_{de}}{2} \ (1 - COS\ 11.07t)$$
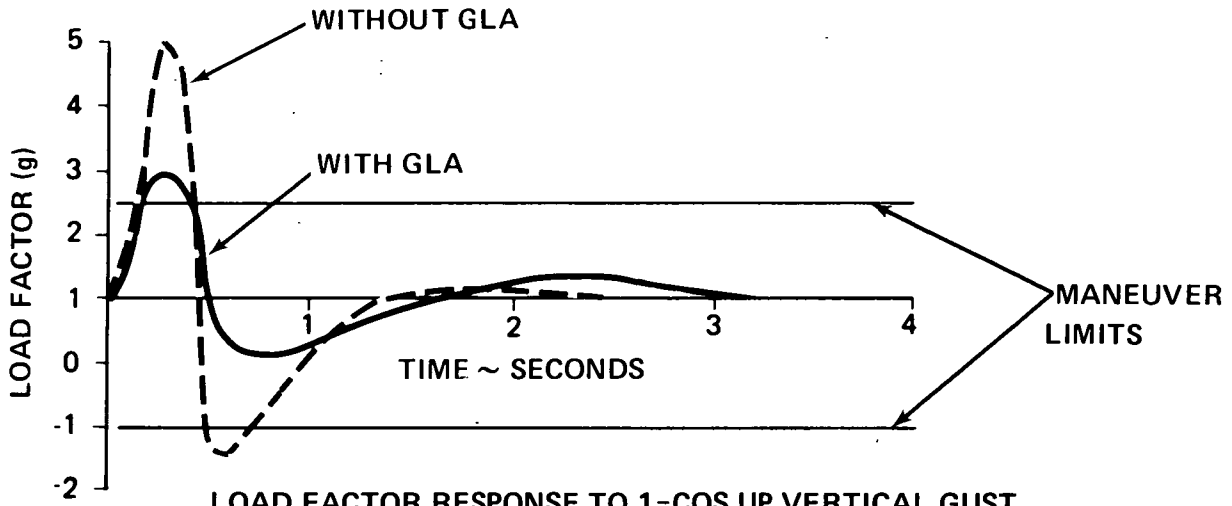
LOAD FACTOR RESPONSE TO 1-COS UP VERTICAL GUST
FIGURE 67

CRUISE CONDITION:

WT = 588,900 N (132,400 lbf) $Wg = -\frac{U_{de}}{2} \ (1 - COS\ 11.07t)$

M = .7

ALT = 5,500 m (18,000 FT)
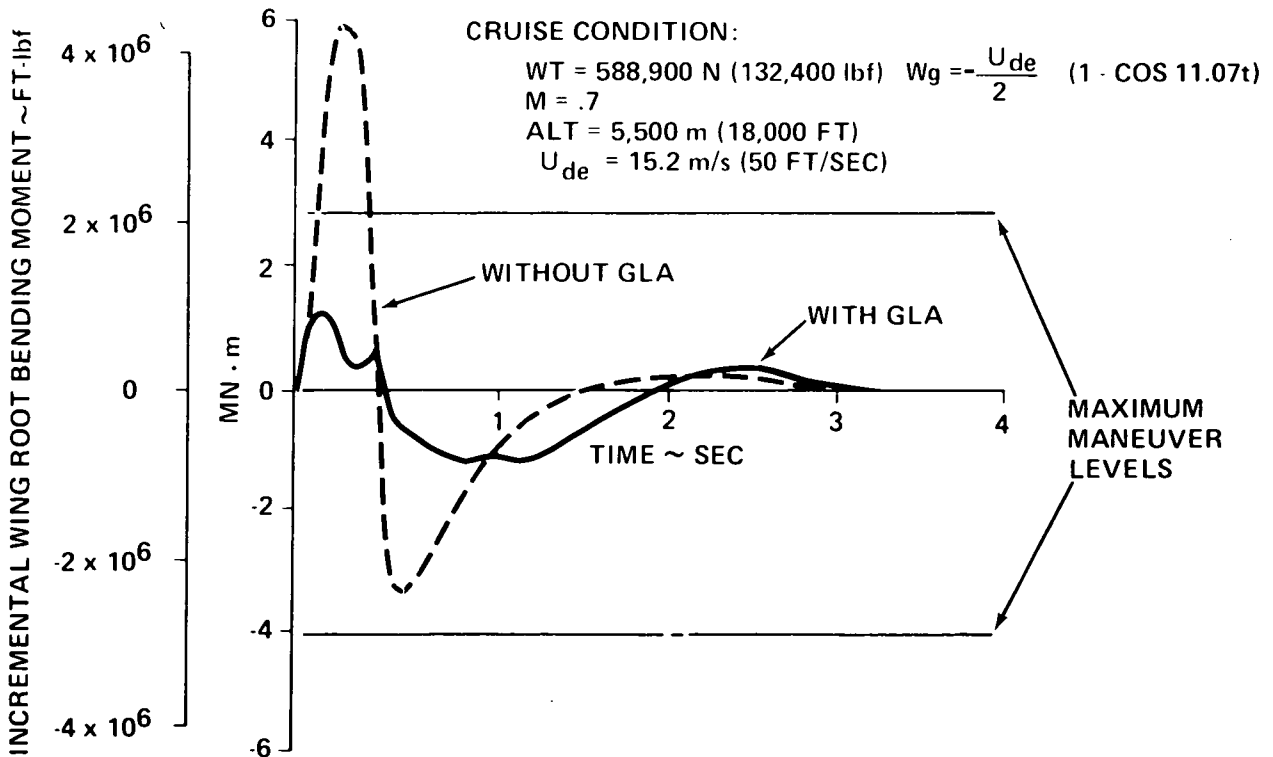
U_{de} = 15.2 m/s (50 FT/SEC)

WING ROOT BENDING MOMENT RESPONSE TO 1-COS UP GUST
FIGURE 68

114
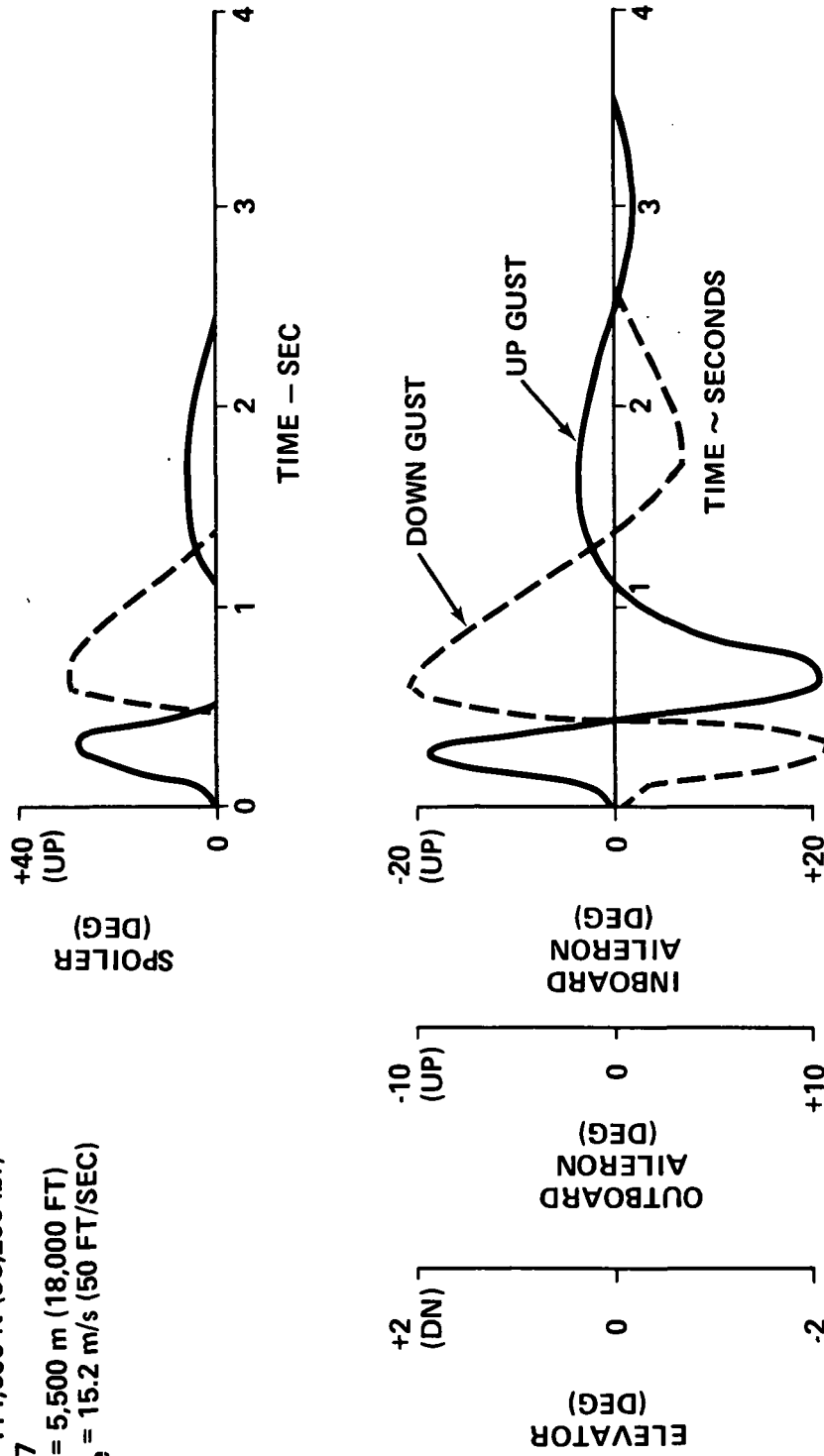
GUST LOAD ALLEVIATION CONTROL SURFACE RESPONSE TO 1-COS GUST
FIGURE 69

115

NOTE: NO WEIGHT INCLUDED FOR GLA SYSTEMS
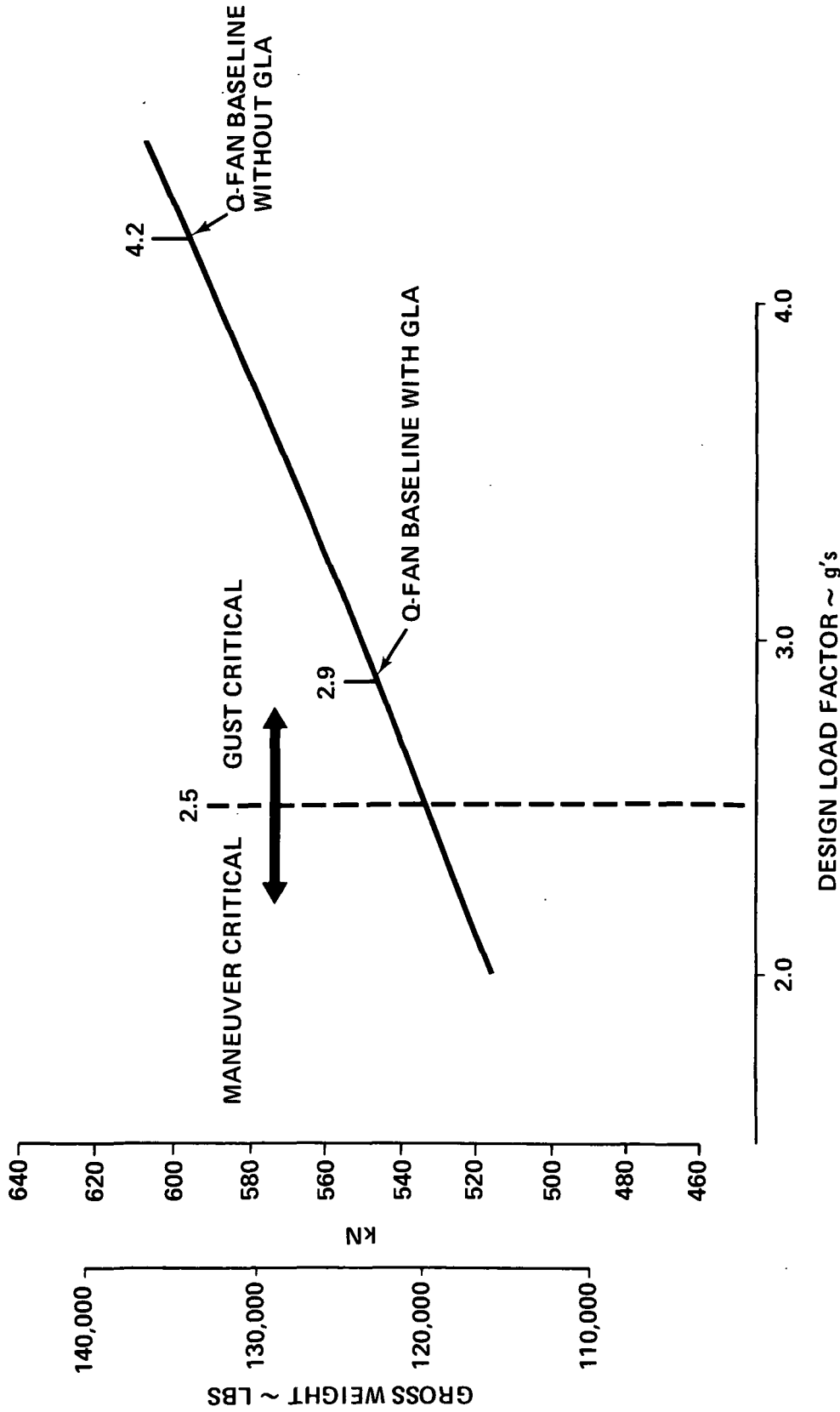
GROSS WEIGHT VARIATION WITH DESIGN LOAD FACTOR
FIGURE 70

further potential improvement would be available by reducing the design gust load factor from 2.9 to 2.5. This possible reduction was not pursued because it was felt that the added system complexity would probably offset the potential reduction in gross weight.

A conventional low-wing-loading short haul transport is feasible with RQI. The benefits of RQI can be determined by comparing a low-wing-loading, short haul configuration to a high-wing-loading configuration designed to accomplish the same mission. This comparison was not accomplished in this study and, as a result, the RQI system has been included in the ACT system weight and cost penalties without any weight benefit contributed to the RQI concept. Therefore, the real ACT benefit is somewhat larger than presented in this study when the saving of low-wing-loading attainable with RQI versus high-wing-loading is included.

<div align="center">Relaxed Static Stability</div>

The objective of this relaxed static stability analysis was to assess the potential weight savings that could accompany reduction in the vertical and horizontal tail surfaces. The relaxed static stability concept deviates from the conventional design practice of sizing the airplane tail to provide the required stability by incorporating a full time stability augmentation system to meet the stability requirement.

The horizontal tail is conventionally sized in the manner presented in "Tail Sizing". With the stability constraint removed, the aft center of gravity becomes limited by a nose-down trim requirement. The horizontal tail sizing schematic, shown in Figure 8, then appears as shown in Figure 71. This design is normally characterized by the wing being moved further forward to obtain a balanced airplane within the center of gravity range. The operating center of gravity range is normally further aft and may encompass or be aft of the inherent neutral point or maneuver point. This center of gravity location is advantageous from an elevator maneuver requirement since the reduced horizontal tail size proportionately decreases the elevator effectiveness ($C_{M_{\delta e}}$). With the center of gravity close to the maneuver point, the elevator deflection per g can be maintained to a reasonable value to meet the maneuver requirement in terms of pulling design maneuver load factor. The elevator per g for a pullup can be approximated as follows:

$$\frac{d\delta_e}{dn_z} = \frac{W}{q \, S \, C_{M_{\delta e}}} \left[\frac{dC_M}{dC_L} + \frac{C_{M_q} \, \bar{c} \, \rho \, g \, S}{4 \, W} \right]$$

NOSE DOWN TRIM — CLIMB

NOSE DOWN TRIM — APPROACH

$\ddot{\theta}_{LIMIT}$

CG

REQUIRED
CG RANGE

TAKEOFF ROTATION (MAIN LANDING
GEAR PLACED FOR STEERING
REQUIREMENT AT AFT CG LIMIT)

NOSE UP TRIM — APPROACH

NOSE UP TRIM — CLIMB

$S_{H/S}$
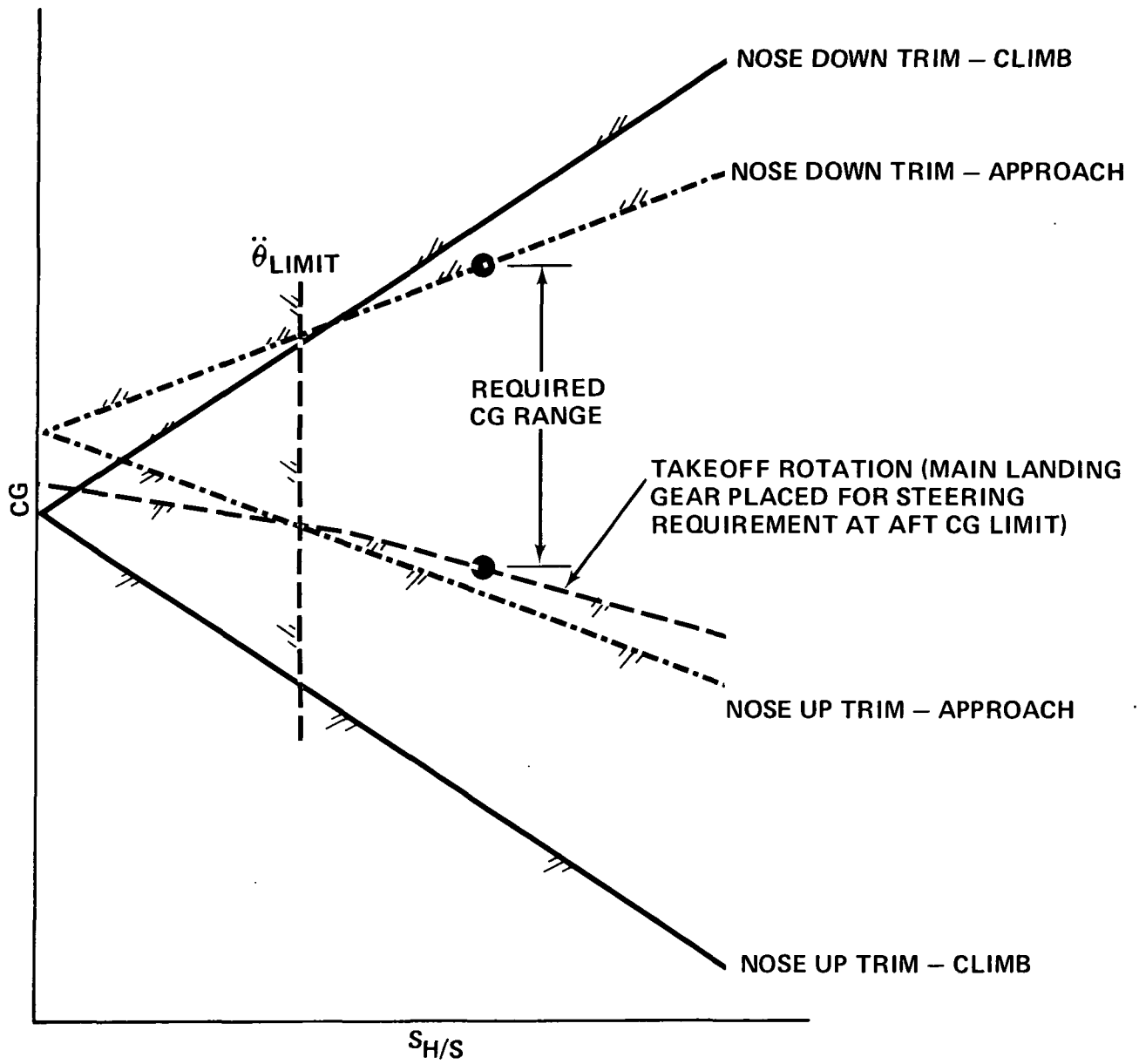
RELAXED STATIC STABILITY HORIZONTAL TAIL SIZING SCHEMATIC
FIGURE 71

118

The vertical tail is conventionally sized in the manner presented in "Vertical Tail Sizing." With the stability constraint removed, the tail size may or may not be affected depending on the engine-out control requirement.

Horizontal Tail Sizing. - The relaxed static stability horizontal tail size was determined for the Q-fan baseline configuration based on the following criteria:

- Maintain the same trim requirements as used to size the baseline airplane horizontal tail.

- Maintain the same maneuver requirements as used to size the baseline airplane horizontal tail.

- Provide the same center of gravity range as used on the baseline airplane.

- No inherent minimum level of static stability required.

- Provide sufficient elevator authority in addition to that required in the second item above to provide the SAS with sufficient authority to stabilize the aircraft throughout the flight envelope.

The variation in horizontal tail area with center of gravity location is shown in Figure 72 for a constant tail arm. The minimum horizontal tail area for a 20 percent center of gravity range is also indicated in Figure 72. The forward center of gravity limit is dictated by the takeoff rotation requirement and the aft center of gravity limit is dictated by the nose-down trim required for the landing approach. To balance the airplane, it was necessary to move the wing 1.78 meters (70 inches) forward. Using the resulting tail arm, a 30 percent reduction in horizontal tail size was obtained.

A check on the maneuver criteria was made by comparing the elevator per g requirements of the baseline configuration to the relaxed stability configuration. The comparison is presented in Figure 73. The center of gravity range of the relaxed stability configuration which was based on trim and maneuver conditions, can be seen to straddle the maneuver point. This center of gravity range allows maximum maneuvering for given elevator authority. During the landing approach, the maximum elevator per g for the relaxed static stability airplane is about half that of the baseline configuration. The SAS authority requirement was evaluated in detail for the ACT configuration.

A summary drawing of the relaxed static stability horizontal tail configuration is presented in Figure 74.
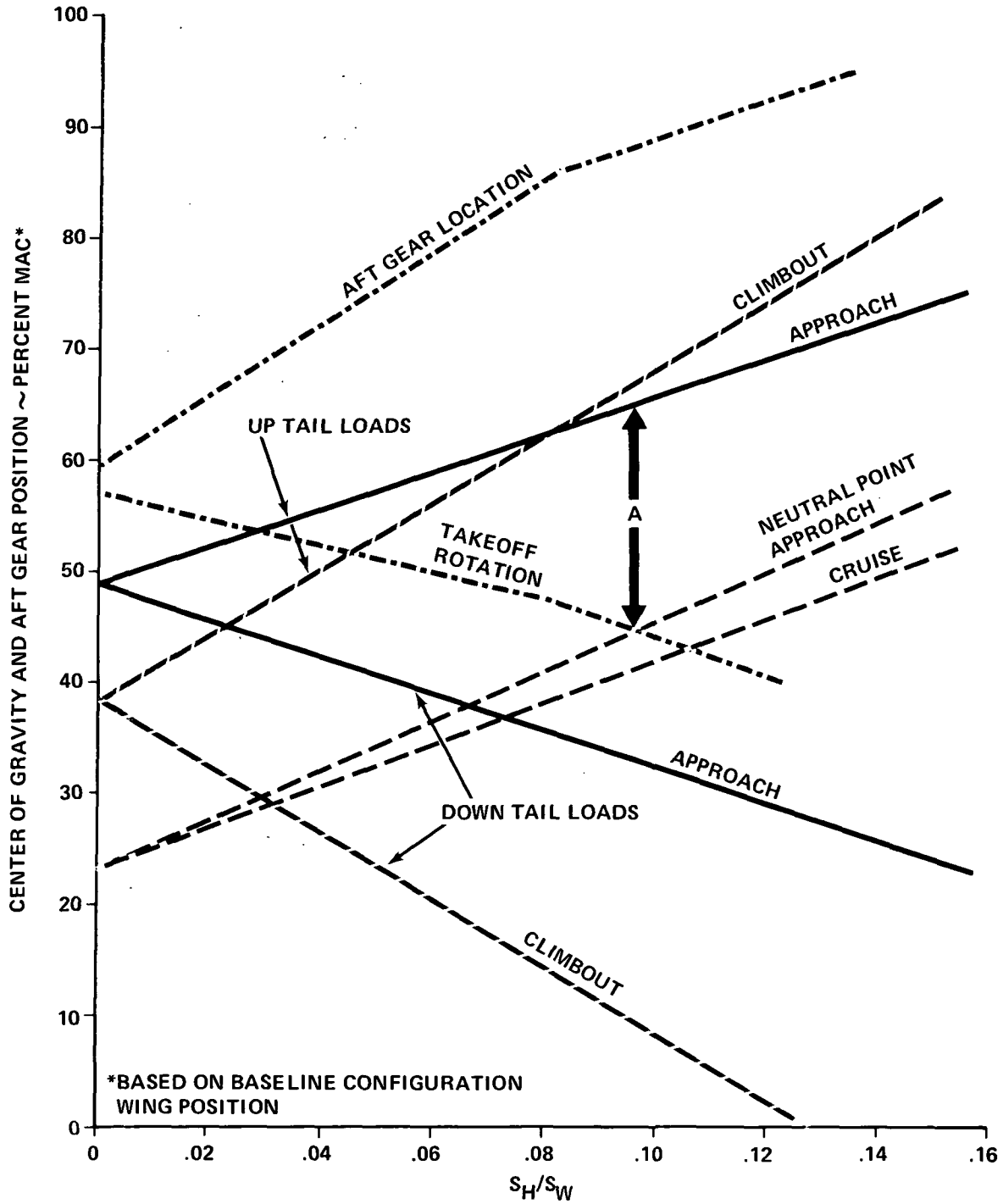
HORIZONTAL TAIL SIZING – RELAXED STATIC STABILITY CONFIGURATION
FIGURE 72
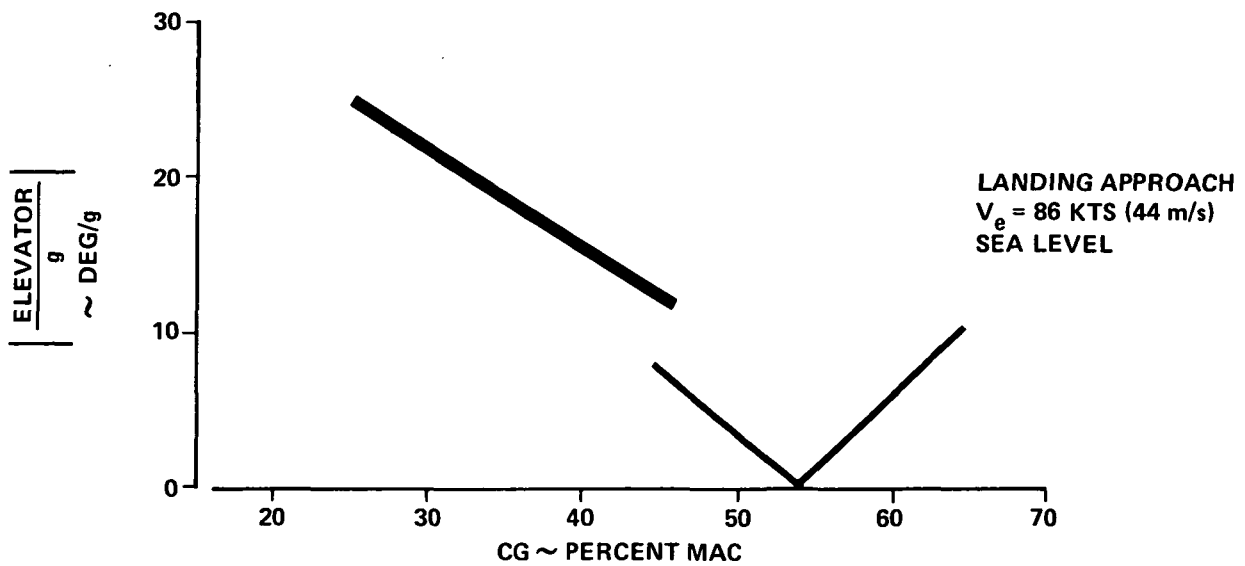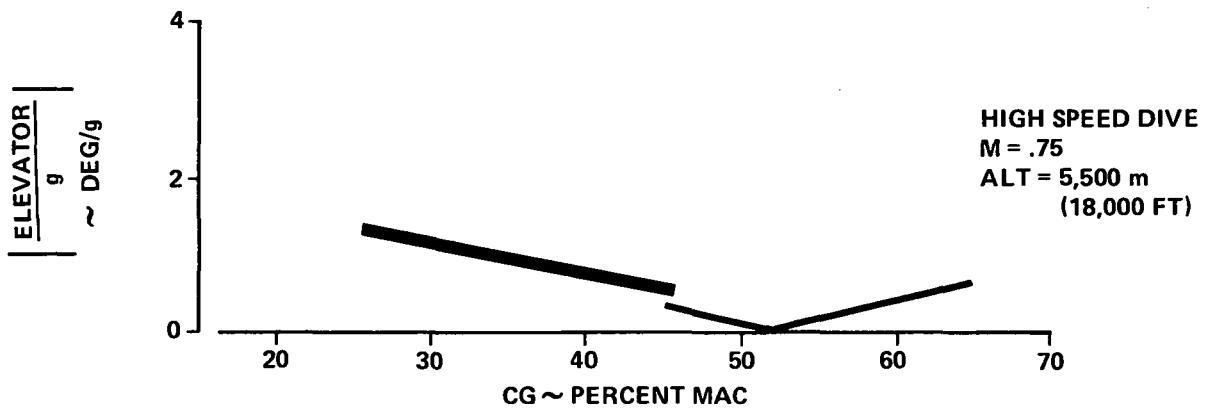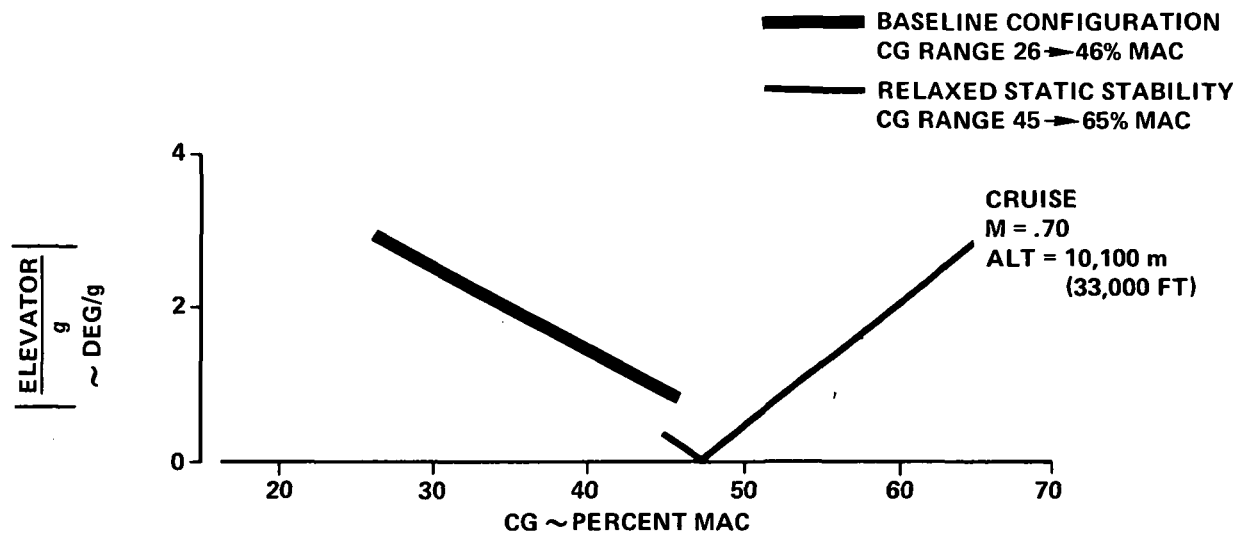
ELEVATOR REQUIRED PER INCREMENTAL LOAD FACTOR
FIGURE 73
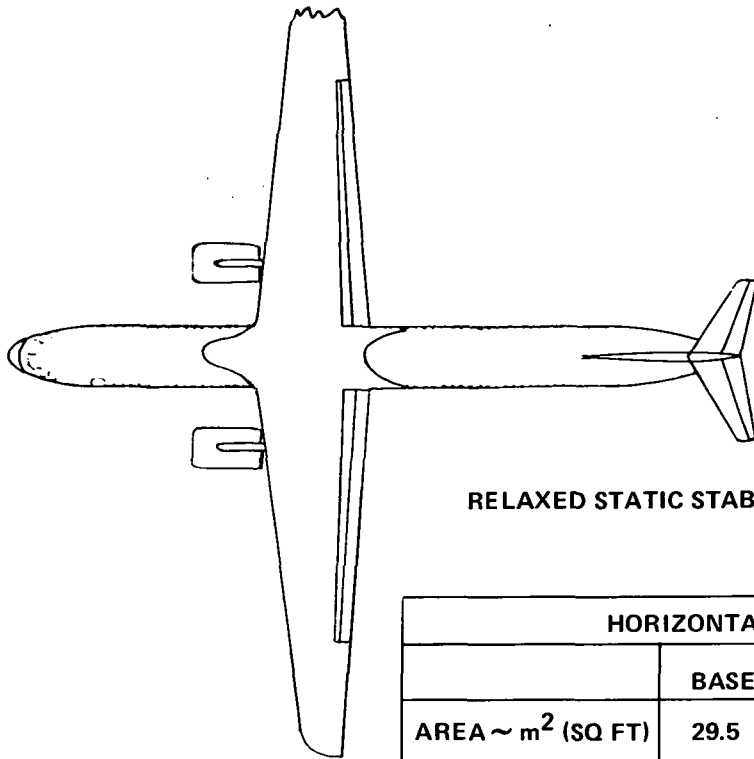
RELAXED STATIC STABILITY CONFIGURATION

HORIZONTAL TAIL
GEOMETRY HELD CONSTANT

ASPECT RATIO	4.5
TAPER RATIO	.3
SWEEP AT C/4	30°

HORIZONTAL TAIL COMPARISON			
	BASELINE	RSS	% REDUCTION
AREA ~ m² (SQ FT)	29.5 (317)	20.2 (217)	30
MAC ~ m (FT)	2.56 (8.4)	2.32 (7.6)	
SPAN ~ m (FT)	11.5 (37.8)	9.54 (31.3)	
TAIL ARM ~ m (FT)	23.7 (77.8)	24.0 (78.9)	
TAIL VOLUME COEFFICIENT	.64	.447	
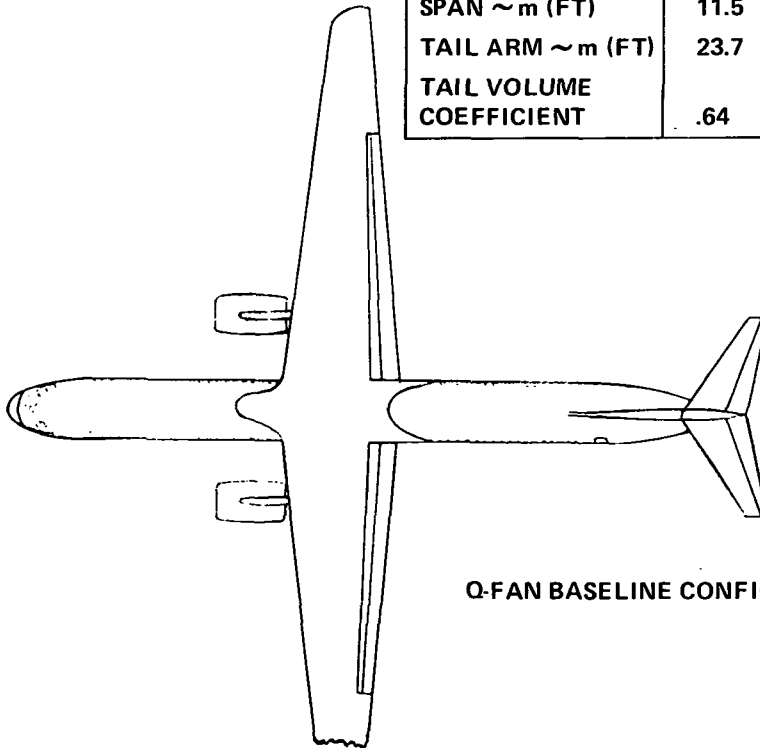
Q-FAN BASELINE CONFIGURATION

RELAXED STATIC STABILITY HORIZONTAL TAIL
CONFIGURATION (NO "SNOWBALL" EFFECT)
FIGURE 74

Vertical Tail Sizing. - The vertical tail size for relaxed static stability was determined based on the same criteria as the baseline, except that the Tameness criteria was based on the automatic flight control system having five degrees of rudder control authority to control an engine out. The variation in vertical tail area with normalized tail arm is presented in Figure 75. The vertical tail sizing requirements based on this Tameness criteria was found to be reduced to the same level as that required to meet the ground minimum control speed.

The vertical tail area is therefore determined by these two requirements, i.e., V_{MCG} and Tameness. The vertical tail area was found to be reduced 23 percent which includes the benefit of the increased moment arm gained from moving the wing forward. A summary drawing of the relaxed static stability vertical tail configuration is presented in Figure 76.

Performance Benefits. - Although substantial reductions in tail size were obtained, the RSS improvement is limited because the horizontal and vertical tail surfaces constitute a relatively low fraction of the total airplane weight (three percent of the baseline Q-fan OWE). Also, the airplane design gross weight is relatively insensitive to a drag decrease because of the relatively short range (low fuel to gross weight ratio). The performance benefits obtained are presented in Table 21.

TABLE 21
RELAXED STATIC STABILITY CONFIGURATION COMPARISON

	Q-Fan Baseline Configuration	Relaxed Static Stability Configuration	Percent Reduction
Horizontal Tail Area m^2 (Ft^2)	29.5 (317)	19.6 (211)	33
Vertical Tail Area m^2 (Ft^2)	23.9 (257)	17.8 (192)	25
Gross Weight N (lbf)	594,300 (133,600)	582,700 (131,000)	2

Note: No weight included for RSS systems

Ride Quality Improvement

The objective of this ride quality analysis was to determine the ride quality of the low-wing-loading Q-fan baseline configuration and ascertain if a ride quality improvement feature is required on the combined ACT configuration. The criteria for evaluating the ride quality is the passenger satisfaction experienced on a current jet transport.
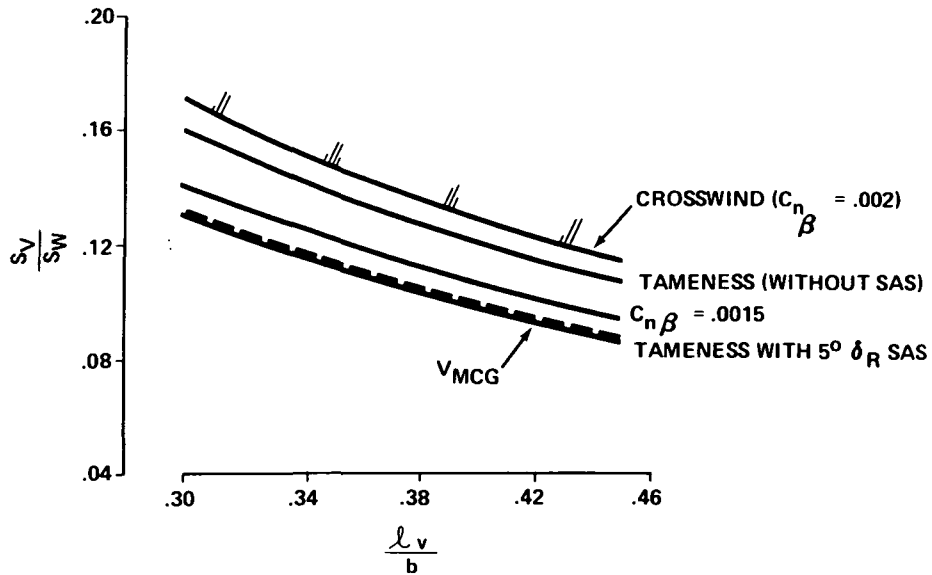
VERTICAL TAIL SIZING — RELAXED STATIC STABILITY CONFIGURATION
FIGURE 75

RELAXED STATIC STABILITY CONFIGURATION
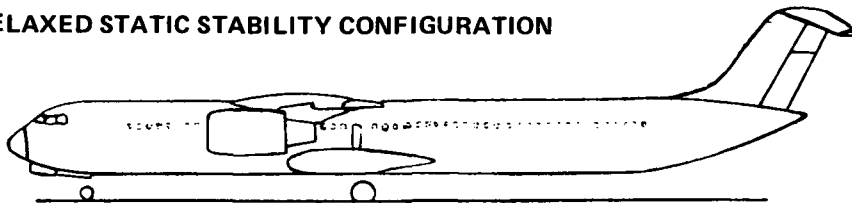
VERTICAL TAIL
GEOMETRY HELD CONSTANT

ASPECT RATIO	1.4
TAPER RATIO	.7
SWEEP AT C/4	35°

Q-FAN BASELINE CONFIGURATION
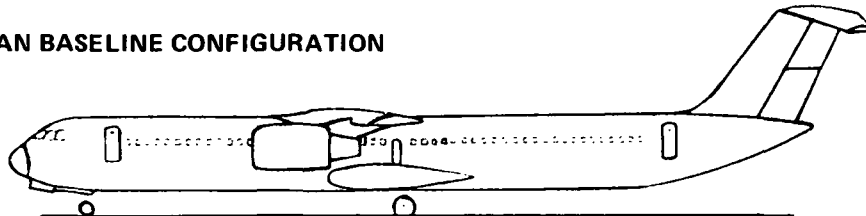
VERTICAL TAIL COMPARISON			
	BASELINE	RSS	% REDUCTION
AREA $\sim$ m² (SQ FT)	23.9 (257)	18.3 (197)	23
MAC $\sim$ m (FT)	4.11 (13.5)	3.66 (12.0)	
SPAN $\sim$ m (FT)	5.79 (19.0)	5.06 (16.6)	
TAIL ARM $\sim$ m (FT)	20.1 (65.8)	21.2 (69.7)	
TAIL VOLUME COEFFICIENT	.0484	.0394	

RELAXED STATIC STABILITY VERTICAL TAIL
CONFIGURATION (NO "SNOWBALL" EFFECT)
FIGURE 76

124

The methodology for comparing the ride quality of the Q-fan propulsion baseline configuration to that of a modern jet transport was to determine first the ride quality of each in terms of passenger satisfaction. The procedure determining passenger satisfaction is that outlined in Reference 18. A schematic diagram outlining this procedure is presented in Figure 77.

The vehicle transfer function is determined from a digital computer program that accepts the airplane stability derivatives and inertia properties and computes the airplane vertical acceleration response to a unit atmospheric gust input. The subjective transfer function and the value transfer function were obtained from References 18 and 19 and are presented in Figures 78 and 79, respectively.

Flight Condition. - A midclimb, cruise and approach flight condition were selected to provide a representative sample of the ride quality on a typical flight. The flight conditions are defined in Table 22 and are lettered for convenient reference.

TABLE 22
RIDE QUALITY IMPROVEMENT DESIGN FLIGHT CONDITIONS

	Ride Quality Improvement Flight Conditions		
	A Climb	B Cruise	C Approach
Configuration	Flaps Up	Flaps Up	Flaps 40
$\nu_e \sim$ m/sec (Kts)	57.3 (188)	121 (235)	44 (86)
Mach No.	.39	.70	.13
Altitude m (Ft)	5,030 (16,500)	10,100 (33,000)	S.L.
Gross Weight $\sim$ lbf	586,700 (131,900)	549,400 (123,500)	562,300 (126,400)
True Airspeed m/s (Ft/Sec)	125 (410)	197 (647)	44 (145)

Atmospheric Model. - The atmospheric turbulence model utilized in this type of analysis has a large effect on the results, particularly in regard to establishing the gust magnitudes to be used for the various flight conditions. The atmospheric turbulence used for this analysis was modeled with a von Karman spectrum having the following spectral density for digital computation of airplane response power spectra.
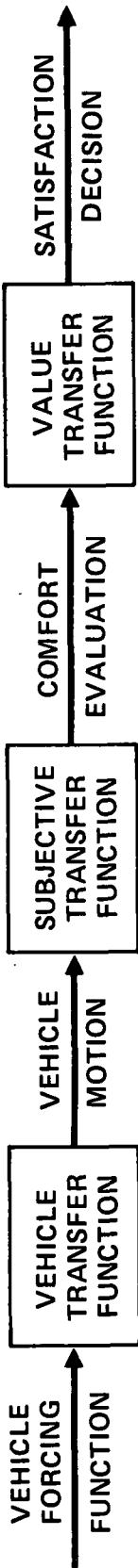
SCHEMATIC FOR DETERMINING PASSENGER
SATISFACTION WITH RIDE QUALITY
FIGURE 77
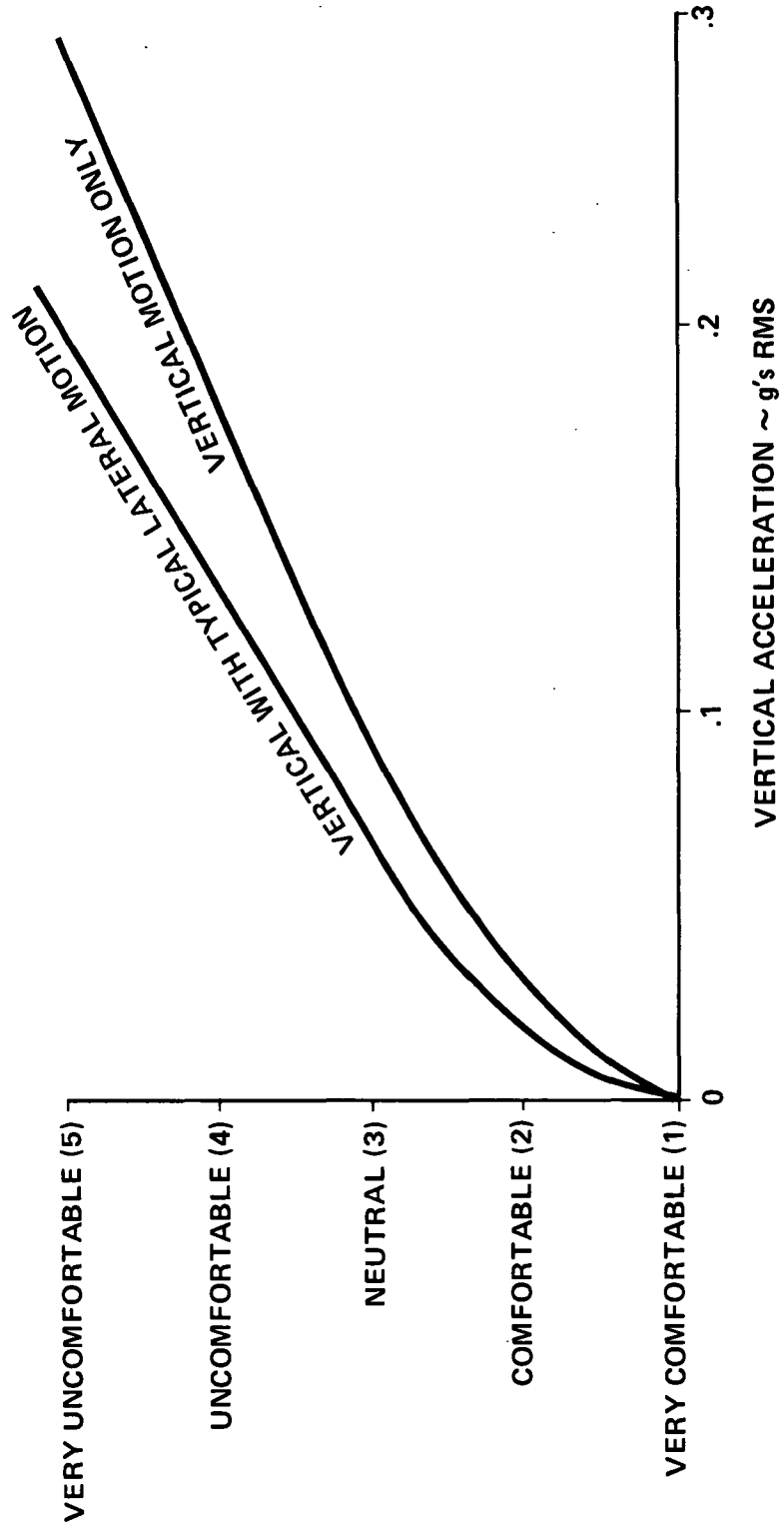
VARIATION IN COMFORT LEVEL WITH VERTICAL ACCELERATION
FIGURE 78
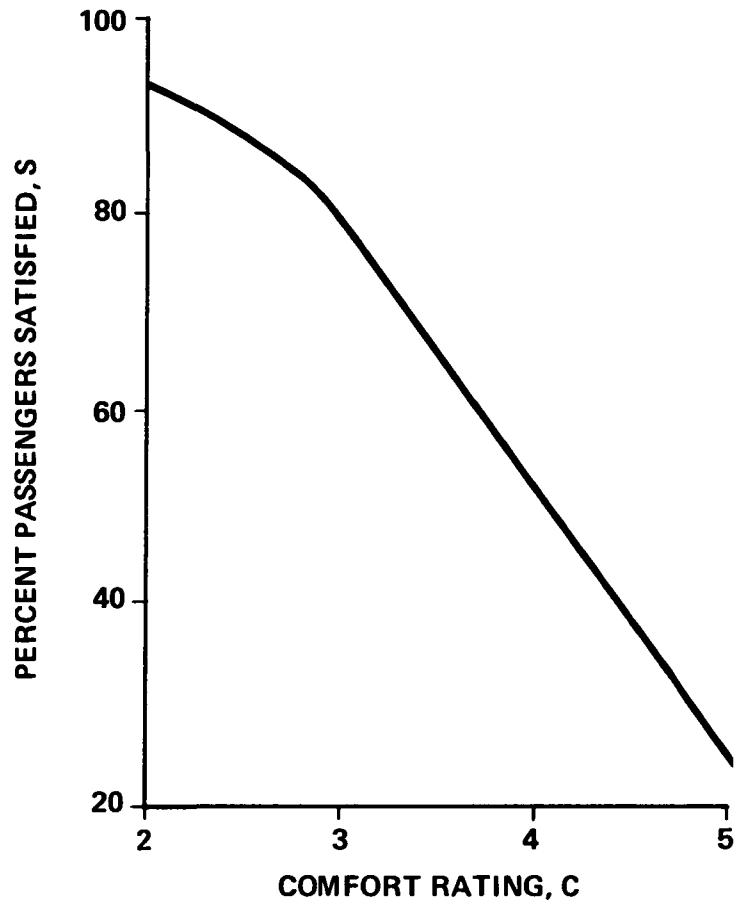
RIDE QUALITY VALUE TRANSFER FUNCTION
FIGURE 79

$$\phi_{w_g} = \frac{\sigma_{w_g}^2 L}{\pi U_o} \frac{\left[1 + \dfrac{8}{3}\left(1.339\dfrac{L}{U_o}\omega\right)^2\right]}{\left[1 + \left(1.339\dfrac{L}{U_o}\omega\right)^2\right]^{11/6}} \quad \frac{(m/sec)^2}{rad/sec}$$

where:

σ_{w_g} = rms gust velocity, m/sec.

U_o = airplane forward velocity, m/sec.

L = turbulence scale length, m.

ω = frequency, rad/sec.

A scale length (L) of 762 meters (2,500 feet) was used for the climb and cruise condition and 152 meters (500 feet) for the landing condition. The atmospheric turbulence RMS gust velocities are presented in Figure 80. These probability data were obtained from References 20, 21 and 22. Taken directly from these reports, they are conservative in that they are based on the time spent in turbulence and do not reflect the probability of encountering turbulence. This procedure was followed so that these results could be compared to the ride quality results presented in References 18 and 19.

Ride Quality. - The vertical ride quality response was initially computed in terms of vertical acceleration response to atmospheric turbulence. The Q-fan baseline airplane vertical acceleration response at the forward passenger seat (B.S. 482), midcenter of gravity (B.S. 1000) and aft passenger seat (B.S. 1541) were determined for each of the flight conditions. The rigid baseline airplane stability and control derivatives for each of the flight conditions are presented in Appendix C. The mathematical model for determining the airplane response include the Wagner and Kussner functions to account for lift growth.

For comparison purposes, the vertical ride quality responses for the Boeing 707 were computed for a comparable best cruise Mach, high cruise Mach and climb/descent flight condition considering rigid body degrees of freedom only. The airplane vertical acceleration cumulative RMS response to vertical atmospheric gust response ($\bar{A}$) were computed for each flight condition. The 707 airplane stability derivatives are also presented in Appendix C.

A summary of the Q-fan baseline airplane and the Boeing 707 vertical acceleration RMS response obtained are presented in Table 23. These results are corrected to exclude that part of the motion that occurs at or below the phugoid response. This correction is made to exclude that portion of the

128

ATMOSPHERIC RMS GUST VELOCITY PROBABILITY
FIGURE 80

TABLE 23
RIDE QUALITY RESPONSE OF Q-FAN BASELINE CONFIGURATION AND MODERN JET TRANSPORT

Fuel Conservative Transport

Flight Condition	Gross Weight N (lbf)		Mach	V_E m/s (Kts)		Altitude m (Ft)		B.S. 482 Å		B.S. 1,000 Å		B.S. 1,541 Å	
A – Climb	586,700	(131,900)	.39	57.3	(188)	5,030	(16,500)	(.0135)	.0443	(.0147)	.0482	(.0160)	.0525
B – Cruise	549,400	(123,500)	.70	121	(235)	10,100	(33,000)	(.0191)	.0627	(.0203)	.0667	(.0215)	.0705
C – Approach L = 152 m (500 Ft)	562,300	(126,400)	.13	.44	(86)	S.L.		(.0120)	.0394	(.0126)	.0413	(.0131)	.0430

Boeing 707 Airplane

Flight Condition	Gross Weight N (lbf)		Mach	V_E m/s (Kts)		Altitude m (Ft)		(480 Inches) FWD of CG 12.2 m Å		CG Å		(480 Inches) AFT of CG 12.2 m Å	
Climb	1,068,000	(240,000)	.57	140	(272)	5,030	(16,500)	(.0090)	.0295	(.0105)	.03444	(.0121)	.0397
.80 Mach Cruise	890,000	(200,000)	.80	138	(268)	10,100	(33,000)	(.0087)	.0285	(.0112)	.0367	(.0138)	.0453
.86 Mach Cruise	801,000	(180,000)	.86	142	(276)	10,700	(35,000)	(.0101)	.0331	(.0133)	.0436	(.0166)	.0545

1. Unless otherwise noted, turbulence scale factor, L = 762 m (2,500 Ft)
2. Kussner lift growth function included
3. Å are without Phugoid or elastic mode contribution
4. Å ~ g's/m/s (g's/Ft/Sec)

motion that is reflected in the airplane total RMS response but is below the passenger sensory perception.

A comparison of the Q-fan baseline airplane response to that of the Boeing 707 as a function of seat location is presented in Figures 81 and 82. During cruise flight, the Q-fan baseline had approximately twice as rough a ride when encountering the same gust as the Boeing 707. During the midclimb/descent flight condition, the Q-fan airplane ride is approximately 50 percent rougher than the 707. For both airplanes, the fore and aft passenger location is a function of the pitch acceleration that develops when the airplane encounters a gust. The pitch acceleration adds to the vertical load factor for seats aft from the center of gravity and subtracts for seats forward. The amount of pitch acceleration depends on the static margin, pitch damping, forward velocity and moment of inertia. A comparison of these parameters shows that the first and last are essentailly the same for these two airplanes but that the Q-fan has twice the pitching damping (C_{M_q}) and operates at 12 percent lower forward velocity. The difference in the ride quality as a function of passenger location is attributed to the contribution of these two parameters.

Previous studies, References 18 and 19, have assessed the ride quality of an airplane in terms of percent travelers satisfied versus flight time percentiles or probability. Using this procedure, the ride quality passenger satisfaction was determined for the Q-fan baseline configuration and for the Boeing 707 in cruise, and the comparison is presented in Figure 83. Also presented is the ride quality for the Q-fan baseline airplane on approach.

Based on these results, the low-wing-loading Q-fan baseline airplane will require a ride quality improvement system to bring the ride quality up to a level of satisfaction equal that of a current jet transport. The system will need to reduce the vertical gust loads approximately in half.

CRUISE
FUEL CONSERVATIVE TRANSPORT
GW = 549,400 N (123,500 lbf)
M = .7
ALT = 10,100 m (33,000 FT)
BOEING 707
GW = 890,000 N (200,000 lbf)
M = .8
ALT = 10,100 m (33,000 FT)

FUEL CONSERVATIVE
TRANSPORT
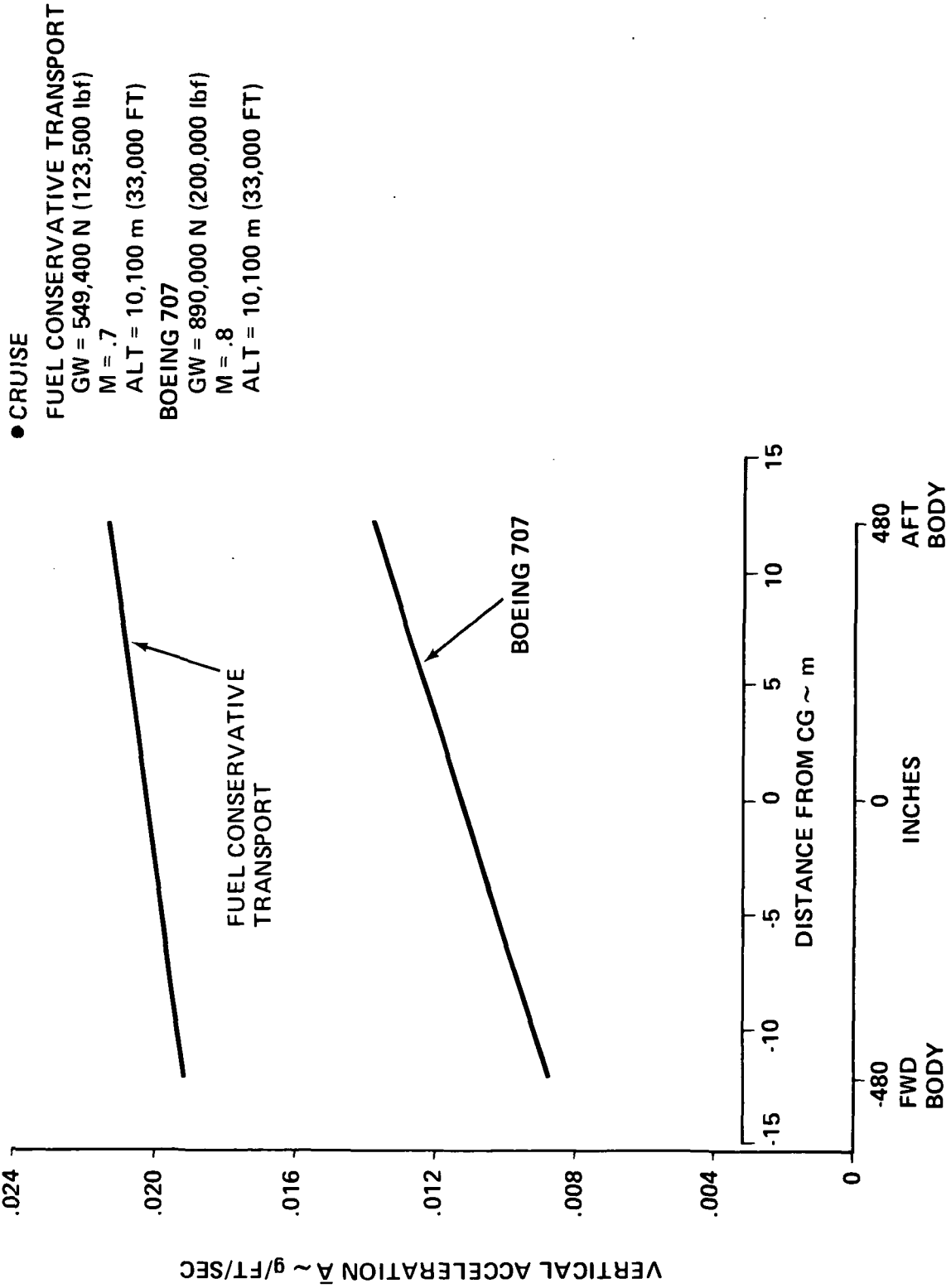
BOEING 707

RIDE QUALITY COMPARISON – CRUISE
(BASELINE AIRPLANE RESPONSE WITHOUT RQI)
FIGURE 81

DISTANCE FROM CG ~ m

INCHES

-480
FWD
BODY

0

480
AFT
BODY

VERTICAL ACCELERATION $\bar{A}$ ~ g/FT/SEC

132

CLIMB

FUEL CONSERVATIVE TRANSPORT
GW = 586,700 N (131,900 lbf)
M = .39
ALT = 5,030 m (16,500 FT)

BOEING 707
GW = 1,068,000 N (240,000 lbf)
M = .57
ALT = 5,030 m (16,500 FT)

FUEL CONSERVATIVE
TRANSPORT

BOEING 707

VERTICAL ACCELERATION A ~ g/FT/SEC

.020

.016

.012

.008

.004

0

DISTANCE FROM CG ~ m

-15   -10   -5   0   5   10   15

FWD
BODY
-480

0
INCHES

480
AFT
BODY
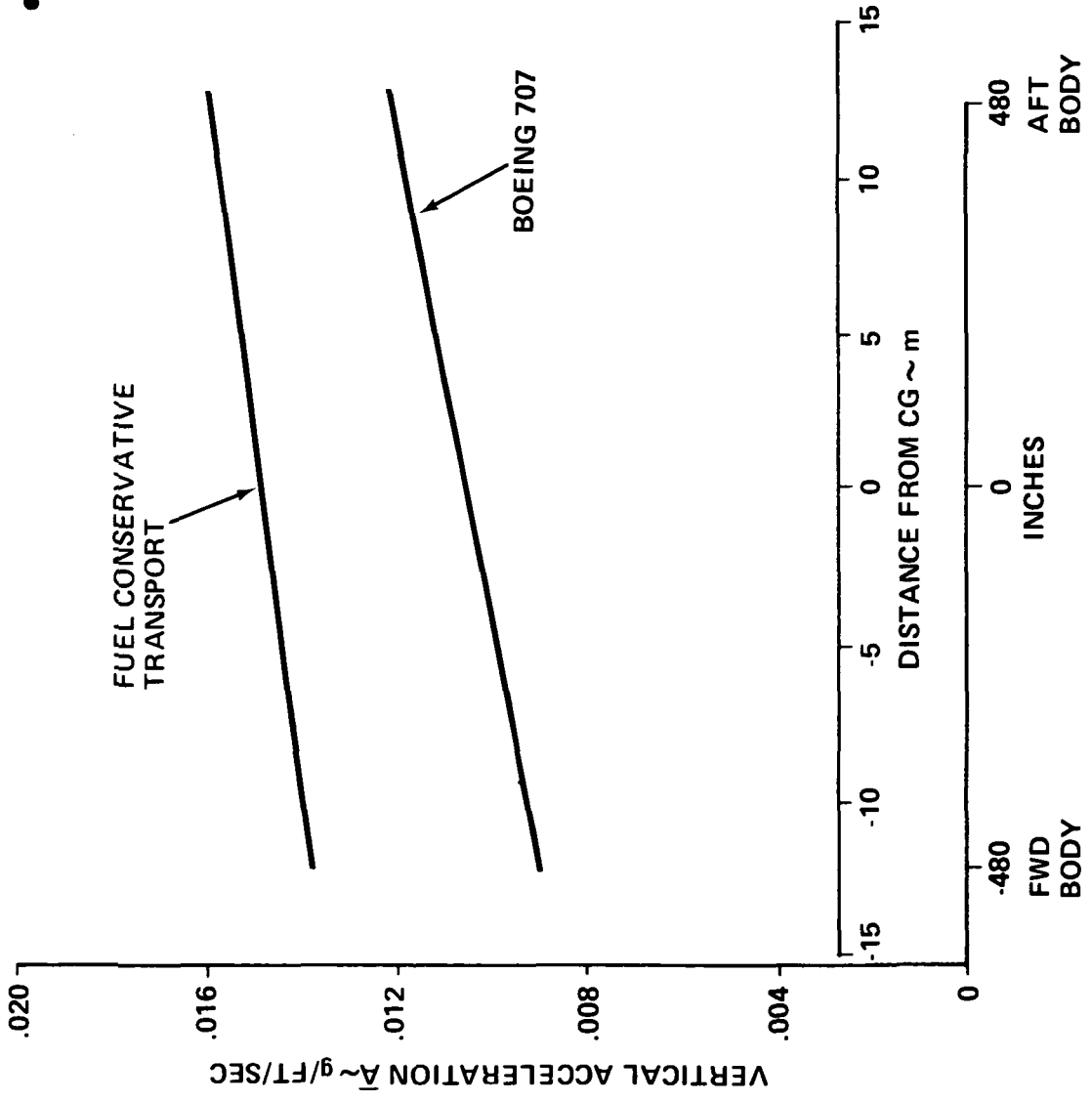
RIDE QUALITY COMPARISON – CLIMB
(BASELINE AIRPLANE RESPONSE WITHOUT RQI)
FIGURE 82

133
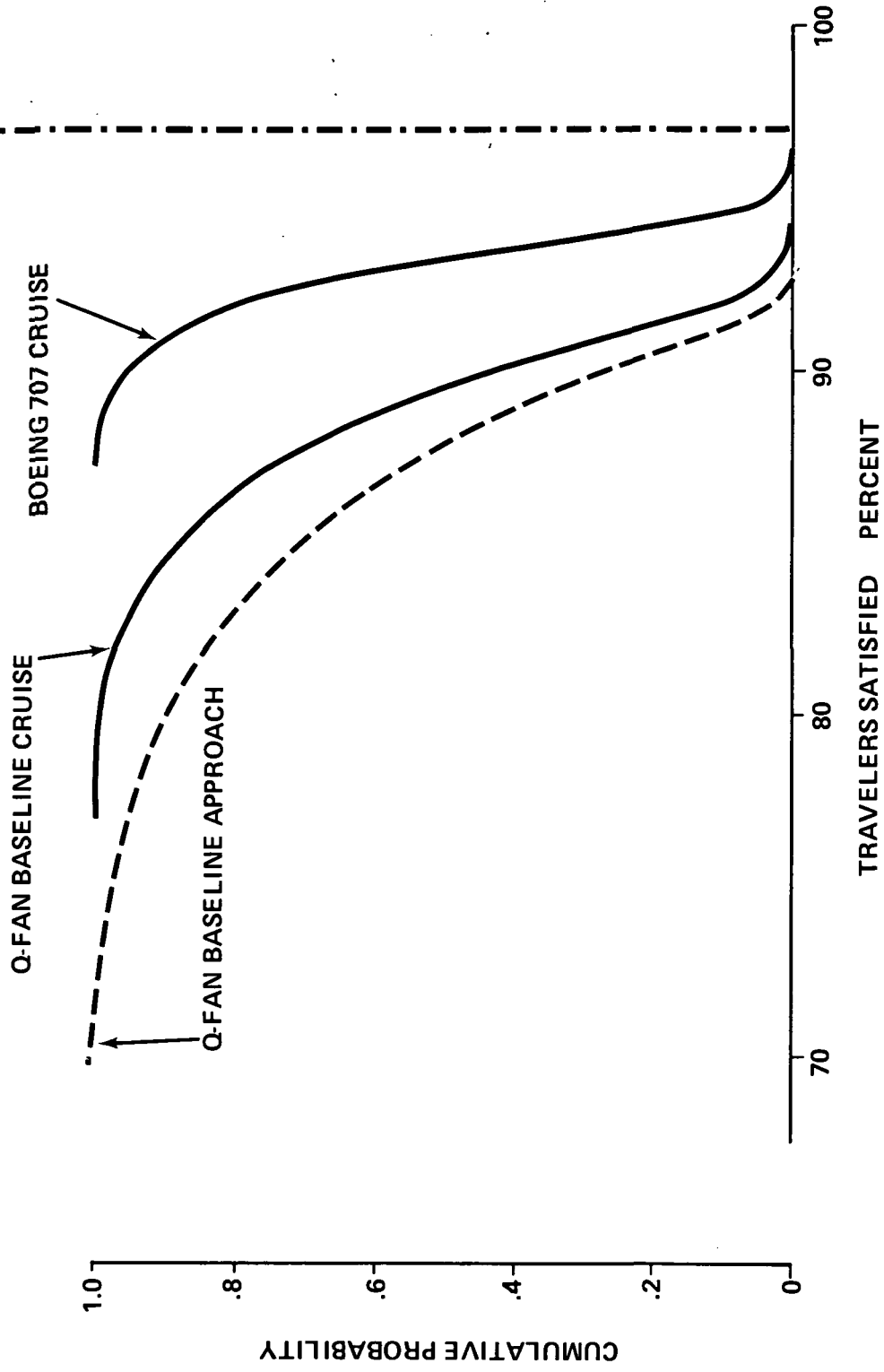
COMPARISON OF Q-FAN BASELINE PASSENGER
SATISFACTION TO MODERN JET TRANSPORT
FIGURE 83

MULTIPURPOSE ACTIVE CONTROLS SYSTEM CONFIGURATION

To evaluate the merits of incorporating active control technology into a low-wing-loading, short haul transport, a multifunction active control system that performs the following functions was defined:

- Gust Load Alleviation
- Relaxed Static Stability
- Ride Quality Improvement

The merits and requirements for each of these functions were based on the separate analyses discussed in the previous section. The gust load alleviation study showed the gust load critical Q-fan baseline (4.21 g's) could potentially be reduced to at least 2.90 g's or within .4 g of the maneuver load factor. This system required a wing control system capable of developing an incremental lift coefficient of .208. The positive wing bending moments were reduced below the maneuvering level. The relaxed static stability study showed the Q-fan baseline vertical tail surface could be reduced 28 percent and the horizontal tail surface 30 percent. It was necessary to move the wing 1.78 meters (70 inches) forward on the body to rebalance the airplane. The ride quality improvement study showed that the low wing loading Q-fan baseline configuration experienced approximately twice as rough a vertical ride as the Boeing 707 during cruise; and, therefore, requires a ride quality improvement system to maintain current jet transport comfort levels.

The reason for evaluating these ACT features as a combined system is that a major portion of the added hardware is in common. For example, the wing direct lift control surfaces and pitch stability augmentation system required for gust load alleviation can be partially shared by the ride quality improvement and relaxed static stability features, respectively.

Design Flight Conditions

The design flight conditions for analyzing the multipurpose active control systems were selected based on the design requirement determined for each of the separate concepts. For the Gust Load Alleviation (GLA) concept, the design condition was the FAR Part 25, V_c requirement. For the Relaxed Static Stability (RSS) concept, the design condition occurs at landing approach. The cruise flight condition was also selected to confirm that satisfactory handling qualities exist during cruise throughout the operating CG range. The cruise condition was selected for the Ride Quality Improvement (RQI) concept

because the major percentage of time is spent at this flight condition (57 percent of the design mission). The mid-climb and landing approach flight conditions were selected because for this relatively short range mission a substantial amount of time is spent in the lower portion of the atmosphere (24 percent below 4880 meters (16,000 feet)) where the turbulence probability is significantly higher. A summary of the design flight conditions is presented in Table 24.

Flight Controls System

Flight Control Surfaces. - The flight control surfaces for the multi-purpose active control system configuration were selected based on the results of the separate studies of the three concepts, GLA, RSS and RQI. The lateral control surfaces include the inboard and outboard ailerons and spoiler segments A and B as described in Figure 60. These surfaces were selected based on their capability to perform the basic airplane roll control required, the gust load alleviation and the ride quality improvement. The horizontal and vertical tail size were reduced to a $\overline{V}_H = 0.447$ and $\overline{V}_V = 0.0394$, respectively, based on the results of the relaxed static stability analysis. The elevator and rudder control surfaces were maintained at the same percent chord as the baseline configuration.

Automatic Flight Control System Synthesis. - An Automatic Flight Control System was synthesized to perform the following multipurpose active control functions:

- Alleviation of Gust Loads
- Relaxed Static Stability
- Improvement of Ride Qualities

A block diagram of the system is presented in Figure 84. The airplane angle of attack feedback to the elevator provides the required effective stability for the relaxed static stability configuration and the vertical acceleration feedback to the wing control surfaces provides gust load alleviation and ride improvement features.

The Gust Load Alleviation/Ride Improvement control system includes a spoiler threshold which serves to actuate only the ailerons in moderate gusts

136

TABLE 24

MULTIPURPOSE ACTIVE CONTROLS SYSTEM DESIGN FLIGHT CONDITIONS

	GLA FAR Part 25 V_C	RSS/RQI Cruise	RSS/RQI Approach	RQI Mid-climb
Mach	.70	.70	.13	.39
$V_E \sim$ m/s (Kts)	167 (325)	121 (236)	44 (86)	97 (188)
Altitude $\sim$ m (Ft)	5,500 (18,000)	10,100 (33,000)	S.L.	4,720 (15,500)
Gross Weight $\sim$ N (lb)	542,200 (121,900)	529,000 (118,900)	518,700 (116,600)	542,700 (122,000)
CG $\sim$ % MAC	Mid	*	*	Mid
$I_{yy} \sim$ kg $\cdot$M^2 (Slug-Ft^2)	5,150,000 (3,800,000)	5,020,000 (3,700,000)	5,020,000 (3,700,000)	5,150,000 (3,800,000)

*RSS at forward CG limit (45% MAC) and aft CG limit (65% MAC)
RQI at mid CG limit (55% MAC)

ACT CONTROL SYSTEM BLOCK DIAGRAM
FIGURE 84

$K_1 = .66$ DEG/m/s^2 (.2 DEG/FT/SEC^2)
$K_2 = 66$ DEG/m/s^2 (20 DEG/FT/SEC^2)

and actuates both ailerons and spoilers at large positive gusts. This concept eliminates unsymmetrical control surface response during moderate random turbulence encounters and reduces the drag due to spoiler activity.

System Weight Analysis. - The ACT system weight increment was estimated by determining the difference in the control system weight for the Q-fan baseline configuration and ACT configuration. The Q-fan baseline configuration has a conventional cable-driven manual flight control system. The ACT configuration was designed with a fly-by-wire (FBW) automatic flight control system. The ground rules and assumptions for the weight estimate are presented in Table 25. Figures 85 and 86 illustrate the simplified block diagram of both concepts. These figures depict the redundancy of the hydraulic and electrical power as well as the actuation and electronic mechanization necessary to achieve a failure probability similar to the baseline.

The weight difference was estimated by using the 737-200 manual flight control system for the baseline weight and extrapolating cable runs for the appropriate fuselage and wing lengths. The FBW system weight was estimated by determining wire bundles, computers, sensors, actuators and power requirements. Since the ground rules required 1975 technology, the 737 rudder dual tandem actuator was used as the common FBW actuator. Table 26 lists the weight by control element for both conventional and FBW systems and Table 27 provides additional weight detail.

Reliability. - A Flight Control System reliability analysis was accomplished by equipment comparisons to similar and existing military (B-52) equipment. The results of this analysis are presented in Table 28.

TABLE 28
ACT SYSTEM RELIABILITY COMPARISON

FCS Configuration	System Failure Probability	System MTBF
Active Control Technology	$3.6 * 10^{-7}$	50 Hours
Conventional	$16.2 * 10^{-7}$	150 Hours

The system MTBF did not include the engine hydraulic and electrical systems.

The system failure probability means the loss of any function (GLA, RSS, RQI) of the ACT system. The loss of a function is not always critical to airplane safety, in that it depends on the function and flight condition. Therefore, probability of airplane loss would be somewhat less. The ACT system reliability is about four times higher than the baseline configuration using conventional flight controls.

TABLE 25
ACT CONTROL SYSTEM GROUND RULES AND ASSUMPTIONS

Configuration	Control Surfaces	Actuation Device (1975 Technology)	Manual System Mechanism	Redundancy	Hydraulic and Electrical Power	Rudder System
Baseline	Elevator Aileron Spoiler A	(Dual Tandem) (Plus Standby) Pure Hydraulic with Mechanical Input	Cables, Pushrods, Bellcranks, Bellows, Springs, Etc.	Single-Fail Operate (Dual Cable)	One Pump and One Generator per Engine Two TR Units	Mechanical Cable with Dual Tandem Actuator + Standby
ACT	Elevator Outb'd Aileron Inb'd Aileron Spoiler A Spoiler B	Pure Hydraulic with Electrical Input	Fly By Wire	Two-Fail Operate Quad Electronics Sensors	One Pump and One Generator per Engine and APU Three TR Units	Electrical Cable Fail-Op Electronics Two Dual Tandem Actuators

TABLE 26
FLIGHT CONTROL SYSTEM WEIGHT SUMMARY

Item	Conventional ~N(lbf)	ACT ~N(lbf)
Elevator Control	2,095 (471)	2,086 (469)
Aileron Control	1,610 (362)	2,856 (642)
Spoiler Control	1,450 (326)	3,407 (766)
Rudder Control	1,303 (293)	1,165 (262)
Miscellaneous: Electronics	–	489 (110)
Sensors	–	214 (48)
Electrical/Hydraulic Power	–	787 (177)
Total	6,459 (1,452)	11,005 (2,474)
Incremental Weight for ACT: 4,546N (1,022 lbf)		

140
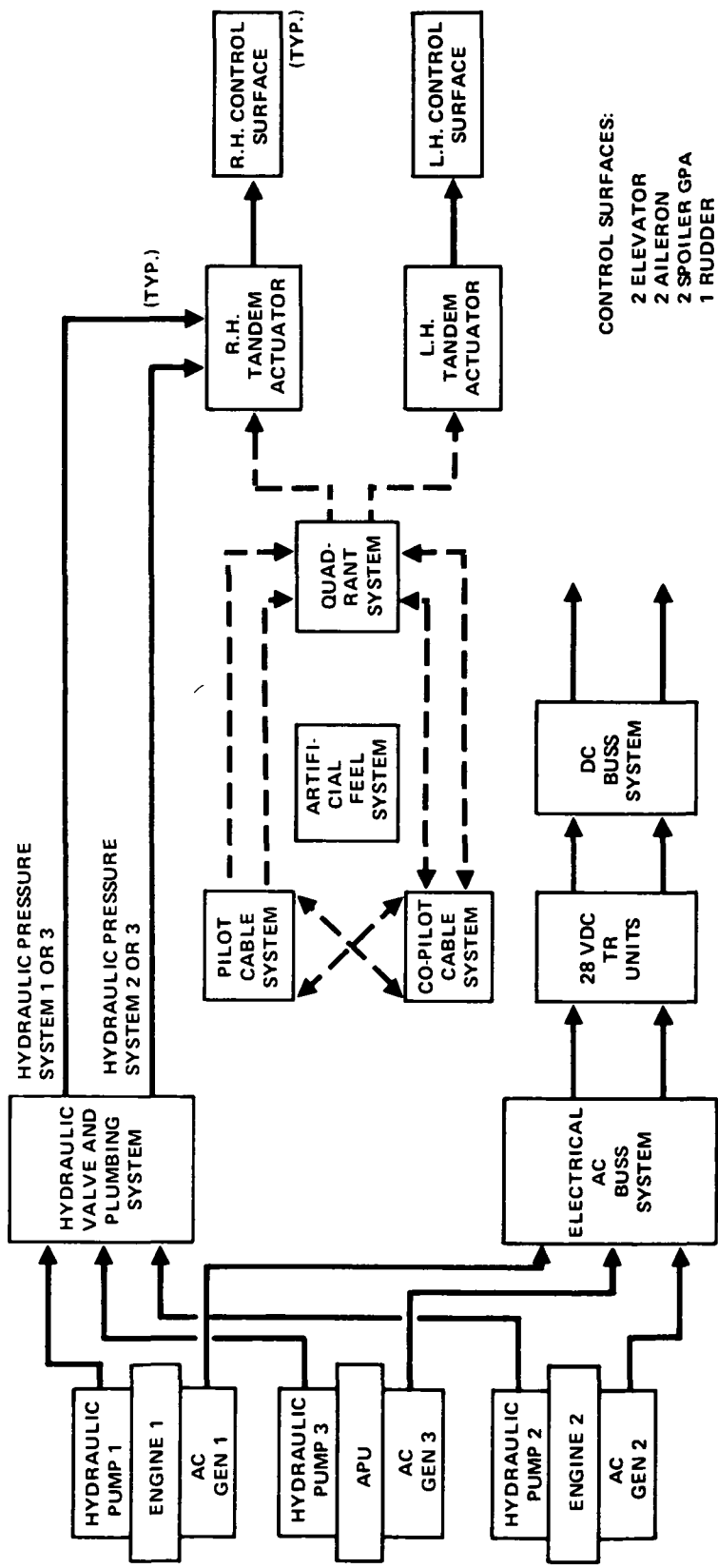
BASELINE AIRPLANE CONVENTIONAL FLIGHT CONTROL SYSTEM
FIGURE 85
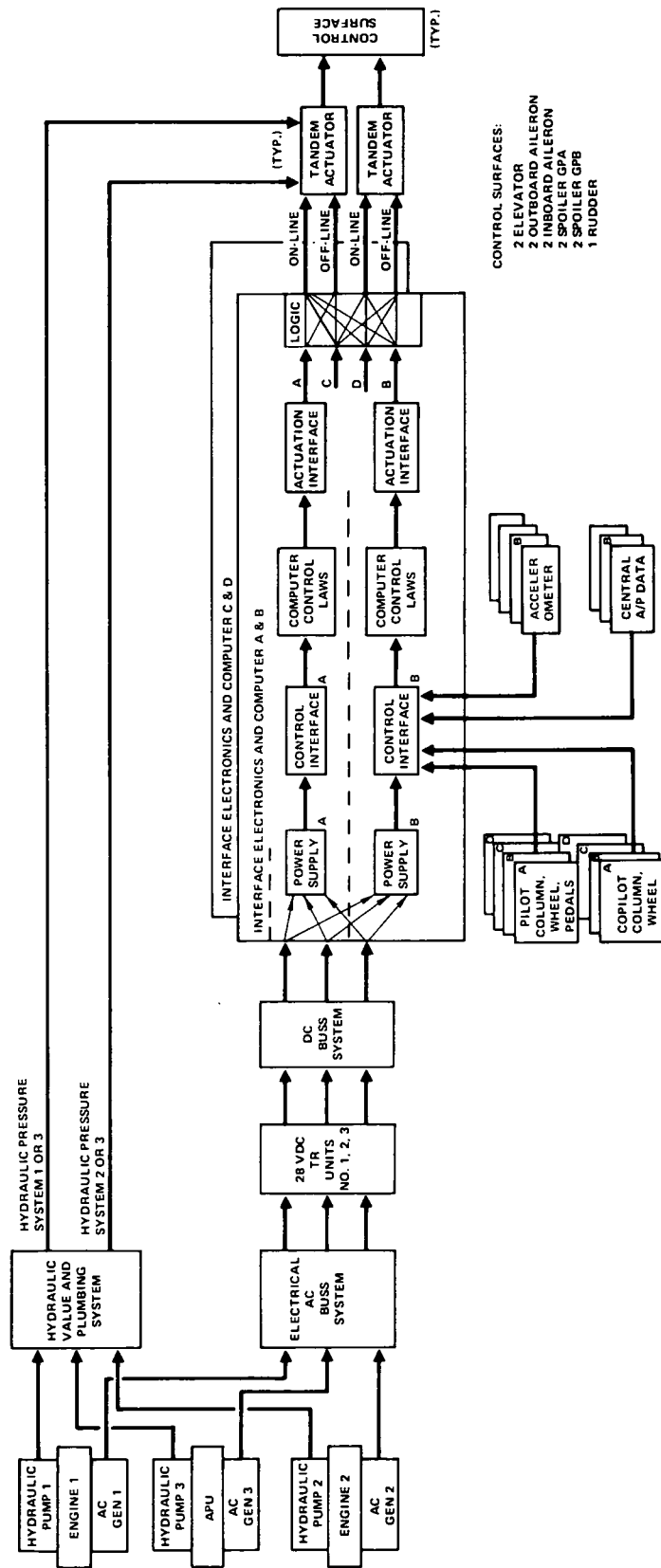
ACT FLY-BY-WIRE FLIGHT CONTROL SYSTEM

FIGURE 86

TABLE 27
FLIGHT CONTROL SYSTEM DETAIL WEIGHT STATEMENT

Item	Conventional N (lbf)	ACT N (lbf)
1.0 Elevator	2,095 (471)	2,086 (469)
1.1 Pilot Pitch and Roll Controls		
1.1.1 2 Columns and Supports	209 (47)	—
1.1.2 4 Hand Controllers	—	71 (16)
1.2 Mechanical Mechanisms		
1.2.1 Cables, Pulleys, etc.	307 (69)	—
1.2.2 Electrical cables from controls to electronics and electronics to power actuators	80 (18)	485 (109)
1.3 Hydraulic Items	1,165 (262)	1,530 (344)
1.3.1 Actuators	525 (118)	105 (236)
1.3.2 Mechanisms	298 (67)	—
1.3.3 Plumbing	156 (35)	311 (70)
1.3.4 Fluid	27 (6)	53 (12)
1.3.5 Valves	44 (10)	—
1.3.6 Trim Motor	116 (26)	116 (26)
1.4 Feel and Centering	334 (75)	—
2.0 Aileron System	1,610 (362)	2,856 (642)
2.1 Pilot Controls	Included with 1.1	
2.2 Mechanical Mechanisms		
2.2.1 Cables, Pulleys, etc.	721 (162)	—
2.2.2 Electrical cables from controls to electronics and electronics to actuators	49 (11)	391 (88)
2.3 Hydraulic Items	841 (189)	2,464 (554)
2.3.1 Actuators	525 (118)	2,100 (472)
2.3.2 Plumbing	156 (35)	311 (70)
2.3.3 Fluid	13 (3)	53 (12)
2.3.4 Controls	147 (33)	—
2.4 Feel System	—	—

TABLE 27 (CONT'D)
FLIGHT CONTROL SYSTEM DETAIL WEIGHT STATEMENT

Item		Conventional N (lbf)	ACT N (lbf)
3.0	Spoiler System	1,450 (326)	3,407 (766)
3.1	Pilot Controls	Included with 1.1	
3.2	Mechanical Mechanisms		
3.2.1	Cables, Pulleys, etc.	187 (42)	—
3.2.2	Electrical Cables	44 (10)	427 (96)
3.3	Hydraulic Items	1,219 (274)	2,980 (670)
3.3.1	Actuators	525 (118)	2,100 (472)
3.3.2	Plumbing	334 (75)	667 (150)
3.3.3	Fluid	107 (24)	214 (48)
3.3.4	Valves	49 (11)	—
3.3.5	Mechanisms	205 (46)	—
4.0	Rudder System	1,303 (293)	1,165 (262)
4.1	Pedals and Support	280 (63)	138 (31)
4.2	Mechanical Mechanisms		
4.2.1	Cables, Pulleys, etc.	147 (33)	—
4.2.2	Electrical Cables	133 (30)	409 (92)
4.3	Hydraulic Items	689 (155)	618 (139)
4.3.1	Actuators	525 (118)	525 (118)
4.3.2	Mechanisms	71 (16)	—
4.3.3	Plumbing	76 (17)	76 (17)
4.3.4	Fluid	18 (4)	18 (4)
4.4	Feel and Centering	53 (12)	—
5.0	Miscellaneous Items	—	1,469 (330)
5.1	Additional Air Data Computer	—	107 (24)
5.2	Accelerometers	—	107 (24)
5.3	Transformer/Rectifier Unit	—	271 (61)
5.4	AC Power Control Box	—	360 (81)
5.5	FBW Computer Boxes	—	489 (110)
5.6	Extra Hydraulic Plumbing	—	133 (30)

Flight Control System Costs. - The estimated cost increment of the ACT flight control system over the cost of the conventional system is a savings of $1,120,000 in nonrecurring costs and an increase of $346,000 in the purchase cost per airplane. These values are based on 1972 dollars to be consistent with the DOC calculations for the baseline airplane. A summary of the cost development is presented in Table 29.

Note that these costs are for the flight control system only and do not reflect the decrease in costs that can be obtained through the lower gross weight of the ACT airplane. The effect of the system costs and weight of the airplane, including engine size, is reflected in the DOC calculations discussed later in this report.

Stability and Control Derivatives

To evaluate the ACT configuration gust load alleviation, relaxed static stability and ride quality improvement, the necessary airplane stability, control and wing root bending moment derivatives were determined for each of the design flight conditions. These derivatives are presented in Appendix C. The wing root bending moment includes the effect of mass relief due to the wing structure, fuel and engines.

ACT System Evaluation

Gust Load Alleviation Analysis. - The control system defined previously for gust load alleviation of discrete (1-cos) gusts provided only approximately 15 percent reduction in vertical acceleration for random turbulence at cruise and produced a biased response from spoiler deflection during random turbulence. Therefore, the system was modified to provide increased ride improvement qualities. The modified system actuates only ailerons and elevator at increased gains for small load factors to provide symmetric control authority for ride improvement during moderate turbulence. The spoilers are actuated only at large positive load factors for additional reduction of large peak gust loads. The modified system maintains the following maximum surface authority:

- Outboard ailerons: ±10 degrees
- Inboard ailerons: ±20 degrees
- Spoilers: +30 degrees
- Elevator: ±5 degrees

Improvements in load factor and wing root bending moment (WRBM) at the design flight condition (V_c) are shown in Figures 87 and 88. Positive values of

TABLE 29
ACT SYSTEM INCREMENTAL COST SUMMARY

Δ = ACT Control System Cost Minus Conventional Control System Cost

Element of Cost	*Δ Cost in 1975 Dollars Nonrecurring		Production	
Manhours				
Engineering	−13,621	M/H	−	
Tooling	−33,422	M/H	−288	M/H
Planning	−29,323	M/H	−	
Production	−729	M/H	−313	M/H
Quality Control	−929	M/H	−313	M/H
Total Hours	−78,024	M/H	−5,354	M/H
Material				
Tool Material	−57,014		−491	
Production Material	−86,050		−285,809	
Purchase Equipment	−226,671		+933,260	
Total Material	−367,735		+646,960	
Element of Cost				
Labor	−571,636		−34,837	
Fringe	−216,433		−13,192	
Material	−369,735		+646,960	
Overhead	−510,156		−82,905	
Total	−1,667,960		+516,026	
1972 Dollars	−1,120,000		+346,000	

*Cost in December 1975 dollars except as noted.
M/H = Manhours

146

CRUISE – V_c

U_o = 223 m/s (732 FPS)
M = .7
ALT = 5,500 m (18,000 FT)
U_{de} = 15.2 m/s (50 FT/SEC)

$$W_{g_{EQV}} = \pm \frac{U_{de}}{2} \, (1 - COS \, 11.07t)$$

——— WITH GLA/RQI AND RSS
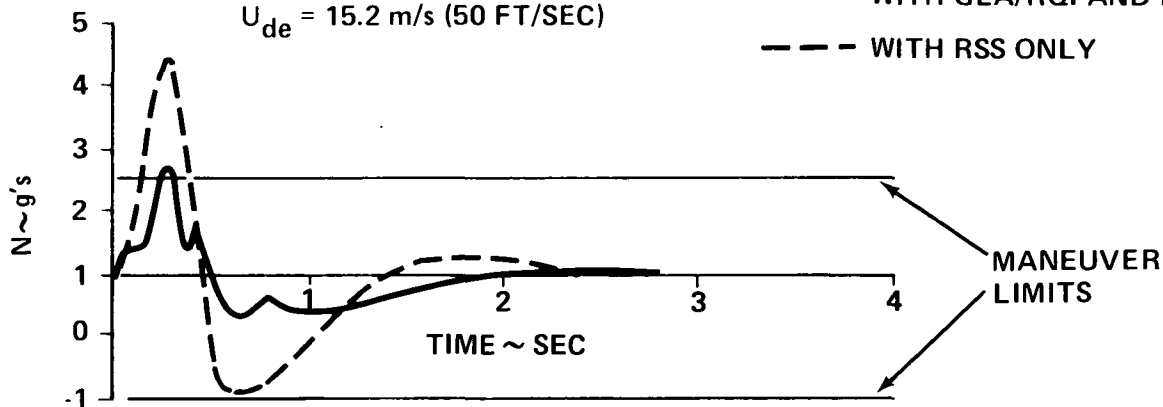
– – – WITH RSS ONLY

A) RESPONSE TO POSITIVE (UP) GUST
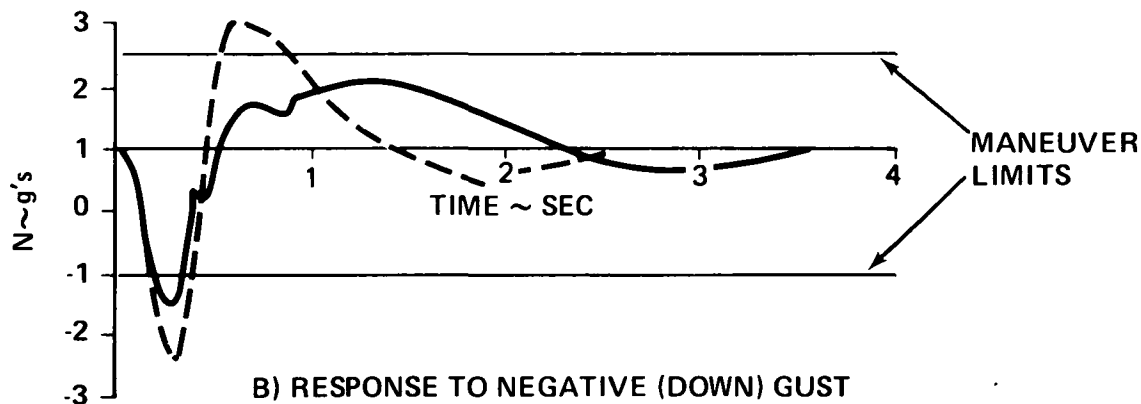
B) RESPONSE TO NEGATIVE (DOWN) GUST

LOAD FACTOR TIME RESPONSE FOR 1-COS GUST
FIGURE 87

147

CRUISE — V_c

$U_o = 223$ m/s (732 FPS)
$M = .7$
ALT = 5,500 m (18,000 FT)
$U_{de} = 15.2$ m/s (50 FT/SEC)

$W_{g_{EQV}} = \pm \dfrac{U_{de}}{2} \ (1\text{-COS }11.07t)$

—— WITH GLA/RQI AND RSS
— — WITH RSS ONLY
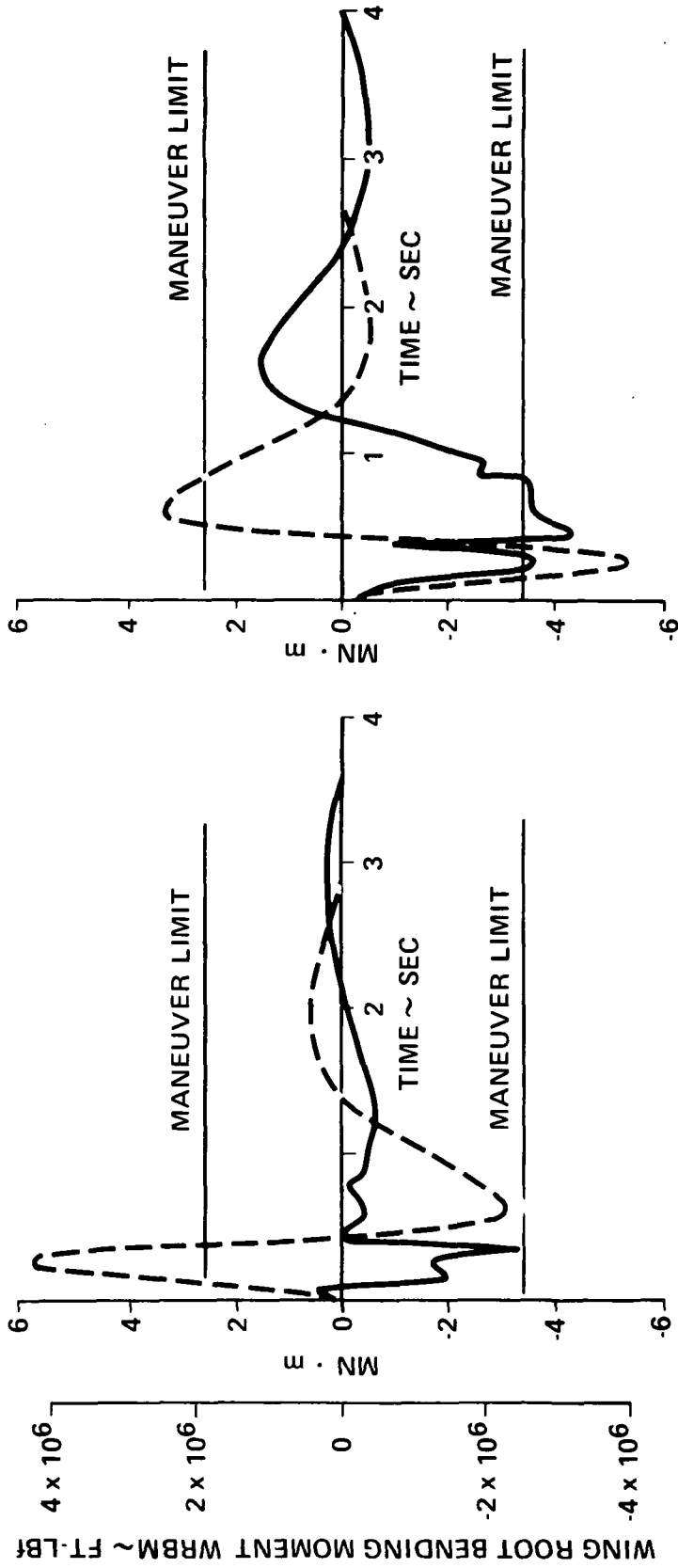
A) RESPONSE TO POSITIVE (UP) GUST

B) RESPONSE TO NEGATIVE (DOWN) GUST

WING ROOT BENDING MOMENT RESPONSE TO 1-COS GUST
FIGURE 88

148

load factor and WRBM due to discrete gusts are reduced substantially with the combination gust load alleviation/ride quality improvement (GLA/RQI) system. Improvements in negative values are small without the spoiler authority available for positive gusts. The positive load factor at maximum gross weight is reduced to approximately 2.65 g's.

Control surface responses due to the design (1-cos) gust at the critical flight condition are shown in Figure 89. The control surface authorities through the GLA/RQI are limited to the values specified above. In general, maximum surface rates occur after the first peak response, and surface response after the first peak is not critical for control of peak load factor and WRBM. The following minimum rates for wing control surfaces are recommended for GLA/RQI operation:

- Outboard ailerons: 100 deg/sec

- Inboard ailerons: 200 deg/sec

- Spoilers: 300 deg/sec

The effects of the various loops of the GLA/RQI on airframe stability are illustrated by the root locus plots of Figure 90. The wing control surface loops destabilize the airplane as shown at the top of Figure 90, and the elevator control loop compensates for the destabilizing effects of the wing control systems as shown at the bottom of Figure 90.

Gain scheduling for the GLA/RQI is shown in Figure 91. Gain scheduling through the GLA/RQI increases control surface authority above that required for gust load alleviation at V_C to obtain a significant improvement in ride qualities at climb and gust penetration cruise. The GLA/RQI produced no significant gust load alleviation or ride quality improvement at approach, even for very high gains. As shown in Figure 92, the GLA/RQI increases the elevator authority requirement for maneuver. Since the GLA/RQI is ineffective at approach, the gain is scheduled low at this critical condition for elevator authority to reduce elevator commands through the GLA/RQI.

The minimal effects of the GLA/RQI on airplane handling qualities are shown in the time response comparison of pitch rate with and without the GLA/RQI in Figure 93.

The reduction of the gust load factor to within .15 g's of the maneuver limit with this control system indicates this remaining .15 g increment could be attained if desired. With the present system, the major portion of the gust load alleviation is accomplished by the spoilers, 70 percent as opposed to
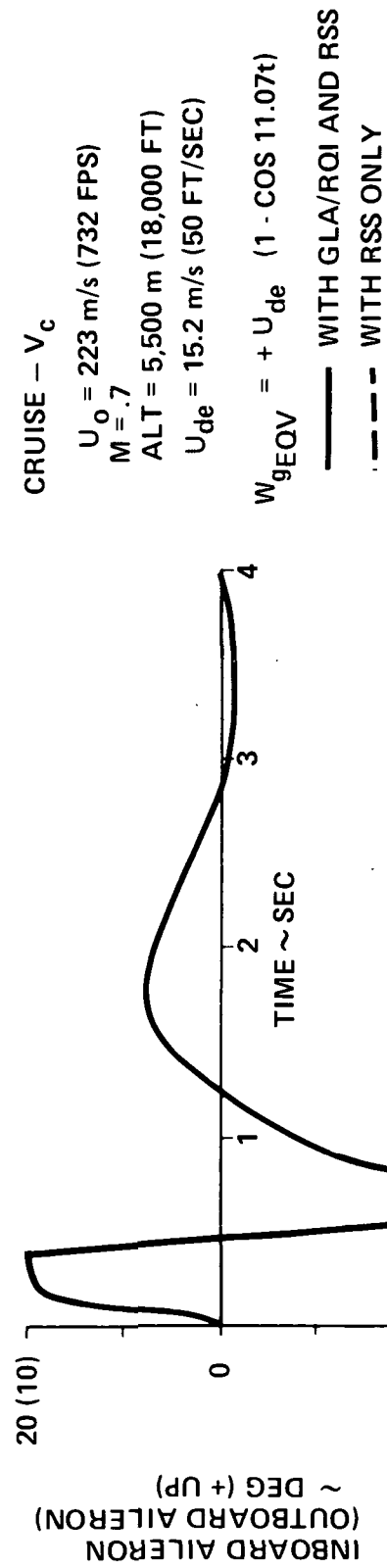
CONTROL SURFACE RESPONSE FOR 1-COS GUST
FIGURE 89

CRUISE

μ_o = 209 m/s (687 FPS)
M = .7
ALT = 10,100 m (33,000 FT)

X POLES
Ⓚ OPERATING GAIN
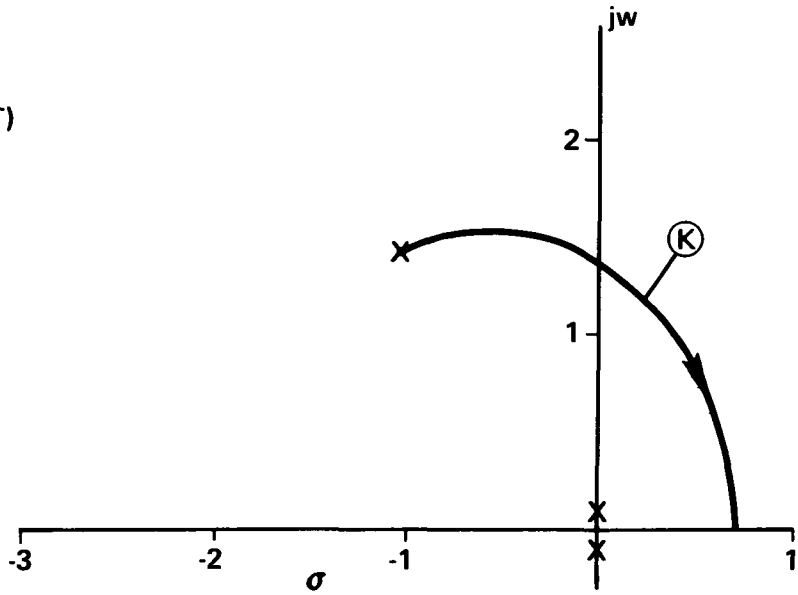
(A) AILERON LOOP ROOT LOCUS WITHOUT ELEVATOR LOOP
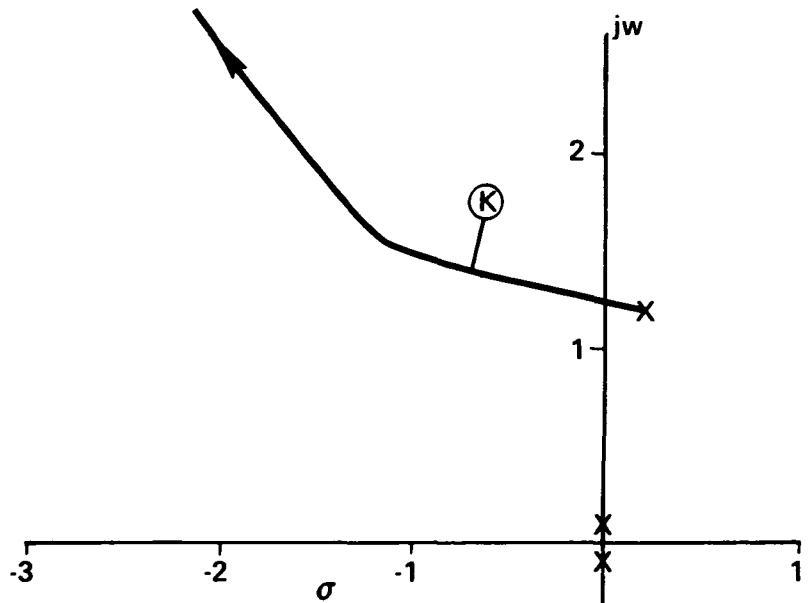
(B) ELEVATOR LOOP ROOT LOCUS WITH AILERON
LOOP AT OPERATING GAIN

GLA/RQI SYSTEM GAIN ROOT LOCUS
FIGURE 90
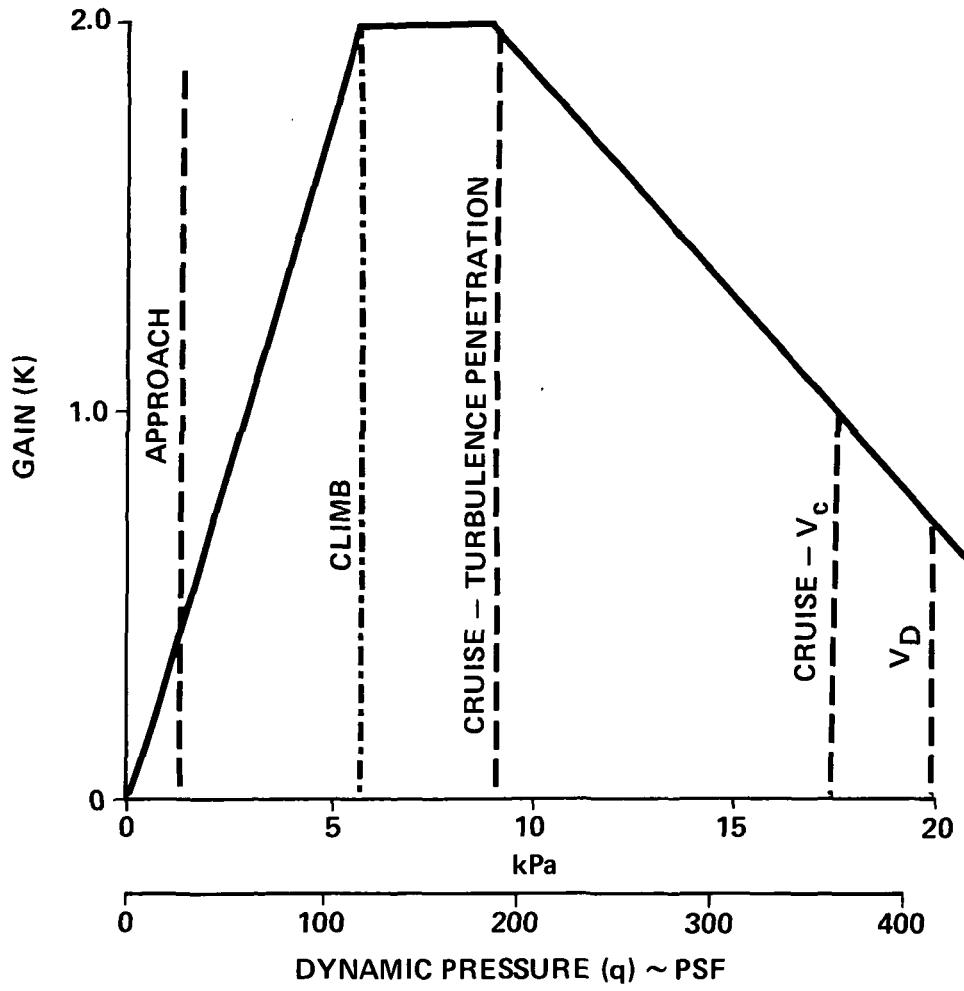
GLA/RQI SYSTEM GAIN SCHEDULE
FIGURE 91

CRUISE — V_c

U_o = 223 m/s (732 FPS)
M = .7
ALT = 5,500 m (18,000 FT)

————— WITH GLA/RQI AND RSS
— — — WITH RSS ONLY

δ ELEV
COMMAND
= -2 DEG
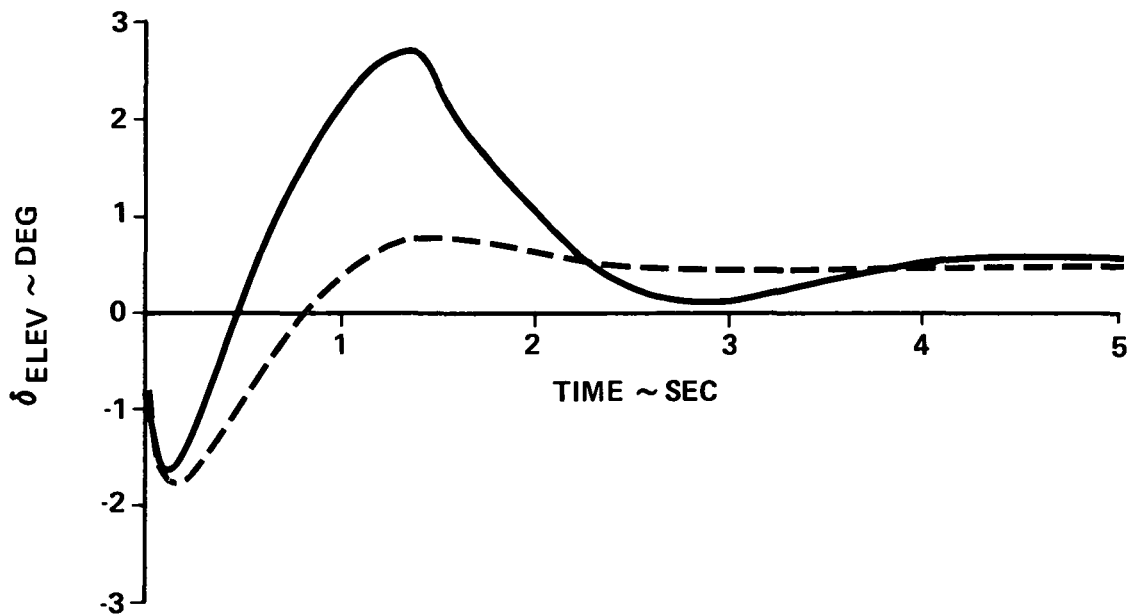
ELEVATOR RESPONSE FOR STEP ELEVATOR COMMAND WITH GLA/RQI SYSTEM
FIGURE 92
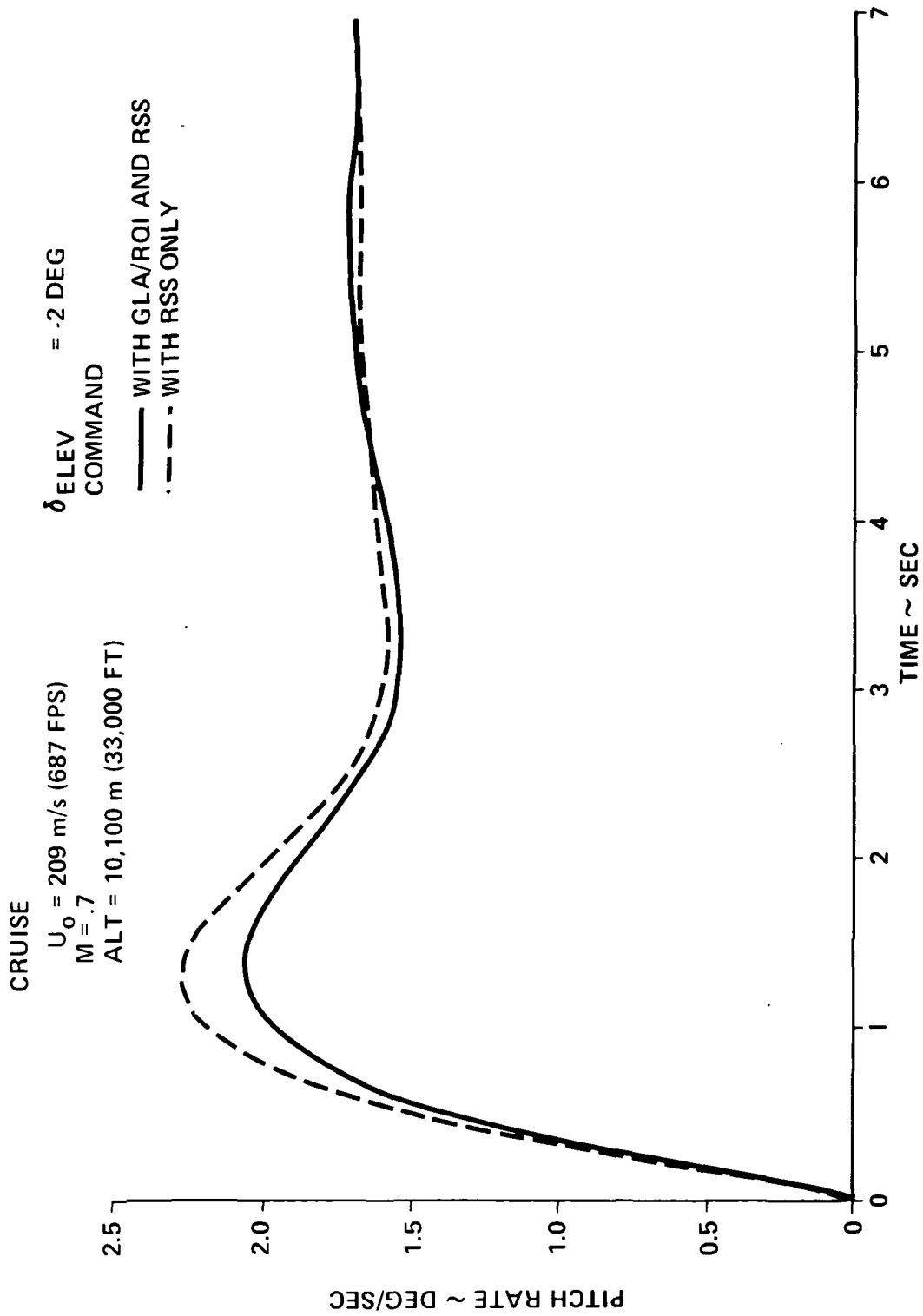
PITCH RATE RESPONSE WITH GLA/RQI SYSTEM
FIGURE 93

CRUISE
U_o = 209 m/s (687 FPS)
M = .7
ALT = 10,100 m (33,000 FT)

δ_{ELEV} = -2 DEG
COMMAND

——— WITH GLA/RQI AND RSS
— — WITH RSS ONLY

21 percent with the inboard ailerons and 9 percent with the outboard ailerons. The .15 g reduction could be attained by increasing the spoiler span from 44 percent to 50 percent or the deflection limit from 30 degrees to 34 degrees. Based on these design alternatives, it is concluded that the ACT system is capable of achieving a 2.5 g gust load alleviation.

Relaxed Static Stability System Analysis. - The Relaxed Static Stability (RSS) system consists of an angle of attack sensor input to elevator. A typical gain root locus for the RSS is shown in Figure 94. The unstable real root moves into the left-hand plane and connects with a branch of the phugoid locus to form new phugoid roots near the free airplane phugoid roots. The other branch of the phugoid locus couples with a stable real root to form oscillatory short period roots. Root loci for vertical accelerometer and pitch rate sensors showed similar formations of short period characteristics, but the unstable real root and a branch of the phugoid approached zeros at or near the origin; therefore; the unstable root was never completely stabilized.

Gain selection of the RSS considered placement of short period and phugoid roots and minimum gain margin on the unstable real root for aft center-of-gravity configurations. Analysis of four flight conditions ranging from approach to cruise indicated that a constant straight gain system provided acceptable handling qualities and stability; however, more desirable performance may be obtained with gain scheduling, sensor filtering and pilot input pre-filtering.

Typical airplane pitch rate response and elevator deflection are shown in Figure 95 for an elevator step command. Pitch rate response is similar to that obtained for a conventional stable airplane configuration. The elevator response shows a transient deflection approaching the command input (+2 degrees) to initiate the maneuver; however, steady state elevator response has a value required to maintain the maneuver opposite in sign to the command input.

Ride Quality Improvement Results. - Ride quality improvement obtained for the ACT configuration is shown in Figure 96, which compares vertical acceleration with and without the GLA/RQI at cruise, climb and approach. The ride quality at climb with the GLA/RQI is equivalent to that of a 707 at a comparable flight condition. At cruise, CG vertical acceleration with the GLA/RQI exceeds that of a 707 by 20 percent with less variation in response along the fuselage than the 707. No improvement in ride quality was obtained at approach.

CRUISE

U_o = 209 m/s
M = .7
ALT = 10,100 m (33,000 FT)

AFT CG

CONTROL SYSTEM:

$\delta_{ELEV} = K(\alpha_A + \alpha_g)$

X   POLES
⊙   ZEROS
Ⓚ   OPERATING GAIN
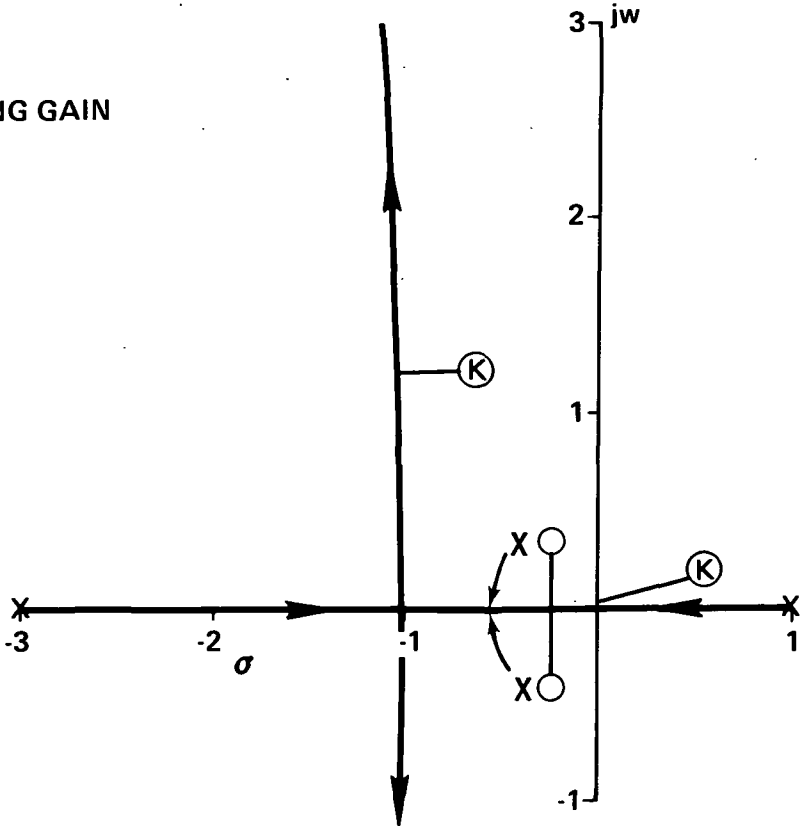
RELAXED STATIC STABILITY SYSTEM ROOT LOCUS
FIGURE 94

156

CRUISE — V_c
U_o = 223 m/s (732 FPS)
M = .7
ALT = 5,500 m (18,000 FT)

δ_{ELEV} = 2.0 DEG
COMMAND
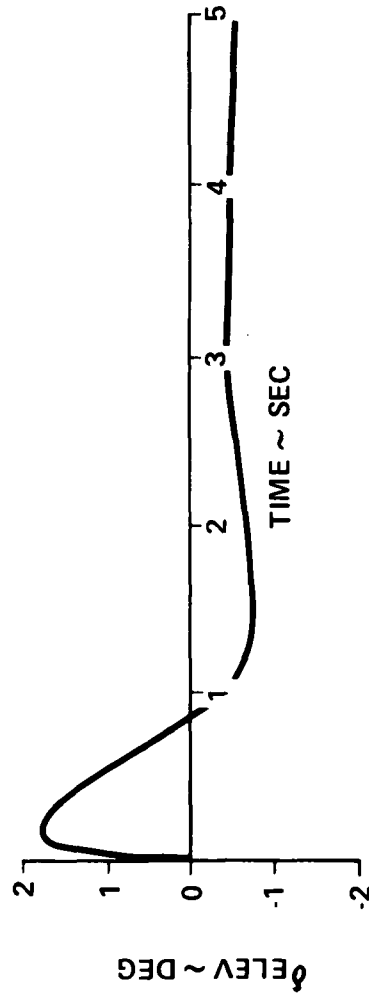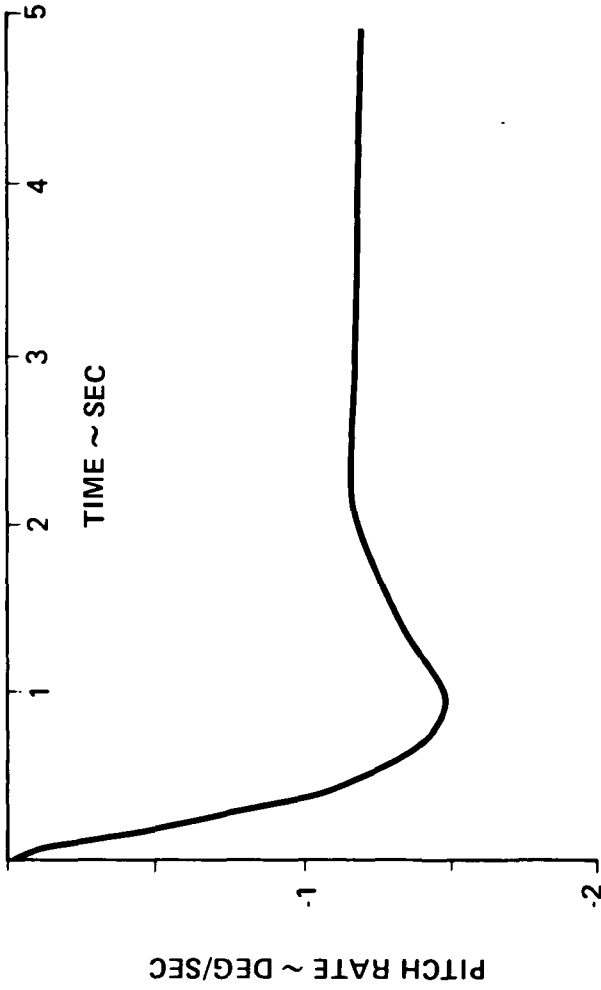
PITCH RATE AND ELEVATOR RESPONSE WITH
RSS TO STEP ELEVATOR WITH RSS
FIGURE 95

157
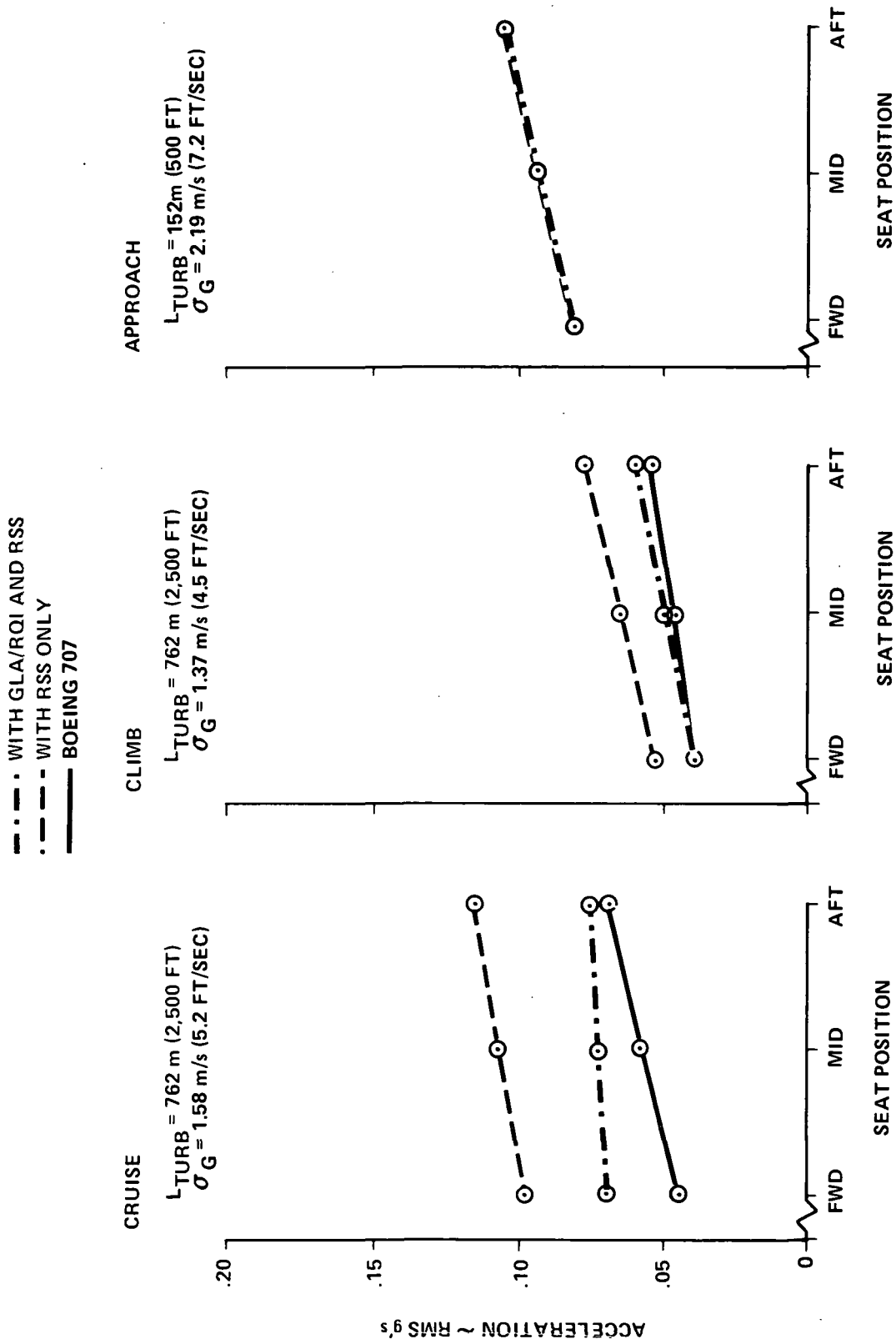
ACT SYSTEM VERTICAL RIDE QUALITY IMPROVEMENT
FIGURE 96

ACT Configuration

The optimized ACT configuration sized by the ASAMP computer program is presented in Figure 97. The airplane was resized using the same Q-fan propulsion system configuration as the baseline, Figure 54. The airplane design load factor was set at 2.5 g's, making the maneuver load factor and gust load factor with gust load alleviation equal. The horizontal and vertical tail volume coefficients were $\overline{V}_H$ = .447 and $\overline{V}_V$ = .0394, respectively. The horizontal and vertical tail arm lengths were 24.7 meters (81.0 feet) and 21.8 meters (71.6 feet) after rebalancing the airplane. The system weight penalties for the ACT installation were as follows:

System	System Weight Multiplication Factor
Hydraulics	1.15
Electronics	1.15
Flight Controls	1.30
Horizontal Tail Surface	1.02
Vertical Tail Surface	1.02

The design was maintained at the same wing loading and thrust to weight ratio as the Q-fan baseline.

A forward wing movement of 2.29 meters (90 inches) relative to the body was required to rebalance with the reduced wing and tail size. This movement is relative to the Q-fan baseline wing position. The weight statement for the optimized ACT configuration is presented in Table 30. The main landing gear moved forward 1.19 meters (47 inches) to maintain the same balance and takeoff rotation capability. It was necessary to recontour the lower aft body slightly to maintain the same rotation angle.

A detail statement of the airplane geometry is presented in Table 31. A comparison to the Q-fan configuration is presented in Figure 98.

ACT Configuration Performance Benefits

The performance improvements were computed in terms of mission fuel quantity saved and reduced direct operating cost. The results as compared to the Q-fan propulsion baseline are summarized in Table 32.
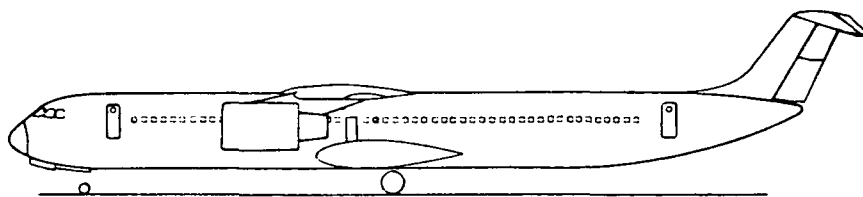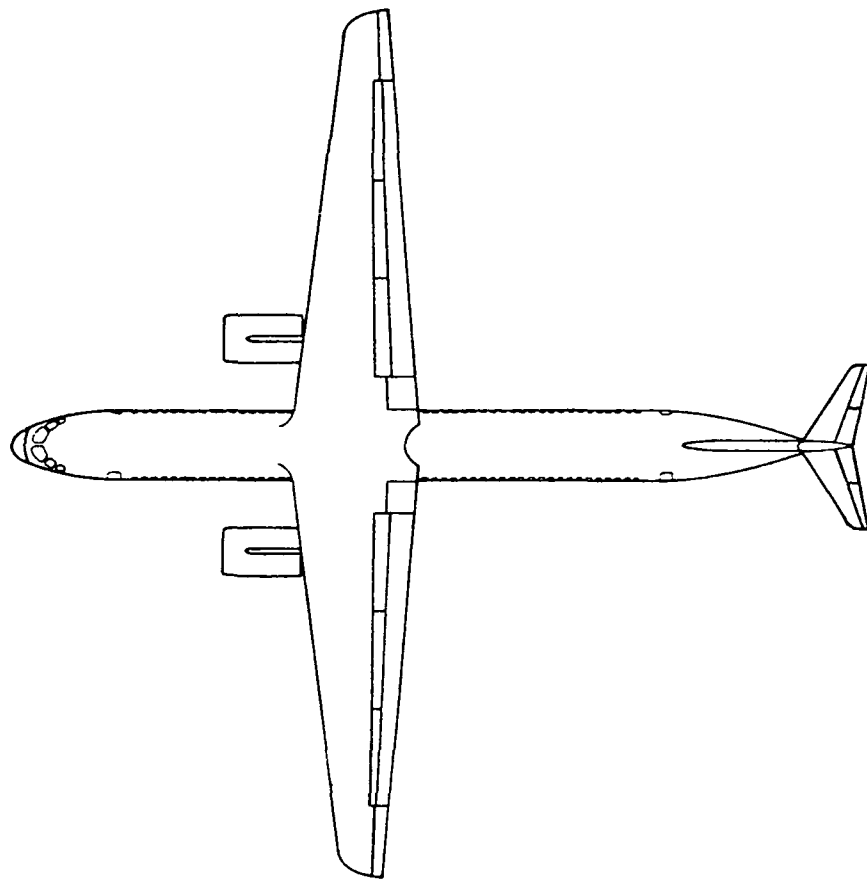
	WING	HORIZONTAL TAIL	VERTICAL TAIL
AREA ∼ m^2 (FT^2)	193 (2075)	16.8 (181)	15.3 (165)
MAC ∼ m (FT)	4.82 (15.8)	1.92 (6.3)	3.57 (11.7)
SPAN ∼ m (FT)	13.4 (144)	8.69 (28.5)	4.27 (14.0)
TAIL ARM ∼ m (FT)	—	24.7 (81.0)	21.8 (71.6)
TAIL VOLUME COEFFICIENT	—	.4470	.0394

MAXIMUM GROSS WEIGHT = 535,300 N (120,350 lbf)

CG RANGE FROM 45 TO 65 PERCENT MAC

ACT OPTIMIZED CONFIGURATION
FIGURE 97

TABLE 30
ACT CONFIGURATION WEIGHT SUMMARY

	WEIGHT	
	N	(lbf)
Propulsion Group		
Primary Engines	31,587	(7,101)
Engine Accessories	1,308	(294)
Engine Controls	667	(150)
Engine Starting System	347	(78)
Thrust Reversers		(0)
Fuel System	1,410	(317)
Total Propulsion Group Weight	35,319	(7,940)
Structures Group		
Wing	87,478	(19,666)
Horizontal Tail	4,101	(922)
Vertical Tail	3,732	(839)
Fuselage	60,927	(13,697)
Landing Gear	21,414	(4,814)
Engine Struts	6,966	(1,566)
Engine Nacelles	9,323	(2,096)
Total Structure Weight	193,942	(43,600)
Fixed Equipment		
Instruments	2,789	(627)
Surface Controls	11,023	(2,478)
Hydraulics	3,510	(789)
Pneumatics	2,362	(531)
Electricals	6,939	(1,560)
Electronics	5,098	(1,146)
Flight Deck Accommodations	3,465	(779)
Passenger Accommodations	48,596	(10,924)
Cargo Accommodation	5,480	(1,232)
Emergency Equipment	1,726	(388)
Air Conditioning	8,069	(1,814)
Anti-icing	1,477	(332)
APU	4,395	(988)
Total Fixed Equipment Weight	104,929	(23,589)
Manufacturers Empty Weight	334,189	(75,129)
Weight of Standard and Operational Items	22,237	(4,999)
Operational Empty Weight	35,643	(80,129)
Payload	134,958	(30,340)
Fuel	43,935	(9,877)
Gross Weight	535,323	(120,346)

TABLE 31
ACT CONFIGURATION AERODYNAMIC GEOMETRY SUMMARY

Fuselage				
LF	Length	41.54 m	(136.3	Ft)
WF	Width	3.66 m	(12.0	Ft)
SF	Wetted Area	433.0 m^2	(4,661.	Sq Ft)

Wing				
AR	Aspect Ratio		10.00	
SW	Area	192.8 m^2	(2,074.9	Sq Ft)
B	Span	43.89 m	(144.0	Ft)
CBARW	Geom. Mean Chord	4.82 m	(15.8	Ft)
LAMBDA C/4	Quarter Chord Sweep		4.3	Deg
LAMBDA	Taper Ratio		0.300	
(T/C)R	Root Thickness		0.183	
(T/C)T	Mean Aerodynamic Thickness		0.140	
WG/SW	Wing Loading	2.8 kPa	(58.0	lb/Sq Ft)

Horizontal Tail				
ARHT	Aspect Ratio		4.50	
SHT	Area	16.81 m^2	(180.9	Sq Ft)
BHT	Span	8.69 m	(28.5	Ft)
CBARHT	Mean Chord	1.92 m	(6.3	Ft)
(T/C)HT	Thickness/Chord		0.120	
LTH	Moment Arm		(81.0	Ft)

Vertical Tail				
ARVT	Aspect Ratio		1.20	
SVT	Area	15.28 m^2	(164.5	Sq Ft)
BVT	Span	4.27 m	(14.0	Ft)
CBARVT	Mean Chord	3.57 m	(11.7	Ft)
(T/C)VT	Thickness/Chord		0.130	
LTV	Moment Arm	21.82 m	(71.6	Ft)

Primary Engine Nacelle				
LN	Length	1.24 m	(13.4	Ft)
DBARN	Mean Diameter	2.16 m	(7.1	Ft)
SN	Wetted Area	54.44 m^2	(586.0	Sq Ft)
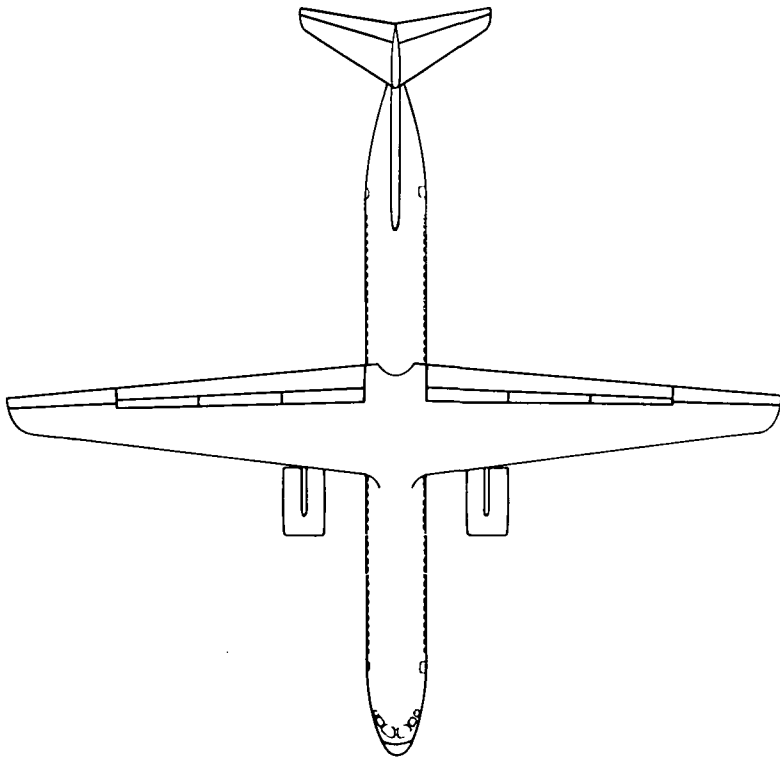
ACT CONFIGURATION
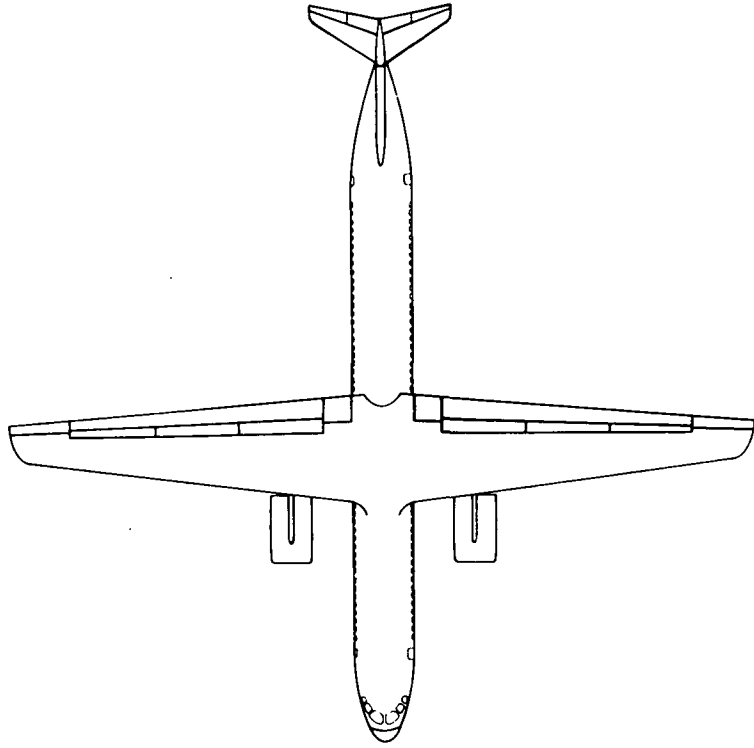
Q-FAN BASELINE CONFIGURATION
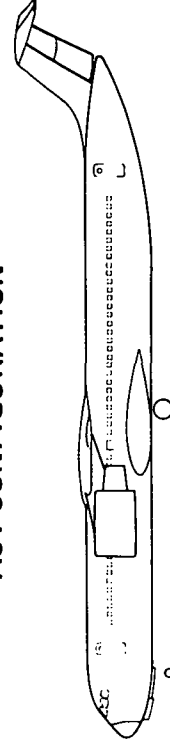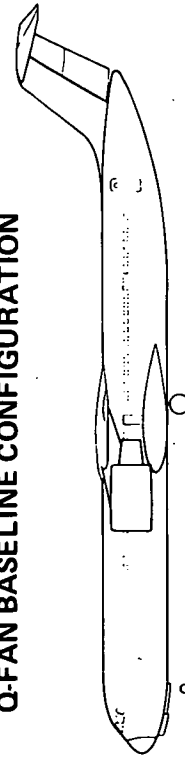
COMPARISON OF ACT CONFIGURATION TO Q-FAN BASELINE CONFIGURATION
FIGURE 98

163

TABLE 32
SUMMARY OF ACT TECHNOLOGY Q-FAN BENEFITS

Cruise at .7 M, 10,100 m (33,000 Ft)

AR = 10

W/S = 2.8 kPa (58 lbf)

λ = .3

	Q-Fan Propulsion	ACT Configuration	Percent Reduction
FPR	1.35	1.35	—
T/W	.33	.33	—
Λc/4 ~ Deg	4.30	4.30	—
OWE ~ N (lbf)	412,081　(92,640)	356,434　(80,130)	14
Payload ~ N (lbf)	134,958　(30,340)	134,958　(30,340)	—
Block Fuel ~ N (lbf)	32,917　(7,400)	30,648　(6,890)	7
Reserve Fuel ~ N (lbf)	14,279　(3,210)	13,256　(2,980)	7
Total Fuel ~ N (lbf)	47,195　(10,610)	43,904　(9,870)	7
Gross Weight ~ N (lbf)	594,235 (133,590)	535,341 (120,350)	10
*DOC ~ Cents/Seat — km (Cents/Seat — Statute Mi)	1.23 (1.98)	1.17 (1.88)	5

*Based on 12 cents/km^3 (46 cents/gal) fuel cost

Federal Airworthiness Regulation Impact

A review of the present Federal Airworthiness Regulation (FAR) Part 25 (Reference 6) that covers this class airplane indicated the ACT configured fuel conservative transport could be certified (Reference 23). This regulation is receptive to incorporating ACT technology provided that first, the airplane handling qualities and flight characteristics with ACT incorporated, remain essentially unchanged from those of a typical conventional certified modern day jet transport. Every effort has been made to maintain these qualities and, where possible, a quantitative evaluation has been presented to substantiate this. A more definite conclusion would require an indepth simulation study.

The second requirement is that the ACT system have the same reliability as the basic airplane structure. The design approach to meet this requirement is to start with a single system of as high a reliability as economically feasible and then to provide redundance to attain the required level of safety. A monitor system is provided to ensure that a failure is detected and isolated in a timely manner. (See Flight Controls System.)

The ability to meet the performance specification of FAR Part 25 is essentially independent of the ACT configuration. The ability of the ACT configuration to meet the Controllability and Maneuverability specification is not obvious because a smaller tail infers less trim and maneuver capability. It is important to realize that, although the ACT configuration has a smaller tail size, the tail is sized to provide the same required trim and maneuver capability as the conventional airplane. This can be seen by comparing the Q-fan tail sizing criteria on Page 27 to that for the ACT configuration presented on Page 120. Therefore, assuming the baseline Q-fan airplane could meet FAR Part 25 trim and maneuver requirements, the ACT configuration should also meet the specification.

A review of the stability section of FAR Part 25 shows that both the static stability and the dynamic stability requirements can be provided by the ACT flight control system. In some ways this requirement can be better met since providing increased stability, to a degree, is only a matter of increasing the system gain or phase, as opposed to increasing tail size on a conventional design.

The control force requirements are provided by the ACT control force feel system which is tailored to the desired force gradients. The positive stability inferred by the force gradients specified in Part 25 is provided by the ACT control system. This system is not unlike the Mach trim compensators on present jet transports that operate in the transonic speed regime. Although the pilot experiences a positive speed stability stick force gradient, i.e., push force

with increase in speed, the inherent airplane is unstable and the stability is provided by the flight control system. The same is true of the stability of the ACT configuration.

A review of the structure subsection of FAR Part 25 indicates the design gust load factors with the gust load alleviation system operating can be a legitimate design criteria. This conclusion is an opinion and would have to be substantiated through proper FAA authorities.

ACT SENSITIVITY TRADE STUDIES

A trade study was conducted to determine the sensitivity of the ACT configuration to variations in the design requirements. The design and operating parameters applicable to the baseline configuration were as follows:

PARAMETERS	REFERENCE BASELINE
Field Length	914 Meters (3,000 Feet)
Thrust to Weight	.331
Wing Loading	2.8 kPa (58.0 PSF)
Cruise Mach Number	.70
Cruise	10100 Meters (33,000 Feet)
Wing Geometry	
Aspect Ratio	10
Sweep	4°
Taper Ratio	.3
Airplane Size	148 Passengers

Since the number of combinations that encompasses a complete permutation of all these variables is unreasonable, the analysis centered on select combinations based on past preliminary design experience involving ACT concepts.

Three field lengths were evaluated: 914 meters (3000 feet), 1067 meters (3500 feet), and 1219 meters (4000 feet). For each field length, the airplane thrust-to-weight and wing-loading required to meet the design mission and payload were determined. The remaining design and operating parameters were held at the reference values. The thrust-to-weight ratio and wing-loading required to meet the design mission and payload were determined. The remaining design and operating parameters were held at the reference values. The thrust-to-weight ratio and wing-loading required to meet takeoff, cruise and landing constraints for 914-meter (3000-feet), 1067-meter (3500-feet) and 1219-meter (4000-feet) field lengths are presented in Figures 99, 100 and 101 respectively.
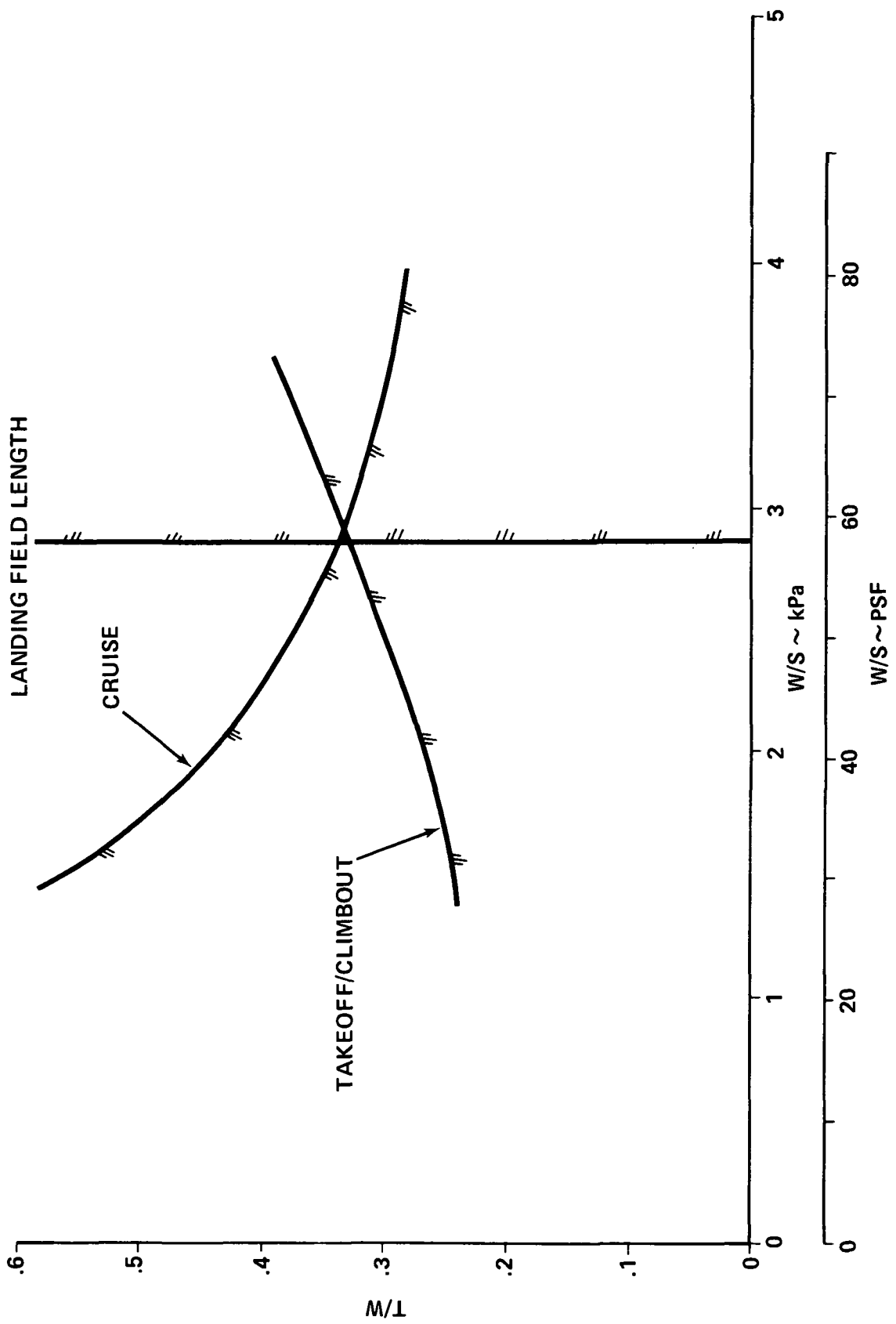
DESIGN CONSTRAINTS FOR 914 m (3,000 FT) FIELD

FIGURE 99

168
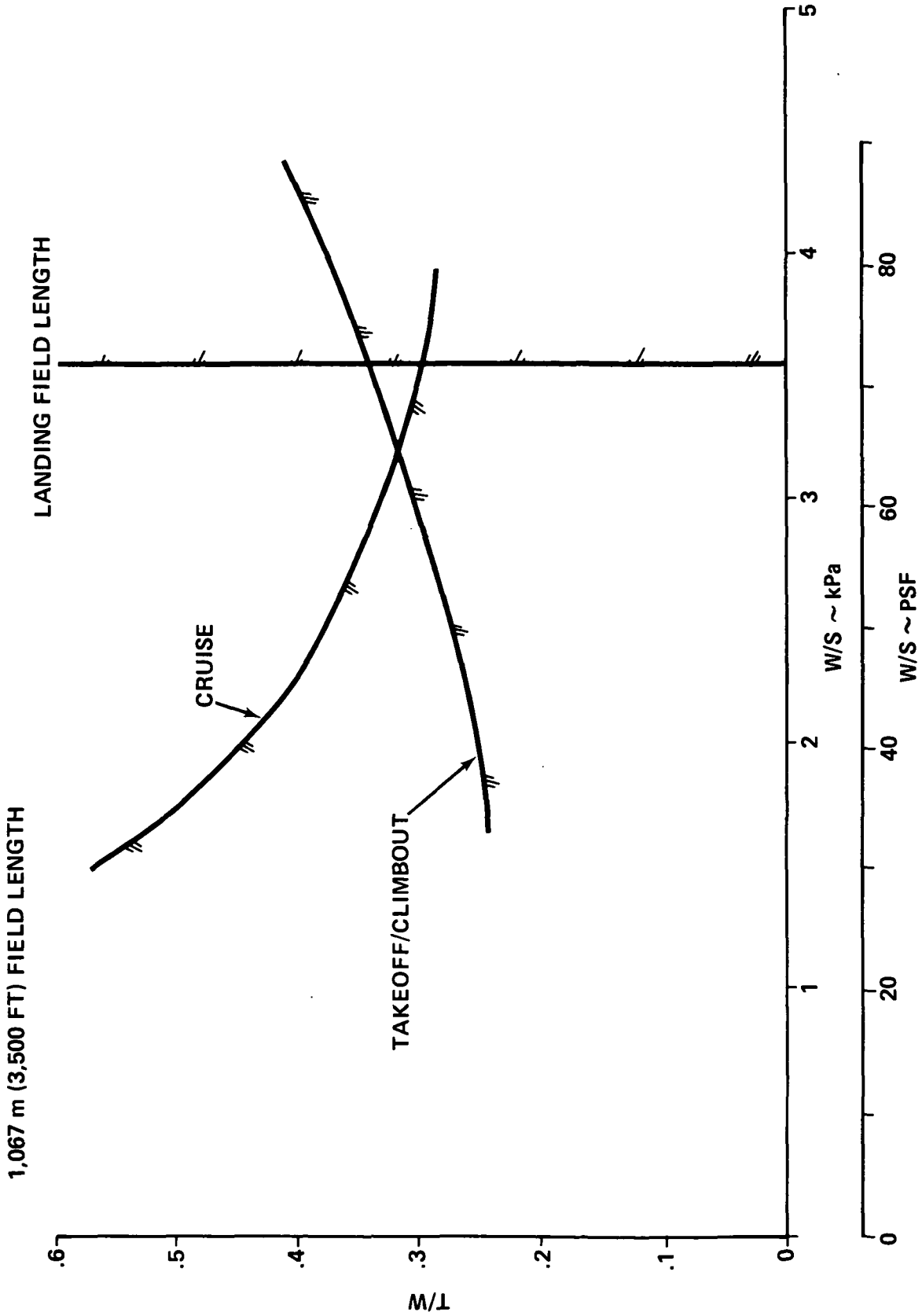
DESIGN CONSTRAINTS FOR 1,067 m (3,500 FT) FIELD
FIGURE 100

169

DESIGN CONSTRAINTS FOR 1,219 m (4,000 FT) FIELD
FIGURE 101

170

The wing loading upper limit that meets the landing requirement can be seen to be 2.8 kPA (58 PSF), 3.4 kPA (72 PSF) and 4.3 kPA (89 PSF) for the respective field lengths. The required T/W ratio at the upper wing loading limits were determined as .343 for 914-meter (3000-foot), .350 for 1067-meter (3500-foot), and .376 for 1219-meter (4000-foot) field lengths. The cruise condition dictated the minimum T/W value for the 914-meter (3000-foot) field length and the takeoff climbout T/W was critical for the longer field lengths. The upper wing loading limit was selected because experience has shown that for high cruise speeds, the minimum fuel consumption favors the higher wing loading because of the higher aerodynamic cruise efficiency (L/D).

The optimum resized airplanes were determined for the three field lengths using the ASAMP computer program. A Q-fan baseline airplane and an ACT configuration were sized for each field length. The performance increment for applying ACT technology as a function of field length are presented in Table 33 in terms of airplane gross weight, mission fuel and DOC. In addition, the airplane noise footprints were computed to evaluate any noise benefit. These results are presented in Table 34 and support the finding of Reference 24; i.e., as the field length increases, the higher wing loading airplanes do not show as large an improvement in performance as with a low wing loading. There are two primary reasons for this. The airplane becomes less gust critical and the smaller wing constitutes a smaller portion of the airplane total weight and drag. The same applies to the relaxed static stability concept, in that the tail constitutes a smaller portion of the airplane total weight. The requirement for ride quality improvement is reduced since the wing loading approaches that of a modern jet transport.

TABLE 34
SUMMARY OF ACT TECHNOLOGY Q-FAN NOISE BENEFITS
AS FUNCTION OF FIELD LENGTH

	FAR PART 25 FIELD LENGTH m (FEET)		
Δ NOISE FOOTPRINT AREA Mm^2 (SQ-MI) (BASELINE Q-FAN - ACT)	(3,000) 914	(3,500) 1,067	(4,000) 1,219
90 EPN dB	(.11) .28	(.05) .13	(.02) .05
80 EPN dB	(.56) 1.45	(.23) .60	(.10) .26

TABLE 33
SUMMARY OF ACT TECHNOLOGY Q-FAN BENEFITS
AS A FUNCTION OF FIELD LENGTH

Cruise at .7 M, 10,100 m (33,000 Ft)

AR = 10

λ = .3

FPR = 1.35

Λ = 4.3

	Field Length		
	914 m (3,000 Ft)	1,067 m (3,500 Ft)	1,219 m (4,000 Ft)
W/S $\sim$ kPa (lb/Ft^2)	2.8 (58)	3.4 (72)	4.3 (89)
T/W	.343	.350	.376
Incremental Savings Due to Active Control Technology (Baseline Q-Fan − ACT)			
Δ OWE $\sim$ N (lbf)	61,719 (13,875)	31,418 (7,063)	14,875 (3,344)
Δ Block Fuel $\sim$ N (lbf)	3,421 (769)	1,784 (401)	930 (209)
Δ Reserve Fuel $\sim$ N (lbf)	1,779 (400)	716 (161)	111 (25)
Δ Total Mission Fuel $\sim$ N (lbf)	5,200 (1,169)	2,500 (562)	1,041 (234)
Δ Gross Weight $\sim$ N (lbf)	66,919 (15,044)	33,918 (7,625)	15,916 (3,578)
Δ DOC $\sim$ Cents/Seat − km (Cents/Seat − Statute Mi)	.08 (.13)	.04 (.06)	.006 (.01)

An increase in cruise Mach number would be at the expense of increased fuel consumption. The .70 Mach number was selected as a compromise in mission duration and fuel consumption. At higher design Mach numbers, the airplane would be more gust load critical; therefore, assuming the gust loading could be alleviated to the maneuver limit, the potential benefits would be proportionately greater for the longer field lengths.

The wind geometry in terms of aspect ratio, taper ratio and sweep were concluded to be near optimum for the longer design field length configurations. Analysis of the baseline configuration showed that for aspect ratios above 10 for this design mission, the increased structural weight penalty offsets the improved aerodynamic efficiency.

Airplane size, in terms of number of passengers, would tend to favor the larger size for maximum ACT benefits. This is based on the experience gained from the Reference 24 study. The ACT electronic costs are not sensitive to airplane size and therefore tend to penalize the smaller size airplanes.

FUTURE RESEARCH AND TECHNOLOGY OBJECTIVES

A summary of the research and technology objectives identified during this study which would be helpful to guide and strengthen the NASA short-haul air transportation program follows. The order does not imply a ranking.

- Continue the development of Q-fan propulsion system and obtain demonstrated performance data.

- A conceptual design analysis method of determining wing weight reduction as a function of nonelliptical lift distribution due to control surface deflections is needed to evaluate the full benefits of a gust load alleviation and/or a maneuver load control system. Present methods rely heavily on predicting wing weight based on previous airplane designs which have been based primarily on a near elliptical lift distribution, thus setting a unique relationship between WRBM and load factor.

- With the reduction of the design gust load factor to the maneuver load factor, the possible further improvement with maneuver load control should be evaluated.

- There is a need for comprehensive study on spoiler effects including a complete set of stability and control derivatives, hinge moments as a function of rate of deflection and lift growth. These data are needed for gust load alleviation analyses where spoilers offer the potential of being the most efficient system. This study should address the effectiveness on the latest supercritical type airfoils, location on the wing, and with and without flaps.

- Develop a atmospheric turbulence model for evaluating control requirements and saturation for relaxed static stability analyses and vertical and lateral accelerations for ride quality improvement analyses. Present models have been primarily developed for structural design purposes and have focused on the low probability of large gust encounters.

- Prepare a quantitative handling qualities criteria for establishing pitch maneuver control required for a short-haul jet type transport. The criteria should include time response requirements that encompass the complete flight envelope from stall to dive.

Page Intentionally Left Blank

CONCLUDING REMARKS

As a continuation of NASA's effort to provide the necessary information to aid in the design of a fuel conservative short-haul transport, two advancements in technology were evaluated, the Q-fan propulsion system and active control technology (ACT). Three concepts were included in the ACT system: gust load alleviation (GLA), relaxed static stability (RSS) and ride quality improvement (RQI). Each concept was evaluated separately and then combined as a multipurpose active control system configuration. The benefits of the Q-fan propulsion system were determined relative to a baseline turbofan powered, low-wing-loading, mechanical flap, fuel conservative transport specified by Reference 2. The ACT benefits were measured relative to the optimized Q-fan propulsion configuration.

The following conclusions were drawn from the results of this study.

- The preliminary design methodology utilized by Boeing produced a satisfactory correlation with the Reference 2 baseline configuration.

- The optimized Q-fan propulsion system configuration showed a 14 percent reduction in mission fuel relative to the baseline configuration.

- The Q-fan configuration did not show a significant improvement in noise. (Both configurations well below FAR Part 36 requirements.)

- All three ACT concepts showed significant performance gains.

    - GLA - 8 percent reduction in design gross weight
    - RSS - 2 percent reduction in design gross weight.
    - RQI - Passenger comfort was equal to that of a modern high performance jet.

- The ACT concepts, when applied collectively, provide essentially the same performance as when applied separately; i.e., the total benefit is essentially the same as the sum of the individual benefits.

- Satisfactory reliability at acceptable cost can be attained for FAR certification.

177

- Satisfactory flying and handling qualities were maintained for all ACT configurations.

- For field lengths longer than 914 meters (3000 feet), the ACT benefits decrease.

APPENDICES

Appendix A Baseline Thrust and Drag Data

The thrust and drag data used in the ASAMP computer program to size the Boeing baseline configuration are presented in Tables 35 through 38. The thrust and specific fuel consumption data are normalized within the thrust subroutines of ASAMP. The thrust subroutines then calculate the necessary rubberized engine data.

Appendix B Q-Fan Thrust and Drag Data

The thrust and drag data used in the ASAMP computer program to size the optimized Q-fan propulsion configuration are presented in Tables 39 through 42. The thrust and specific fuel consumption data are normalized within the thrust subroutines of ASAMP. The thrust subroutines then calculate the necessary rubberized engine data.

Appendix C Stability, Control and WRBM Derivatives

The stability, control and wing-root-bending-moment derivatives used to evaluate the gust load alleviation system are presented in Tables 43 through 45. The derivatives used to evaluate the Q-fan propulsion system baseline configuration and Boeing 707 ride qualities are presented in Tables 46 and 47, respectively. The derivatives used to evaluate the ACT configuration are presented in Table 48.

The stability, control and wing root bending moment derivatives were developed from data contained in References 9 through 15.

TABLE 35
BASELINE FCT THRUST

TAKEOFF THRUST~ N (lbf) SEA LEVEL, 308°K (95°F)

Alt~m (ft)	MACH NO.						
	0	.10	.20	.30	.40	.50	.60
0	118200. (26572)	101890. (22905)	88440. (19882)	77880. (17508)	69210. (15558)	62300. (14006)	56130. (12619)

MAXIMUM CLIMB THRUST~N (lbf)

Alt~m (ft)	MACH NO.					
	0	.20	.35	.50	.65	.80
0	120710. (27136.)	81360. (18290.)	65420. (14708.)	54880. (12338.)	46600. (10475.)	40310. (9063.)
3048. (10000)	134390. (30212.)	99920. (22463.)	83030. (18665.)	71150. (15996.)	61910. (13919.)	54750. (12309.)
6096. (20000)	147980. (33268.)	115680. (26006.)	98730. (22195.)	88110. (19809.)	79250. (17815.)	71860. (16154.)
9144. (30000)	140550. (31597.)	112140. (25210.)	99220. (22305.)	91300. (20524.)	86950. (19546.)	87040. (19567.)
12192 (40000)	123300. (27718.)	108090. (24300.)	99060. (22269.)	91070. (20473.)	86600. (19469.)	86560. (19460.)

MAXIMUM CRUISE THRUST ~ N (lbf)

Alt~m (ft)	MACH NO.					
	0	.20	.35	.50	.65	.80
0	97360. (21887.)	71750. (16130.)	57360. (12895.)	47570. (10694.)	40070. (9009.)	34430. (7741.)
3048. (10000.)	117640. (26447.)	89180. (20049.)	74520. (16752.)	62490. (14048.)	53650. (12062.)	46750. (10509.)
6096. (20000)	130570. (29354.)	106640. (23973.)	91260. (20515.)	79680. (17912.)	71050. (15770.)	62610. (14075.)
9144. (30000)	142190. (31966.)	113630. (255546.)	99220. (22305.)	91300. (20524.)	86950. (19546.)	81770. (18383.)
12192 (40000)	164710. (37029.)	123060. (27664.)	99060. (22269.)	91070. (20473.)	86600. (19469.)	86560. (19460.)

TABLE 36
BASELINE FCT SFC

ALTITUDE = 0   SFC ~ Mkg/N • S (lbm/lbf • hr)

Net Thrust ~ N (lbf)	MACH NO.			
	0	.20	.35	.50
8896. (2000)	16.37 (.578)	21.24 (.750)	26.06 (.920)	31.87 (1.125)
17793. (4000.)	10.91 (.385)	16.91 (.597)	18.41 (.650)	22.94 (.810)
26689. (6000.)	9.63 (.340)	12.41 (.438)	16.15 (.570)	19.83 (.700)
35586. (8000.)	9.01 (.318)	11.56 (.408)	14.90 (.526)	17.96 (.634)
44482. (100000)	8.58 (.303)	11.13 (.393)	14.02 (.495)	16.91 (.597)
53378. (12000)	8.36 (.295)	10.76 (.380)	13.48 (.476)	16.15 (.570)
62275. (14000)	8.21 (.290)	10.45 (.369)	13.14 (.464)	15.78 (.557)
71171. (16000)	7.93 (.280)	9.91 (.350)	12.97 (.458)	15.58 (.550)
80068. (18000)	7.65 (.270)	9.91 (.350)	12.75 (.450)	15.58 (.550)
88964. (20000)	7.51 (.265)	9.91 (.350)	12.75 (.450)	15.58 (.550)
97860. (22000)	7.25 (.256)	9.91 (.350)	12.75 (.450)	15.58 (.550)
106757. (24000)	7.11 (.251)	9.91 (.350)	12.75 (.450)	15.58 (.550)
115653. (26000)	6.91 (.244)	9.91 (.350)	12.75 (.450)	15.58 (.550)
124550. (28000)	6.91 (.244)	9.91 (.350)	12.75 (.450)	15.58 (.550)

TABLE 36
BASELINE FCT SFC (CONT'D)

ALTITUDE = 3048 (10000)   SFC~ Mkg/N · S   (lbm/lbf · hr)

Net Thrust ~ N(lbf)	MACH NO.			
	.35	.50	.65	.80
8896. (2000.)	25.92 (.915)	31.87 (1.125)	39.23 (1.385)	46.03 (1.625)
17793. (4000.)	18.41 (.650)	22.69 (.801)	27.99 (.988)	33.20 (1.172)
26689. (6000.)	15.86 (.560)	19.74 (.697)	23.79 (.840)	27.87 (.984)
35586. (8000.)	14.73 (.520)	18.07 (.638)	21.33 (.753)	25.12 (.887)
44482. (10000.)	13.94 (.492)	16.94 (.598)	19.94 (.704)	23.23 (.820)
53378. (12000.)	13.40 (.473)	16.15 (.570)	18.98 (.670)	21.90 (.773)
62275. (14000.)	13.03 (.460)	15.64 (.552)	18.18 (.642)	20.96 (.740)
71171. (16000.)	12.86 (.454)	15.30 (.540)	17.87 (.631)	20.22 (.714)
80068. (18000.)	12.75 (.450)	15.27 (.539)	17.62 (.622)	19.83 (.700)

TABLE 36
BASELINE FCT SFC (CONT'D)

ALTITUDE = 6096 (20000) SFC~ Mkg/N · S (lbm/lbf · hr)

Net Thrust ~ N (lbf)	MACH NO.			
	.35	.50	.65	.80
8896. (2000.)	26.34 (.930)	31.87 (1.125)	39.66 1.400)	48.86 (1.725)
17793. (4000.)	18.69 (.660)	23.23 (.820)	28.10 (.992)	33.76 (1.192)
26689. (6000.)	16.09 (.568)	19.97 (.705)	23.82 (.841)	27.96 (.987)
35586. (8000.)	14.76 (.521)	18.07 (.638)	21.47 (.758)	24.93 (.880)
44482. (10000.)	13.94 (.492)	16.85 (.595)	19.94 (.704)	23.23 (.820)
53378. (12000.)	13.43 (.474)	16.15 (.570)	18.98 (.670)	21.98 (.776)
62275. (14000.)	13.09 (.462)	15.61 (.551)	18.21 (.643.)	21.19 (.748)
71171. (16000.)	12.97 (.458)	15.35 (.542)	17.87 (.631)	20.59 (.727)
80068. (18000.)	12.80 (.452)	15.30 (.540)	17.70 (.625)	20.14 (.711)
88964. (20000.)	12.77 (.451)	15.24 (.538)	17.70 (.625)	19.86 (.701)
97860. (22000.)	12.89 (.455)	15.30 (.540)	17.87 (.631)	19.83 (.700)

TABLE 36
BASELINE FCT SFC (CONT'D)

ALTITUDE = 9144 (30000)   SFC ~ Mkg/N · S   (lbm/lbf · hr)

Net Thrust ~ N(lbf)	MACH NO.			
	.35	.50	.65	.80
8896. (2000.)	27.08 (.956)	33.71 (1.190)	39.94 (1.410)	48.38 (1.708)
17793. (4000.)	19.60 (.692)	23.57 (.832)	28.86 (1.019)	34.81 (1.229)
26689. (6000.)	16.54 (.584)	20.34 (.718)	24.30 (.858)	28.52 (1.007)
35586. (8000.)	15.04 (.531)	18.41 (.650)	21.75 (.768)	25.35 (.895)
44482. (10000.)	14.13 (.499)	17.14 (.605)	20.16 (.711)	23.48 (.829)
53378. (12000.)	13.54 (.478)	16.20 (.572)	19.03 (.672)	22.12 (.781)
62275. (14000.)	13.14 (.464)	15.69 (.554)	18.41 (.650)	21.22 (.759)
71171. (16000.)	12.97 (.458)	15.47 (.546)	18.04 (.637)	20.68 (.730)
80068. (18000.)	12.89 (.455)	15.30 (.540)	17.85 (.630)	20.39 (.720)
88964. (20000.)	12.97 (.458)	15.35 (.542)	17.76 (.627)	20.22 (.714)
97860. (22000.)	13.03 (.460)	15.58 (.550)	17.73 (.626)	20.17 (.712)

TABLE 36
BASELINE FCT SFC (CONT'D)

ALTITUDE = 12,192 (40000)   SFC~Mkg/N · S   (lbm/lb · hr)

Net Thrust ~N(lbf)	MACH NO.			
	.35	.50	.65	.80
8896. (2000.)	31.58 (1.115)	37.79 (1.334)	45.89 (1.620)	53.17 (1.877)
17793. (4000.)	20.59 (.727)	25.46 (.899)	30.25 (1.068)	35.89 (1.267)
26689. (6000.)	17.48 (.617)	21.19 (.748)	25.12 (.887)	29.40 (1.038)
35586. (8000.)	15.98 (.564)	18.98 (.670)	22.35 (.789)	26.20 (.925)
44482. (10000.)	14.96 (.528)	17.65 (.623)	20.79 (.734)	24.08 (.850)
53378. (12000.)	14.16 (.500)	16.77 (.592)	19.66 (.694)	22.63 (.799)
62275. (14000.)	13.71 (.484)	16.20 (.572)	18.92 (.668)	21.73 (.767)
71171. (16000.)	13.40 (.473)	15.89 (.561)	18.44 (.651)	21.05 (.743)
80068. (18000.)	13.26 (.468)	15.72 (.555)	18.24 (.644)	20.71 (.731)
88964. (20000.)	13.17 (.465)	15.72 (.555)	18.10 (.639)	20.59 (.727)
97860. (22000.)	13.31 (.470)	15.86 (.560)	18.16 (.641)	20.62 (.728)

Page Intentionally Left Blank

TABLE 37 BASELINE FCT DRAG BREAKDOWN

10,060 m (33,000 ft.)

MACH NO. = 0.70   CL = 0.31

GEOMETRY TOTAL DRAG	PARASITE DRAG	FLAT PLATE FRICTION DRAG	PRESSURE DRAG	DRAG RISE	VORTEX DRAG
0.019054	0.015554	0.009823	0.005710	0.000025	0.003496

COMPONENT DRAG					INDUCED DRAG
					0.003266
WING	0.006467	0.004326	0.002141	0.0	TRIM DRAG
BODY	0.004139	0.003432	0.000708	0.0	0.000130
HORZ TAIL	0.000943	0.000736	0.000208	0.0	
VERT TAIL	0.000683	0.000528	0.000155	0.0	
NACELLE	0.001592	0.000617	0.000975	0.000025	
STRUT	0.000261	0.000185	0.000076	0.0	
HI CAP	0.0	0.0	0.0	0.0	
BODY POD	0.0	0.0	0.0	0.0	
WING POD	0.0	0.0	0.0	0.0	
FLAP TRACK	0.0	0.0	0.0	0.0	
BUBBLE EXCRESCENCE	0.0 0.001449	0.0	0.0	0.0	

TABLE 38 BASELINE FCT DRAG POLAR

ALT = 0.0

CL/M	0.0	0.0500	0.1000	0.1500	0.2000	0.2500	0.3000	0.3500
0.0	0.0008	0.0251	0.0224	0.0210	0.0201	0.0194	0.0189	0.0184
0.1000	0.0011	0.0239	0.0214	0.0201	0.0192	0.0186	0.0181	0.0177
0.2000	0.0022	0.0248	0.0223	0.0210	0.0201	0.0195	0.0190	0.0186
0.3000	0.0039	0.0267	0.0242	0.0228	0.0220	0.0214	0.0209	0.0205
0.4000	0.0064	0.0294	0.0266	0.0255	0.0247	0.0240	0.0235	0.0231
0.5000	0.0096	0.0329	0.0303	0.0290	0.0281	0.0274	0.0269	0.0265
0.6000	0.0135	0.0373	0.0346	0.0332	0.0323	0.0317	0.0312	0.0307
0.7000	0.0181	0.0428	0.0400	0.0386	0.0377	0.0370	0.0364	0.0360

ALT = 0.0

CL/M	0.4000	0.4500	0.5000	0.5500	0.6000	0.6500	0.7000
0.0	0.0181	0.0178	0.0175	0.0173	0.0170	0.0169	0.0167
0.1000	0.0173	0.0170	0.0168	0.0166	0.0164	0.0162	0.0161
0.2000	0.0183	0.0180	0.0177	0.0175	0.0173	0.0172	0.0170
0.3000	0.0201	0.0198	0.0196	0.0194	0.0192	0.0190	0.0188
0.4000	0.0228	0.0225	0.0222	0.0220	0.0218	0.0216	0.0215
0.5000	0.0262	0.0259	0.0256	0.0254	0.0252	0.0250	0.0249
0.6000	0.0304	0.0301	0.0298	0.0296	0.0294	0.0292	0.0295
0.7000	0.0356	0.0353	0.0351	0.0348	0.0346	0.0344	0.0390

ALT = 10,060 m (33,000 ft.)

CL/M	0.0	0.0500	0.1000	0.1500	0.2000	0.2500	0.3000	0.3500
0.0	0.0008	0.0251	0.0224	0.0210	0.0201	0.0194	0.0189	0.0184
0.1000	0.0011	0.0239	0.0214	0.0201	0.0192	0.0186	0.0181	0.0177
0.2000	0.0022	0.0248	0.0223	0.0210	0.0201	0.0195	0.0190	0.0186
0.3000	0.0039	0.0267	0.0242	0.0228	0.0220	0.0214	0.0209	0.0205
0.4000	0.0064	0.0294	0.0268	0.0255	0.0247	0.0240	0.0235	0.0231
0.5000	0.0096	0.0329	0.0303	0.0290	0.0281	0.0274	0.0269	0.0265
0.6000	0.0135	0.0373	0.0346	0.0332	0.0323	0.0317	0.0312	0.0307
0.7000	0.0181	0.0428	0.0400	0.0386	0.0377	0.0370	0.0364	0.0360

ALT = 10,060 m (30,000 ft.)

CL/M	0.4000	0.4500	0.5000	0.5500	0.6000	0.6500	0.7000
0.0	0.0181	0.0178	0.0175	0.0173	0.0170	0.0169	0.0167
0.1000	0.0173	0.0170	0.0168	0.0166	0.0164	0.0162	0.0161
0.2000	0.0183	0.0180	0.0177	0.0175	0.0173	0.0172	0.0170
0.3000	0.0201	0.0198	0.0196	0.0194	0.0192	0.0190	0.0188
0.4000	0.0228	0.0225	0.0222	0.0220	0.0218	0.0216	0.0215
0.5000	0.0262	0.0259	0.0256	0.0254	0.0252	0.0250	0.0249
0.6000	0.0304	0.0301	0.0298	0.0296	0.0294	0.0292	0.0295
0.7000	0.0356	0.0353	0.0351	0.0348	0.0346	0.0344	0.0390

TABLE 39
Q-FAN PROPULSION THRUST

TAKEOFF THRUST ~ N (lbf) ' SEA LEVEL, 308°K (95°F)

ALT ~ M (ft)	MACH NO.						
	0	.10	.20	.35	.50	.65	.80
0	114568. (25756.)	97113. (21832.)	83728. (18823.)	70824. (15922.)	62448. (14039.)	57662. (12963.)	54268. (12200.)

MAXIMUM CLIMB THRUST ~ N (lbf)

ALT ~ M (ft)	MACH NO.						
	0	.10	.20	.35	.50	.65	.80
0	103110. (23180.)	86000. (19334.)	72710. (16,346.)	58640. (13182.)	49090. (11036.)	40660. (9140.)	34050. (7654.)
3048. (10000.)	122250. (27483.)	106080. (23848.)	91850. (20648.)	76020. (17089.)	64630. (14529.)	55520. (12482.)	48340. (10867.)
6086. (20000.)	141320. (31771.)	126810. (28507.)	113450. (25504.)	96020. (21587.)	82880. (18632.)	72270. (16247.)	64040. (14397.)
9144. (30000.)	141550. (31822.)	133310. (29970.)	124330. (27950.)	111570. (25081.)	100965. (22698.)	92550. (20806.)	84300. (18950.)
12192. (40000.)	144200. (32417.)	134830. (30310.)	127370. (28635.)	116380. (26163.)	106880. (24028.)	99760. (22427.)	95560. (21482.)

MAXIMUM CRUISE THRUST ~ N (lbf)

ALT ~ M (ft)	MACH NO.						
	0	.10	.20	.35	.50	.65	.80
0	84070. (18900.)	73170. (16450.)	63610. (14300.)	52040. (11698.)	42660. (9590.)	34960. (7859.)	28740. (6460.)
3048. (10000.)	116190. (26120.)	91850. (20648.)	81500. (18322.)	67920. (15269.)	57280. (12878.)	49060. (11029.)	42130. (9472.)
6069. (20000.)	132420. (27745.)	112290. (25243.)	101640. (22849.)	86930. (19543.)	74240. (16690.)	64300. (14456.)	56590. (12723.)
9144. (30000.)	136310. (30644.)	126730. (28489.)	118340. (26603.)	105460. (23708.)	94280. (21195.)	83620. (18798.)	62170. (16976.)
12192. (40000.)	142040. (31931.)	132900. (29878.)	123770. (27825.)	110990. (24952.)	100830. (22667.)	93490. (21017.)	85780. (19284.)

188

TABLE 40
Q-FAN PROPULSION SFC

ALTITUDE = 0   SFC ~ Mkg/N · S   (lbm/lbf · hr)

Net Thrust~N (lbf)	MACH NO.				
	0	.10	.20	.35	.50
8896. (2000.)	19.26 (.680)	20.68 (.730)	22.12 (.781)	24.36 (.860)	31.16 (1.100)
13345. (3000.)	14.30 (.505)	15.78 (.557)	17.14 (.605)	19.29 (.681)	24.67 (.871)
17793. (4000.)	12.18 (.430)	13.62 (.481)	15.01 (.530)	17.00 (.600)	21.56 (.761)
26689. (6000.)	9.91 (.350)	11.36 (.401)	12.75 (.450)	14.87 (.525)	18.41 (.650)
35586. (8000.)	8.78 (.310)	10.20 (.360)	11.61 (.410)	13.77 (.486)	16.77 (.592)
44482. (10000.)	8.04 (.284)	9.52 (.336)	10.91 (.385)	13.14 (.464)	15.86 (.560)
53378. (12000.)	7.56 (.267)	8.92 (.315)	10.42 (.368)	12.60 (.445)	15.18 (.536)
62275. (14000.)	7.22 (.255)	8.50 (.300)	10.06 (.355)	12.32 (.435)	14.73 (.520)
71171. (16000.)	7.00 (.247)	8.33 (.294)	9.91 (.350)	12.15 (.429)	14.50 (.512)
80068. (18000.)	6.85 (.242)	8.21 (.290)	9.77 (.345)	12.04 (.425)	14.33 (.506)
88964. (20000.)	6.80 (.240)	8.21 (.290)	9.74 (.344)	11.95 (.422)	14.30 (.505)
106757. (24000.)	6.80 (.240)	8.21 (.290)	9.72 (.343)	11.92 (.421)	14.25 (.503)
142342. (32000.)	7.31 (.258)	8.78 (.310)	10.20 (.360)	12.35 (.436)	14.62 (.516)

TABLE 40
Q-FAN PROPULSION SFC (CONT'D)

ALTITUDE = 3048 (10000)   SFC~ Mkg/N · S (LBM/LBF · HR)

Net Thrust ~ N (lbf)	MACH NO.			
	.35	.50	.65	.80
8896. (2000.)	24.08 (.850)	30.31 (1.070)	41.19 (1.454)	52.06 (1.838)
13345. (3000.)	19.69 (.695)	25.78 (.910)	30.76 (1.086)	37.11 (1.310)
17793. (4000.)	17.19 (.607)	21.53 (.760)	26.63 (.940)	31.61 (1.116)
26689. (6000.)	14.87 (.525)	18.27 (.645)	22.24 (.785)	26.54 (.937)
35586. (8000.)	13.77 (.486)	16.71 (.590)	20.11 (.710)	24.16 (.835)
44482. (10000.)	13.09 (.462)	15.81 (.558)	18.75 (.662)	21.95 (.775)
53378. (12000.)	12.49 (.441)	15.15 (.535)	17.96 (.634)	20.90 (.738)
62275. (14000.)	12.26 (.433)	14.73 (.520)	17.39 (.614)	20.17 (.712)
71171. (16000.)	12.07 (.426)	14.45 (.510)	17.00 (.600)	19.71 (.696)
80068. (18000.)	12.04 (.425)	14.28 (.504)	16.77 (.592)	19.43 (.686)

TABLE 40
Q-FAN PROPULSION SFC (CONT'D)

ALTITUDE = 6096 (20000)   SFC~ Mkg/N · S (LBM/LBF · HR)

Net Thrust ~ N (lbf)	MACH NO.			
	.35	.50	.65	.80
8896. (2000.)	24.78 (.875)	30.45 (1.075)	41.07 (1.450)	51.69 (1.825)
13345. (3000.)	21.10 (.745)	24.93 (.880)	31.58 (1.115)	39.66 (1.400)
17793. (4000.)	18.35 (.648)	21.81 (.770)	26.91 (.950)	32.97 (1.164)
26689. (6000.)	15.15 (.535)	18.58 (.656)	22.52 (.795)	26.91 (.950)
35586. (8000.)	13.88 (.490)	16.83 (.594)	20.17 (.712)	23.85 (.842)
44482. (10000.)	13.17 (.465)	15.86 (.560)	18.84 (.665)	22.09 (.780)
53378. (12000.)	12.72 (.449)	15.27 (.539)	17.99 (.635)	20.96 (.740)
62275. (14000.)	12.38 (.437)	14.79 (.522)	17.42 (.615)	20.22 (.714)
71171. (16000.)	12.18 (.430)	14.47 (.511)	17.05 (.602)	19.66 (.680)
80068. (18000.)	12.01 (.424)	14.28 (.504)	16.77 (.592)	19.26 (.680)
88964. (20000.)	11.90 (.420)	14.11 (.498)	16.57 (.585)	18.98 (.670)
97860. (22000.)	11.90 (.420)	14.02 (.495)	16.43 (.580)	18.81 (.664)

TABLE 40
Q-FAN PROPULSION SFC (CONT'D)

ALTITUDE = 9144 (30000)   SFC ~ Mkg/N · S (LBM/LBF · HR)

Net Thrust ~ N (lbf)	MACH NO.			
	.35	.50	.65	.80
8896. (2000.)	27.19 (.960)	35.83 (1.265)	44.47 (1.570)	53.11 (1.875)
17793. (4000.)	18.69 (.660)	23.43 (.827)	28.33 (1.000)	33.99 (1.200)
26689. (6000.)	15.58 (.550)	19.12 (.675)	22.94 (.810)	27.19 (.960)
35586. (8000.)	14.33 (.506)	17.31 (.611)	20.54 (.725)	24.08 (.850)
44482. (10000.)	13.48 (.476)	16.15 (.570)	19.09 (.674)	22.29 (.787)
53378. (12000.)	12.92 (.456)	15.47 (.546)	18.24 (.644)	21.19 (.748)
62275. (14000.)	12.55 (.443)	14.96 (.528)	17.62 (.622)	20.39 (.720)
71171. (16000.)	12.29 (.434)	14.59 (.515)	17.19 (.607)	19.83 (.700)
80068. (18000.)	12.09 (.427)	14.45 (.510)	16.94 (.598)	19.46 (.687)
88964. (20000.)	12.04 (.425)	14.30 (.505)	16.83 (.594)	19.26 (.680)
97860. (22000.)	11.89 (.423)	14.30 (.505)	16.77 (.592)	19.12 (.675)
106757. (24000.)	12.04 (.425)	14.30 (.505)	16.85 (.595)	19.12 (.675)
115653. (26000.)	12.18 (.430)	14.45 (.510)	16.94 (.598)	19.26 (.680)

TABLE 40
Q-FAN PROPULSION SFC (CONT'D)

ALTITUDE = 12192 (40000)   SFC~ Mkg/N · S   (LBM/LBF· HR)

Net Thrust~ N (lbf)	MACH NO.			
	.35	.50	.65	.80
8896. (2000.)	27.19 (.960)	32.43 (1.145)	38.24 (1.350)	44.61 (1.575)
17793. (4000.)	19.83 (.700)	24.64 (.870)	29.32 (1.035)	36.82 (1.300)
26689. (6000.)	16.60 (.586)	20.11 (.710)	24.53 (.866)	29.03 (1.025)
35586. (8000.)	15.07 (.532)	17.99 (.635)	21.39 (.755)	24.87 (.878)
44482. (10000.)	14.11 (.498)	16.74 (.591)	19.71 (.696)	22.92 (.809)
53378. (12000.)	13.48 (.476)	16.00 (.565)	18.72 (.661)	21.67 (.765)
62275. (14000.)	13.03 (.460)	15,44 (.545)	18.04 (.637)	20.85 (.736)
71171. (16000.)	12.69 (.448)	15.01 (.530)	17.56 (.620)	20.28 (.716)
80068. (18000.)	12.46 (.440)	14.73 (.520)	17.28 (.610)	19.86 (.701)
88964. (20000.)	12.32 (.435)	14.59 (.515)	17.05 (.602)	19.57 (.691)
97860. (22000.)	12.29 (.434)	14.59 (.515)	17.00 (.600) ·	19.40 (.685)
106757. (24000.)	12.32 (.435)	14.62 (.516)	17.00 (.600)	19.32 (.682)
115653. (26000.)	12.46 (.440)	14.73 (.520)	17.05 (.602)	19.32 (.682)
124550. (28000.)	12.66 (.447)	14.87 (.525)	17.22 (.608)	19.40 (.685)

Page Intentionally Left Blank

TABLE 41 Q-FAN PROPULSION DRAG BREAKDOWN

10,060 m

MACH NO. = 0.70   CL = 0.31   ALT = (33,000 ft.)

MACH NO. = C.7C   CL = 0.31   RE/FT = 0.17945E 07   ALT = 0.33000E 05

GEOMETRY TOTAL DRAG	PARASITE DRAG	FLAT PLATE FRICTION DRAG	PRESSURE DRAG	DRAG RISE	VORTEX DRAG
0.019354	0.015831	0.009988	0.005843	0.000026	0.003497

COMPONENT DRAG				INDUCED DRAG
				0.003370
WING	0.006456	0.004313	0.002142	0.0	TRIM
BODY	0.004332	0.003593	0.000739	0.0	DRAG
				0.000127
HORZ TAIL	0.000922	0.000719	0.000203	0.0
VERT TAIL	0.000667	0.000516	0.000152	0.0
NACELLE	0.001687	0.000654	0.001033	0.000026
STRUT	0.000273	0.000193	0.000080	0.0
HL CAB	0.0	0.0	0.0	0.0
BODY POD	0.0	0.0	0.0	0.0
WING POD	0.0	0.0	0.0	0.0
FLAP TRACK	0.0	0.0	0.0	0.0
BUBBLE EXCRESCENCE	0.0 0.001449	0.0	0.0	0.0

TABLE 42 Q-FAN PROPULSION DRAG POLAR

ALT = 0.0

CL/M	0.0	0.0500	0.1000	0.1500	0.2000	0.2500	0.3000	0.3500
0.0	0.0008	0.0217	0.0195	0.0183	0.0176	0.0170	0.0166	0.0162
0.1000	0.0012	0.0207	0.0186	0.0176	0.0169	0.0164	0.0160	0.0156
0.2000	0.0022	0.0216	0.0196	0.0185	0.0178	0.0173	0.0169	0.0166
0.3000	0.0040	0.0235	0.0214	0.0204	0.0197	0.0191	0.0187	0.0184
0.4000	0.0066	0.0261	0.0241	0.0230	0.0223	0.0218	0.0214	0.0210
0.5000	0.0096	0.0296	0.0275	0.0264	0.0257	0.0252	0.0247	0.0244
0.6000	0.0135	0.0338	0.0317	0.0306	0.0298	0.0293	0.0289	0.0285
0.7000	0.0181	0.0391	0.0369	0.0357	0.0350	0.0344	0.0340	0.0337

ALT = 0.0

CL/M	0.4000	0.4500	0.5000	0.5500	0.6000	0.6500	0.7000
0.0	0.0160	0.0157	0.0155	0.0153	0.0151	0.0150	0.0148
0.1000	0.0154	0.0151	0.0149	0.0147	0.0146	0.0144	0.0143
0.2000	0.0163	0.0161	0.0159	0.0157	0.0155	0.0154	0.0152
0.3000	0.0181	0.0179	0.0177	0.0175	0.0174	0.0172	0.0171
0.4000	0.0208	0.0205	0.0203	0.0201	0.0200	0.0198	0.0197
0.5000	0.0241	0.0239	0.0237	0.0235	0.0233	0.0232	0.0231
0.6000	0.0283	0.0280	0.0278	0.0276	0.0275	0.0273	0.0279
0.7000	0.0334	0.0331	0.0329	0.0327	0.0325	0.0324	0.0390

10,060 m
ALT = (33,000 ft.)

CL/M	0.0	0.0500	0.1000	0.1500	0.2000	0.2500	0.3000	0.3500
0.0	0.0008	0.0256	0.0228	0.0214	0.0204	0.0198	0.0192	0.0188
0.1000	0.0012	0.0244	0.0218	0.0204	0.0196	0.0189	0.0184	0.0180
0.2000	0.0022	0.0252	0.0227	0.0213	0.0205	0.0198	0.0193	0.0189
0.3000	0.0040	0.0271	0.0245	0.0232	0.0223	0.0217	0.0212	0.0208
0.4000	0.0064	0.0298	0.0272	0.0259	0.0250	0.0244	0.0238	0.0234
0.5000	0.0096	0.0333	0.0307	0.0293	0.0284	0.0278	0.0273	0.0268
0.6000	0.0135	0.0376	0.0349	0.0335	0.0326	0.0320	0.0314	0.0310
0.7000	0.0181	0.0430	0.0402	0.0388	0.0379	0.0372	0.0367	0.0362

10,060 m
ALT = (33,000 ft.)

CL/M	0.4000	0.4500	0.5000	0.5500	0.6000	0.6500	0.7000
0.0	0.0184	0.0181	0.0178	0.0176	0.0174	0.0172	0.0170
0.1000	0.0177	0.0174	0.0171	0.0169	0.0167	0.0165	0.0164
0.2000	0.0186	0.0183	0.0180	0.0178	0.0176	0.0175	0.0173
0.3000	0.0205	0.0202	0.0199	0.0197	0.0195	0.0193	0.0191
0.4000	0.0231	0.0228	0.0225	0.0223	0.0221	0.0219	0.0218
0.5000	0.0265	0.0262	0.0259	0.0257	0.0255	0.0253	0.0252
0.6000	0.0307	0.0304	0.0301	0.0299	0.0297	0.0295	0.0301
0.7000	0.0358	0.0355	0.0353	0.0350	0.0348	0.0346	0.0412

	Outb'd Gust Load Alleviation		Outb'd/Inb'd Gust Load Alleviation	
	A	B	A	B
C_{L_o}	.138	.097	.138	.097
C_{L_α}/Rad	9.14	9.14	9.14	9.14
$C_{L_{\dot\alpha}}$/Rad	2.20	2.20	2.20	2.20
$C_{L_{\dot q}}$/Rad	6.78	6.78	6.78	6.78
$C_{L_{\delta E}}$/Deg	.0062	.0062	.0062	.0062
$C_{L_{\delta\,Ail.\,Inb'd}}$/Deg/Side			.00184	.00184
$C_{L_{\delta\,Ail.\,Outb'd}}$/Deg/Side	.00351	.00351	.00150	.00150
$C_{L_{\delta\,Spoiler\,A}}$/Deg/Side	-.00206	-.00206	-.00187	-.00187
$C_{L_{\delta\,Spoiler\,B}}$/Deg/Side			-.00242	-.00242
C_{D_o}	.0158	.0154	.0158	.0154
C_{D_α}/Rad	.0713	.0713	.0713	.0713
C_D/C_L	.0078	.0078	.0078	.0078
$C_{D_{\delta E}}$/Deg	–	–	–	–
$C_{D_{\delta\,Ail.\,Inb'd}}$/Deg/Side			.000141	.000141
$C_{D_{\delta\,Ail.\,Outb'd}}$/Deg/Side	.000324	.000324	.000122	.000122
$C_{D_{\delta\,Spoiler\,A}}$/Deg/Side	.000420	.000420	.000350	.000350
$C_{D_{\delta\,Spoiler\,B}}$/Deg/Side			.000480	.000480
C_{M_o}	–	–	–	–
C_{M_α}/Rad	-1.02	-1.02	-1.02	-1.02
$C_{M_{\dot\alpha}}$/Rad	-10.3	-10.3	-10.3	-10.3
$C_{M_{\dot q}}$/Rad	-31.7	-31.7	-31.7	-31.7
$C_{M_{\delta E}}$/Deg	-.0280	-.0280	-.0280	-.0280
$C_{M_{\delta\,Ail.\,Inb'd}}$/Deg/Side			-.00100	-.00100
$C_{M_{\delta\,Ail.\,Outb'd}}$/Deg/Side	-.00147	-.00147	-.00079	-.00079
$C_{M_{\delta\,Spoiler\,A}}$/Deg/Side	.00040	.00040	.00040	.00040
$C_{M_{\delta\,Spoiler\,B}}$/Deg/Side			.00040	.00040
WRBM δ Ail. Inb'd m-N/Deg/Side (Ft-lbs/Deg/Side)			22,600	22,600
WRBM δ Ail. Outb'd m-N/Deg/Side (Ft-lbs/Deg/Side)	293,000 (216,000)	293,000 (216,000)	136,500 (100,700)	136,500 (100,700)
WRBM δ Spoiler A m-N/Deg/Side (Ft-lbs/Deg/Side)	-123,800 (-91,300)	-123,800 (-91,300)	-119,600 (-88,200)	-119,600 (-88,200)
WRBM δ Spoiler B m-N/Deg/Side (Ft-lbs/Deg/Side)			-118,400 (-87,300)	-118,400 (-87,300)
WRBM α m-N/Deg (Ft-lbs/Deg)	2,236,000 (1,649,000)	1,969,000 (1,452,000)	2,236,000 (1,649,000)	1,969,000 (1,452,000)

TABLE 44
GLA STABILITY, CONTROL AND WRBM DERIVATIVES
FOR FLIGHT CONDITIONS C AND D

	Outb'd Gust Load Alleviation		Outb'd/Inb'd Gust Load Alleviation	
	C	D	C	D
C_{L_0}	.159	.112	.159	.112
C_{L_α}/Rad	8.65	8.65	8.65	8.65
$C_{L_\alpha}^{\wedge}$/Rad	2.01	2.01	2.01	2.01
$C_{L_q}^{\wedge}$/Rad	6.56	6.56	6.56	6.56
$C_{L_{\delta E}}$/Deg	.0060	.0060	.0060	.0060
$C_{L_{\delta\ Ail.\ Inb'd}}$/Deg/Side			.00189	.00189
$C_{L_{\delta\ Ail.\ Outb'd}}$/Deg/Side	.00351	.00351	.00150	.00150
$C_{L_{\delta\ Spoiler\ A}}$/Deg/Side	-.00195	-.00195	-.00178	-.00178
$C_{L_{\delta\ Spoiler\ B}}$/Deg/Side			-.00229	-.00229
C_{D_0}	.0162	.0158	.0162	.0158
C_{D_α}/Rad	.184	.184	.184	.184
C_D/C_L	.0225	.0225	.0225	.0225
$C_{D_{\delta E}}$/Deg	—	—	—	—
$C_{D_{\delta\ Ail.\ Inb'd}}$/Deg/Side			.000141	.000141
$C_{D_{\delta\ Ail.\ Outb'd}}$/Deg/Side	.000324	.000324	.000122	.000122
$C_{D_{\delta\ Spoiler\ A}}$/Deg/Side	.000389	.000389	.000324	.000324
$C_{D_{\delta\ Spoiler\ B}}$/Deg/Side			.000444	.000444
C_{M_0}	—	—	—	—
C_{M_α}/Rad	-1.02	-1.02	-1.02	-1.02
$C_{M_\alpha}^{\wedge}$/Rad	-9.42	-9.42	-9.42	-9.42
$C_{M_q}^{\wedge}$/Rad	-30.6	-30.6	-30.6	-30.6
$C_{M_{\delta E}}$/Deg	-.0280	-.0280	-.0280	-.0280
$C_{M_{\delta\ Ail.\ Inb'd}}$/Deg/Side			-.00100	-.00100
$C_{M_{\delta\ Ail.\ Outb'd}}$/Deg/Side	-.00147	-.00147	-.00079	-.00079
$C_{M_{\delta\ Spoiler\ A}}$/Deg/Side	.00040	.00040	.00040	.00040
$C_{M_{\delta\ Spoiler\ B}}$/Deg/Side			.00040	.00040
WRBM δ Ail. Inb'd m-N/Deg/Side (Ft-lbs/Deg/Side)			19,500	19,500
WRBM δ Ail. Outb'd m-N/Deg/Side (Ft-lbs/Deg/Side)	271,000(200,000)	271,000 (200,000)	117,500 (86,700)	117,500(86,700)
WRBM δ Spoiler A m-N/Deg/Side (Ft-lbs/Deg/Side)	-100,800 (-74,400)	-100,800 (-74,400)	-97,500 (-71,900)	-97,500(-71,900)
WRBM δ Spoiler B m-N/Deg/Side (Ft-lbs/Deg/Side)			-96,500 (71,200)	-96,500(-71,200)
WRBM α m-N/Deg (Ft-lbs/Deg)	1,814,000 (1,338,000)	1,593,000 (1,175,000)	1,814,000 (1,338,000)	1,593,000 (1,175,000)

TABLE 45
GLA STABILITY, CONTROL AND WRBM DERIVATIVES
FOR FLIGHT CONDITIONS E AND F

	Outb'd Gust Load Alleviation		Outb'd/Inb'd Gust Load Alleviation	
	E	F	E	F
C_{L_o}	.512	.517	.512	.517
C_{L_α} /Rad	7.22	7.10	7.22	7.10
$C_{L_{\hat\alpha}}$ /Rad	1.49	1.45	1.49	1.45
$C_{L_{\hat q}}$ /Rad	5.82	5.75	5.82	5.75
$C_{L_{\delta E}}$ /Deg	.00702	.00695	.00702	.00695
C_{L_δ} Ail. Inb'd /Deg/Side			.00189	.00189
C_{L_δ} Ail. Outb'd /Deg/Side	.00351	.00351	.00150	.00150
C_{L_δ} Spoiler A /Deg/Side	-.00161	-.00158	-.00146	-.00144
C_{L_δ} Spoiler B /Deg/Side			-.00189	-.00186
C_{D_o}	.027	.027	.027	.027
C_{D_δ} /Rad	.271	.266	.271	.266
C_D/C_L	.0375	.0375	.0375	.0375
$C_{D_{\delta E}}$ /Deg	–	–	–	–
C_{D_δ} Ail. Inb'd /Deg/Side			.000141	.000141
C_{D_δ} Ail. Outb'd /Deg/Side	.000324	.000324	.000122	.000122
C_{D_δ} Spoiler A /Deg/Side	.00033	.00032	.00027	.00026
C_{D_δ} Spoiler B /Deg/Side			.00037	.00036
C_{M_o}	–	–	–	–
C_{M_α} /Rad	-1.12	-1.10	-1.12	-1.10
$C_{M_{\hat\alpha}}$ /Rad	-6.69	-6.80	-6.69	-6.80
$C_{M_{\hat q}}$ /Rad	-27.3	-26.9	-27.3	-26.9
$C_{M_{\delta E}}$ /Deg	-.0328	-.0330	-.0328	-.0330
C_{M_δ} Ail. Inb'd /Deg/Side			-.00100	-.00100
C_{M_δ} Ail. Outb'd /Deg/Side	-.00147	-.00147	-.00079	-.00079
C_{M_δ} Spoiler A /Deg/Side	.00040	.00040	.00040	.00040
C_{M_δ} Spoiler B /Deg/Side			.00040	.00040
WRBM δ Ail. Inb'd m-N/Deg/Side (Ft-lbs/Deg/Side)			6,100	4,200
WRBM δ Ail. Outb'd m-N/Deg/Side (Ft-lbs/Deg/Side)	79000 (58,320)	55000 (40,600)	36900 (27,200)	25600 (18,900)
WRBM δ Spoiler A m-N/Deg/Side (Ft-lbs/Deg/Side)	-26200 (-19,300)	-17900 (-13,200)	-25200 (-18,600)	-17200 (-12,700)
WRBM δ Spoiler B m-N/Deg/Side (Ft-lbs/Deg/Side)			-24900 (-18,400)	-17100 (-12,600)
WRBM$_\alpha$ m-N/Deg (Ft-lbs/Deg)	469000 (346,000)	283000 (209,000)	469000 (346,000)	283000 (209,000)

TABLE 46
STABILITY AND CONTROL DERIVATIVES RIDE QUALITY
IMPROVEMENT BASELINE CONFIGURATION

	Ride Quality Improvement Flight Conditions		
	A Climb	B Cruise	C Approach
C_{L_o}	.478	.300	2.23
C_{L_α}/Rad	7.22	8.65	7.73
$C_{L_{\hat{\alpha}}}$ /Rad	1.49	2.01	1.38
$C_{L_{\hat{q}}}$ /Rad	5.82	6.56	5.66
$C_{L_{\delta_E}}$/Deg	.00702	.00600	.0072
C_{D_o}	.026	.0192	.4462
C_{D_α}/Rad	.271	.184	1.113
C_D/C_L	.0375	.0225	.144
$C_{D_{\delta_E}}$/Deg	—	—	—
C_{M_α} /Rad	-1.12	-1.02	-.873
$C_{M_{\hat{\alpha}}}$/Rad	-6.69	-9.42	-6.44
$C_{M_{\hat{q}}}$ /Rad	-27.3	-30.6	-26.5
$C_{M_{\delta_E}}$/Deg	-.0331	-.0283	-.034

TABLE 47
BOEING 707 RIDE QUALITY FLIGHT CONDITIONS AND STABILITY DERIVATIVES

	Flight Conditions		
	Cruise		Climb/Desc.
Configuration	Clean	Clean	Clean
Mach No.	.80	.86	.57
$V_E \sim$ m/s (Kts)	138 (268)	142 (276)	140 (272)
GW $\sim$ N (lbs)	890,000 (200,000)	800,700 (180,000)	1,068,000 (240,000)
$I_{yy} \sim$ kg - m^2 (Slugs-Ft^2)	4,750,000 (3,500,000)	4,660,000 (3,440,000)	4,990,000 (3,680,000)
CG $\sim$ % MAC	25	25	25
C_{L_o}	.335	.288	.386
C_{L_α}/Rad	5.07	5.41	4.67
$C_{L_{\hat{\alpha}}}$/Rad	—	—	—
$C_{L_{\hat{q}}}$/Rad	—	—	—
C_{D_o}	.0181	.020	.021
C_{D_α}/Rad	.178	.178	.191
C_{M_α}/Rad	-1.02	-1.209	-.630
$C_{M_{\hat{\alpha}}}$/Rad	-7.00	-6.40	-5.75
$C_{M_{\hat{q}}}$/Rad	-15.18	-13.37	-13.60

TABLE 48
ACT STABILITY, CONTROL AND WRBM DERIVATIVES

	ACT-1 GLA FAR Part 25 V_c	ACT-2 RSS/RQI Cruise	ACT-3 RSS/RQI Approach	ACT-4 RQI Midclimb
C_{L_o}	.160	.300	2.23	.480
C_{L_α} /Rad	8.46	8.46	7.56	7.05
$C_{L_{\hat{\alpha}}}$ /Rad	1.37	1.37	.934	1.02
$C_{L_{\hat{q}}}$ /Rad	4.51	4.51	3.89	4.05
$C_{L_{\delta E}}$ /Deg	.00364	.00364	.00440	.00450
$C_{L_{\delta Ail. Inb'd}}$ /Deg/Side	.00189	.00189	.00189	.00189
$C_{L_{\delta Ail. Outb'd}}$ /Deg/Side	.00150	.00150	.00150	.00150
$C_{L_{\delta Spoiler A}}$ /Deg/Side	-.00178			
$C_{L_{\delta Spoiler B}}$ /Deg/Side	-.00229			
C_{D_o}	.0164	.0198	.445	.0252
C_{D_α} /Rad	.093	.191	1.09	.247
C_D/C_L	.011	.0225	.144	.035
$C_{D_{\delta E}}$ /Deg	–	–	–	–
$C_{D_{\delta Ail. Inb'd}}$ /Deg/Side	.000141	.000141	.000141	.000141
$C_{D_{\delta Ail. Outb'd}}$ /Deg/Side	.000122	.000122	.000122	.000122
$C_{D_{\delta Spoiler A}}$ /Deg/Side	.000324	–	–	–
$C_{D_{\delta Spoiler B}}$ /Deg/Side	.000444	–	–	–
C_{M_o}	0	0	0	0
C_{M_α} /Rad	1.21	▷1	▷2	.810
$C_{M_{\hat{\alpha}}}$ /Rad	-7.25	-7.25	-4.94	-5.40
$C_{M_{\hat{q}}}$ /Rad	-23.9	-23.9	-20.6	-21.4
$C_{M_{\delta E}}$ /Deg	-.0190	-.0190	-.0232	-.0230
$C_{M_{\delta Ail. Inb'd}}$ /Deg/Side	-.00100	-.00100	-.00100	-.00100
$C_{M_{\delta Ail. Outb'd}}$ /Deg/Side	-.00079	-.00079	-.00079	-.00079
$C_{M_{\delta Spoiler A}}$ /Deg/Side	.00040	–	–	–
$C_{M_{\delta Spoiler B}}$ /Deg/Side	.00040	–	–	–
ΔWRBM δ Ail. Inb'd m-N/Deg/Side (Ft-lbs/Deg/Side)	24,000 (18,000)	12,700 (9,400)	1,680 (1,240)	8,190 (6,040)
ΔWRBM δ Ail. Outb'd m-N/Deg/Side (Ft-lbs/Deg/Side)	103,300 (76,200)	54,000 (39,800)	7,050 (5,200)	34,600(25,500)
ΔWRBM δ Spoiler A m-N/Deg/Side (Ft-lbs/Deg/Side)	-100,900 (-74,400)	–	–	–
ΔWRBM δ Spoiler B m-N/Deg/Side (Ft-lbs/Deg/Side)	-99,900(-73,700)	–	–	–
ΔWRBM α m-N/Deg (Ft-lbs/Deg)	1,631,000 (1,203,000)	846,000 (623,800)	98,800 (72,900)	455,500 (336,000)

▷1

CG ~ % MAC	C_{M_α} ~/Rad
45 (Fwd)	0.364
55 (Mid)	1.21
56 (Aft)	2.06

▷2

CG ~ % MAC	C_{M_α} ~/Rad
45 (Fwd)	0.279
55 (Mid)	1.13
65 (Aft)	1.97

Page Intentionally Left Blank

REFERENCES

1. NASA CR 2320, "The Influence of Wing Loading on Turbofan Powered STOL Transports With and Without Externally Blown Flaps".

2. NASA CR 137525 and 137526, "Evaluation of Advance Lift Concepts and Fuel Conservative Short-Haul Aircraft, Volumes I and II".

3. NASA CR 137634, "Evaluation of Active Control Technology For Short-Haul Aircraft".

4. Boeing Document, "User's Manual for ASAMP, Aircraft and Mission Performance Program", D3-7949, 1968.

5. Boeing Document, "Parametric/Statistical Weight Estimating Methods (Class I)", D6-15095TN, Revision C, 1972.

6. Department of Transportation, Federal Aviation Administration, Federal Aviation Regulations, Volume III, Part 25 Airworthiness Standards: Transport Category Airplanes.

7. Department of Transportation, Federal Administration: Federal Aviation Regulations, Volume III, Part 36 Noise Standards: Aircraft Type Certification.

8. Holloway, R. B., Thompson G. O., Rohling, W. J., "Prospects For Low-Wing-Loading STOL Transports With Ride Smoothing , Journal of Aircraft, August 1972.

9. Hoak, D. E. and Finck, R. D., "USAF Stability and Control Datcom", 1972 Revision.

10. Anon: Data Sheets, Royal Aeronautical Society, 1972 Revision.

11. Boeing Document, "Low-Speed Aerodynamic Prediction Method", D6-26011, 1970.

12. Barnes, C. S., "A Developed Theory of Spoilers on Airfoils", Aeronautical Research Council, C.P. No. 887, 1966.

13. Fischel, J. and Tamburello, V., "Investigation of Effect of Span, Span-Wise Location and Chordwise Location of Spoilers on Lateral Control Characteristics of a Tapered Wing", NACA TN 1294, 1947.

14. Luoma, A. A., "An Investigation of the Lateral-Control Characteristics of Spoilers on a High-Aspect Ratio Wing of NACA 65-210 Section in the Langley 8-Foot High-Speed Tunnel", NACA RM No. L7D21, 1947.

15. Wentz, W. H. Jr., "Effectiveness of Spoilers on the GA(W)-1 Airfoil With a High Performance Fowler Flap", NASA CR-2538, 1975.

16. NASA CR-137635, "Development of Longitudinal Handling Qualities Criteria For Large Advanced Supersonic Aircraft".

17. AFFDL-TR-74-92, Volume I, "B-52 CCV Program Summary".

18. Jacobson, I. D., Kuhlthau, A. R., and L. G. Richards, "Application of Ride Quality Technology to Predict Ride Satisfaction For Commuter-Type Aircraft", NASA TM X-3295, 1975.

19. Conner, D. W., and Thompson, G. O., "Potential Benefits to Short-Haul Transports Through Use of Active Controls", AGARD-CP-157, 1974.

20. Boeing Document D-13272-362A, "Flight Test Results of HICAT Turbulence Survey Program".

21. Air Force Report, AFFDL TR-68-127, "Project HICAT, High Altitude Clear Air Turbulence Measurements and Meteorological Correlation."

22. Air Force Report AFFDL TR-70-10, "Low Altitude Atmospheric Turbulence LO-LOCAT Phase III".

23. Schoenman, R. L. and Shomber, H. A., "Impact of Active Controls on Future Transport Design, Performance and Operation", SAE 751051, 1975

24. Morris, R. L., Hanke, C. R., Pasley, L. H., and Rohling, W. J., "The Influence of Wing Loading on Turbofan Powered STOL Transports With and Without Externally Blown Flaps", NASA CR-2320, 1973.